Eukaryotic initiation factor 4E binding proteins (4EBPs): Deciphering their functions in the cellular response to glucose deprivation and as drivers of tumor aggressiveness in pediatric neuroblastoma

Inaugural-Dissertation

zur Erlangung des Doktorgrades
der Mathematisch-Naturwissenschaftlichen Fakultät
der Heinrich-Heine-Universität Düsseldorf

vorgelegt von

Kai Philipp Völtzke
aus Mönchengladbach

Düsseldorf, Dezember 2021

Aus dem Institut für Neuropathologie
der Heinrich-Heine-Universität Düsseldorf

Gedruckt mit der Genehmigung der
Mathematisch-Naturwissenschaftlichen Fakultät der
Heinrich-Heine-Universität Düsseldorf

Berichterstatter:

1. Prof. Dr. Guido Reifenberger

2. Prof. Dr. Andreas Reichert

Tag der mündlichen Prüfung:

28.04.2022

Ich versichere an Eides Statt, dass die Dissertation von mir selbständig und ohne unzulässige fremde Hilfe unter Beachtung der „Grundsätze zur Sicherung guter wissenschaftlicher Praxis an der Heinrich-Heine-Universität Düsseldorf“ erstellt worden ist.

Die Dissertation wurde in dieser oder ähnlicher Weise noch an keiner anderen Fakultät vorgelegt und es wurde kein vorheriger Promotionsversuch unternommen.

_____

Kai Philipp Völtzke

Düsseldorf, Dezember 2021

Table of contents

Acknowledgements

First, I would like to thank Professor Reifenberger for his supervision. I sincerely appreciate that you opened your doors for our group and that you gave me the opportunity to finish my doctoral thesis in your Institute.

Also, I am profoundly grateful to Professor Reichert for being my second supervisor and for taking the time to discuss experimental approaches within the great world of yeast.

I consider myself privileged to have received a grant from *Elterninitiative Kinderkrebsklinik e.V.* Keep up your great work for the children.

Gabriel, your enthusiasm for science and your gusto for a glass of fine wine are contagious. I sincerely thank you for the support and supervision throughout my PhD journey.

Laura, we both might have not suspected that initially, but I think we grew together as a team that supported each other. For the future, I wish for you to find the most fulfilling job there is.

Jon, you always lend an ear while radiating resilience. I am sure you will become a renowned scientist.

Kati and Alisa, you both couldn't have been more different. Yet, both of you had one thing in common: your intelligence. And that will bring you everywhere you want. I seriously couldn't have wished for other students.

Next, I would like to thank the whole institute of neuropathology – Kerstin and Kirstin, the Diagnostics team, the Korth lab, the Weggen lab, Christiane and Janine, Bastian, Jörg, Kerstin, and Marietta. Thanks to all of you for being extremely welcoming and helpful. And, of course, I shall not forget to thank the research group of Neurosurgery for the cheerful talks.

The people from the biochemistry and molecular biology lab gave me invaluable help though I was the "outsider". A special thanks to Katja, Tanja, Andrea, Laura, Ruchika, Rajesh, and Marcel. PS: I think I still owe the lab money for the coffee I drank ;)

I want to appreciate the friends and colleagues I found at the KMT-lab; A big thanks to the lovely people from our lunch and Kiosk gang including Daniel Picard, Daniel Hein, and Daniel the Nigel, Ciro, Melanie, Julian, and all the others joining from time to time. I miss my old office, which thanks to Scholti, Idriss, and Melf felt like an oasis in the dessert. Finally, a special thanks to Bianca and Silke, you two are the actual heart and head of the lab - everybody knows that.

Importantly, I want to express my gratitude to all the collaborators that made this thesis possible. In particular, I am extremely grateful to the enthusiastic young scientists from both the Rotblat and the Toiber lab for welcoming me so warmly in Be'er Sheva, Israel.

Last but not least, I want to thank my friends and family. You are the reason I am still hanging on. Küsschen & knuffel to my people from Mönchengladbach and Nijmegen! Extra viel Liebe an meine Eltern und meinen Brudi. Und natürlich an Marina – o amor da minha vida. ♡

Für Oppi

Summary

Cells frequently encounter nutrient stress, such as glucose starvation, forcing them to reprogram their metabolism in order to survive. It is critical to define the factors mediating such an adaptive response. This thesis aimed at delineating the role of the translational repressors and mTOR substrates eukaryotic initiation factor 4E binding proteins (4EBP1/2) in the response to changes in glucose levels. Unlike the current model, stating that 4EBP1/2 are inactivated by mTOR when glucose is available, the own work uncovered that a fraction of 4EBP1/2 is active under basal conditions, and selectively regulate specific sets of transcripts. 4EBP1/2 function was investigated under glucose deprivation using various cellular models of 4EBP-deficiency, which uncovered that 4EBP1/2 are preventing cell death in response to glucose deprivation. Functional *in vitro* assays demonstrated that under such conditions 4EBP1/2 are preventing oxidative stress by repressing fatty acid synthesis, which normally consume NADPH, in turn allowing cells to survive. The molecular dissection of the mechanisms underlying 4EBP1/2 function revealed that 4EBP1/2 selectively repress the translation of *ACACA*, which encodes the rate-limiting enzyme of fatty acid synthesis. Remarkably, *in vivo* studies in budding yeast revealed that the protective function of 4EBP1/2 under glucose depletion is evolutionarily conserved. Since cancer is a pathological condition of glucose deprivation, the potential clinical relevance and the regulation of 4EBP1 in this disease was additionally investigated, with a focus on the neuroblastoma, the most common solid cancer type in pediatric patients. Bioinformatics analyses showed that *EIF4EBP1*, the gene coding for 4EBP1, is overexpressed in this tumor entity and this increased expression is linked to poor prognosis. Hence, 4EBP1 expression may serve to stratify patients with high-risk neuroblastoma. This was confirmed by immunohistochemistry of 4EBP1 in neuroblastoma tissue samples, which connected high 4EBP1 levels to aggressive tumor subtypes. Furthermore, *in vitro* gene reporter assays and manipulation of gene expression showed that *EIF4EBP1* transcription is controlled by binding of the MYCN oncoprotein to the *EIF4EBP1* promoter, thus linking 4EBP1 upregulation to *MYCN* gene amplification and overexpression, which is an established factor for poor prognosis in neuroblastoma.

Taken together, the studies summarized in this thesis reveal that 4EBPs are evolutionary conserved mediators of the metabolic response to glucose starvation by selectively regulating mRNA translation. In addition, increased 4EBP1 expression could be implicated as a novel pathomechanism linked to aggressive clinical behavior in neuroblastoma, suggesting that cancer cells may hijack 4EBPs to adapt to nutrient stress.

Zusammenfassung

Zellen sind häufig mit Stresssituationen, wie zum Beispiel Glukosemangel, konfrontiert und daher gezwungen, ihren Stoffwechsel umzuprogrammieren, um zu überleben. Es ist von entscheidender Bedeutung, die Faktoren zu bestimmen, die eine solche Adaptation möglich machen. Diese Dissertationsarbeit zielte darauf ab, die Rolle der Translationsrepressoren und mTOR-Substrate "Eukaryotische Initiationsfaktor 4E bindende Proteine (4EBP1/2)" bei der zellulären Reaktion auf Veränderungen des Glukosespiegels zu beschreiben. Im Gegensatz zum derzeitigen Modell, welches besagt, dass 4EBP1/2 durch mTOR inaktiviert werden, wenn Glukose verfügbar ist, konnte nachgewiesen werden, dass 4EBPs bereits unter basalen Bedingungen aktiv sein können und selektiv bestimmte Gruppen von Transkripten regulieren. Die Funktion von 4EBP1/2 wurde hierfür unter Glukosemangel anhand verschiedener zellulärer Modelle mit 4EBP-Defizienz untersucht und es wurde festgestellt, dass 4EBP1/2 den Zelltod als Reaktion auf Glukosemangel verhindern. Funktionelle *in vitro* Experimente zeigten, dass 4EBP1/2 unter solchen Bedingungen oxidativen Stress verhindern, indem sie die NADPH-konsumierende Fettsäuresynthese unterdrücken und so den Zellen das Überleben ermöglichen. Die molekulare Entschlüsselung der Mechanismen, die der Funktion von 4EBP1/2 zugrunde liegen, ergab, dass 4EBP1/2 selektiv die Translation von *ACACA* unterdrücken. *ACACA* kodiert für ACC1, welches das initiierende Enzym der Fettsäuresynthese ist. Bemerkenswerterweise zeigten *in vivo* Studien in Hefezellen, dass die Schutzfunktion von 4EBP1/2 unter Glukosemangel evolutionär konserviert ist. Da Krebs einen pathologischen Zustand des Glukosemangels darstellt, wurde zusätzlich die klinische Bedeutung und die Regulation von 4EBP1 in Neuroblastom, den häufigsten soliden Tumoren im Kindesalter, untersucht. Bioinformatische Analysen zeigten, dass *EIF4EBP1* (das Gen, das 4EBP1 kodiert) in dieser Tumorentität überexprimiert ist und dass diese erhöhte Expression mit einer ungünstigeren Prognose assoziiert ist und somit zur molekularen Stratifizierung von Hochrisiko-Patienten beitragen kann. Dies wurde auch durch immunhistochemische Untersuchungen von 4EBP1 in Neuroblastom-Gewebeproben bestätigt, die zeigten, dass eine erhöhte 4EBP1-Proteinexpression signifikant mit histologischen Merkmalen von Hochrisiko-Neuroblastomen korreliert. Darüber hinaus konnte mit Hilfe von *in vitro* Genreporter-Assays gezeigt werden, dass der Promotor und die Transkriptionsrate von *EIF4EBP1* durch das Onkoprotein MYCN kontrolliert wird, welches in aggressiven Neuroblastomen häufig amplifiziert und überexprimiert ist und einen bereits etablierten Marker für eine ungünstigere Prognose darstellt.

Insgesamt zeigen die in dieser Dissertationsschrift zusammengefassten Arbeiten, dass 4EBPs evolutionär konservierte Regulatoren der metabolischen Reaktion auf Glukosemangel sind und Zellen schützen, indem sie selektiv die mRNA Translation regulieren. Darüber hinaus konnte eine erhöhte 4EBP1-Expression als neuer Pathomechanismus im Zusammenhang mit

einem aggressivem klinischem Verhalten bei Neuroblastomen identifiziert werden, was darauf hindeutet, dass Krebszellen 4EBPs zur Anpassung an Nährstoffstress im Tumorgewebe nutzen können.

1. Introduction

1.1. Glucose deprivation

Cells have continuous need for nutrients, as they are the building blocks of biomass and essential to cellular growth. Irrespective of the size or organization of an organism, whether it is a unicellular or a multicellular organism, every living creature needs energy and biomolecules for maintaining cellular viability, for regeneration, and to grow and divide. Undisputedly, glucose is the most frequently occurring monosaccharide in nature and the major source of cellular energy. While prokaryotes and plants can synthesize glucose on their own, higher organisms such as mammals must meet their glucose requirements through food intake. In mammals, glucose molecules are absorbed in the small intestine and transported to individual cells via the bloodstream (Berg et al. 2002). In addition, excess glucose stored as glycogen or fat can be degraded to compensate for glucose scarcity. Nevertheless, in nature, glucose deprivation is a common physiological condition that is faced by every living organism, and which needs to be coped with to ensure survival. At the cellular level, glucose starvation reduces adenosine triphosphate (ATP)-generating processes, such as glycolysis, resulting in ATP depletion and thus energy stress (Joyner et al. 2016). Furthermore, withdrawal of glucose has been shown to increase oxidative stress, both by generation of reactive oxygen species (ROS) and by decreased availability of reducing agents and thus antioxidant activity (Ren und Shen 2019). Hence, under glucose deprivation energy depletion and failure to maintain redox balance will rapidly result in cell death if the cells do not initiate metabolic countermeasures to conserve energy and prevent accumulation of oxidants. While cells die after prolonged periods of glucose starvation, it was not conclusively characterized by which type of cell death this occurs, as the reported forms of cell death range from apoptosis over programmed non-apoptotic types of cell death to necrosis (Alves et al. 2006; Caro-Maldonado et al. 2010; Suzuki et al. 2003; Ding et al. 2016).

Cancer is a pathological condition characterized by glucose starvation, which is due to the immature and leaky vascularized microenvironment of macroscopic tumors (Lugano et al. 2020; Schaaf et al. 2018). In addition, at the first steps of tumor initiation, oncogene activation leads to a metabolic reprogramming that preconditions cancer cells to be glucose addicted. In particular, cancer cells commonly overuse the glycolytic pathway, which rapidly generates ATP and precursors for lipid and nucleotide syntheses (Deberardinis et al. 2008; Hsu und Sabatini 2008). All these processes provide the biomolecules needed for cellular growth and support rapid proliferation of cancer cells, in turn driving tumor expansion. While this promotes a selective growth advantage to cancer cells, it also increases their demand for glucose. Consequently, this initially renders cancer cells sensitive to low glucose conditions, creating a selective pressure for cellular adaptation.

1.2. Metabolic response to glucose deprivation

The metabolism of a cell is defined by the activity of anabolic and catabolic processes. While the former consumes/hydrolyses ATP to synthesize the biomolecules needed for cellular growth, the latter degrades energy-rich molecules into smaller units to harvest ATP and antioxidants. Metabolic homeostasis results from the proper balance between anabolism and catabolism under physiological conditions. When sufficient amounts of glucose are accessible, anabolic processes will be favored in the cell to promote the synthesis of biomolecules, including proteins, nucleotides and lipids, needed for cellular growth. However, in nature, when facing periods of glucose scarcity, living organisms will adjust their metabolism to cope with this stress condition at the cellular level. Such a cellular adjustment to glucose starvation corresponds to a metabolic switch that causes a blocking of anabolic processes, while at the same time promotes catabolic processes as depicted in Figure 1.1.

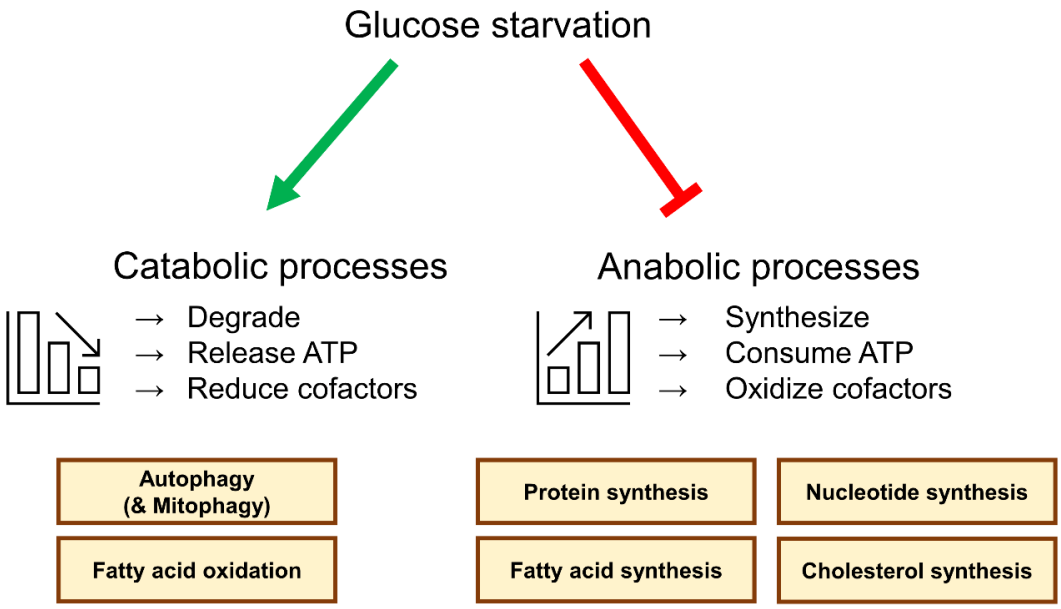

Figure 1.1: Glucose starvation-induced metabolic switch. *When encountering low levels of glucose, metabolic adaptation is crucial to ensure cell survival. On one hand, catabolic processes that provide energy and reduce cofactors for antioxidant reactions are promoted. While on the other hand, anabolic processes that build complex macromolecules by consuming ATP need to be suppressed. Together, this ensures maintenance of both the energetic and redox balance under conditions of glucose deprivation.*

When glucose is available, cells will take up the sugar and feed it into pathways generating energy and antioxidants for further metabolic processes. In particular, glycolysis will generate energy in the form of ATP, as well as precursors for lipid and protein production. Next to that, glucose can also branch off to the pentose phosphate pathway (PPP) to provide the cell with nucleotide precursors, while converting nicotinamide adenine dinucleotide phosphate ($NADP^+$) to its reduced form, NADPH, which is critical for antioxidant reactions. When glucose levels are low, cells need to accommodate a variety of metabolic processes in order to maintain energy homeostasis and prevent cell death. Notably, highly energy-consuming processes

need to be stopped under such conditions. This includes the most ATP consuming processes protein synthesis (Buttgereit und Brand 1995; Lindqvist et al. 2018; Holcik und Sonenberg 2005), as well as nucleotide synthesis and fatty acid synthesis (FAS) (Jeon et al. 2012; Liu und Sabatini 2020; Leprivier und Rotblat 2020; Leprivier et al. 2015). In addition to energy homeostasis, cells need to maintain the redox balance when glucose is low. This occurs in part by restricting antioxidant-consuming processes, such as FAS, which is the most NADPH consuming process. NADPH is a cofactor, which is required for numerous cellular antioxidant reactions. In particular, NADPH is the major electron donor for the regeneration of glutathione (GSH). One NADPH molecule can be utilized to reduce a molecule of oxidized disulfide glutathione (GSSG) to two GSH molecules. GSH is an essential antioxidant defense that can detoxify peroxides in living cells. Under glucose deprivation, since the major source of NADPH, the PPP, cannot be fed sufficiently, the conservation of reducing power is essential for survival (Berg et al. 2002).

In parallel to blocking anabolic processes when glucose levels drop, cells activate catabolic processes including the degradation, i.e. the oxidation of fatty acids (FAO) (Vacanti et al. 2014; Weber et al. 2020). This generates precursors for the production of ATP and NADPH, which are thus critical for the maintenance of cellular energetic balance and redox homeostasis (Bellance et al. 2009; Carracedo et al. 2013). Another important catabolic procedure is the lysosomal degradation of cellular components by autophagy. Autophagy is considered a self-recycling process that serves to clear accumulated waste from the cell and, in parallel, provides necessary ATP (Mehrpour et al. 2010). In mammalian cells, low levels of glucose can initiate autophagic degradation of macromolecules (Lee et al. 2021; Moruno et al. 2012; Marambio et al. 2010; Singh und Cuervo 2011). In yeast, acute depletion of glucose induces, next to FAO, autophagic flux to provide the starved cell with sufficient levels of energy (Weber et al. 2020). Surprisingly, another study showed that autophagy is inhibited in yeast cells under prolonged glucose starvation (Lang et al. 2014). In conclusion, the role of autophagy under glucose starvation remains not fully understood and its importance could vary in a duration-dependent manner.

In cancer cells, in contrast to normal cells, metabolism is initially not switched in response to glucose starvation. Indeed, oncogenic signaling renders cell metabolism unresponsive to energy stress. This disables them to reprogram metabolic processes upon changes of nutrients availability, including glucose availability. As a consequence, glucose starvation does not lead to blocking of anabolic processes in cancer cells initially. Instead, cancer cells sustain high glucose consumption independent of changes in glucose availability, so that anabolic processes are still active when glucose is low (Ward und Thompson 2012; Hsu und Sabatini 2008; Aykin-Burns et al. 2009). This initially increases the sensitivity of cancer cells to glucose-deprived conditions. Indeed, oncogene activation, by pushing anabolic processes, renders

cells more susceptible to glucose deprivation-induced cell death (Buzzai et al. 2005; Palorini et al. 2016; Shim et al. 1998). Insufficient inhibition of anabolism under glucose deprived conditions is thought to increase generation of ROS and oxidative damage, and to deplete ATP in cells (Aykin-Burns et al. 2009; Simons et al. 2009). This microenvironmental condition creates a selective pressure, driving the adaptation of some tumor cell clones to glucose deprivation (Flavahan et al. 2013). For instance, a study aiming to understand cancer cell adaptation to metabolic stress found transformed cells, which were initially reprogrammed to sustain unlimited growth by maintaining high levels of mRNA translation, to struggle to survive upon nutrient deprivation (Leprivier et al. 2013). Strikingly, nutrient deprivation selectively promoted survival of tumor cells that adapted by re-expressing high levels of a negative regulator of mRNA translation elongation: eukaryotic elongation factor 2 kinase (eEF2K). This utilization of the eEF2K pathway is a classic example of how cancer cells, that were initially glucose-addicted, hijack conserved pathways to adapt their metabolism to environmental changes such as low levels of glucose.

1.3. Glucose-responsive signaling networks – the opponents AMPK and mTOR

Throughout evolution, cells have developed complex networks for sensing glucose level and adapting their metabolism accordingly. The following paragraphs provide an overview of the two major hubs that connect glucose/energy-sensing to downstream signaling networks controlling metabolic processes.

1.3.1. AMPK

All eukaryote organisms have protein complexes that sense and maintain energy balance. A highly conserved energy-sensor that is activated upon low ATP levels, and therefore glucose deprivation, is the AMP-activated kinase (AMPK) (Lin und Hardie 2018; Salt et al. 1998). AMPK is known to control numerous metabolic pathways and to guide a metabolic switch from anabolic to catabolic processes, thereby enabling the cell to survive in glucose poor environments (Ren und Shen 2019; Russell et al. 2014; Hardie et al. 2012). AMPK is a heterotrimeric protein complex with a kinase function that enables the tight and fast control of downstream targets, including metabolic enzymes (Kim et al. 2011). An increase of the AMP/ATP or ADP/ATP ratio, which is induced by glucose starvation, directly activates AMPK. In addition, AMPK is activated by phosphorylation through the action of upstream kinases such as LKB1, which is a tumor suppressor that gets stimulated upon energy stress (Shackelford und Shaw 2009; Shaw et al. 2004).

Once activated, AMPK regulates the function of several downstream proteins involved in metabolism and cell growth (Hardie et al. 2012). On the one hand, AMPK induces catabolic processes, such as fatty acid oxidation (FAO) and autophagy (Herzig und Shaw 2018), to maintain redox balance under glucose starvation (Ren und Shen 2019). To do so, AMPK inhibits acetyl-CoA carboxylase 2 (ACC2), which activates FAO and supplies the cell with precursors needed for generating ATP and antioxidants (Weber et al. 2020; Pike et al. 2011; Ren und Shen 2019; Jeon et al. 2012; Winder und Hardie 1996). In addition, by phosphorylating Unc-51-like autophagy activating kinase 1 (ULK1), AMPK promotes autophagy and thereby ensures that the cell recycles macromolecules to gain energy, reducing agents and building blocks for molecule synthesis (Kim et al. 2011). Furthermore, phosphorylation of ULK1 and mitochondrial fission factor (MFF) by AMPK raises the recycling of mitochondria by an autophagy-like process referred to as mitophagy (Herzig und Shaw 2018). Strikingly, AMPK regulates, in parallel to the degradation, the biogenesis of mitochondria, through activation of peroxisome proliferator-activated receptor gamma coactivator 1 alpha (PGC1α), suggesting that tight control of mitochondrial flux is essential to maintain energy balance under glucose deprived conditions (Herzig und Shaw 2018).

On the other hand, AMPK inhibits anabolic processes such as protein and lipid syntheses to maintain cellular bioenergetic balance. One major substrate of AMPK that controls protein, lipid and nucleotide syntheses is the mechanistic target of rapamycin (mTOR) protein (Laplante und Sabatini 2012). By inhibiting mTOR, AMPK restricts the activity of the above-mentioned anabolic processes. More specifically, AMPK mediates the shutdown of mTORC1 signaling by targeting the regulatory protein Raptor and the tuberous sclerosis complex (TSC). While inhibition of Raptor decreases stability of the mTOR complex, activation of TSC prevents mTOR activation. Next to the counterplay with mTOR, AMPK inhibits ACC1, the rate limiting enzyme of fatty acid synthesis (FAS), thereby preventing the highly NADPH-consuming lipid synthesis (Herzig und Shaw 2018). Similarly, snf1, the yeast AMPK, gets activated upon low glucose availability to negatively regulate FAS (Wilson et al. 1996; Woods et al. 1994). The shutdown of such an anabolic pathway is essential in maintaining the assets of cells to cope with energy and antioxidant stress (Jeon et al. 2012). Thus, AMPK coordinates the inhibition of anabolic pathways with the activation of catabolic processes such as FAO to cope with energy and redox stress under glucose deprivation as summarized in Figure 1.2 (Ren und Shen 2019; Jeon et al. 2012).

Given that AMPK functions to block anabolic processes, it is not surprising that AMPK was initially considered as a tumor suppressor (Liang und Mills 2013). This was further supported by the fact that AMPK is induced by the tumor suppressor LKB1, which is often lost in cancer (Ciccarese et al. 2019). However, this view has been challenged by findings that showed AMPK to promote cellular growth and survival under nutrient poor conditions. More specifically,

Jeon et al. showed that AMPK-mediated inhibition of FAS is essential for maintaining NADPH levels and support cancer cell survival under glucose starvation *in vivo* (Jeon et al. 2012). In addition, AMPK was found to facilitate tumor growth by upregulating catabolic processes, such as lysosomal activity or glycolysis and mitochondrial activity, in mouse models of non-small-cell lung carcinoma (Eichner et al. 2019) and glioblastoma (Chhipa et al. 2018), respectively. In summary, the role of AMPK in cancer can be growth-inhibitory under nutrient rich conditions but growth- and survival-promoting in an unfavorable environmental context.

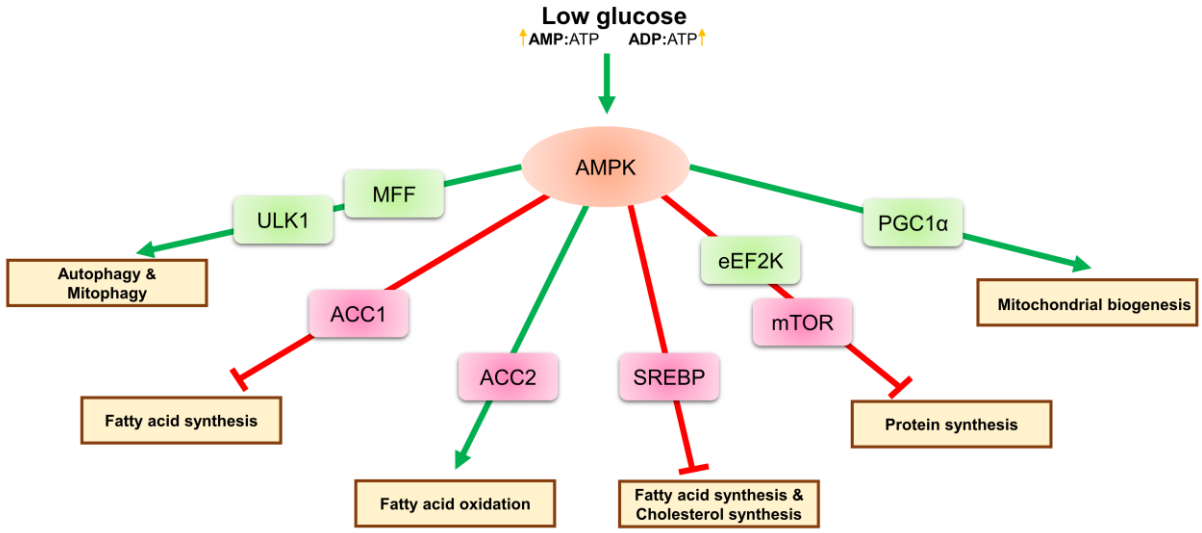

Figure 1.2: Overview of the AMPK signaling pathways. *The scheme summarizes the major AMPK substrates and corresponding metabolic processes controlled upon glucose starvation. The green or pink color of proteins indicates either an activating or inhibitory effect of AMPK, respectively. The green arrow or red blunt end lines denote either activation or suppression of the depicted metabolic process, respectively. The role of AMPK is to inhibit anabolism and promote catabolism to maintain energetic and redox balance upon cellular energetic stress.*

1.3.2. mTOR

Another major nutrient sensing hub is the already mentioned AMPK counterpart mTOR. This kinase is conserved from yeast to mammals, emphasizing its importance. mTOR is a master regulator coupling nutrient availability to cellular metabolism (Kim und Guan 2019). To be able to act as the focal point in nutrient sensing and signaling, mTOR works coordinately together with other proteins (Laplante und Sabatini 2012). In particular, two distinct complexes can be formed by mTOR: mTORC1 and mTORC2, by assembly with either one of the two regulatory proteins Raptor or Rictor (Laplante und Sabatini 2012), respectively. While mTORC1 is the focal point where nutrient sensing meets control of a wide range of cellular processes including protein, lipid and nucleotide syntheses, autophagy and proliferation (Dowling et al. 2010), mTORC2 mainly controls the organization of the cytoskeleton (Sarbassov et al. 2004). This thesis will focus on mTORC1, since mTORC2 does not respond to glucose but solely to growth factors (Foster und Fingar 2010; Sabatini 2017).

The activity of mTORC1 is regulated by several nutrients, such as leucine, arginine and glucose, both directly and through independent upstream sensors and signaling pathways (Laplante und Sabatini 2009; Saxton und Sabatini 2017; Liu und Sabatini 2020; Orozco et al. 2020). In general, mTORC1 gets activated at the lysosome, where, under nutrient rich conditions, GTP-bound Rheb stimulates mTORC1 activity (Laplante und Sabatini 2012). Upon glucose starvation, the TSC complex is activated by AMPK signaling and in turn prevents Rheb-mediated mTORC1 activation. Moreover, phosphorylation of Raptor by AMPK directly blocks mTORC1 formation when glucose levels are low (Gwinn et al. 2008). Next to Rheb, other proteins including the lysosomal vacuolar-type H^+-ATPase (v-ATPase) control mTORC1 activation at the lysosome (Zhang et al. 2014; Leprivier und Rotblat 2020). Interestingly, the v-ATPase was found to robustly orchestrate the metabolic switch by stimulating either mTORC1 or AMPK when ATP and glucose levels are high or low, respectively (Zhang et al. 2014).

MTORC1 controls metabolic processes to promote cell growth by multiple means (Laplante und Sabatini 2012; Sabatini 2017). In particular, mTORC1 fosters protein biosynthesis by inhibiting negative regulators of mRNA translation initiation, including eukaryotic initiation factor 4E binding proteins (4EBPs), to support cellular growth (Laplante und Sabatini 2012). MTORC1 inactivate 4EBPs by phosphorylation, preventing 4EBPs to repress mRNA translation initiation. In addition, mTORC1 drives protein synthesis by phosphorylating ribosomal protein S6 kinase (S6K), which in turn activates ribosomal protein S6. Furthermore, activation of distinct transcriptional programs by mTORC1 induces the synthesis of ATP, nucleotides and lipids to provide the building blocks for DNA synthesis and the lipid layer of the membrane, thus promoting cell growth and cell division (Saxton und Sabatini 2017). In particular, mTORC1 drives the expression of activating transcription factor 4 (ATF4), leading to increased nucleotide (and non-essential amino acids) synthesis (Saxton und Sabatini 2017). Furthermore, activation of hypoxia-inducible factor 1 (HIF-1) and sterol regulatory element-binding protein (SREBP) by mTORC1 promotes cellular growth by upregulating glycolysis, the pentose phosphate pathway and the synthesis of lipids, including fatty acids and cholesterol (Saxton und Sabatini 2017; Eberlé et al. 2004; Laplante und Sabatini 2009). While anabolic processes are supported by mTORC1, catabolic processes are inhibited by it. For instance, in contrast to the AMPK-mediated phosphorylation, ULK1 phosphorylation by mTOR prevents autophagy (Kim et al. 2011; Russell et al. 2014). Summing up, this allows mTORC1 to promote biosynthesis and cell growth under nutrient sufficiency (see Figure 1.3).

For survival under glucose deprivation, it is crucial to prevent mTORC1 signaling, as failure to do so leads to ATP depletion and cell death (Choo et al. 2010; Zhang et al. 2020). This is due in part to the inhibition of mRNA translation, following mTOR blockage, as this process is the most energy consuming process occurring in cells (Lindqvist et al. 2018; Buttgereit und Brand 1995; Holcik und Sonenberg 2005). In support to that, Choo *et al.* successfully blocked glucose

starvation-induced cell death in TSC knock down cells, which fail to inhibit mTORC1, by treatment with low doses of the translational inhibitor cycloheximide (Choo et al. 2010). Glucose starvation-induced suppression of mTORC1 further blocks several anabolic and thus ATP-consuming pathways while releasing inhibition of catabolic pathways like autophagy. Together, this mediates the metabolic shift needed to preserve the balance of cellular bioenergetics and thus to ensure survival under glucose deprivation (Choo et al. 2010).

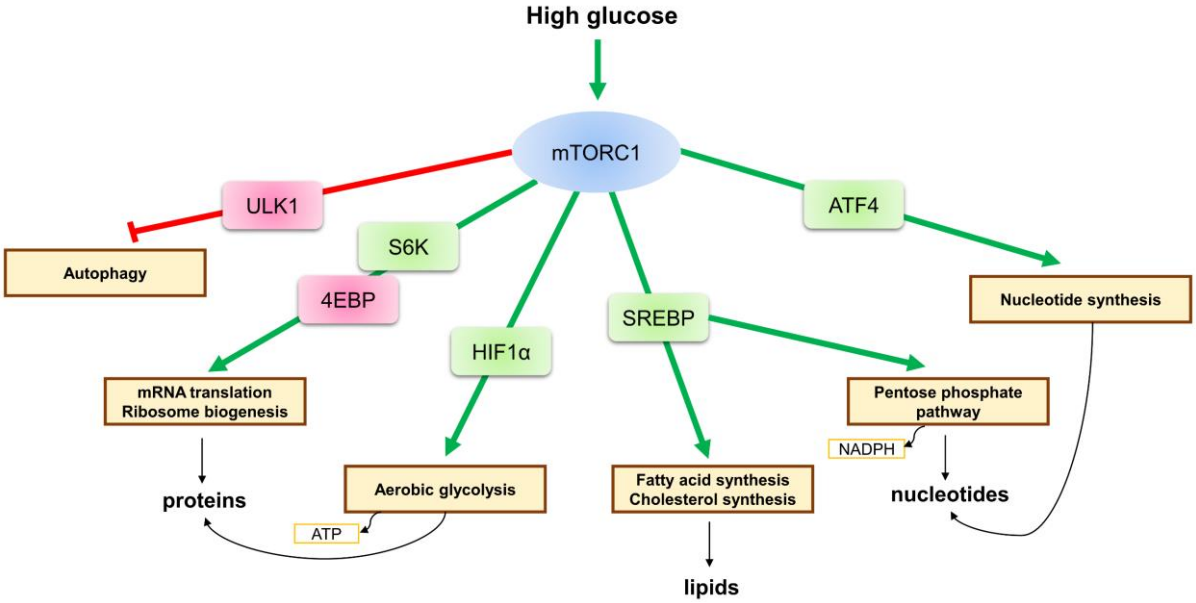

Figure 1.3: Overview of the mTORC1 signaling pathways. *The scheme highlights the targets of mTORC1 and corresponding metabolic processes regulated under glucose deprivation. The green or pink color of proteins indicates either an activating or inhibitory effect of mTORC1, respectively. The green arrow or red blunt end lines denote activation or suppression of the depicted metabolic process, respectively. Summing up, mTORC1 promotes anabolic processes involved in cellular growth while suppressing catabolic pathways including FAO and autophagy. Since low levels of glucose inactivate mTORC1 signaling, anabolic processes will be blocked while a shift towards catabolic processes will occur.*

In cancer, mTORC1 signaling is commonly found to be overactive (Laplante und Sabatini 2012; Saxton und Sabatini 2017). Elevated mTORC1 activity is associated with rapid tumor growth and chemoresistance, which is the reason for the focus on therapeutic targeting of this pathway to treat cancer (Mossmann et al. 2018). Strikingly, the success of mTORC1 targeting therapies in cancer seems to be complex and dependent on the tumor microenvironment, as it was reported that mTORC1 inhibition only reduced proliferation of tumor tissues within well-vascularized regions (Palm et al. 2015). Some tumor regions being less vascularized and thus potentially nutrient deprived showed the reverse effect, i.e., that mTORC1 inhibition resulted in increased tumor cell proliferation. Together, mTORC1 signaling drives anabolic growth, however, inhibition of mTORC1 might stimulate growth under unfavorable conditions, i.e. when catabolic processes should be favored to promote survival.

1.4. 4EBPs – regulators of mRNA translation

The mTORC1 substrates 4EBPs are eukaryotic initiation factor 4E (eIF4E)-binding proteins that regulate the rate-limiting step of protein biosynthesis, namely the initiation of mRNA translation (Haghighat et al. 1995). In mammals, three 4EBP homologs have been identified, namely 4EBP1, 2 and 3 (Poulin et al. 1998), which are encoded by different genes, *EIF4EBP1*, *-2* and *-3* respectively. However, their amino acid sequence is about 60% alike and all three share the conserved eIF4E binding motif (YXXXXLφ, φ = any hydrophobic amino acid) (Poulin et al. 1998; Cho et al. 2020; Mader et al. 1995). Strikingly, this motif is highly conserved throughout evolution as pointed out by the virtually unchanged sequence that can be found in other species ranging from yeast to mammals (Cosentino et al. 2000; Mader et al. 1995; Carroll et al. 2006; Oulhen et al. 2009; Miron et al. 2001). Next to the shared conserved eIF4E binding motif, 4EBP proteins share an N-terminal (RAIP) and a C-terminal (TOS/FEMDI) motif, which can be recognized by regulatory proteins such as Raptor (Böhm et al. 2021). A schematic outline of the protein structure of (human) 4EBPs is shown in Figure 1.4.

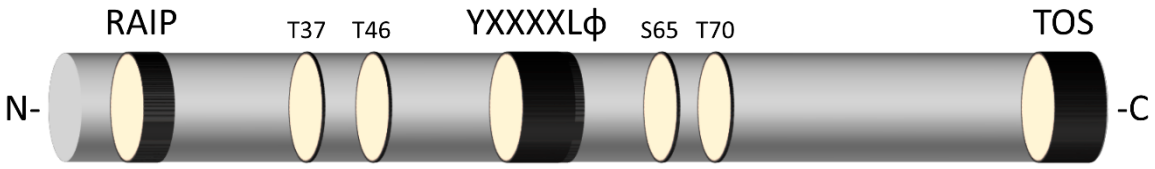

Figure 1.4: Schematic overview of the 4EBP protein structure. *The mTOR-directed phosphorylation sites at Threonine (T) 37, T46, T70 and Serine (S) 65 are highlighted (amino acid position based on human 4EBP1 sequence). The highly conserved Raptor binding motifs RAIP and TOS (amino acid sequence FEMDI) are depicted at the N- and C-terminus, respectively. The eIF4E binding motif is represented by the consensus amino acid sequence YXXXXLφ. Scheme based on Musa et al. 2016.*

The strong sequence conservation of the motifs highlights their importance for 4EBPs functions and suggests that the different 4EBP proteins, both within and between species, have similar functions (see Table 1.1). Several studies investigated the biological activity of 4EBP1- and -2 in mammals and found them to be functionally redundant with only minor differences that are potentially caused by distinct expression levels between the two homologs (Ayuso et al. 2010; Ding et al. 2018; Nehdi et al. 2014; Rousseau et al. 1996a). Moreover, Poulin et al. showed that 4EBP3 controls eIF4E-dependent translation similarly to 4EBP1/2 (Poulin et al. 1998). In yeast, the 4EBP orthologues cap-associated factor 20 (Caf20) (Altmann et al. 1997) and the eIF4E-associated protein (Eap1) (Cosentino et al. 2000) both carry the conserved eIF4E binding motif (Dever et al. 2016), but regulate next to an overlapping set of transcripts also distinct mRNAs individually (Castelli et al. 2015). To conclude, in mammals it is generally accepted that the three homologs of 4EBP (1-3) have redundant molecular functions and mainly differ with regards to cell-type-specific expression levels (Sikalidis et al.

2013). The following paragraphs detail how the activity of 4EBPs is regulated and further describe the functions of active 4EBPs.

Table 1.1: Overview of the conservation of the two Raptor binding motifs RAIP and TOS/FEMDI, and the eIF4E binding motif YXXXXLφ between 4EBP homologs/orthologs from different species. *Amino acid residues that diverge from the conserved consensus sequences are depicted in red. Data retrieved from National Center for Biotechnology Information (NCBI). [1988] – [cited 2021 Sep 06]. Available from: https://www.ncbi.nlm.nih.gov/ (National Center for Biotechnology Information (NCBI)[Internet].; Altschul 1993)*

species	RAIP	YXXXXLφ	TOS
Human 4EBP1	RAIP	YDRKFLM	FEMDI
Human 4EBP2	RAIP	YDRKFLL	FEMDI
Human 4EBP3	CPIP	YDRKFLL	FEMDI
Mouse 4ebp1	RAIP	YDRKFLM	FEMDI
Mouse 4ebp2	RAIP	YDRKFLL	FEMDI
Mouse 4ebp3	CPIP	YDRKFLL	FEMDM
Zebrafish 4ebp1	QAIP	YDRKFLL	FEMDI
Zebrafish 4ebp2	RAIP	YDRKFLL	FEMDI
Zebrafish 4ebp3	CPIP	YDRKFLL	FEMDI
Drosophila 4ebp	QALP	YERAFMK	FQLDL
Yeast Eap1	-	YSMNELY	-
Yeast Caf20	-	YTIDELF	-

1.4.1. Regulation of expression and activity of 4EBPs

The activity of 4EBPs is post-translationally regulated through recognition and subsequent phosphorylation by mTORC1 (Gingras et al. 1998). As highlighted before, mTORC1 activity is inhibited by a wide range of cellular stress signals, including glucose deprivation (Saxton und Sabatini 2017). Logically, inhibition of mTORC1 results in loss of phosphorylation and thus activation of 4EBPs under these stress conditions. For 4EBP1, seven putative phosphorylation sites are known, of which at least four are coordinated by mTORC1. The threonine (T) residues 46, 37 and 70 are stepwise phosphorylated, followed by phosphorylation of serine (S) 65 (Averous und Proud 2006; Wang et al. 2005). Strikingly, phosphorylation of all four sites are needed for efficient release from eIF4E binding (Gingras et al. 2001). 4EBP1 is an intrinsically disordered protein that changes its conformation upon initial phosphorylation at residues T^{37} and T^{46}, which allows Raptor to access residues T^{70} and S^{65} for subsequent phosphorylation (Böhm et al. 2021), in turn abolishing the binding to eIF4E. In addition, other kinases besides mTOR have been found to be able to phosphorylate 4EBP, including the (mitogen activated kinase (MAPK)) extracellular signal regulated kinase (ERK) (Qin et al. 2016). Important for the phosphorylation and thus inhibition of 4EBPs is the recognition by mTORC1. The binding of

the mTORC1 component Raptor is guided by the 4EBPs RAIP and FEMDI motifs. For efficient recognition, both motifs are needed (Böhm et al. 2021). However, in 4EBP3, the N-terminal motif has one distinct residue compared to 4EBP1 or -2 (Cho et al. 2020; Böhm et al. 2021). This could suggest that the regulation of 4EBP3 underlies a slightly different recognition pattern as compared to 4EBP1/2.

Next to the post-translational regulation of 4EBPs, the expression of 4EBPs may be transcriptionally regulated, as few transcription factors including ATF4, ATF5 and HIF-1α have been identified to drive *EIF4EBP1* promoter activity and transcription in human cells upon ER stress or hypoxia, respectively *(Azar et al. 2013; Yamaguchi et al. 2008)*. In addition, members of the MYC family including c-MYC and MYCN, master regulators of transcription, were found to bind the promoter region of human *EIF4EBP1* and stimulate its transcription *(Balakumaran et al. 2009; Cheung et al. 2019; Hsu et al. 2016)*. This potentially positive regulation of *EIF4EBP1* expression by MYC proteins could have important clinical implications in cancer since *MYC and MYCN* are commonly amplified and overexpressed oncogenes in diverse types of human cancer. The effects of *EIF4EBP1* expression in cancer development will be reviewed in a later chapter. In addition, increased *EIF4EBP1* mRNA levels were detected in mice starved or fed with an insufficient composition of amino acids (Sikalidis et al. 2013; Jagoe et al. 2002). In *Drosophila*, amino acid-restricted diet induced a similar increase (Kang et al. 2017). Moreover, amino acid or serum starvation induced *EIF4EBP3* transcription in cell lines (Tsukumo et al. 2016). The same authors observed that *EIF4EBP3* expression is increased in mice upon therapeutic inhibition of mTOR. Taken together, these data highlight again the involvement of 4EBPs in the response to cellular stress.

1.4.2. Functions of 4EBPs

4EBPs were identified to control several molecular and cellular processes, which are briefly described in the following sections.

1.4.2.1. Regulation of mRNA translation

The lack of nutrient availability causes a decrease of the rate of overall protein biosynthesis, as this is the most energy consuming process occurring in cells (Lindqvist et al. 2018; Buttgereit und Brand 1995). Initiation of mRNA translation is the rate limiting step and the most complex segment of protein biosynthesis (Sonenberg und Hinnebusch 2009). In eukaryotes, the initiation process is often mediated by recognition of the 7-methyl-guanosine structure (or cap) located at the 5’ end of mRNA. For successful initiation of translation of these transcripts, recognition and binding of the cap by eIF4E is essential. Upon recognition of the cap structure by eIF4E, recruitment of the helicase eIF4A and the scaffolding protein eIF4G is initiated to form a protein complex (Sonenberg und Hinnebusch 2009). Together, the eIF4E/A/G complex,

abbreviated as eIF4F, recruits the ribosomal 43S pre-initiation complex to the mRNA to initiate translation of the respective transcripts (Gebauer und Hentze 2004). It is noteworthy that eIF4E is the least abundant protein of the translational initiation machinery and thus eIF4E availability dictates rates of formation of the initiation apparatus (Alain et al. 2012; Benedetti und Graff 2004). Translation of transcripts, which is being regulated through cap recognition and formation of the eIF4F complex is considered to be cap-dependent. Since most, if not all, mRNAs contain a 5' cap, this complex has a broad regulatory function in initiating mRNA translation (Hinnebusch et al. 2016).

4EBPs were shortly after their discovery identified to negatively control mRNA translation (Lin et al. 1994; Lawrence 1997; Sonenberg und Hinnebusch 2009). As the name suggests, eukaryotic initiation factor 4E binding proteins, 4EBPs bind to eIF4E, thereby preventing interaction between eIF4E and eIF4G and thus inhibiting the formation of the eIF4F complex (Hay und Sonenberg 2004). This leads to a global decrease of cap-dependent protein biosynthesis rates (Ma und Blenis 2009). The repressive regulators of translation 4EBPs compete with eIF4G for eIF4E binding, because of a shared conserved motif (YXXXLφ, mentioned above) with which they recognize eIF4E (Mader et al. 1995). Next to the consensus eIF4E binding motif YXXXLφ, both 4EBPs and eIF4G have secondary binding sequences for eIF4E that are less conserved and seem to regulate the difference in association and dissociation (Abiko et al. 2007; Umenaga et al. 2011; Igreja et al. 2014). While 4EBPs have an increased binding preference compared to eIF4G, the release from eIF4E is more rapid for the former compared to the latter protein. This means that 4EBPs are by default preset to both bind and release eIF4E rapidly upon cellular stimuli. The eIF4E/4EBP ratio determines the extent to which 4EBPs can block cap dependent translation as some eIF4E molecules can escape 4EBP binding and allow for eIF4F complex formation (Alain et al. 2012).

Next to inhibiting the overall cap-dependent translation initiation, 4EBPs were found to selectively block the translation initiation of specific mRNAs (Jin et al. 2020; Hsieh et al. 2012; Thoreen et al. 2012; Morita et al. 2013). This is not surprising as eIF4E has been shown to selectively promote translation initiation of specific mRNAs (Hinnebusch et al. 2016). However, it is not fully understood how the differential selectivity for certain transcripts is regulated. It has long been proposed that some mRNAs depend more than others on the eIF4F complex because their long and highly structured 5'UTR requires robust eIF4A-mediated helicase activity (Sonenberg und Hinnebusch 2009; Amorim et al. 2018; Svitkin et al. 2001). This assumption was in line with the oncogenic effect of eIF4E overexpression, as these mRNAs with long and complex 5'UTRs often code for growth-promoting proteins and their synthesis could thus be promoted by eIF4E (Pickering und Willis 2005). Active 4EBPs could therefore selectively exert an inhibition on the expression of these transcripts. However, this hypothesis has recently been challenged by studies that found mRNAs which are specifically regulated by

the mTORC1-4EBP-eIF4E axis possess specific motifs in their 5'UTR rather than a complex secondary structure (Thoreen et al. 2012; Pende et al. 2004). Two independent studies aimed to identify mRNAs translationally regulated by mTORC1 provided information about 4EBP-sensitive transcripts. Thoreen et al. inhibited the function of mTORC1 and analyzed the translatome by ribosome profiling, to identify the subset of transcripts specifically regulated by mTORC1 signaling. The mRNAs identified to be decreased upon mTORC1 suppression coded for proteins involved in protein biosynthesis, such as ribosomal proteins and elongation factors (Thoreen et al. 2012). In addition, prolonged mTOR inhibition restricts the rate of overall protein biosynthesis by suppressing mRNA translation of these protein synthesis transcripts. The authors further revealed a terminal oligopyrimidine (TOP) sequence to be a common motif for recognition of these mTORC1-sensitive genes. Strikingly, depletion of 4EBP1/2 abrogated the effect of mTORC1 inhibition on translation of TOP mRNAs (Thoreen et al. 2012), while this was not the case in S6K knockout cells (Pende et al. 2004). Therefore, the authors concluded that 4EBPs are mTORC1 downstream effectors responsible of controlling selective translation of TOP containing transcripts (Thoreen et al. 2012). Next to this study, Hsieh et al. similarly inhibited mTORC1 signaling to investigate which mRNAs are mTORC1-dependent and found a set enriched for pro-growth and invasion transcripts (Hsieh et al. 2012). Notably, they confirmed the TOP motif to determine sensitivity to mTORC1 signaling. In addition, they identified another sequence, the pyrimidine-rich translational element (PRTE), that together with the TOP motif defines around 90% of all mTORC1-sensitive transcripts (Hsieh et al. 2012). The translation of these mTORC1-dependent transcripts was proven to be regulated by 4EBPs (Hsieh et al. 2012). In addition, genome-wide translational profiling revealed no increased length or complexity of the 5'UTR of eIF4E/4EBP-dependent target transcripts compared to the whole genome (Truitt et al. 2015). With this approach Truitt et al. identified a common cytosine-enriched regulator of translation (CERT) motif in the 5'UTR of eIF4E-sensitive transcripts, which included mRNAs coding for antioxidant proteins (Truitt et al. 2015). This motif diverges from the TOP and PRTE motifs, however, another study confirmed the presence of different motifs underlying 4EBP-mediated repression of cap-dependent mRNA translation in *Drosophila* (Jin et al. 2020). The authors suggested that distinct motifs can control the extent of translational repression between distinct transcripts (Jin et al. 2020).

Next to cap-dependent mRNA translation, there are mechanisms of cap-independent mRNA translation. However, these are inefficient and represent only a minor fraction of actively translated mRNAs under basal conditions. Noteworthy, glucose deprivation can trigger a relative shift towards increased cap-independent mRNA translation (Khan et al. 2015; Fernandez et al. 2002; Gilbert et al. 2007). This shift could be mediated by 4EBPs blocking the eIF4F formation specifically, as has been shown for different stress conditions including hypoxia (Dennis et al. 2013; Braunstein et al. 2007; Svitkin et al. 2005). The blockage of eIF4F

assembly allows for free ribosomes and released eIF4G to associate with transcripts in a cap-independent fashion and use alternate routes to initiate translation. For instance, the presence of internal ribosome entry site (IRES) permits initiation of translation in the middle of a transcript (Komar und Hatzoglou 2011). Interestingly, transcripts that are involved in regulating cellular homeostasis and survival contain both a 5'UTR that guides cap-dependent mRNA translation initiation and an IRES allowing for cap-independent translation. Thus, while 4EBPs decrease the overall rate of protein biosynthesis under metabolic stress to spare ATP, translation of essential transcripts is maintained to promote cellular regeneration and survival or if needed apoptosis (Graber und Holcik 2007). In particular, transcripts, which translation is selectively stimulated by active 4EBPs in response to metabolic stress include HIF-1α and VEGF (Braunstein et al. 2007).

1.4.2.2. Mitochondrial activity and biogenesis

Mitochondrial-related metabolism processes are involved in both catabolism and anabolism, and TCA cycle intermediates are crucial in cellular signaling (Martínez-Reyes und Chandel 2020). Nutrient stress, such as glucose deprivation, reduces production of cellular ATP levels from both glycolysis and mitochondria. ATP production by mitochondria can facilitate the maintenance of energy levels under such unfavorable conditions, but for that to work, a tight regulation of mitochondria synthesis and activity is crucial. In addition, shutdown of highly energy-consuming processes, such as protein biosynthesis, needs to be reduced to a minimum to spare energy. Thus, signaling of mTORC1 may couple the availability of nutrients to mitochondrial activity, thereby controlling ATP generation to feed protein synthesis activity. Morita et al. found 4EBP activation to selectively inhibit the translation of transcripts encoding mitochondrial proteins (Morita et al. 2013). Consequently, 4EBPs restrict mitochondrial activity and revert mTORC1 promotion of glycolysis and mitochondrial respiration. In contrast, Zid et al. found 4EBPs to selectively upregulate translation of transcripts encoding mitochondrial proteins in Drosophila upon calorie restriction (Zid et al. 2009). The subsequent increase of mitochondrial activity, however, can lead to increased accumulation of ROS and mitochondrial dysfunctions. 4EBP1 was found to be essential in promoting the mitochondrial unfolded protein response and thus helps repairing mitochondria and protecting cells from proteotoxicity (Dastidar et al. 2020). Thus, 4EBPs not only facilitate adaptation of mitochondrial metabolism to certain stress stimuli but further maintain the proper function of mitochondria. This way, 4EBPs connect the stress signaled by mTOR to a translational response that mediates metabolic adaptation and promotes survival.

1.4.2.3. Cell growth

MTORC1 is a key promoter of anabolism and growth and a tight regulation of protein biosynthesis is essential for controlling cell growth (Kim und Guan 2019). Cellular growth can be subdivided into three classes: 1) proliferation, thus the multiplicative growth of cell numbers by division after completed cell cycle progression, 2) cell size, hence the enlargement of cellular volume without mitotic division, and 3) accretionary growth meaning the excretion of extracellular mass (Wolpert 2011). To date, no publications have aimed to investigate the role of 4EBPs in growth by accretion. Therefore, this section will focus on the effects of 4EBPs on proliferation and cell size.

Overexpression of eIF4E in mammalian cells was found to selectively increase the expression of mRNAs that are associated with proliferation and cell cycle progression (Rousseau et al. 1996b; Smith et al. 1990), suggesting that 4EBPs by negatively regulating their translation in turn restrict cell division. Conversely, knockdown of eIF4E, which resembles activation of 4EBPs, suppressed proliferation of ovarian cancer cells (Wan et al. 2015). In yeast, expression of a mutant eIF4E with reduced cap binding affinity resulted in cell cycle arrest (Brenner et al. 1988), suggesting that a functional eIF4E is needed for cell cycle progression. Paradoxically, the yeast 4EBP Caf20 was essential for entering the S-phase (Castelli et al. 2015). This could explain the reasons why yeast 4EBP-mutant cells have aberrant cell morphology and form bigger and rounder cells compared to their parental control (Ibrahimo et al. 2006). In *Drosophila*, genetic manipulation resulting in an unfunctional eIF4E protein caused growth arrest at early larval stage (Lachance et al. 2002). In line, therapeutic inhibition of mTOR and thus activation of 4EBPs inhibited both proliferation and cell cycle progression in mouse embryonic fibroblasts (MEFs), albeit to a lesser extent compared to eIF4E depletion combined with mTORC1 inhibition (Alain et al. 2012). Likewise, a constitutively active form of 4EBP1 was sufficient to block cell cycle progression in rat fibroblasts (Lynch et al. 2004). Overall protein biosynthesis and cell size were not affected in this study, highlighting that under nutrient rich conditions active 4EBPs prevent proliferation without impacting the rate of overall protein biosynthesis. Moreover, vascular injuries of muscles activated mTORC1 *in vivo*, which was followed by inactivation of 4EBP and, in parallel, expression of cell cycle proteins (Braun-Dullaeus et al. 2001), again emphasizing the necessity of blocking 4EBP to enable cell cycle progression. Fingar et al. claimed that 4EBPs are regulating both the proliferation rate and cell size of mammalian cells (Fingar et al. 2004; Fingar et al. 2002), however, their study revolved around measuring percentages of cells in specific cell cycle phases and did not measure proliferation or cell size directly. Similar to the results of these studies, forced expression of *Drosophila* 4EBP in fruit fly larvae resulted in reduced wing size, on account of both cell number and volume (Miron et al. 2001).

The effects of 4EBPs on cell size growth have been challenged. Dowling et al. found 4EBPs to control proliferation but not cell size (Dowling et al. 2010), contradicting the findings of Fingar et al. (Fingar et al. 2002). They argued that each of the mTOR effectors 4EBP and S6K are independently regulating proliferation and cell size separately in mammals, while in *Drosophila* either of the two growth processes were involved both mTOR effectors (Dowling et al. 2010). In mammalian cells, upon serum or amino acid starvation, or pharmacological inhibition of mTOR, 4EBP1/2 double knockout (DKO) cells failed to stop cell cycle progression, while in control 4EBP1/2 wild type cells this progression was blocked and proliferation prevented (Dowling et al. 2010). The underlying mechanism of 4EBPs regulation of cellular proliferation is by selective repression of translation of eIF4E-dependent pro-proliferative transcripts, such as ornithine decarboxylase (*ODC*) and cyclin D3 (Dowling et al. 2010).

To conclude, it becomes evident that active 4EBPs manage selective mRNA translation to regulate cell cycle progression, thereby tightly regulating proliferation rates. Their effect on cell size, however, is less clear and could be species specific. The role of 4EBPs to control proliferation or cell size under glucose starvation remains an open question.

1.4.2.4. Differentiation

Since 4EBPs are likely to coordinate cell cycle progression, it is tempting to assume that they also control cell differentiation, which typically requires tight control of the cell cycle (Soufi und Dalton 2016). MTORC1 signaling was found to steer neuronal differentiation by blocking 4EBPs activity (Hartman et al. 2013). Conversely, 4EBPs are crucial for maintaining the stemness of hematopoietic stem cells, by suppressing mRNA translation (Signer et al. 2016). Moreover, 4EBPs were found to maintain in T-cells in a quiescent state, ready to rapidly induce differentiation into effector cells through selective regulation of mRNA translation of metabolic transcripts (Ricciardi et al. 2018). Tahmasebi et al. confirmed 4EBPs to be crucial for the induction of pluripotency in MEFs. However, the authors delineated in detail that this is p53-dependent, as a combined loss of both the translational repressors 4EBP1/2 and p53 augmented the reprogramming into pluripotent stem cells (Tahmasebi et al. 2014). In conclusion, tight regulation of mRNA translation by the mTORC1-4EBP axis is a critical process for both differentiation or the induction and maintenance of stemness but is also dependent on the action of stemness factors and cell cycle proteins.

1.4.2.5. Physiological responses

The control of mRNA translation is critical to the organization of physiological responses, normal development, and diseases. This paragraph provides a brief overview of the role of 4EBPs in (patho)physiology. It is generally accepted that calorie restriction can increase

longevity in a variety of organisms including yeast, flies, mice and primates (Masoro 2000; Pifferi et al. 2018). In *Drosophila,* 4EBP was found to be activated upon nutrient restriction to decrease energy-consuming metabolic processes (Teleman et al. 2005). As a consequence, flies lacking 4EBP expression showed a significantly reduced survival under nutrient starvation (Teleman et al. 2005). Conversely, mTORC1 inactivation or 4EBPs activation sufficed to prevent the negative effects of obesity, including heart failure, caused by a high fat diet in *Drosophila* (Birse et al. 2010). These results underscore the importance of 4EBPs in regulating protein biosynthesis to cope with metabolic stress conditions. Knockdown of fatty acid synthase (so inhibition of fatty acid synthesis) similarly prevented obesity and heart dysfunction, hinting towards a potential role of mTORC1/4EBP in translationally controlling the balance between fat anabolism and catabolism. Zid et al. showed that expression of 4EBPs were needed to govern the response to caloric restriction by promoting selective translation of transcripts encoding mitochondrial proteins in *Drosophila* (Zid et al. 2009). Also in mice, 4EBP1 expression prevented obesity induced by a high fat diet, however, only in male rodents (Tsai et al. 2016; Le Bacquer et al. 2007). This suggests that 4EBPs act not only in a tissue-dependent but also in a sex-dependent manner. 4EBPs-mediated translational regulation also protected against aging-related obesity or muscle loss in mice and fly models (Tsai et al. 2015; Tsai et al. 2016; Demontis und Perrimon 2010). In *S. cerevisae,* inactivation of yeast 4EBPs Caf20 or Eap1 was associated with distorted responses to oxidative stress, nitrogen starvation and heat stress (Mascarenhas et al. 2008; Cridge et al. 2010; Cosentino et al. 2000). In an autism mouse model, knockdown of *eIF4EBP2* was found to cause autistic disorders by failed repression of eIF4E-dependent translation (Wiebe et al. 2019; Gkogkas et al. 2013). Upon neurovascular ischemia-reperfusion-stress, 4EBP1 and -2 were similarly activated to regulate protein synthesis (Ayuso et al. 2010). Le Bacquer et al. found that silencing 4EBP1/2 can prevent muscle degradation through regulation of protein biosynthesis (Le Bacquer et al. 2019). 4EBP1/2 DKO mice had significantly decreased FAO, suggesting that 4EBP1/2 function to translationally control metabolism (Le Bacquer et al. 2019). Paradoxically, in a kidney disease model, Holditch et al. found that overexpression of 4EBPs promoted proliferation and cyst formation, while deletion of 4EBPs suppressed proliferation (Holditch et al. 2019). This seems contradictory as 4EBPs are known to prevent eIF4E-dependent mRNA translation and proliferation. However, it cannot be ruled out that 4EBPs selectively repress translation of growth-suppressive transcripts and thus promote cyst formation and proliferation in this specific cellular context. Taken together, it becomes evident that 4EBPs are involved in a variety of physiological and pathophysiological processes. The effects of altered 4EBP signaling are heterogeneous but all processes have in common that the control of mRNA translation is perturbed, which eventually appears to affect the regulation of metabolic processes and the response to cellular stress.

1.4.2.6. The dual role of 4EBPs in cancer

One disease that must be considered distinctly is cancer. On the one hand, glucose deprivation is a pathological condition of macroscopic tumors and, on the other hand, the mTORC1-4EBP axis is critical for the control of proliferation and anabolic processes in cancer cells (Liu und Sabatini 2020). There are contradictory findings regarding the role of 4EBPs in tumorigenesis. Therefore, the following paragraphs give a deepened overview of the functions of 4EBPs on tumor outgrowth.

1.4.2.6.1. Tumor suppressive potential

The effects of eIF4E on cell transformation and carcinogenesis has been intensively reviewed (Bhat et al. 2015; Benedetti und Graff 2004; Graff et al. 2008; Averous und Proud 2006; Lazaris-Karatzas et al. 1990). All reviews present *eIF4E* as an oncogene involved in transformation, rapid tumor growth, invasion, and metastasis, and assume that sequestration of eIF4E by 4EBPs has a tumor suppressive effect. This is further underscored by studies aiming at reversing the effect of eIF4E-induced transformation. For instance, Rousseau et al. found that both 4EBP1 and 4EBP2 were able to reverse eIF4E-mediated transformation *in vitro* (Rousseau et al. 1996a). In addition, the earlier mentioned block of cell cycle progression mediated by active 4EBPs was associated to reduced transformation (Lynch et al. 2004). In a mouse model of Akt-driven lymphomagenesis, expression of constitutively active 4EBP1 (4EBP1 that escapes phosphorylation and thus inhibition by mTORC1) prevented tumor formation in about two thirds and significantly delayed tumor formation in the remaining third of mice (Hsieh et al. 2010). Likewise, in a mouse model of prostate cancer induced by phosphatase tensin homolog (PTEN) deficiency, non-phosphorylatable 4EBP1 inhibited carcinogenesis (Hsieh et al. 2015). Moreover, in a hepatocellular cancer mouse model, the expression of a constitutively active form of 4EBP1 sufficed to prevent carcinogenesis induced by overexpressed eIF4E signaling (Wang et al. 2015). Petroulakis et al. found DKO of 4EBP1/2 to decrease the survival time of tumor-bearing mice lacking functional p53 (Petroulakis et al. 2009). Also, in a mouse model of head and neck cancer, knockout of *4ebp1/2* expression significantly increased tumor growth (Wang et al. 2019). Conversely, inhibition of mTORC1 or forced expression of constitutively active 4EBPs prevented oncogenic growth in the same model. Genetically engineered mouse models lacking 4EBP1 expression did not develop tumors sporadically (Tsukiyama-Kohara et al. 2001). Thus, it becomes evident that 4EBPs are not classic tumor suppressors according to the traditional definition since neither 4EBP1 KO nor 4EBP1/2 DKO mice develop tumors over time.

In a cancer metastasis model, loss of 4EBP1 expression promoted cancer cell migration and metastasis to adjacent tissues by selective translation of transcripts involved in migration (Cai et al. 2014). During the development and outgrowth of malignant tumors, eIF4E-dependent

mRNA translation was associated to increased chances of tissue invasion and metastasis (Benedetti und Graff 2004). 4EBP was found to selectively block the translation of pro-invasive genes (Hsieh et al. 2012), and thus it is not surprising that in mouse models, eIF4E promoted metastasis while genetic or therapeutic inactivation of eIF4E established resistance to breast cancer-derived lung metastasis (Robichaud et al. 2015; Pettersson et al. 2015). Conversely, the release of eIF4E inhibition by short-hairpin mediated knockdown of 4EBP1 promoted liver metastasis in murine models (Cai et al. 2014). Summing up, 4EBP1 may act as a suppressor of tumor invasion and metastasis *in vivo*.

In human tumor samples, reduced 4EBP1 expression was found to correlate with poor survival in lung cancer patients (Seki et al. 2010). However, most studies put their focus on 4EBP activity (i.e. phosphorylation), rather than expression. Elevated levels of phospho-4EBP1 have been frequently reported in cancer including prostate, gastric, ovarian, renal, and head and neck tumors (Graff et al. 2008; Lee et al. 2018; Alabdullah et al. 2019; Zhang et al. 2018; Qu et al. 2016; Huang et al. 2019). This apparent inactivation of 4EBP1 has been associated to poor patient outcomes in some of these cancer types. However, these studies neglected the chance that the increased levels of phospho-4EBP1 may be due to an increased total pool of 4EBP1 proteins. Thus, measuring high phospho-4EBP1 levels in tumor tissues does not necessarily mean that 4EBP1 is inactive in these tissues. Moreover, it has been shown that eIF4E is the limiting factor of the eIF4F complex and thus the ratio of eIF4E/4EBPs determines the competition between 4EBPs and eIF4G (Alain et al. 2012). Therefore, future research should focus on analyzing both the total and the phosphorylated fraction of 4EBPs and the level of eIF4E in human tumor samples, which can improve the understanding of the dynamic situation between eIF4E and their sequestration by 4EBPs in cancer.

1.4.2.6.2. Tumorigenic potential

Next to the tumor suppressive functions attributed to 4EBPs, there is accumulating evidence for a pro-oncogenic function. 4EBP1 was found to be overexpressed in a range of cancer entities. For instance, the common 8p11.12 amplicon in breast cancer causes amplification of *EIF4EBP1.* Moreover, the expression of *EIF4EBP1* was found to be elevated in prostate cancer (Hsieh et al. 2015; Ding et al. 2018), colorectal cancer (Chao et al. 2015), renal cell carcinoma (Schultz et al. 2011) and breast cancer (Karlsson et al. 2013; Karlsson et al. 2011; Rutkovsky et al. 2019). In all these cancers, increased expression was associated with a more aggressive and/or therapy-resistant tumor. Moreover, a recent study representing an extensive *The Cancer Genome Atlas* (TCGA) data analysis showed that increased *EIF4EBP1* expression significantly predicts poor patient survival in all TCGA cancer entities combined (Wu und Wagner 2021). In the same study, multivariate analysis highlighted high *EIF4EBP1*

expression to be a stronger determinant for decreased chances of survival in patients compared to high *eIF4E* or even high *MYC* levels. This suggests *EIF4EBP1* expression as a strong predictor of poor survival in human cancer.

MEFs lacking 4EBP1/2 expression, while p53 is functioning, are able to resist oncogene-induced transformation by premature senescence (Petroulakis et al. 2009). The same study found that injection of oncogenic RAS expressing 4EBP1/2 DKO MEFs into nude mice did not result in tumor formation (Petroulakis et al. 2009). Hsieh et al. reported that the abundance of 4EBPs facilitates resistance against drugs targeting the PI3K/Akt/mTOR pathway in prostate cancer, (Hsieh et al. 2015). In addition, 4EBPs were found to be crucial for cancer cell survival under hypoxia, as loss of their expression resulted in tumors with increased sensitivity to both hypoxia and radiation (Dubois et al. 2009). In line, Braunstein et al. described in detail a mechanism by which 4EBPs are activated by hypoxia in a breast cancer model to promote selective translation of HIF-1α and VEGF, which support angiogenesis, survival under hypoxia and growth of tumor xenografts (Braunstein et al. 2007). Ding et al. showed that 4EBP1/2 on the one hand reduced tumor growth of prostate cancer, but on the other hand improved survival under hypoxia, likely by inhibiting protein biosynthesis and pushing selective translation of transcripts involved in the stress/hypoxia response (Ding et al. 2018). This is in line with the characterization of 4EBPs as a 'metabolic break' (Teleman et al. 2005) and highlights that the ambivalent role of 4EBPs between a tumor-suppressive and a pro-oncogenic effector is determined by the microenvironmental context, i.e. the abundance of nutrients. This means that while in the earlier phases of tumorigenesis rapid growth and thus mTOR-steered protein biosynthesis gives the cancer cells an advantage to outcompete adjacent healthy cells, at later stages of the tumor development, nutrient and oxygen scarcity could activate 4EBP-mediated translational regulation to function as a parachute under unfavorable conditions.

1.5. Aims of this thesis

The comprehension of how cells adapt their metabolism towards glucose starvation improved intensively, yet the specific targets driving and orchestrating such a biological adaptation are still not well defined. A rapid and effective means for cellular metabolism to adapt to such conditions is by translational regulation. Indeed, many cellular processes were shown to be translationally regulated by 4EBPs, yet many questions remain unanswered. The work summarized in this thesis aimed at answering the question whether 4EBPs protect cells under glucose starvation. When considering the functions reported for 4EBPs, there is evidence that 4EBPs can act as a metabolic break to ensure survival of *Drosophila* under dietary restriction. Thus, it is likely that 4EBPs function similarly upon glucose removal. Assuming that 4EBPs protect glucose-deprived cells, a better understanding of how they can translationally adapt

the metabolism of cells to cope with glucose starvation would be highly desirable. Furthermore, the question should be answered whether this function is conserved throughout evolution. Also, while it is widely accepted that under nutrient-rich conditions 4EBPs are phosphorylated and inactive, it is not known whether a fraction of 4EBPs can escape mTORC1-mediated phosphorylation and exert activity under basal conditions. This may particularly be important in cancers with increased *EIF4EBP1*/4EBP1 expression. Therefore, **paper 1** aimed at answering the question whether 4EBPs are active under optimal growth conditions, i.e. when mTORC1 is active. It was found that a pool of 4EBP1/2 molecules can escape the inactivation by mTORC1 and selectively regulates translation of specific transcripts. Next, the function of 4EBPs under glucose starvation was studied. Glucose deprivation causes depletion of ATP and antioxidant power. Therefore, it is crucial for a cell to rewire its metabolism accordingly to the reduction in glucose availability in order to prevent cell death. Since the translational repressors 4EBPs were shown to be activated as metabolic brakes under serum starvation, amino acid starvation or pharmacological inhibition of mTOR, the question should be clarified whether glucose deprivation could similarly activate 4EBPs to ensure cell survival. Thus, **manuscript 2** hypothesized that tight control of mRNA translation by 4EBPs may be essential in coping with the energy and redox stress triggered by low glucose levels. To this end, it could be elucidated that 4EBPs are essential to translationally regulate fatty acid synthesis, in turn maintaining the redox balance to protect cells under glucose starvation. Moreover, 4EBPs were characterized as protective regulators that are conserved in *S. cerevisae* to gain a survival advantage within glucose-deprived microenvironments. Finally, **manuscript 3** aimed to decipher the clinical relevance of 4EBP1 expression and its regulation in cancer tissues. A cancer entity that often faces nutrient unfavorable conditions during tumorigenesis is neuroblastoma (NB). This malignancy is the most common solid tumor in children with a mortality rate of 15% (Colon und Chung 2011). The expression of *EIF4EBP1* mRNA was significantly elevated in NB tumors as compared to normal adrenal control tissues, and increased expression of *EIF4EBP1*/4EBP1 was significantly associated with poor patient survival. Furthermore, overexpression of MYCN, which frequently drives aggressive NB, can directly upregulate *EIF4EBP1* promoter activity and transcription. The results summarized here are critically evaluated in subsequent discussion. Altogether, this thesis presents 4EBPs as translational regulators of metabolism exerting a protective function under glucose deprivation. This function is evolutionarily conserved as shown in budding yeast. Moreover, since *EIF4EBP1* is frequently overexpressed in cancer, the survival-supportive role of 4EBPs under low glucose likely plays a major role in cancer regions with impaired nutrient supply and may thereby drive tumor progression and aggressive clinical behavior.

2. Paper 1 – 4EBP1/2 are active under standard cell culture conditions to regulate the translation of specific mRNAs

Alasad et al. Cell Death and Disease (2020) 11:968
https://doi.org/10.1038/s41419-020-03182-6

Cell Death & Disease

COMMENT Open Access

4EBP1/2 are active under standard cell culture conditions to regulate the translation of speci c mRNAs

Khawla Alasad[1], Kai Voeltzke[2], Liron Levin[3], Guido Reifenberger[2,4], Gabriel Leprivier[2] and Barak Rotblat[1,3]

The mammalian target of rapamycin (mTOR) kinase is a nutrient sensor coordinating cellular anabolic and catabolic processes[1]. During favourable metabolic conditions, mTOR promotes protein synthesis by phosphorylating its substrates, including eIF4E binding proteins 1-3 (4EBP1-3). Upon conditions where mTOR is inactive, the hypo-phosphorylated and active 4EBPs bind to eukaryotic initiation factor 4E (eIF4E), competing with the recruitment of eIF4G thus disrupting the formation of the eIF4F complex, in turn leading to inhibition of cap-dependent translation initiation[2].

It is not known whether 4EBPs regulate mRNA translation in optimal growth conditions, in which mTOR is active and 4EBPs thus phosphorylated and presumed to be inactive. This question is particularly relevant in pathological and physiological conditions where the expression of 4EBPs are up- or down-regulated while mTOR is active.

To assess the activity of 4EBP1/2 under basal cell culture conditions, we used lysates of 4EBP1/2 knockdown (KD) and control scramble shRNA (shSCR) HEK293 cells[3] to pull down eIF4E and its interacting proteins using m^7GTP-agarose beads (Fig. 1a). We found more eIF4G bound to eIF4E in KD lysates as compared to shSCR cell lysates (Fig. 1a). This finding was confirmed using 4EBP1/2WT and double KO (DKO) $p53^{-/-}$ MEFs[3] (Fig. 1a), suggesting that an active cellular fraction of 4EBPs is detectable in optimal cell culture conditions, even in the presence of active mTOR.

However, we did not find a statistically significant effect of the active 4EBPs fraction on overall protein synthesis using AHA labelling[4] under basal conditions, although there was a trend towards increased protein synthesis in DKO cells (Fig. S1a). Nevertheless, using a bicistronic reporter vector in which Renilla luciferase (Rluc) is translated in a cap-dependent manner, while Firefly luciferase (Fluc) is translated in a cap-independent manner (Fig. 1b)[5], we found that KD cells exhibited a significantly higher Rluc/Fluc ratio as compared to controls (Fig. 1b). These data suggest that while 4EBP1/2 restrict cap-dependent translation in normal cell culture conditions, this has minimal impact on overall protein synthesis, pointing to a selective regulation of mRNA translation.

We then identified transcripts whose translation is selectively influenced by 4EBP1/2 under basal conditions, by performing polysome profiling using a non-linear sucrose gradient (the Larsson protocol)[6] (Fig. 1c). Total and polysomal mRNA, obtained from KD and shSCR cells, were identified and quantified by RNAseq. Analysis of total mRNA expression showed that only 26 genes were differentially expressed between KD and shSCR cells (Fig. S1b and Supplementary Table 1). We calculated the translation efficiency (TE) of each mRNA as the ratio between polysomal and total mRNA levels in KD and shSCR samples (Fig. S1c) and found 516 transcripts with lower TE in KD cells (cluster #1) and 569 transcripts whose translation was increased in KD cells (cluster #2) (Supplementary Table 1). KEGG analysis of transcripts whose TE was affected by 4EBP1/2 identified pathways previously linked to 4EBP1/2 functions including ribosomes, oxidative phosphorylation, metabolic pathways and neurodegeneration (Fig. S1d)[3,7,8]. Overall, these data show that 4EBP1/2 selectively affect the translatome in normal cell culture conditions.

Correspondence: Barak Rotblat (rotblat@bgu.ac.il)
[1]Department of Life Sciences, Ben-Gurion University of the Negev, Beer Sheva, Israel
[2]Institute of Neuropathology, Medical Faculty, University Hospital Düsseldorf, Düsseldorf, Germany
Full list of author information is available at the end of the article

SPRINGER NATURE
CDDpress

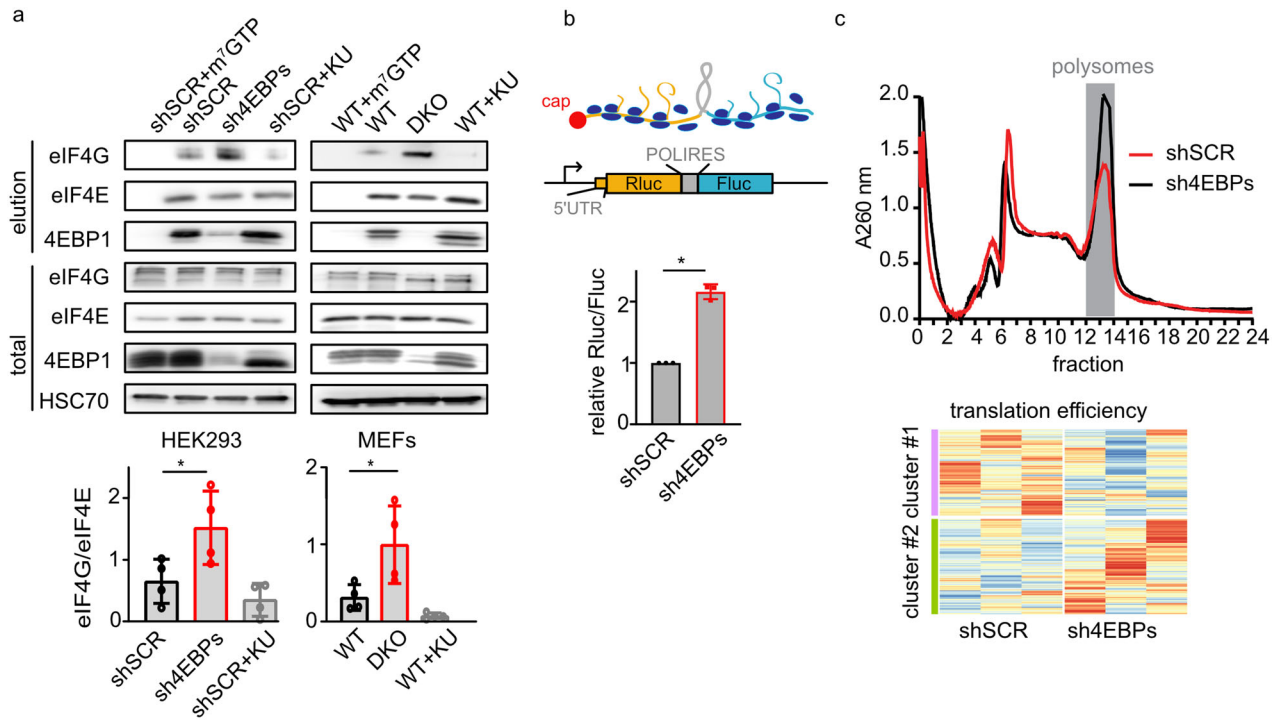

Fig. 1 Detection of an active 4EBP1/2 pool under basal conditions. a The indicated cells were grown in normal cell culture media, treated or not with 1 μM of the mTOR inhibitor KU-0063794 (KU) for 4h, were lysed and incubated with m^7GTP coated beads. When indicated, cell lysates were pre-incubated with free m^7GTP (shSCR+m^7GTP) to detect nonspecific binding. Eluted and total proteins were analyzed by immunoblot using the indicated antibodies. Protein levels of m^7GTP bound eIF4G and eIF4E were quantified using ImageJ and presented in a bar graph; *p <0.05. b Scheme of the bicistronic Luciferase reporter; Rluc is driven by cap-dependent mRNA translation through an artificial 5′UTR, Fluc is produced by cap-independent mRNA translation through a poliovirus IRES (POLIRES). HEK293 shSCR and sh4EBP stransfected with pcDNA3-RLUC-POLIRES-FLUC bicistronic vector were grown in normal media. 24h post-transfection, cells were lysed and levels of Rluc and Fluc were sequentially measured. Results are expressed as Rluc/FLuc ratio (n = 3 biologically independent experiments). Data are reported as means± SD with indicated significance (*p <0.05). c HEK293 shSCR and sh4EBPs cells were lysed, separated on non-linear sucrose gradients and polysome profiles were generated by measuring absorbance at 260 nm. Polysomal fractions, highlighted in grey, were collected together with total mRNA. mRNA was then extracted and sequenced. Heat map representation of transcripts whose TE is significantly different between the HEK293 shSCR and sh4EBPs cells, highlighting the three biological replicates.

Acknowledgements
This research was supported by the Israel Science Foundation (grant No. 1436/19), by the Israeli Cancer Association (grant #20180012) and the NIBN. G.L. is supported by the Deutsche Forschungsgemeinschaft (LE 3751/2-1), the German Cancer Aid (70112624) and the Elterninitiative Kinderkrebsklinik.

Author details
[1]Department of Life Sciences, Ben-Gurion University of the Negev, Beer Sheva, Israel. [2]Institute of Neuropathology, Medical Faculty, University Hospital Düsseldorf, Düsseldorf, Germany. [3]The National Institute for Biotechnology in the Negev, Beer Sheva, Israel. [4]German Cancer Consortium (DKTK), partner site Essen/Düsseldorf, Düsseldorf, Germany

Con ict of interest
The authors declare that they have no conflict of interest.

Publisher's note
Springer Nature remains neutral with regard to jurisdictional claims in published maps and institutional affiliations.

Supplementary Information accompanies this paper at (https://doi.org/10.1038/s41419-020-03182-6).

Received: 27 July 2020 Revised: 9 October 2020 Accepted: 13 October 2020
Published online: 11 November 2020

References

1. Kim, J. & Guan, K.-L. mTOR as a central hub of nutrient signalling and cell growth. Nat. Cell Biol. 21,63 –71 (2019).
2. Haghighat, A., Mader, S., Pause, A. & Sonenberg, N. Repression of cap-dependent translation by 4E-binding protein 1: competition with p220 for binding to eukaryotic initiation factor-4E. EMBO J. 14, 5701–5709 (1995).
3. Dowling, R. R. J. O. et al. mTORC1-mediated cell proliferation, but not cell growth, controlled by the 4E-BPs. Science 328,1172–1177 (2010).
4. Marciano, R., Leprivier, G. & Rotblat, B. Puromycin labeling does not allow protein synthesis to be measured in energy-starved cells correspondence. Cell Death Dis. https://doi.org/10.1038/s41419-017-0056-x (2018).
5. Tsukumo, Y., Sonenberg, N. & Alain, T. Transcriptional induction of 4E-BP3 prolongs translation repression. Cell Cycle 0,1–2(2016).
6. Liang, S. et al. Polysome-profiling in small tissue samples. Nucleic Acids Res 46, 1–13 (2017).
7. Thoreen, C. C. et al. A unifying model for mTORC1-mediated regulation of mRNA translation. Nature 485, 109–113 (2012).
8. Hsieh, A. C. et al. The translational landscape of mTOR signalling steers cancer initiation and metastasis. Nature 485,55 –61 (2012).

3. Manuscript 2 – 4EBP1/2 support cell survival under metabolic stress by translationally regulating fatty acid synthesis

4EBP1/2 support cell survival under metabolic stress by translationally regulating fatty acid synthesis

Tal Levy[1,2*], Kai Voeltzke[3*], Laura Hauffe[3*], Khawla Alasad[1,2*], Marteinn Snaebjörnsson[4], Ran Marciano[1,2], Katerina Scharov[3,5], Melanie Planque[6], Kim Vriens[6], Stefan Christen[6], Christina Hassiepen[3], Alisa Kahler[3], Beate Heider[3], Daniel Picard[3,5,7], Katja Bendrin[8], Andres Vargas-Toscano[9], Ulf Kahlert[9], Christiane Knobbe-Thomsen[3], Marc Remke[3,5,7], Moshe Elkabets[10,11], Thomas GP Grünewald[12,13,14,15], Andreas Reichert[8], Sarah-Maria Fendt[6], Almut Schulze[4], Guido Reifenberger[3], Barak Rotblat[1,2#], Gabriel Leprivier[3#]

[1]The National Institute for Biotechnology in the Negev, Ben-Gurion University of the Negev, Beer Sheva 84105, Israel.

[2]Department of Life Sciences, Faculty of Life Science, Ben-Gurion University of the Negev, Beer-Sheva 84105, Israel.

[3]Institute of Neuropathology, Heinrich Heine University, Medical Faculty, Düsseldorf, Germany.

[4]Biochemistry and Molecular Biology, Theodor-Boveri-Institute, Biocenter, Am Hubland, 97074 Würzburg, Germany; Division of Tumor Metabolism and Microenvironment, German Cancer Research Center, Im Neuenheimer Feld 581, 69120 Heidelberg, Germany.

[5]Department of Pediatric Oncology, Hematology, and Clinical Immunology, Medical Faculty, Heinrich Heine University, Düsseldorf, Germany.

[6]Laboratory of Cellular Metabolism and Metabolic Regulation, VIB-KU Leuven Center for Cancer Biology, VIB, Leuven, Belgium; Laboratory of Cellular Metabolism and Metabolic Regulation, Department of Oncology, KU Leuven and Leuven Cancer Institute (LKI), Leuven, Belgium.

[7]German cancer consortium (DKTK) partner site Essen/Düsseldorf, Munich, Germany.

[8]Institute for Biochemistry and Molecular Biology I, Medical Faculty, Heinrich-Heine University Düsseldorf, Germany

[9]Clinic for Neurosurgery, Medical Faculty Heinrich-Heine University, Moorenstrasse 5, 40225, Duesseldorf, Germany.

[10]The Shraga Segal Department of Microbiology, Immunology and Genetics, Faculty of Health Science, Ben-Gurion University of the Negev, Beer-Sheva 84105, Israel.

[11]Faculty of Health Sciences, Ben-Gurion University of the Negev, Beer-Sheva 84105, Israel.

[12]Max-Eder Research Group for Pediatric Sarcoma Biology, Institute of Pathology, Faculty of Medicine, LMU Munich, Munich, Germany.

[13]Division of Translational Pediatric Sarcoma Research, German Cancer Research Center (DKFZ), Heidelberg, Germany.

[14]Hopp Children's Cancer Center (KiTZ), Heidelberg, Germany.

[15]Institute of Pathology, Heidelberg University Hospital, Heidelberg, Germany.

*These authors contributed equally

Key words: nutrient stress response, 4EBP1, mRNA translation, tumorigenesis

[#]**Corresponding authors:**

Dr. Barak Rotblat, Department of Life Sciences, Faculty of Life Science and The National Institute for Biotechnology in the Negev, Ben-Gurion University of the Negev, Beer Sheva 84105, Israel; E-mail: rotblat@bgu.ac.il.

Dr. Gabriel Leprivier, Institute of Neuropathology, Heinrich Heine University Düsseldorf, Moorenstrasse 5, D-40225 Düsseldorf, Germany; E-mail: gabriel.leprivier@med.uni-duesseldorf.de.

SUMMARY

Metabolic stress compels cells to evolve adaptive mechanisms to maintain homeostasis. The regulation of such cellular response is not well understood. Here, we found that eukaryotic initiation factor 4E binding proteins 1/2 (4EBP1/2) are essential to promote the survival of mammalian cells and budding yeast under glucose starvation. 4EBP1/2 block fatty acid synthesis, sparing NADPH and in turn preserving intracellular redox balance upon energy stress via 4EBP1/2-mediated inhibition of *Acetyl-CoA Carboxylase Alpha* (*ACACA*) mRNA translation. This has important relevance in cancers, as we uncovered that oncogenically transformed cells and glioma cells exploit 4EBP1/2 regulation of *ACACA* and redox balance to combat metabolic stress, thereby supporting transformation and tumorigenicity. Clinically, high *eIF4EBP1* expression (4EBP1 gene) is associated with poor outcome in several cancers, including glioma. Our data reveal that 4EBP1/2 are conserved mediators of the survival response to metabolic stress by translationally controlling fatty acid synthesis.

INTRODUCTION

Glucose is one of the most important nutrients for living organisms. Lack of glucose has a profound biological impact on cell fate. Therefore, in order to adapt to glucose deprivation, cells have evolved highly coordinated and conserved metabolic responses. When glucose levels drop, anabolic processes, such as protein synthesis and fatty acid synthesis, are inhibited while catabolic processes, such as autophagy and fatty acid oxidation, are activated. Together, these responses preserve energetic and redox balances, thus maintaining cellular homeostasis (Caro-Maldonado, 2011). A well-characterized pathological condition of glucose deprivation occurs in cancer (Warburg, 1956). Cancer cells growing within solid tumors are experiencing glucose deprivation due high glucose consumption combined with defects in tumor vasculature (Nagy et al., 2009; Warburg, 1956). While such stress condition initially restricts cell division and induces cell death in some instances, it may on the long-term drive adaptation and emergence of more highly tumorigenic and chemo-resistant cancer clones (Flavahan et al., 2013; Jones and Thompson, 2009). Furthermore, similarly to glucose deprivation, matrix detachment triggers energy stress characterized by ATP depletion and elevated reactive oxygen species (Schafer et al., 2009). Mechanisms promoting cell survival under matrix detachment, a hallmark of transformation and tumorigenicity, are also supporting cancer cell adaptation to glucose deprivation (Jeon et al., 2012). It is therefore important to delineate the mechanisms underlying metabolic adaptation to glucose deprivation.

Protein synthesis, as the most highly energy consuming cellular process (Buttgereit and Brand, 1995), is tuned to cellular energetics. While this process is inhibited under energy stress, failure to do so leads to cell death in both normal and tumor cells, in part due to ATP depletion (Choo et al., 2010; Leprivier et al., 2013; Ng et al., 2012). Protein synthesis is regulated at both the initiation and elongation steps by key evolutionary conserved signaling pathways that sense cellular metabolic state (Leibovitch and Topisirovic, 2018; Leprivier et al., 2015). One major cellular energetics sensor is AMP-activated protein kinase (AMPK), which is allosterically activated when intracellular AMP:ATP or ADP:ATP ratios raise (Trefts and Shaw, 2021). In response to glucose deprivation, AMPK inhibits mRNA translation elongation

by activating eukaryotic translation elongation factor 2 kinase (eEF2K) (Horman et al., 2002), which in turn phosphorylates and inactivates the translation elongation factor eEF2 (Ryazanov et al., 1988). EEF2K-mediated inhibition of mRNA translation elongation is essential for survival of normal and tumor cells during nutrient starvation, a function that is conserved in *C. elegans* (Leprivier et al., 2013). Importantly, the expression and activity of eEF2K was found to be increased in numerous cancers (Leprivier et al., 2013), altogether supporting the notion that negative regulators of mRNA translation have evolved to promote cell survival during energetic stress and are hijacked by cancer cells to mediate metabolic adaptation.

Another key regulator of protein synthesis is the nutrient sensing kinase complex mechanistic target of rapamycin complex 1 (mTORC1), which couples the rate of mRNA translation initiation to glucose availability (Leprivier and Rotblat, 2020; Orozco et al., 2020). In keeping with the notion raised above, mTORC1 inhibition is required to preserve viability of normal and cancer cells under glucose starvation (Choo et al., 2010; Inoki et al., 2003). When glucose is abundant, mTORC1 is active and promotes mRNA translation initiation by phosphorylating and activating 70-kDa ribosomal protein S6 kinase (p70S6K) and inhibiting the eukaryotic initiation factor 4E binding protein 1-3 (4EBP-1/-2/-3). During glucose deprivation mTORC1 is inhibited, in turn releasing 4EBP-1/-2/-3 from inhibition, which leads to inhibition of mRNA translation initiation (Liu and Sabatini, 2020; Valvezan and Manning, 2019).

4EBP-1/-2/-3 (4EBPs) are major repressors of protein synthesis regulated by glucose levels (Pause et al., 1994; Poulin et al., 1998), and thus may represent underappreciated regulators of the cellular and metabolic response to glucose starvation. In response to various stresses, 4EBPs inhibit mRNA translation initiation by binding eukaryotic initiation factor 4E (eIF4E) to prevent the formation of the eIF4E-containg pre-initiation complex required for cap-dependent mRNA translation (Silvera et al., 2010; Truitt and Ruggero, 2016). Initially, 4EBPs was thought to exert a general inhibitory effect on the rate of protein synthesis (Sonenberg and Hinnebusch, 2009). However, recent findings highlight that 4EBPs exert a selective regulatory function on mRNA translation, by preferentially blocking the translation of a subset of transcripts (Dowling et al., 2010; Hsieh et al., 2012; Morita et al., 2013; Thoreen et al., 2012).

This allows 4EBPs to inhibit the activity of specific cellular processes, such as cellular proliferation, mitochondrial activity and tumor cell invasion (Dowling et al., 2010; Hsieh et al., 2012; Morita et al., 2013; Thoreen et al., 2012). Whether these processes are controlled by 4EBPs in response to glucose starvation is unknown. 4EBP was shown to promote survival of Drosophila larva under nutrient starvation (Teleman et al., 2005; Tettweiler et al., 2005; Zid et al., 2009), nevertheless, the cellular functions of 4EBPs in eukaryotic cells challenged by energetic stress are not known. In addition, the functions of 4EBPs in cancer are still under debate (Musa et al., 2016). On one hand, numerous reports support a tumor suppressive function of 4EBPs, as 4EBP1/2 double knock out leads to reduced tumor-free survival of p53-/- mice (Petroulakis et al., 2009) and accelerates tumor development in genetically engineered mouse models of head and neck squamous cell carcinoma and prostate cancer (Ding et al., 2018; Wang et al., 2019). On the other hand, 4EBPs were shown to exert a pro-tumorigenic function by mediating oncogenic RAS transformation (Petroulakis et al., 2009) and supporting breast cancer progression in vivo through promoting angiogenesis (Braunstein et al., 2007).

Here, we found that 4EBP1/2 are fundamental regulators of the cellular and metabolic response to glucose starvation, conserved in yeast, mouse and human. Mechanistically, 4EBP1/2 curb fatty acid synthesis in response to glucose starvation by selectively repressing the translation of acetyl-CoA carboxylase 1 (ACC1) mRNA. This allows preserving NADPH levels, which are normally consumed by fatty acid synthesis, and thus prevents oxidative stress and cell death during glucose starvation. Furthermore, we report that 4EBP1/2 regulation of ACC1 is exploited by cancer and transformed cells to survive in anchorage-independent conditions and grow tumors *in vivo*. Finally, we reveal that 4EBP1 expression has clinical relevance in multiple cancers and is functional in glioma to promote tumor growth and aggressiveness, altogether highlighting a pro-tumorigenic function for the mRNA translation inhibitor 4EBP1.

RESULTS

4EBP1/2 promote cell survival under glucose deprivation by controlling mRNA translation

We investigated the functions of 4EBPs in the cellular response to glucose starvation. To do so, we used cells deficient for 4EBP activity, such as 4EBP1/2 double knock out (DKO) mouse embryonic fibroblasts (MEFs) or stable 4EBP1/2 knock down (kd) (sh4EBP1/2) HEK293 cells (Dowling et al., 2010). We assessed the impact of 4EBP1/2 depletion on cell survival during glucose starvation. Glucose starvation led to massive cell death of 4EBP1/2 DKO MEFs or sh4EBP1/2 HEK293 cells compared to the respective control counterparts (WT and shScr, respectively), which was not the case in basal conditions (Fig. 1A&B). This was confirmed in other cell lines of different origins, including induced pluripotent stem cells (iPSC), glioblastoma U-87 MG cells, breast cancer MCF7 cells, and neuroblastoma cells. In these cells, stable kd of both 4EBP1 and 4EBP2, or of 4EBP1 alone, severely restricted survival under glucose deprivation (Fig. S1A-E). Conversely, overexpression of a constitutively active 4EBP1 mutant, 4EBP1 (T37A/T46A) (4EBP1^{AA}), was sufficient to protect glucose withdrawal-sensitive HeLa cells against induction of cell death under glucose-deprived conditions (Fig. 1C). In sharp contrast, manipulating 4EBP1/2 expression levels had no impact on the rates of cell death triggered by amino acid starvation (Fig. 1A-C), pointing towards a specific role of 4EBP1/2 in the response to glucose starvation.

We next determined the cellular processes involved in mediating 4EBP1/2 protective function under glucose starvation. We first tested whether this was due to 4EBP1/2 control of cell proliferation, as reported upon serum starvation (Dowling et al., 2010). Unexpectedly, while the rate of proliferation was severely reduced following 24 hrs glucose deprivation, there was no difference between WT and 4EBP1/2 DKO MEFs, nor between shScr and sh4EBP1/2 HEK293 cells under these conditions (Fig. 1D&E). In addition, we found no evidence that autophagy was responsible for the observed function of 4EBP1/2, as rates of autophagy were similar in control and 4EBP1/2 deficient MEFs and HEK293 cells under glucose starvation (Fig. S1F&G).

Since 4EBP1/2 are major repressors of mRNA translation initiation, we examined the contribution of mRNA translation activity to 4EBP1/2 protective function under glucose starvation. Pharmacological inhibition of protein synthesis, using cycloheximide (CHX), fully rescued 4EBP1/2 deficient MEFs and HEK293 cells from glucose starvation-induced cell death (Fig. 1F&G) and significantly reduced cell death in sh4EBP1 MCF7 cells (Fig. S1C). This suggests that uncontrolled protein synthesis contributes to glucose starvation-induced cell death observed in cells lacking 4EBP1/2. Unexpectedly, we measured similar rates of overall protein synthesis under glucose starvation in control and 4EBP1/2 deficient MEFs and HEK293 cells using AHA labeling and Click Chemistry (Marciano et al., 2018) (Fig. 1H&I). In contrast, 4EBP1/2 deficient cells showed high rates of global protein synthesis vs. control cells upon pharmacological inhibition of mTORC1 (using KU-0063794) (Fig. S1H), suggesting that 4EBPs protective function under glucose starvation is independent from inhibiting total protein synthesis. Putting our data together suggests that selective, rather than global, regulation of mRNA translation by 4EBP1/2 promotes cell viability under glucose deprivation.

Given that 4EBP1/2 function by binding to eIF4E to selectively repress the translation of a subset of transcripts (Dowling et al., 2010; Hsieh et al., 2012; Morita et al., 2013; Thoreen et al., 2012), we tested the involvement of eIF4E in the protective function of 4EBP1/2. Knock down of eIF4E in both 4EBP1/2 DKO MEFs and sh4EBP1/2 HEK293 cells led to a significant reduction of cell death under glucose starvation (Fig. 1J&K). In addition, forced expression of an eIF4E- non-binding mutant of 4EBP1^{AA}, 4EBP1 (Y54A/L59A) (4EBP1$^{AA, YL}$; REF), failed to prevent cell death of HeLa cells upon glucose depletion, in contrast to 4EBP1^{AA} (Fig. 1L), indicating that binding of 4EBP1/2 to eIF4E is required for 4EBP1/2-mediated cellular protection under glucose-deprived conditions. Together, these data highlight that 4EBP1/2 exert a pro-survival function under glucose deprivation by binding eIF4E to regulate mRNA translation.

4EBP1/2 maintain redox balance to preserve cell viability under glucose deprivation

To dissect how 4EBP1/2 protect cells under glucose-deprived conditions, we assessed the impact of 4EBP1/2 on the energetic and redox balances, which are major cellular parameters influenced by glucose availability. While ATP levels were reduced following glucose starvation as anticipated, 4EBP1/2 deficient MEFs and HEK293 cells showed the same amount of ATP as compared with the corresponding control cells under these conditions (Suppl. Fig. S2A&B). Given that protein synthesis is the most ATP-consuming process within a cell (Buttgereit and Brand, 1995), this result is consistent with the lack of impact of 4EBP1/2 on rates of overall protein synthesis under these conditions (Fig. 1H&I). In contrast, levels of endogenous H_2O_2 were higher under glucose deprivation in 4EBP1/2 DKO MEFs and sh4EBP1/2 HEK293 cells compared to their respective controls (WT and shScr, respectively) (Fig. 2A&B). In addition, overexpression of $4EBP1^{AA}$ prevented increases of H_2O_2 levels in HeLa cells during glucose depletion (Fig. 2C). These findings suggest a role for 4EBP1/2 in controlling redox balance upon glucose starvation. Glutathione is a major cellular anti-oxidant and cells recycle the oxidized form, GSSG, to the reduced form, GSH. The GSH to GSSG ratio is an indication for oxidative stress (Flohe, 2013). 4EBP1/2 DKO MEFs and sh4EBP1/2 HEK293 cells exhibited a lower GSH/GSSG ratio as compared with the respective control cells under glucose starvation, indicative of lower anti-oxidant capacity in 4EBP1/2 deficient cells (Fig. 2D&E). Conversely, $4EBP1^{AA}$ overexpression precluded severe depletion of GSH/GSSH ratio in HeLa cells during glucose removal (Fig. 2F). Since we did not observe changes in the level of total glutathione in 4EBP1/2 deficient MEFs and HEK293 nor $4EBP1^{AA}$ overexpressing cells during glucose deprivation, in comparison to the respective control cells (Fig. S2C-E), we reasoned that in glucose starved cells, 4EBP1/2 may contribute to glutathione recycling rather than its biosynthesis.

The conversion of GSSG to GSH requires the oxidation of NADPH to $NADP^+$, whose levels are determinant for cellular survival during glucose deprivation (Jeon et al., 2012). In comparison to the respective control cells, 4EBP1/2 DKO MEFs and sh4EBP1/2 HEK293 cells were characterized by severe reduction of NADPH/$NADP^+$ ratio under glucose withdrawal

(Fig. 2G&H). Furthermore, 4EBP1^{AA} overexpression led to a significant increase of NADPH/NADP^{+} ratio in HeLa cells during glucose starvation (Fig. 2I). These results are consistent with a role of 4EBP1/2 in promoting NADPH levels under glucose depletion. We next asked whether increased oxidative stress, observed in glucose starved 4EBPs depleted cells, is linked to increased sensitivity to glucose starvation. We thus supplemented glucose starved 4EBP1/2 DKO MEFs and sh4EBP1/2 HEK293 cells with anti-oxidants, N-acetyl cysteine (NAC) or Catalase (CAT), and found these anti-oxidants significantly reduce cell death compared to vehicle (Fig. 2J&K). Therefore, 4EBP1/2 protective function under glucose deprivation relies on curbing oxidative stress by promoting NADPH levels.

4EBP1/2 controls fatty acid synthesis under glucose deprivation to preserve NADPH levels

We next asked how 4EBP1/2 support NADPH levels under glucose deprivation. We reasoned that to do so, 4EBP1/2 either promote NADPH production or restrict NADPH consumption. Noteworthy, the most NADPH-consuming process within a cell, namely fatty acid synthesis (Fan et al., 2014), is inhibited in response to glucose starvation to preserve NADPH levels and promote cell survival (Jeon et al., 2012). Therefore, we asked whether 4EBP1/2 contribute to the inhibition of fatty acid synthesis during glucose starvation. Using ^{14}C acetate labeling, we measured the impact of 4EBP1/2 on fatty acid synthesis activity by quantifying ^{14}C incorporation in the cellular lipid fraction under basal conditions and after 16 hrs of glucose starvation. We found that under glucose deprivation 4EBP1/2 DKO MEFs as well as sh4EBP1/2 HEK293 cells accumulated higher amounts of ^{14}C-labelled lipids as compared to corresponding control cells (Fig. 3A&B). Noteworthy, in control cells levels of ^{14}C-labelled lipid was reduced upon glucose withdrawal, which is consistent with expected inhibition of fatty acid synthesis activity in response to glucose deprivation. We therefore concluded that 4EBP1/2 restrict fatty acid synthesis activity in response to glucose removal.

We next wondered whether increased fatty acid synthesis is responsible for reduced NADPH levels and increased ROS observed in glucose starved 4EBPs depleted cells.

Pharmacological inhibition of fatty acid synthesis, using the acetyl-CoA carboxylase (ACC) inhibitor TOFA, in 4EBP1/2 DKO MEFs and sh4EBP1/2 HEK293 cells led to significant elevation of NADPH/$NADP^+$ ratio (Fig. 3B&C) and reduced ROS levels during glucose withdrawal (Fig. 3D&E). Thus, 4EBP1/2 control redox balance under glucose-limited conditions by curbing fatty acid synthesis. Given that fatty acid synthesis activity is determinant for cell viability under glucose starvation, we next assessed whether increased fatty acid synthesis contributes to glucose starvation sensitivity of 4EBP1/2 depleted cells. Treatment of 4EBP1/2 deficient MEFs and HEK293 cells with TOFA efficiently protected cells under glucose deprivation (Fig. 3F&G). This was confirmed by selectively targeting the NADPH consuming enzyme fatty acid synthase (FASN). Si-RNA mediated knockdown of *FASN* in 4EBP1/2 DKO MEFs and sh4EBP1/2 HEK293 cells significantly reduced the levels of glucose withdrawal-induced cell death, as compared to control siRNA (scr) (Fig. 3H&I). Altogether, our findings suggest that during glucose starvation, 4EBP1/2 promote cell viability by inhibiting fatty acid synthesis to preserve NADPH levels and reduce ROS accumulation.

4EBP1/2 selectively regulate the translation of ACC1 to preserve cell viability under glucose deprivation

We next wondered by which mechanisms 4EBP1/2 regulate fatty acid synthesis in response to glucose starvation. Since 4EBP1/2 were reported to selectively block the translation of specific transcripts, we asked whether 4EBP1/2 restrict the synthesis of one of the fatty acid synthesis enzymes. Immunoblots analysis showed that levels of ATP citrate lyase (ACLY), ACC2 and FASN were similar in control and 4EBP1/2 DKO MEFs and sh4EBP1/2 HEK293 cells under glucose starvation (Fig. 4A&B). In contrast, ACC1 expression was severely decreased in control MEFs and HEK293 cells by 16 hrs glucose depletion, which was not the case in the corresponding 4EBP1/2 deficient cells, thus revealing that ACC1 is highly expressed in 4EBP1/2 deficient cells under glucose starvation (Fig. 4A&B). In agreement, $4EBP1^{AA}$ overexpression led to reduction of ACC1 levels in HeLa cells under glucose deprivation (Fig. S3A). The difference of ACC1 expression between control and 4EBP1/2

deficient HEK293 cells under glucose deprivation was not due to changes in *ACACA* (gene encoding ACC1) mRNA level (Fig. 4C), suggesting a potential regulation at the translational level. To discern whether 4EBP1/2 preferentially control *ACACA* translation under glucose starvation, we quantified levels of *ACACA* transcripts in polysomal and total mRNA and calculated the translation efficiency (TE) as the ratio of polysomal to total mRNA levels. We found that TE of *ACACA* transcript was significantly higher in sh4EBP1/2 HEK293 cells compared to control cells under glucose deprivation (Fig. 4D).

Given that 4EBPs/eIF4E-mediated selective translational control is mediated by the target's 5'UTR, we investigated the potential regulation of *ACACA* 5'UTR by 4EBP1/2 in response to glucose starvation. Since *ACACA* encodes several isoforms harboring different 5'UTR (Damiano et al., 2018), we focused on the 5'UTR most highly expressed in our cell models (data not shown). This 5'UTR, present in human *ACACA* transcript variant 3 (Damiano et al., 2018), is highly conserved in mouse. We observed that *ACACA* 5'UTR activity, as monitored with a luciferase reporter, was significantly decreased upon glucose starvation in control MEFs and HEK293 cells (Fig. 4E&F). In addition, *ACACA* 5'UTR activity was higher in 4EBP1/2 DKO MEFs and sh4EBP1/2 HEK293 cells under glucose starvation compared to respective control cells (Fig. 4E&F). To determine the contribution of the 5'UTR to 4EBP1/2 regulation of ACC1 expression in the context of the *ACACA* transcript, we ectopically expressed HA tagged *ACACA*, flanked or not by the 5'UTR, and monitored the impact of 4EBP1/2 on exogenous ACC1 protein levels during glucose starvation. While the expression of ACC1 with no 5'UTR did not differ between sh4EBP1/2 and control cells under glucose starvation, the level of 5'UTR containing ACC1 was higher in sh4EBP1/2 cells as compared with controls during glucose starvation (Fig. 4G). Altogether, these data support that *ACACA* 5' UTR is essential for 4EBP1/2 inhibition of *ACACA* translation under glucose-deprived conditions.

To determine the contribution of increased ACC1 expression to the sensitivity of 4EBP1/2 DKOs and sh4EBP1/2 HEK293 cells to glucose starvation, we knocked down ACC1 and assessed the impact on cell viability during glucose starvation (Fig. 4H&I). We found that *ACACA* knockdown rescued 4EBP1/2 deficient cells from glucose starvation-induced cell

death (Fig. 4H&I). These data are in line with our findings using an ACC inhibitor (Fig. 3G&H). The simplest interpretation of these results is that 4EBP1/2 protect cells from glucose starvation by inhibiting the translation of *ACACA* in a 5'UTR dependent manner thus reducing fatty acid synthesis, preserving NADPH and limiting oxidative stress.

The 4EBP1/2 orthologue Eap1 preserves viability of yeast under glucose deprivation

Since living organisms need to cope with glucose-starved conditions, we asked whether 4EBP1/2 protective function under glucose starvation represents an evolutionary conserved biological response to such a stress. In support to that, it was previously reported that 4EBP facilitates survival of Drosophila under nutrient deprivation. We aimed to delineate the function of 4EBP under glucose deprivation in the evolutionary distant model organism *Saccharomyces cerevisiae*, by studying the two functional 4EBP orthologues in yeast, namely Eap1p and Caf20p (Cosentino et al., 2000; Lanker et al., 1992). In rich glucose-containing YPD media, disruption of *EAP1* (*EAP1Δ*) or *CAF20* (*CAF20Δ*) had no impact on the growth rate of serially diluted yeast cultures on agar in comparison to WT strain (Fig. 5A), which is in agreement with previous reports stating that *EAP1* and *CAF20* are not essential genes (Cosentino et al., 2000; Lanker et al., 1992). In sharp contrast, the growth of *EAP1Δ* strain, but not of *CAF20Δ* strain, was severely compromised in solid rich glucose-free YP media, as compared to WT strain (Fig. 5A). Deletion of both *EAP1* and *CAF20* (*EAP1Δ*/*CAF20Δ*) had no further impact on growth in glucose-free media when compared to *EAP1Δ* strain (Fig. 5A). Our data indicate that the 4EBP orthologue Eap1p, but not Caf20p, supports growth of *Saccharomyces cerevisiae* in glucose-deprived conditions. Such functional difference between Eap1p and Caf20p is in line with differential requirements of these proteins for growth under other types of nutrient depleted conditions, and can be due to differences in the set of transcripts translationally regulated by Eap1p and Caf20p, as reported (Cridge et al., 2010). We confirmed that in liquid media *EAP1* disruption had a pronounced negative effect on growth in glucose-free YP media compared to WT strain (Fig. 5B). We next assessed whether

such phenotype was due to a reduction in survival under glucose-deprived conditions. Clonogenic assays of WT and *EAP1Δ* strains grown in liquid conditions in absence of glucose indicated that disruption of *EAP1* prevented survival of yeast upon glucose withdrawal (Fig. 5C). Our data points to a role of Eap1p in protecting yeast under glucose starvation, supporting the premise that 4EBP1/2 protective function, under such stress conditions, is conserved in the evolution.

Next, we determined whether *EAP1* and its orthologue *EIF4EBP1* respond to glucose deprivation, as part of a transcriptional program, as is expected from genes evolved to function during such stress. We observed that levels of *EAP1* were induced following 24 hrs of glucose removal in yeast cultures (Fig. 5D). Similarly, *EIF4EBP1* expression was increased upon glucose starvation in a three mammalian cell lines (Fig. 5E). Together, these data suggest that 4EBPs are conserved components of the biological response to glucose starvation.

4EBP1/2 promote oncogenic transformation by mitigating oxidative stress and controlling ACC1 level

Cellular response to glucose starvation is closely linked to oncogenic transformation and tumorigenicity, as similar mechanisms controlling redox balance and fatty acid synthesis are involved in these biological processes (Jeon et al., 2012; Schafer et al., 2009; Truitt et al., 2015). While 4EBP1/2 are required for oncogenic RAS transformation of primary fibroblasts (Petroulakis et al., 2009), it is not known whether 4EBP1/2 support transformation by other oncogenes or contribute to the maintenance of the oncogenic transformation state, as is expected if indeed 4EBP1/2 promote survival during energetic stress (Jeon et al., 2012). Using soft agar assays, we uncovered that 4EBP1/2 is necessary for HER2 transformation of mouse mammary epithelial cells (NT2197) in vitro (Fig. 6A). In addition, we found that 4EBP1/2 kd restricted the ability of immortalized NIH3T3 $KRAS^{V12}$ transformed fibroblasts to form colonies in soft agar (Suppl. Fig. 4A). These data show that 4EBP1/2 pro-tumorigenic functions are not restricted to RAS oncogene nor to initiation of cellular transformation. To determine how 4EBP1/2 deficiency leads to restricted oncogenic transformation, we assessed the possible

involvement of oxidative stress and uncontrolled fatty acid synthesis. Treatment of 4EBP1/2 DKO NT2197 cells with anti-oxidants – CAT, NAC or Trolox – or with an ACC inhibitor – TOFA – largely rescued colony formation in soft agar (Fig. 6B). Similarly, anti-oxidants treatment restored colony formation of NIH3T3 KRAS^{V12} 4EBP1/2 kd cells in soft agar (Suppl. Fig. 4B). Importantly, we found that genetic inhibition of ACC1 expression, by CRISPRi-mediated knockdown, was sufficient to restore colony formation of 4EBP1/2 deficient NT2197 cells (Fig. 6C). Thus, 4EBP1/2 support oncogenic transformation by negatively regulating ACC1 and oxidative stress.

We next tested our model in vivo and found that 4EBP1/2 DKO NT2197 cells were unable to form any detectable tumors when injected in the flank of immunocompromised mice, in sharp contrast to WT NT2197 cells (Fig. 6D&E). Analysis of tumor tissues indicated that 4EBP1/2 DKO NT2197 tumors were characterized by higher amounts of oxidative stress, as measured by the protein oxidation marker dityrosine, when compared to WT NT2197 tumors (Fig. 6F). To ascertain the contribution of ACC1 to the observed phenotype in NT2197 tumors in vivo, we assessed the impact of targeting ACC1 expression on the growth of 4EBP1/2 DKO NT2197 tumors. Remarkably, Acc1 knockdown (shAcaca) led to a major increase of tumor mass as compared to control (shScr) 4EBP1/2 DKO NT2197 tumors (Fig. 6G&H).

Next, we characterized the impact of ectopic expression of 4EBP1 on tumorigenicity. In support to our data obtained with 4EBP1/2 deficient cells, we found that overexpression of 4EBP1^{AA} in HeLa cells led to a significant increase in colony formation in soft agar as compared to control cells (EV) (Fig. 6I). This was recapitulated in vivo as 4EBP1^{AA} HeLa cells developed larger tumors than control HeLa cells when injected in the flank of immunocompromised mice (Fig. 6J&K). Collectively, these data support a model whereby 4EBP1/2 promote oncogenic transformation, tumorigenicity and survival during glucose starvation through a common mechanism entailing reduced ACC1 expression to restrain fatty acid synthesis and, thus, oxidative stress.

4EBP1 is clinically relevant and functional in brain tumors

Having found that 4EBP1/2 promote survival upon glucose starvation, a condition encountered in solid tumors, and that 4EBP1/2 support oncogenic transformation, we investigated the clinical relevance of 4EBP1/2 in cancer. By analyzing levels of *EIF4EBP1* and *EIF4EBP2* in patient samples (using TCGA and GTEx datasets), we uncovered that *EIF4EBP1* is overexpressed in 17 different tumor types as compared to corresponding normal tissues (Fig. S5A). In contrast, *EIF4EBP2* was only found to be overexpressed in 3 out of the 17 tumor types (Fig. S5B), therefore we focused our analyses on *EIF4EBP1*. Furthermore, high *EIF4EBP1* expression correlated with significantly decreased overall survival in 3 different tumor types (Fig. S5C-E), including glioma (Fig. S5E), highlighting *EIF4EBP1* expression as a potential prognostic biomarker in these tumor entities.

Glucose levels are low in the interstitial compartment of the brain as compared with blood (Fellows and Boutelle, 1993; Gruetter et al., 1992), because, for the most part, glucose is up taken and metabolized by astroglial cells (Pellerin, 2008). To survive in the low glucose microenvironment existing in the brain, cancer cells metastazing to the brain or glioma tumors acquire resistance to glucose starvation (Chen et al., 2015; Flavahan et al., 2013). To further investigate the relevance of *EIF4EBP1* in cancer, we turned out attention to the most common form of brain tumor in which low glucose levels have been detected, glioma (Tanaka et al., 2021). *EIF4EBP1* expression is higher in glioma versus non-tumorigenic brain tissues (NTT) (Fig. 7A) and is increased according to tumor grade, with highest expression in the most aggressive grade IV glioblastoma (GB) compared to low grade glioma (grades 2 and 3) (Fig. 7B). Proteomics data analyses further indicated that 4EBP1 protein is overexpressed in GB tissues compared to non-tumorigenic brain (Fig. S5F). Furthermore, high *EIF4EBP1* expression was associated with reduced overall survival in one additional independent and non-overlapping glioma cohort (Fig. 7C). This trend is observed in GB patients but to a lower extent (Fig. S5G), illustrating the clinical relevance of *EIF4EBP1* in such a highly malignant form of adult brain tumor.

To functionally dissect the role of 4EBP1 in glioma, we analyzed the impact of 4EBP1 kd on tumorigenic potential of human and mouse glioma cells, U87 and GL261 respectively. We first confirmed that 4EBP1 kd sensitizes glioma cells to glucose starvation-induced cell death (Fig. S5H), as with other cell lines. In addition, 4EBP1 kd severely restricted the ability of glioma cells to form colonies in soft agar (Fig. S6A&B). Importantly, inhibiting ACC with TOFA or supplementing cells with anti-oxidants rescued colony formation of the different 4EBP1 deficient cells (Fig. S6C-F). These data indicate that in glioma cells, 4EBP1 promotes tumorigenicity in vitro by means of controlling redox balance and fatty acid synthesis.

We next evaluated in vivo 4EBP1 pro-tumorigenic functions in glioma cells by first injecting control (shScr) and 4EBP1 kd U87 cells to the flanks of NOD-SCID mice. 4EBP1 depleted cells grew significantly smaller tumors as compared with controls (Fig. 7D&E).

To decipher whether 4EBP1 is also important for tumor maintenance, we used a doxycycline inducible shRNA system to target 4EBP1 expression in established tumors. 4EBP1 kd was induced once tumors formed by injection of engineered U87 models had reached 100 mm^3 in size. We observed an inhibition of tumor growth in doxycycline treated mice harboring the sh4EBP1-U87 tumors but not in shScr-U87 tumors or tumors in mice unexposed to doxycycline (Fig. 7I). These data suggest that 4EBP1 promotes growth of established glioma tumors in vivo.

To determine whether 4EBP1 supports tumor growth in brain, we performed orthotopic injection of control and sh4EBP1-U87 cells. While both control and 4EBP1 deficient cells generated tumors, mice bearing sh4EBP1-U87 tumors survived longer as compared with controls (Fig. 7J). To assess 4EBP1 function in an immunocompetent mouse model, we injected control and sh4EBP1 GL261 to brains of C57 mice. Mice carrying sh4EBP1 GL261 tumors showed a significant extension of survival compared to mice with control (shScr) tumors (Fig. 7L), suggesting that 4EBP1 promotes glioma aggressiveness also in presence of a functional immune system. Acc1 KD in sh4EBP1 GL261 cells tumor aggressiveness supporting the model where 4EBP1 is exploited by tumor cells to reduced Acc1 expression to promote tumor aggressiveness. Collectively, our data highlight that *EIF4EBP1* has clinical

relevance in various human tumor types, including glioma, and that 4EBP1 exerts a pro-tumorigenic function in glioma by reducing ACC1 expression.

DISCUSSION

4EBP1/2 are evolutionary conserved factors promoting cell survival under glucose deprivation

Glucose starvation represents a physiological stress, which requires/triggers a proper cellular response to prevent cell death. Here we report that 4EBPs promote cell survival during glucose starvation, a biological function conserved in human, mouse and yeast cells. The yeast orthologue of 4EBPs, Eap1p, shows little sequence homology with mammalian 4EBPs, although, similarly to mammalian 4EBPs, it binds yeast eIF4E to inhibit cap-dependent translation (Cosentino et al., 2000) and promotes survival under glucose starvation. Unlike its mammalian orthologue, Eap1 protects against other forms of metabolic stress, such as ammonium sulfate, serine or glutamate depletion (Cridge et al., 2010) suggesting that promoting viability specifically during glucose starvation, is an evolutionary conserved 4EBPs function.

In addition, we found that EIF4EBP1 has evolved as a glucose starvation-responsive gene. Both yeast *EAP1* and mammalian *EIF4EBP1* expression are induced by glucose starvation, in line with observations made in adipocytes (Agudelo et al., 2021) and in muscle tissues of food-deprived mice (Jagoe et al., 2002). Given that glucose starvation induced expression of another pro-survival factor and negative regulator of mRNA translation, namely eEF2K (Leprivier et al., 2013), this raises the notion that negative regulators of mRNA translation, and 4EBPs in particular, have evolved to protect cells against glucose starvation.

4EBP1/2 act as metabolic switches by translationally restricting fatty acid synthesis

Cellular response to glucose starvation proceeds through profound metabolic reprogramming, during which anabolic processes are blocked and catabolic processes are activated (Caro-Maldonado, 2011). These mechanisms are hijacked by cancer cells to adapt to the glucose

deprived conditions of the tumor microenvironment (Flavahan et al., 2013; Jones and Thompson, 2009). We uncovered that 4EBPs are key mediators of the metabolic switch induced by glucose withdrawal, and that they do so by binding eIF4E to restrict fatty acid synthesis and promote NADPH levels, thus linking mRNA translation to energy levels and regulation of fatty acid synthesis, and cellular redox balance. The regulation of cell metabolism by 4EBPs, through inhibition of fatty acid synthesis, proliferation (Dowling et al., 2010) and mitochondrial activity (Morita et al., 2013), is compatible with 4EBPs acting as metabolic switches responding to stress which steer cells to a more quiescent or low energy state.

4EBPs control metabolic processes rely on their ability to selectively restrict the translation of specific transcripts, including pro-proliferative *cyclin D3* and *ornithine decarboxylase* (Dowling et al., 2010) as well as mitochondrial coding *ATP5O* and *TFAM* (Morita et al., 2013). Here we uncovered that 4EBPs restrain fatty acid synthesis by selectively inhibiting the synthesis of the fatty acid synthesis rate limiting enzyme ACC1. Previously it was reported that eIF4E selectively promotes *ACACA* translation in T-cells (Ricciardi et al., 2018) and in liver tissue of mice fed with a high fat diet (Conn et al., 2021). In particular, the transition of CD4+ T cell from quiescence to activation, which metabolically mirror changes in glucose availability, is driven by eIF4E-promoted of *ACACA* translation which is dependent upon the 5'UTR of *ACACA* (Ricciardi et al., 2018). Similarly, we report that another 5'UTR of *ACACA* supports 4EBPs-mediated control of *ACACA* translation, highlighting that this *ACACA* 5'UTR represents a genetic element linking fatty acid synthesis activity to the energetic state of the cell. Altogether, our data support the model whereby in addition to AMPK-mediated phosphorylation of ACC1, cells evolved a parallel mechanism to inhibit ACC1 in response to energetic stress, through 4EBPs-mediated translational repression of ACACA mRNA. These may represent two complementary mechanisms, as phosphorylation is fast but easily reversible, especially due to the action of phosphatases, while mRNA translation repression is slower but may be more efficient at blocking ACC1 on the long-term. Noteworthy, in bacteria ACC is also regulated both at the translational and post-translational levels in response to glucose availability

(Broussard et al., 2013), in agreement with the possibility that the modes of ACC1 regulation are evolutionary conserved.

4EBP1 exerts a pro-tumorigenic function in glioma

The role of 4EBP1 in cancer is still unclear (Musa et al., 2016). While 4EBP1 exhibits tumor suppressive function in mouse models of lymphoma, head and neck squamous cell carcinoma and prostate cancer (Ding et al., 2018; Wang et al., 2019), 4EBP1 knockout mice per se do not develop tumor excluding that 4EBP1 is a tumor suppressor (Tsukiyama-Kohara et al., 2001). More than that, 4EBP1 has been shown to exert pro-tumorigenic functions, as it is required for oncogenic RAS transformation (Petroulakis et al., 2009) and it promotes breast cancer development in vivo (Braunstein et al., 2007). Our data support a pro-tumorigenic function of 4EBP1, as we uncovered that 4EBP1 mediates HER2 transformation and tumorigenicity of glioma cells in vitro and in vivo.

It is possible that the role of 4EBP1 in cancer is determined by the levels of metabolic stress present in tumors and that 4EBP1 pro-tumorigenic function predominates in metabolically challenged tumor environment, as was previously proposed for AMPK (Chhipa et al., 2018; Eichner et al., 2019; Faubert et al., 2014). In particular, glucose concentrations in the brain are low compared to plasma glycemia (Fellows and Boutelle, 1993; Gruetter et al., 1992), and aggressive glioma are characterized by the presence of large necrotic areas (Homma et al., 2006), indicative of oxygen and nutrient deprivation. To survive the low glucose microenvironment of the brain, glioma tumors or breast cancer cells metastazing to the brain, acquire resistance to glucose starvation (Chen et al., 2015; Flavahan et al., 2013), which adversely select for more highly tumorigenic cancer cell clones (Flavahan et al., 2013). We propose that 4EBP1 confers glioma cells the ability to adapt to metabolic stress by preserving the redox balance and restricting ACC1 expression, similarly to the mechanisms of 4EBP1 function in response to glucose deprivation. This is in line with the proposed function of AMPK in mediating cell survival under glucose starvation and tumorigenesis through inhibition of

ACC1 and prevention of oxidative stress (Jeon et al., 2012). 4EBP1 is, therefore, a metabolic regulator exploited by cancer cells to adapt adverse conditions of the tumor microenvironment. Since 4EBP1 is post-translationally inhibited by mTORC1, which is overactive in numerous cancers, it is assumed that 4EBP1 is inactive in tumors as evidenced by increased levels of phosphorylated 4EBP1 reported in various tumor tissues (Musa et al., 2016). However, the amount of total 4EBP1 protein is rarely monitored. Importantly, the activity of 4EBP1 in glioblastoma was shown to be directly dependent on the proximity to blood vessels, with highest 4EBP1 activity detected in areas furthest from blood vessels, corresponding to oxygen and glucose deprived areas (Kumar et al., 2019). This raises the possibility that upregulation of *EIF4EBP1*, as observed in numerous cancer types (Wu and Wagner, 2021), leads to increased 4EBP1 activity in metabolically challenged tumor areas. It is noteworthy that oncogenic transcription factors, such as MYC, MYCN, ETS1 and MYBL2 (Tameire et al., 2019) promote *EIF4EBP1* overexpression, further supporting the clinical relevance of *EIF4EBP1* as a pro-tumorigenic gene.

Our findings together with our previous work (Leprivier et al., 2013) support a model whereby translational repressors promote cell survival under glucose starvation and are hijacked by tumor cells to cope with energy stress.

EXPERIMENTAL PROCEDURES

Resource Availability

Lead Contacts

Further information and requests for reagents may be directed to, and will be fulfilled by the corresponding authors (rotblat@bgu.ac.il and gabriel.leprivier@med.uni-duesseldorf.de).

Material Availability

The unique reagents generated in this study are available from the Lead Contacts.

Experimental Model and Subject Details

Cell culture

Cells were maintained using standard tissue culture procedures in a humidified incubator at 37°C with 5% CO_2 and atmospheric oxygen. Stable HEK293 (human, female) control (shScr) and knock down for 4EBP1/4EBP2 (sh4EBP1/2) cell lines, WT ($p53^{-/-}$) and 4EBP1/4EBP2 double knockout (DKO) ($p53^{-/-}$) MEFs (mouse, sex unspecified) were kind gifts from Prof. Nahum Sonenberg (McGill University, Canada). NMuMG-NT2197 (mouse, female) (NT2197) control and 4EBP1/4EBP2 DKO cell lines were kind gifts from Dr. Ivan Topisirovic (McGill University, Canada). GL261 (mouse) glioma cell line was a kind gift from Prof. Reuven Stein (Tel Aviv University, Israel). NIH 3T3 cells (mouse, male) stably expressing K-Ras^{V12} have been previously described (Leprivier et al., 2013). Wild type HEK293, HEK293-T (human, female), HeLa (human, female), U-87 MG (human, male), MCF7 (human, female), Kelly (human, female) and IMR-32 (human, male). cell lines were originally obtained from American Type Culture Collections (ATCC).

NT2197 were cultured in Dulbecco's modified Eagle medium (DMEM) supplemented with 10% fetal bovine serum (FBS), 1% penicillin/streptomycin (pen/strep), 10 µg/ml insulin, and 20 mM HEPES, pH 7.5. NIH 3T3 K-Ras^{V12} were cultured in DMEM supplemented with 10% bovine calf serum. All other cell lines were maintained in DMEM supplemented with 10% FBS, 1% penicillin/streptomycin (pen/strep).

All cell lines were routinely confirmed to be mycoplasma-free using Venor®GeM Classic kit (Minerva Biolabs, Berlin, Germany). All human cell lines were authenticated by STR-profiling (Genomics and Transcriptomics Laboratory, Heinrich-Heine University, Germany).

Yeast culture

Yeast strains (all isogenic to BY4742, see table below) were grown in complex medium containing 1% (w/v) yeast extract and 2% (w/v) peptone without (YP) or with (YPD) 2% glucose. To pour solid agar plates, 2% agar was added to medium. For dot spot assays, yeast strains were grown to an OD600 of approximately 1, washed and diluted in a series of fivefold

dilutions before eventually being stamped on the corresponding agar plate before incubation at 30°C or 37°C for 3-5 days. For incubation in liquid complete YPD or glucose-free YP medium, suspensions were adjusted to an OD600 of 0.1 prior to incubation at 200 rpm at 30°C. The OD600 was measured throughout the experiment with a spectrophotometer. For survival analysis, BY4742 control or Eap1Δ yeast strains were incubated in liquid YP medium at an OD600 of 0.1 for 2 weeks at 30°C shaking at 300 rpm prior to streaking serial dilutions onto complete YPD agar plates.

Name	**Genotype**
BY4742	MATα his3Δ1 leu2Δ0 lys2Δ0 ura3Δ0
Eap1Δ	MATα his3Δ1 leu2Δ0 lys2Δ0 ura3Δ0 eap1Δ::NatMX4
Caf20Δ	MATα his3Δ1 leu2Δ0 lys2Δ0 ura3Δ0 caf20Δ::KanMX4
Eap1Δ/Caf20Δ	MATα his3Δ1 leu2Δ0 lys2Δ0 ura3Δ0 eap1Δ::NatMX4 caf20Δ::KanMX4

Animal models

All mouse work was performed in accordance with the institutional animal care use committee and relevant guidelines at the Ben-Gurion University, with protocols 34-06-2016, 35-06-2016 and 59-08-2019E. C57WT, nod-scid and nod-scid-Gama mice. Both male and female mice from 5-8 weeks of age were used for all experiments in this study. In specific experiment all mice were from the same sex and same age. All mice were housed under specific-pathogen-free (SPF) condition at the Ben-Gurion University facility.

Xenograft tumor models

For sub-cutaneous injection, cancer cells ($5X10^6$-$1X10^7$) were injected into the flank of mice. Tumors size were monitor-using caliper. When tumors reach the wanted size, mice were sacrificed, tumor were excised and weighed. Each tumor were cut in half and either fixed in formaldehyde 4% or snap-frozen in liquid nitrogen. When inducible system were used, mice received 10 mg/kg/day, such that 0.05 mg/mL of doxycycline was added to the drinking water twice a week.

For orthotropic/ intracranial injection, cancer cells were engrafted into a mouse brain using stereotactic device. For MRI imaging, mice were anesthetized by isoflurane inhalation

anesthesia (1.5 l O_2/min and 2.5% isoflurane), placed in the MRI T2 cranial images were acquired. Mice survival/mortality rate were monitored. At the end of the experiment, mice were sacrificed; their brains were excised and processed for IHC.

Method Details
Reagents

Cycloheximide (CHX), N-acetylcysteine (NAC), Catalase (CAT), 5-(Tetradecyloxy)-2-furoic acid (TOFA), and 6-hydroxy-2,5,7,8-tetramethylchroman-2-carboxylic acid (Trolox) were from Sigma-Aldrich.

Glucose and amino acids starvation of cell culture

Glucose or amino acids starvation was performed with subconfluent cultures (~50% confluency). For glucose starvation, full media was replaced with DMEM (RPMI for the IMR-32 and Kelly) containing no glucose and no sodium pyruvate supplemented with 10% dialyzed FBS and 1 mM glucose. For amino acid starvation, full media was replaced with Earle's Balanced Salt Solution (EBSS) supplemented with 10% dialyzed FBS and 25 mM glucose. When indicated, cells were treated with either CHX (2 μg/ml), NAC (3 mM), Catalase (400 U/ml), TOFA (5 μM) at the time of media replacement.

Vectors for genetically manipulating cell lines

shRNA expression plasmids

To make the shRNA expression vectors which were not commercially available, complementary oligonucleotides corresponding to shRNAs targeting mouse *eif4ebp1 or* mouse *acaca* were custom cloned (Genewiz) into AgeI and EcoRI restriction sites of the pLKO.1-neo cloning vector (Addgene 13425), or of the pLKO.1-puro (Addgene 10878), or of the Tet-pLKO-puro (Addgene 21915), or into EcoRI and PacI restriction sites of the pLKO.3G (Addgene). All other pLKO.1 lentiviral shRNA vectors were pLKO.1-puro based and were

retrieved from the arrayed Mission TRC genome-wide shRNA collections purchased from Sigma-Aldrich Corporation.

CRISPRi/Cas9 plasmids

To construct CRISPRi/Cas9 targeting vectors, single guide RNAs (sgRNAs) targeting human *EIF4EBP1* or mouse *acaca* were synthesized and custom cloned (Genewiz) into BsmBI restriction site of gRNA-dCas9-KRAB GFP (Addgene 71237).

cDNA expression plasmids

The cDNA sequences of human 4EBP1 (T37A/T46A) [4EBP1^{AA}] and 4EBP1^{AA} (Y54A/L59A) (4EBP1$^{AA, YL}$) were synthesized and custom cloned (Genewiz) into the EcoRI restriction site of the pLJM1 expression vector (Addgene 91980).

siRNA transfections

Cells were transfected at ~25% confluency in 6-well plates with 25 nM control ON TARGET plus non-targeting siRNA (Dharmacon) or with 25 nM of single siRNAs targeting human or mouse *EIF4E*, human or mouse *FASN*, human or mouse *ACACA*, mouse *EIF4EBP1* and *EIF4EBP2* using siLentFect transfection reagent (Bio-Rad) according to the manufacturer's instructions. When indicated, cells were glucose starved 48 hours post-transfection.

Virus production and viral transduction of cell lines

HEK293T cells were transfected with expression vectors and lentiviral packaging plasmids psPAX2 (Addgene 12260) and pMD2.G (Addgene 12259) in a ratio of 4:3:1 using CalFectin transfection reagent (Signagen) according to the manufacturer's guidelines. Media was harvested 72 hours post-transfection, passed through a 0.45 μm nitrocellulose filter and frozen at -80°C. Recipient cells were seeded in 6-well plates and were infected the next day when reaching ~50% confluency. For infection, 0.3 ml of virus-containing media was added to each

well in a final volume of 2 mL media containing 8 µg/ml polybrene. Stable cell lines were either selected with 2 µg/ml puromycin or 1 mg/ml G418, or FACS sorted for cells expressing GFP.

Immunoblot analyses of protein expression

Cells were lysed in RIPA buffer (150 mM NaCl, 50 mM Tris-HCl, pH 8, 1% Triton X-100, 0.5% sodium deoxycholate, and 0.1% SDS) supplemented with cOmplete™, EDTA-free Protease Inhibitor Cocktail (Sigma) and phosphatase inhibitors (PhosphoSTOP, Roche). Cell lysates were centrifuged at 14,000 x g for 15 min at 4°C and supernatants were collected. Protein concentration was measured using the BCA kit (Pierce) according to manufacturer's protocol. Protein lysates were resolved by SDS-PAGE and transferred to nitrocellulose membranes (GE Healthcare). Membranes were blocked with 5% BSA TBS-Tween (20 mM Tris-HCl, pH 7.4, 150 mM NaCl, 0.1% Tween 20) and probed with the primary antibodies indicated in supplementary table. Secondary anti-mouse (926-32210, Li-Cor) or anti-rabbit (926-32211, Li-Cor) antibodies were used and fluorescent signal was detected with the LI-COR Odyssey CLx system.

RNA analysis

RNA was extracted using the RNeasy mini kit (QIAgen) according to manufacturer's instruction. cDNAs were synthesized from total RNAs using either QuantiTect Reverse Transcription Kit (Quiagen) or High-Capacity cDNA Reverse Transcription Kit (Applied Biosystems) according to manufacturer's instruction. The cDNAs were quantified by real-time PCR analysis using SYBR Green Master Mix (Bio-Rad, CA). The primer sequences are listed in Table below. As internal controls, PPIA, GusB and β-actin were amplified.

Gene	Primer Sequence
eIF4EBP1	FW: AGCCCTTCCAGTGATGAGC RV: TGTCCATCTCAAACTGTGACTCTT

PPIA	F: CCAGACTGAGATGCACAAGTG R: GTGGCGGATTTGATCATTTGG
GusB	F: GTTTTTGATCCAGACCCAGATG R: GCCCATTATTCAGAGCGAGTA
ACTB	F: TCCCCCAACTTGAGATGTATG R: ACTGGTCTCAAGTCAGTGTACAGG
Act1 (yeast)	F: CCAGAAGCTTTGTTCCATCC R:CGGACATAACGATGTTACCG
Eap1 (yeast)	F: CAGCCGCTACTCACAAATC R: GCTTTCTTTATTGTTACCGCTC

ROS measurements

Cells were incubated with 5 µM chloromethyl-2′,7’-dichlorodihydrofluorescein diacetate (CM-H2DCFDA) at 37°C for 20 minutes. Cells were harvested and resuspended in PBS. Green fluorescence intensity was measured with a CytoFLEX flow cytometer (Beckmann Coulter). Data analysis was performed with FlowJo 10 software (FlowJo).

Reduced and oxidized glutathione measurements

Cells were seeded into 12-well plates and allowed to attach overnight. Cells were collected and cellular concentrations of reduced and total GSH were quantified using the GSH-Glo assay kit, according to the manufacturer’s protocol (Promega). Luminescence was measured using the Spark® plate reader (Tecan).

$NADP^+$/NADPH measurements

Cells were lysed in a base solution (100 mM sodium carbonate, 20 mM sodium bicarbonate, 10 mM nicotinamide, 0.05% Triton X-100) containing 1% of Dodecyltrimethylammoniumbromid (DTAB). Cell lysates were split in two equal fractions. The

pH of one of the fraction was adjusted by adding 0.4 N HCl according to the manufacturer's protocol. Both fractions were then heated for 15 minutes at 60°C and subsequently incubated at RT for 10 minutes. According to the manufacturer's protocol, before adding the detection reagent, Trizma base or HCl/Trizma solution were used to adjust pH each fraction. Finally, luminescence of each fraction was analyzed with Spark® plate reader (Tecan) to measure NADP+ and NADPH levels, and the $NADP^+$/NADPH ratio was calculated.

Protein synthesis rate

To quantify levels of newly synthesized proteins, 50 µM of azidohomoalanine (AHA) (C10102, Thermo Fisher Scientific, Massachusetts) was added to the cell culture medium and cells were incubated for 4 hours. Cells were then washed with ice-cold PBS, collected and lysed with EDTA-free RIPA lysis buffer (150 mM NaCl, 50 mM Tris pH 8, 1% Triton X-100, 0.5% sodium deoxycholate, 0.1% SDS). The concentration of proteins was measured by bicinchoninic acid assay using Pierce™ BCA Protein Assay Kit (PIR-23227, Thermo Fisher Scientific), and a Click reaction was performed with Click-iT® Protein Reaction Buffer Kit (C10276, Thermo Fisher Scientific) according to manufacturer's instructions.

Cell proliferation

To assess cell proliferation, cells plated in 6-wells were incubated in fresh media containing 10 µM 5-ethynyl-2'-deoxyuridine (EdU) (Invitrogen) for 60 min at 37°C. EdU staining was conducted using Click-iT™ EdU Alexa Fluor™ 488 Flow Cytometry Assay Kit (Invitrogen, Carlsbad, CA) according to the manufacturer's protocol. Briefly, cells were harvested, fixed with 4% paraformaldehyde in phosphate buffer saline (PBS) for 15 min, and permeabilized with 1X Click-iT™ saponin-based permeabilization reagent. Cells were incubated with a Click-iT™ reaction cocktail containing Click-iT™ reaction buffer, $CuSO_4$, Alexa Fluor® 488 Azide, and reaction buffer additive for 30 min while protected from light. Green fluorescence intensity was measured with a CytoFLEX flow cytometer (Beckmann Coulter). Data analysis was performed with FlowJo 10 software (FlowJo).

Cell death assays

Cell death was measured by flow cytometry using Propidium iodide (PI) staining. Briefly, attached and detached cells were harvested, centrifuged and resuspended in PBS containing 1 µg/ml PI (Sigma). Cell death quantification was performed using a CytoFLEX flow cytometer (Beckmann Coulter). A minimum of 50.000 events were recorded for each replicate. Data analysis was performed with FlowJo 10 software (FlowJo).

Soft agar colony assays

Cells were plated in 6-well plates with 8,000 cells per well in DMEM 10% FBS or DMEM 10% bovine calf serum in a top layer of 0.25% agar added over a base layer of 0.4% agar in DMEM 10% FBS or DMEM 10% bovine calf serum. Cells were fed once a week with 1ml of corresponding medium onto the top layer. Where indicated, NAC (5 mM), Catalase (200 U/ml), Trolox (100 µM), or TOFA (10 µM) were added to the top agar layer, as well as every 2-3 days in the feeder medium. After 2-4 weeks at 37°C, colonies were stained with 0.01% crystal violet and 10 random fields were counted manually for each well. The percentage of colony forming cells was calculated.

^{14}C labeling and fatty acid synthesis activity

Cells were labeled with 10 µCi of [1-^{14}C]-acetate (Perkin Elmer) in basal media or in glucose starved media for 16 h. Cells were snapped frozen and lipids were extracted by methanol-water-chloroform extraction. Phase separation was achieved by centrifugation at 4°C and the methanol-water phase containing polar metabolites was used as negative control. Radioactivity in the chloroform phase containing fatty acids was quantified by liquid scintillation counting and values were normalized to protein concentration determined in the dried protein interphase.

5'UTR Luciferase assays

The 5'UTR Firefly Luciferase reporter plasmids were custom cloned (Genewiz) by inserting the 5'UTR of human *ACACA* isoform 3 into the SacI and BglII restriction sites of pGL3 control vector (Promega).

For transfection, HEK293 cells were seeded in 12-well plates and transfected with 250 ng of each 5'UTR Firefly Luciferase reporter and 3 ng Renilla Luciferase expressing pRL null plasmid (Promega), completed to 500 ng DNA with pcDNA3.1 plasmid, using CalFectin transfection reagent (Signagen) according to the manufacturer's guidelines. Cells were harvested 48 hours post-transfection and activity of Firefly and Renilla Luciferase were sequentially determined using the Dual-Luciferase Reporter Assay System (Promega) and analyzed with the Spark® plate reader (Tecan). All samples were performed in triplicate and the final luciferase quantification was formulated as the ratio of Firefly luciferase to Renilla luciferase luminescence.

Polysome analysis

Cells were treated with 10 µg/ml of cycloheximide for 10 min, washed twice with PBS containing 100 µg/ml cycloheximide, then cells were scrapped and collected. Cells were pelleted by centrifugation (300 x g, 5 min, 4°C), lysed with 434 µl of lysis buffer (50 mM Tris-base pH 8, 2.5 mM $MgCl_2$, 1.5 mM KCl, 115 µg/ml cycloheximide, 2.3 mM DTT and 0.27 U/µl RNaseOUT [10777019, Thermo Fisher Scientific]), and vortexed. 25 µl of 100% Triton X-100 and 25 µl of 10% sodium deoxycholate were added to the cell lysates, which were vortexed and centrifuged (17,800 x g, 2 min, 4°C). 50 µl of the lysates were saved as the total fraction and the remaining were loaded on top of a three layers sucrose gradient (5%, 34% and 55% sucrose) that were prepared by dissolving sucrose in gradient buffer (4 mM HEPES pH 7.6, 20 mM KCl, 1 mM $MgCl_2$). The lysates loaded on top of the sucrose gradient were subjected to ultracentrifugation (229,884 x g, 2.5 hours, 4°C). The polysome profile was read using a piston gradient collector (Biocomp) fitted with a UV detector (Tirax). Three polysomal fractions

were collected and placed in Trizol (Sigma-Aldrich Company, location). RNA was extracted from frozen fractions using manufacturer's instructions.

Bioinformatics analyses of gene expression patterns in human tissue samples

For expression analysis, RNA-seq data from TCGA and the GTEx projects were analyzed with Gepia (PMID: 28407145). For survival analysis, RNA-seq and microarrays data were analyzed with Kaplan-Meier Plotter (PMID: 34527184) or Chinese Glioma Genome Atlas (CGGA; PMID: 33662628).

Quantification and Statistical Analysis

All experiments were, if not otherwise stated, independently carried out three times. Statistical significance was calculated using Student's t-test in GraphPad Prism 8. The data is represented as means +/- standard deviation. A p-value of less than 0,05 was considered to be significant.

FIGURE LEGENDS

Figure 1. 4EBP1/2 prevent cell death in response to glucose starvation through control of eIF4E and mRNA translation

(A) WT or 4EBP1/4EBP2 DKO MEF were grown in complete media, depleted for amino acids (AA) or for glucose (Glc) starved for 48 hrs. Cell death was measured by propidium iodide (PI) staining, and analyzed by flow cytometry.

(B) Control (shScr) or stable 4EBP1/4EBP2 knocked down (sh4EBP1/2) HEK293 cells were grown in complete media, depleted for amino acids (AA) or for glucose (Glc) starved for 48 hrs. Cell death was measured by propidium iodide (PI) staining, and analyzed by flow cytometry.

(C) Control (MSCV) or stable $4EBP1^{AA}$ overexpressing HeLa cells were grown in complete media, depleted for amino acids (AA) or for glucose (Glc) starved for 48 hrs. Cell death was measured by propidium iodide (PI) staining, and analyzed by flow cytometry.

(D) WT or 4EBP1/4EBP2 DKO MEF were grown in complete media or glucose starved (Glc strv)

for the indicated times and labeled with EdU. EdU incorporation was analyzed by flow cytometry.

(E) ShScr or sh4EBP1/2 HEK293 cells were grown in complete media or glucose starved (Glc strv) for the indicated times and labeled with EdU. EdU incorporation was analyzed by flow cytometry.

(F) 4EBP1/4EBP2 DKO MEF were grown in glucose starved media (Glc strv) and treated or not with cycloheximide (CHX) for 48 hrs. Cell death was measured by propidium iodide (PI) staining, and analyzed by flow cytometry.

(G) Sh4EBP1/2 HEK293 cells were grown in glucose starved media (Glc strv) and treated or not with cycloheximide (CHX) for 48 hrs. Cell death was measured by propidium iodide (PI) staining, and analyzed by flow cytometry.

(H) WT or 4EBP1/4EBP2 DKO MEF were grown in complete media or glucose starved (Glc strv)

for the indicated times and labeled with azidohomoalanine (AHA). Levels of AHA-labelled proteins was detected by immunoblotting with a streptavidin conjugate.

(I) ShScr or sh4EBP1/2 HEK293 cells were grown in complete media or glucose starved (Glc strv)

for the indicated times and labeled with azidohomoalanine (AHA). Levels of AHA-labelled proteins was detected by immunoblotting with a streptavidin conjugate.

(J) 4EBP1/4EBP2 DKO MEF were transfected with control siRNA (scr) or siRNAs targeting *eif4e* and were grown in glucose starved media (Glc strv) for 48 hrs. Cell death was measured by propidium iodide (PI) staining, and analyzed by flow cytometry.

(K) Sh4EBP1/2 HEK293 cells were transfected with control siRNA (scr) or siRNAs targeting *EIF4E* and were grown in glucose starved media (Glc strv) for 48 hrs. Cell death was measured by propidium iodide (PI) staining, and analyzed by flow cytometry.

(L) HeLa cells stably expressing empty vector (EV), 4EBP1^{AA} or 4EBP1^{AA,YL} were grown in glucose starved media (Glc strv) for 48 hrs. Cell death was measured by propidium iodide (PI) staining, and analyzed by flow cytometry.

Figure 2. 4EBP1/2 preserve the redox balance under glucose starvation by maintaining antioxidant power

(A) WT or 4EBP1/4EBP2 DKO MEF grown in complete media or glucose (Glc) starved for 24 hrs were assayed for H_2O_2 levels by flow cytometry using DCFDA.

(B) ShScr or sh4EBP1/2 HEK293 cells grown in complete media or glucose (Glc) starved for 24 hrs were assayed for H_2O_2 levels by flow cytometry using DCFDA.

(C) MSCV or 4EBP1^{AA} overexpressing HeLa cells grown in complete media or glucose (Glc) starved for 24 hrs were assayed for H_2O_2 levels by flow cytometry using DCFDA.

(D) WT or 4EBP1/4EBP2 DKO MEF were grown in complete media or glucose (Glc) starved for 24 hrs, and reduced and total glutathione were measured and expressed as the ratio of reduced (GSH) to oxidized (GSSG) glutathione.

(E) ShScr or sh4EBP1/2 HEK293 cells were grown in complete media or glucose (Glc) starved for 24 hrs, and reduced and total glutathione were measured and expressed as the ratio of reduced (GSH) to oxidized (GSSG) glutathione.

(F) MSCV or 4EBP1^{AA} overexpressing HeLa cells were grown in complete media or glucose (Glc) starved for 24 hrs, and reduced and total glutathione were measured and expressed as the ratio of reduced (GSH) to oxidized (GSSG) glutathione.

(G) WT or 4EBP1/4EBP2 DKO MEF were grown in complete media or glucose (Glc) starved for 24 hrs, and $NADP^+$ and NADPH were measured.

(H) ShScr or sh4EBP1/2 HEK293 cells were grown in complete media or glucose (Glc) starved for 24 hrs, and $NADP^+$ and NADPH were measured.

(I) MSCV or 4EBP1^{AA} overexpressing HeLa cells were grown in complete media or glucose (Glc) starved for 24 hrs, and $NADP^+$ and NADPH were measured.

(J) 4EBP1/4EBP2 DKO MEF were grown in glucose starved media (Glc strv) and treated with vehicle (V), N-acetyl cysteine (NAC) or Catalase (CAT) for 48 hrs. Cell death was measured by propidium iodide (PI) staining, and analyzed by flow cytometry.

(K) Sh4EBP1/2 HEK293 cells were grown in glucose starved media (Glc strv) and treated with vehicle (V), N-acetyl cysteine (NAC) or Catalase (CAT) for 48 hrs. Cell death was measured by propidium iodide (PI) staining, and analyzed by flow cytometry.

Figure 3. 4EBP1/2 controls fatty acid synthesis activity in response to glucose starvation to preserve redox balance and protects cells

(A) WT or 4EBP1/4EBP2 DKO MEF were grown in complete media or glucose starved media and labelled with [^{14}C] acetate for 16 hrs. Lipids were extracted and amounts of labelled lipids were quantified with a scintillation counter and normalized to protein content.

(B) ShScr or sh4EBP1/2 HEK293 cells were grown in complete media or glucose starved media and labelled with [^{14}C] acetate for 16 hrs. Lipids were extracted and amounts of labelled lipids were quantified with a scintillation counter and normalized to protein content.

(C) 4EBP1/4EBP2 DKO MEF were grown in glucose starved media (Glc strv) for 24 hrs, treated or not with TOFA, and $NADP^+$ and NADPH were measured.

(D) Sh4EBP1/2 HEK293 cells were grown in glucose starved media (Glc strv) for 24 hrs, treated or not with TOFA, and $NADP^+$ and NADPH were measured.

(E) 4EBP1/4EBP2 DKO MEF grown in glucose starved media (Glc strv) for 24 hrs and treated or not with TOFA were assayed for H_2O_2 levels by flow cytometry using DCFDA.

(F) Sh4EBP1/2 HEK293 cells grown in glucose starved media (Glc strv) for 24 hrs and treated or not with TOFA were assayed for H_2O_2 levels by flow cytometry using DCFDA.

(G) 4EBP1/4EBP2 DKO MEF grown in glucose starved media (Glc strv) were treated or not with TOFA for 48 hrs. Cell death was measured by propidium iodide (PI) staining, and analyzed by flow cytometry.

(H) Sh4EBP1/2 HEK293 cells grown in glucose starved media (Glc strv) were treated or not with TOFA for 48 hrs. Cell death was measured by propidium iodide (PI) staining, and analyzed by flow cytometry.

(I) 4EBP1/4EBP2 DKO MEF were transfected with control siRNA (scr) or siRNAs targeting *fasn* and were grown in glucose starved media (Glc strv) for 48 hrs. Cell death was measured by propidium iodide (PI) staining, and analyzed by flow cytometry.

(J) Sh4EBP1/2 HEK293 cells were transfected with control siRNA (scr) or siRNAs targeting *FASN* and were grown in glucose starved media (Glc strv) for 48 hrs. Cell death was measured by propidium iodide (PI) staining, and analyzed by flow cytometry.

Figure 4. 4EBP1/2 represses *ACACA* translation under glucose starvation

(A) WT or 4EBP1/4EBP2 DKO MEF were grown in complete media or glucose starved (Glc strv) for the indicated times, and analyzed by immunoblotting using the indicated antibodies.

(B) ShScr or sh4EBP1/2 HEK293 cells were grown in complete media or glucose starved (Glc strv) for the indicated times, and analyzed by immunoblotting using the indicated antibodies.

(C) ShScr or sh4EBP1/2 HEK293 cells were grown in complete media or glucose starved (Glc strv) for 16 hrs, and *ACACA* mRNA expression was analyzed by qRT-PCR.

(D) ShScr or sh4EBP1/2 HEK293 cells were grown in complete media or glucose starved (Glc strv) for 6 hrs, and translation efficiency (TE) of *ACACA* mRNA was calculated by measuring the levels of polysomal and total *ACACA* mRNA by qRT-PCR

(E) WT or 4EBP1/4EBP2 DKO MEF were transfected with an *ACACA* 5'UTR-containing Firefly Luciferase construct and a control *Renilla* Luciferase vector. Cells grown in complete media or glucose starved (Glc strv) for 6 hrs, and luminescence was measured.

(F) ShScr or sh4EBP1/2 HEK293 cells were transfected with an *ACACA* 5'UTR-containing Firefly Luciferase construct and a control *Renilla* Luciferase vector. Cells grown in complete media or glucose starved (Glc strv) for 6 hrs, and luminescence was measured.

(G) 293 cells were transfected with HA tagged ACC1 expressing vector containing or not *ACACA* 5'UTR. Cells were grown in complete media or glucose starved (Glc strv) for the indicated times, and analyzed by immunoblotting using the indicated antibodies.

(H) 4EBP1/4EBP2 DKO MEF were transfected with control siRNA (scr) or siRNAs targeting *acaca* and were grown in glucose starved media (Glc strv) for 48 hrs. Cell death was measured by propidium iodide (PI) staining, and analyzed by flow cytometry.

(I) Sh4EBP1/2 HEK293 cells were transfected with control siRNA (scr) or siRNAs targeting *ACACA* and were grown in glucose starved media (Glc strv) for 48 hrs. Cell death was measured by propidium iodide (PI) staining, and analyzed by flow cytometry.

Figure 5. Yeast 4EBPs orthologue promotes survival under glucose deprivation

(A) WT, *EAP1Δ*, *CAF20Δ or EAP1Δ*, *CAF20Δ* strains were platted by serial dilution on solid complex medium with (YPD) or without (YP) 2% glucose.

(B) WT or *EAP1Δ* were grown in liquid medium with (YPD) or without (YP) 2% glucose for the indicated times at which OD was measured.

(C) WT or *EAP1Δ* were grown in liquid medium containing (YP) no glucose for 2 weeks at 30°C and then were platted by serial dilutions onto complete YPD agar plates.

(D) WT strains were grown in liquid medium with (YPD) or without (YP) 2% glucose, and *EAP1* mRNA expression was analyzed by qRT-PCR.

(E) HEK293, MEF and HeLa were grown in complete media or glucose starved (Glc strv) for 24 hrs indicated times, and *EIF4EBP1* mRNA expression was analyzed by qRT-PCR.

Figure 6. 4EBP1 supports oncogenic transformation in vitro and in vivo

(A) WT or 4EBP1/4EBP2 DKO NT2197 cells were grown in soft agar for 21 days. Colonies and single cells were counted, and colony formation efficiency was calculated.

(B) 4EBP1/4EBP2 DKO NT2197 cells were grown in soft agar for 21 days and treated with DMSO, NAC, CAT, TROLOX or TOFA. Colonies and single cells were counted, and colony formation efficiency was calculated.

(C) Control or ACC1 targeting CRISPRi (sgAcc1) 4EBP1/4EBP2 DKO NT2197 cells were grown in soft agar for 21 days. Colonies and single cells were counted, and colony formation efficiency was calculated.

(D, E) WT or 4EBP1/4EBP2 DKO NT2197 cells were injected in the flank of NOD-SCIDgamma mice. Tumors were harvested, photographed (D) and weighed (E).

(F) Tumors of (D, E) were analyzed for levels of dityrosine proteins by immunoblotting. Quantification of dityrosine proteins intensity is represented.

(G, H) Control or stable ACC1 knocked down 4EBP1/4EBP2 DKO NT2197 cells were injected in the flank of NOD-SCIDgamma mice. Tumors were harvested, photographed (G) and weighed (H).

(I) HeLa cells stably expressing empty vector (EV) or $4EBP1^{AA}$ were grown in soft agar for 21 days. Colonies and single cells were counted, and colony formation efficiency was calculated.

(J, K) HeLa cells stably expressing empty vector (EV) or $4EBP1^{AA}$ were injected in the flank of NOD-SCIDgamma mice. Tumors were harvested, photographed (J) and weighed (K).

Figure 7. 4EBP1 has clinical relevance in glioma and promotes glioma tumorigenesis

(A) Expression levels of *EIF4EBP1* expression in non-tumorigenic brain tissue (NTT) and glioma tissues in the FRENCH cohort.

(B) Expression levels of *EIF4EBP1* per glioma stage in the CCGA cohort.

(C) Kaplan-Meier survival estimates of overall survival of glioma patients stratified by their *EIF4EBP1* mRNA (median first quartile) in the CCGA cohort.

(D, E) Control (shScr) or stable 4EBP1 knocked down (sh4EBP1#1 and #2) U-87 MG cells were injected in the flank of NOD-SCIDgamma mice. Tumors were harvested, photographed (D) and weighed (E).

(F) Tumors of (D, E) were analyzed for levels of dityrosine proteins by immunoblotting. Quantification of dityrosine proteins intensity is represented.

(G) Tumors of (D, E) were analyzed by immunoblotting and levels of ACC1 was quantified.

(H) Tumors of (D, E) were analyzed by qRT-PCR to assess *ACACA* mRNA expression.

(I) ShScr or stable inducible 4EBP1 knocked down (sh4EBP1) U-87 MG cells were injected in the flank of NOD-SCIDgamma mice. When tumors reached 100 mm^3, mice were given or not doxycycline (DOX). Tumor volumes were measured at the indicated times.

(J) ShScr or stable 4EBP1 knocked down (sh4EBP1) U-87 MG cells were injected intracranially in NOD-SCIDgamma mice. Survival of mice was monitored post injection.

(K) Tumors of (J) were analyzed for levels of 8-oxo-dG by immunohistochemical staining. Quantification of 8-oxo-dG intensity is represented.

(L) ShScr or stable 4EBP1 knocked down (sh4EBP1) GL261 cells were injected intracranially in C57WT mice. Survival of mice was monitored post injection.

SUPPLEMENTARY FIGURE LEGENDS

Supplementary Figure 1. Related to Figure 1.

(A) Control (shScr) or stable 4EBP1/4EBP2 knocked down (sh4EBP1/2) iPSC were grown in complete media or glucose (Glc) starved for 48 hrs. Cell death was measured by propidium iodide (PI) staining, and analyzed by flow cytometry.

(B) Control (shScr) or stable 4EBP1 knocked down (sh4EBP1#1 and #2) U-87 MG cells were grown in complete media or glucose (Glc) starved for 48 hrs. Cell death was measured by propidium iodide (PI) staining, and analyzed by flow cytometry.

(C) Control (shScr) or stable 4EBP1 knocked down (sh4EBP1#1 and #2) MCF-7 cells were grown in complete media or glucose (Glc) starved for 48 hrs. Cell death was measured by propidium iodide (PI) staining, and analyzed by flow cytometry.

(D) Control (shScr) or stable 4EBP1 knocked down (sh4EBP1#1 and #2) IMR-32 cells were grown in complete media or glucose (Glc) starved for 48 hrs. Cell death was measured by propidium iodide (PI) staining, and analyzed by flow cytometry.

(E) Control (shScr) or stable 4EBP1 knocked down (sh4EBP1#1 and #2) Kelly cells were grown in complete media or glucose (Glc) starved for 48 hrs. Cell death was measured by propidium iodide (PI) staining, and analyzed by flow cytometry.

(F) ShScr and Sh4EBP1/2 HEK293 cells were grown complete media or glucose starved (GS) for the indicated times and treated or not with chloroquine (CHQ). Cell lysates were analyzed by immunoblotting using the indicated antibodies.

(G) WT or 4EBP1/4EBP2 DKO MEF were grown complete media or glucose starved (GS) for the indicated times and treated or not with chloroquine (CHQ). Cell lysates were analyzed by immunoblotting using the indicated antibodies.

(H) ShScr and Sh4EBP1/2 HEK293 cells were grown in complete media, treated or not with rapamycin (Rapa) or Ku-0063794 (KU), and labeled with azidohomoalanine (AHA). Levels of AHA-labelled proteins was detected by immunoblotting with a streptavidin conjugate.

Supplementary Figure 2. Related to Figure 2.

(A) WT or 4EBP1/4EBP2 DKO MEF were grown in complete media or glucose (Glc) starved for 24 hrs, and ATP levels was measured by GC-MS.

(B) ShScr or sh4EBP1/2 HEK293 cells were grown in complete media or glucose (Glc) starved for 24 hrs, and ATP levels was measured by GC-MS.

(C) WT or 4EBP1/4EBP2 DKO MEF were grown in complete media or glucose (Glc) starved for 24 hrs, and total glutathione was measured.

(D) ShScr or sh4EBP1/2 HEK293 cells were grown in complete media or glucose (Glc) starved for 24 hrs, and total glutathione was measured.

(E) MSCV or 4EBP1^{AA} overexpressing HeLa cells were grown in complete media or glucose (Glc) starved for 24 hrs, and total glutathione was measured.

Supplementary Figure 3. Related to Figure 4.

(A) MSCV or 4EBP1^{AA} overexpressing HeLa cells were grown in complete media or glucose starved (Glc strv) for the indicated times, and analyzed by immunoblotting using the indicated antibodies.

Supplementary Figure 4. Related to Figure 6.

(A) NIH 3T3 transfected with control (scr) and *eif4ebp1* and *eif4ebp2* targeting siRNAs were grown in soft agar for 21 days. Colonies and single cells were counted, and colony formation efficiency was calculated.

(B) NIH 3T3 transfected with *eif4ebp1* and *eif4ebp2* targeting siRNAs were grown in soft agar for 21 days and treated with DMSO, NAC, CAT or TROLOX. Colonies and single cells were counted, and colony formation efficiency was calculated.

Supplementary Figure 5. Related to Figure 7.

(A, B) Expression levels of *EIF4EBP1* (A) and *EIF4EBP1* (B) in tumor tissues and corresponding non-tumorigenic tissues (NTT) from TCGA.

(C, D, E) Kaplan-Meier survival estimates of overall survival of bladder urothelial carcinoma (C), kidney renal clear cell carcinoma (D), and glioma (E) patients stratified by their *EIF4EBP1* mRNA (median first quartile) in the CCGA cohort.

(H) Control (shScr) or stable 4EBP1 knocked down (sh4EBP1#1 and #2) GL261 cells were grown in complete media or glucose (Glc) starved for 48 hrs. Cell death was measured by propidium iodide (PI) staining, and analyzed by flow cytometry.

(G) Kaplan-Meier survival estimates of overall survival of glioblastoma patients stratified by their *EIF4EBP1* mRNA (median first quartile) of CCGA cohort.

Supplementary Figure 6. Related to Figure 7.

(A) Control or *EIF4EBP1* targeting CRISPRi (sg4EBP1#1 and #2) U-87 MG cells were grown in soft agar for 21 days. Colonies and single cells were counted, and colony formation efficiency was calculated.

(B) Control (Scrl) or stable 4EBP1/4EBP2 knocked down (sh4EBP1/2) GL261 cells were grown in soft agar for 21 days. Colonies and single cells were counted, and colony formation efficiency was calculated.

(C, D) *EIF4EBP1* targeted CRISPRi (sg4EBP1#1 and #2) U-87 MG cells were grown in soft agar for 21 days and treated with DMSO, NAC, CAT, TROLOX or TOFA. Colonies and single cells were counted, and colony formation efficiency was calculated.

(E, F) 4EBP1/4EBP2 knocked down (sh4EBP1/2) GL261 cells were grown in soft agar for 21 days and treated with DMSO, NAC, CAT, TROLOX or TOFA. Colonies and single cells were counted, and colony formation efficiency was calculated.

REFERENCES

Agudelo, L.Z., Tuyeras, R., Llinares, C., Morcuende, A., Park, Y., Sun, N., Linna-Kuosmanen, S., Atabaki-Pasdar, N., Ho, L.-L., Galani, K.*, et al.* (2021). Metabolic resilience is encoded in genome plasticity. bioRxiv, 2021.2006.2025.449953.

Braunstein, S., Karpisheva, K., Pola, C., Goldberg, J., Hochman, T., Yee, H., Cangiarella, J., Arju, R., Formenti, S.C., and Schneider, R.J. (2007). A Hypoxia-Controlled Cap-Dependent to Cap-Independent Translation Switch in Breast Cancer. Molecular Cell *28*, 501-512.

Broussard, T.C., Price, A.E., Laborde, S.M., and Waldrop, G.L. (2013). Complex formation and regulation of Escherichia coli acetyl-CoA carboxylase. Biochemistry *52*, 3346-3357.

Buttgereit, F., and Brand, M.D. (1995). A hierarchy of ATP-consuming processes in mammalian cells. The Biochemical journal *312 (Pt 1*, 163-167.

Caro-Maldonado, A. (2011). Dying for Something to Eat: How Cells Respond to Starvation. The Open Cell Signaling Journal *3*, 42-51.

Chen, J., Lee, H.J., Wu, X., Huo, L., Kim, S.J., Xu, L., Wang, Y., He, J., Bollu, L.R., Gao, G.*, et al.* (2015). Gain of glucose-independent growth upon metastasis of breast cancer cells to the brain. Cancer Res *75*, 554-565.

Chhipa, R.R., Fan, Q., Anderson, J., Muraleedharan, R., Huang, Y., Ciraolo, G., Chen, X., Waclaw, R., Chow, L.M., Khuchua, Z.*, et al.* (2018). AMP kinase promotes glioblastoma bioenergetics and tumour growth. Nat Cell Biol *20*, 823-835.

Choo, A.Y., Kim, S.G., Vander Heiden, M.G., Mahoney, S.J., Vu, H., Yoon, S.O., Cantley, L.C., and Blenis, J. (2010). Glucose Addiction of TSC Null Cells Is Caused by Failed mTORC1-Dependent Balancing of Metabolic Demand with Supply. Molecular Cell *38*, 487-499.

Conn, C.S., Yang, H., Tom, H.J., Ikeda, K., Oses-Prieto, J.A., Vu, H., Oguri, Y., Nair, S., Gill, R.M., Kajimura, S.*, et al.* (2021). The major cap-binding protein eIF4E regulates lipid homeostasis and diet-induced obesity. Nat Metab *3*, 244-257.

Cosentino, G.P., Schmelzle, T., Haghighat, A., Helliwell, S.B., Hall, M.N., and Sonenberg, N. (2000). Eap1p, a novel eukaryotic translation initiation factor 4E-associated protein in Saccharomyces cerevisiae. Mol Cell Biol *20*, 4604-4613.

Cridge, A.G., Castelli, L.M., Smirnova, J.B., Selley, J.N., Rowe, W., Hubbard, S.J., McCarthy, J.E., Ashe, M.P., Grant, C.M., and Pavitt, G.D. (2010). Identifying eIF4E-binding protein translationally-controlled transcripts reveals links to mRNAs bound by specific PUF proteins. Nucleic Acids Res *38*, 8039-8050.

Damiano, F., Testini, M., Tocci, R., Gnoni, G.V., and Siculella, L. (2018). Translational control of human acetyl-CoA carboxylase 1 mRNA is mediated by an internal ribosome entry site in response to ER stress, serum deprivation or hypoxia mimetic CoCl2. Biochim Biophys Acta Mol Cell Biol Lipids *1863*, 388-398.

Ding, M., Van der Kwast, T.H., Vellanki, R.N., Foltz, W.D., McKee, T.D., Sonenberg, N., Pandolfi, P.P., Koritzinsky, M., and Wouters, B.G. (2018). The mTOR Targets 4E-BP1/2 Restrain Tumor Growth and Promote Hypoxia Tolerance in PTEN-driven Prostate Cancer. Mol Cancer Res *16*, 682-695.

Dowling, R.J.O., Topisirovic, I., Alain, T., Bidinosti, M., Fonseca, B.D., Petroulakis, E., Wang, X., Larsson, O., Selvaraj, A., Liu, Y.*, et al.* (2010). mTORC1-mediated cell proliferation, but not cell growth, controlled by the 4E-BPs. Science (New York, NY) *328*, 1172-1176.

Eichner, L.J., Brun, S.N., Herzig, S., Young, N.P., Curtis, S.D., Shackelford, D.B., Shokhirev, M.N., Leblanc, M., Vera, L.I., Hutchins, A.*, et al.* (2019). Genetic Analysis Reveals AMPK Is Required to Support Tumor Growth in Murine Kras-Dependent Lung Cancer Models. Cell Metab *29*, 285-302 e287.

Fan, J., Ye, J., Kamphorst, J.J., Shlomi, T., Thompson, C.B., and Rabinowitz, J.D. (2014). Quantitative flux analysis reveals folate-dependent NADPH production. Nature *510*, 298-302.

Faubert, B., Vincent, E.E., Poffenberger, M.C., and Jones, R.G. (2014). The AMP-activated protein kinase (AMPK) and cancer: Many faces of a metabolic regulator. Cancer Letters.

Fellows, L.K., and Boutelle, M.G. (1993). Rapid changes in extracellular glucose levels and blood flow in the striatum of the freely moving rat. Brain Res *604*, 225-231.

Flavahan, W.a., Wu, Q., Hitomi, M., Rahim, N., Kim, Y., Sloan, A.E., Weil, R.J., Nakano, I., Sarkaria, J.N., Stringer, B.W.*, et al.* (2013). Brain tumor initiating cells adapt to restricted nutrition through preferential glucose uptake. Nature neuroscience *16*, 1373-1382.

Flohe, L. (2013). The fairytale of the GSSG/GSH redox potential. Biochim Biophys Acta *1830*, 3139-3142.

Gruetter, R., Novotny, E.J., Boulware, S.D., Rothman, D.L., Mason, G.F., Shulman, G.I., Shulman, R.G., and Tamborlane, W.V. (1992). Direct measurement of brain glucose concentrations in humans by 13C NMR spectroscopy. Proc Natl Acad Sci U S A *89*, 1109-1112.

Homma, T., Fukushima, T., Vaccarella, S., Yonekawa, Y., Di Patre, P.L., Franceschi, S., and Ohgaki, H. (2006). Correlation among pathology, genotype, and patient outcomes in glioblastoma. J Neuropathol Exp Neurol *65*, 846-854.

Horman, S., Browne, G., Krause, U., Patel, J., Vertommen, D., Bertrand, L., Lavoinne, A., Hue, L., Proud, C., and Rider, M. (2002). Activation of AMP-activated protein kinase leads to the

phosphorylation of elongation factor 2 and an inhibition of protein synthesis. Current biology : CB *12*, 1419-1423.

Hsieh, A.C., Liu, Y., Edlind, M.P., Ingolia, N.T., Janes, M.R., Sher, A., Shi, E.Y., Stumpf, C.R., Christensen, C., Bonham, M.J.*, et al.* (2012). The translational landscape of mTOR signalling steers cancer initiation and metastasis. Nature *485*, 55-61.

Inoki, K., Zhu, T., and Guan, K.-L. (2003). TSC2 mediates cellular energy response to control cell growth and survival. Cell *115*, 577-590.

Jagoe, R.T., Lecker, S.H., Gomes, M., and Goldberg, A.L. (2002). Patterns of gene expression in atrophying skeletal muscles: response to food deprivation. FASEB J *16*, 1697-1712.

Jeon, S.M., Chandel, N.S., and Hay, N. (2012). AMPK regulates NADPH homeostasis to promote tumour cell survival during energy stress. Nature *485*, 661-665.

Jones, R.G., and Thompson, C.B. (2009). Tumor suppressors and cell metabolism: A recipe for cancer growth. Genes and Development *23*, 537-548.

Kumar, S., Sharife, H., Kreisel, T., Mogilevsky, M., Bar-Lev, L., Grunewald, M., Aizenshtein, E., Karni, R., Paldor, I., Shlomi, T.*, et al.* (2019). Intra-Tumoral Metabolic Zonation and Resultant Phenotypic Diversification Are Dictated by Blood Vessel Proximity. Cell Metab *30*, 201-211 e206.

Lanker, S., Muller, P.P., Altmann, M., Goyer, C., Sonenberg, N., and Trachsel, H. (1992). Interactions of the eIF-4F subunits in the yeast Saccharomyces cerevisiae. J Biol Chem *267*, 21167-21171.

Leibovitch, M., and Topisirovic, I. (2018). Dysregulation of mRNA translation and energy metabolism in cancer. Adv Biol Regul *67*, 30-39.

Leprivier, G., Remke, M., Rotblat, B., Dubuc, A., Mateo, A.R.F., Kool, M., Agnihotri, S., El-Naggar, A., Yu, B., Prakash Somasekharan, S.*, et al.* (2013). The eEF2 kinase confers resistance to nutrient deprivation by blocking translation elongation. Cell *153*.

Leprivier, G., and Rotblat, B. (2020). How does mTOR sense glucose starvation? AMPK is the usual suspect. Cell Death Discov *6*, 27.

Leprivier, G., Rotblat, B., Khan, D., Jan, E., and Sorensen, P.H. (2015). Stress-mediated translational control in cancer cells. Biochimica et Biophysica Acta - Gene Regulatory Mechanisms *1849*, 845-860.

Liu, G.Y., and Sabatini, D.M. (2020). mTOR at the nexus of nutrition, growth, ageing and disease. Nat Rev Mol Cell Biol *21*, 183-203.

Marciano, R., Leprivier, G., and Rotblat, B. (2018). Puromycin labeling does not allow protein synthesis to be measured in energy-starved cells. Cell Death Dis *9*, 39.

Morita, M., Gravel, S.P., Chénard, V., Sikström, K., Zheng, L., Alain, T., Gandin, V., Avizonis, D., Arguello, M., Zakaria, C.*, et al.* (2013). MTORC1 controls mitochondrial activity and biogenesis through 4E-BP-dependent translational regulation. Cell Metabolism *18*, 698-711.

Musa, J., Orth, M.F., Dallmayer, M., Baldauf, M., Pardo, C., Rotblat, B., Kirchner, T., Leprivier, G., and Grünewald, T.G.P. (2016). Eukaryotic initiation factor 4E-binding protein 1 (4E-BP1): a master regulator of mRNA translation involved in tumorigenesis. Oncogene.

Nagy, J.a., Chang, S.H., Dvorak, a.M., and Dvorak, H.F. (2009). Why are tumour blood vessels abnormal and why is it important to know? British journal of cancer *100*, 865-869.

Ng, T.L., Leprivier, G., Robertson, M.D., Chow, C., Martin, M.J., Laderoute, K.R., Davicioni, E., Triche, T.J., and Sorensen, P.H. (2012). The AMPK stress response pathway mediates anoikis resistance through inhibition of mTOR and suppression of protein synthesis. Cell Death Differ *19*, 501-510.

Orozco, J.M., Krawczyk, P.A., Scaria, S.M., Cangelosi, A.L., Chan, S.H., Kunchok, T., Lewis, C.A., and Sabatini, D.M. (2020). Dihydroxyacetone phosphate signals glucose availability to mTORC1. Nat Metab *2*, 893-901.

Pause, A., Belsham, G.J., Gingras, A.C., Donze, O., Lin, T.A., Lawrence, J.C., Jr., and Sonenberg, N. (1994). Insulin-dependent stimulation of protein synthesis by phosphorylation of a regulator of 5'-cap function. Nature *371*, 762-767.

Pellerin, L. (2008). Brain energetics (thought needs food). Curr Opin Clin Nutr Metab Care *11*, 701-705.

Petroulakis, E., Parsyan, A., Dowling, R.J.O., LeBacquer, O., Martineau, Y., Bidinosti, M., Larsson, O., Alain, T., Rong, L., Mamane, Y.*, et al.* (2009). p53-Dependent Translational Control of Senescence and Transformation via 4E-BPs. Cancer Cell *16*, 439-446.

Poulin, F., Gingras, A.C., Olsen, H., Chevalier, S., and Sonenberg, N. (1998). 4E-BP3, a new member of the eukaryotic initiation factor 4E-binding protein family. J Biol Chem *273*, 14002-14007.

Ricciardi, S., Manfrini, N., Alfieri, R., Calamita, P., Crosti, M.C., Gallo, S., Muller, R., Pagani, M., Abrignani, S., and Biffo, S. (2018). The Translational Machinery of Human CD4(+) T Cells Is Poised for Activation and Controls the Switch from Quiescence to Metabolic Remodeling. Cell Metab *28*, 895-906 e895.

Ryazanov, a.G., Shestakova, E.a., and Natapov, P.G. (1988). Phosphorylation of elongation factor 2 by EF-2 kinase affects rate of translation. Nature *334*, 170-173.

Schafer, Z.T., Grassian, A.R., Song, L., Jiang, Z., Gerhart-Hines, Z., Irie, H.Y., Gao, S., Puigserver, P., and Brugge, J.S. (2009). Antioxidant and oncogene rescue of metabolic defects caused by loss of matrix attachment. Nature *461*, 109-113.

Silvera, D., Formenti, S.C., and Schneider, R.J. (2010). Translational control in cancer. Nat Rev Cancer *10*, 254-266.

Sonenberg, N., and Hinnebusch, A.G. (2009). Regulation of Translation Initiation in Eukaryotes: Mechanisms and Biological Targets. Cell *136*, 731-745.

Tameire, F., Verginadis, II, Leli, N.M., Polte, C., Conn, C.S., Ojha, R., Salas Salinas, C., Chinga, F., Monroy, A.M., Fu, W.*, et al.* (2019). ATF4 couples MYC-dependent translational activity to bioenergetic demands during tumour progression. Nat Cell Biol *21*, 889-899.

Tanaka, K., Sasayama, T., Nagashima, H., Irino, Y., Takahashi, M., Izumi, Y., Uno, T., Satoh, N., Kitta, A., Kyotani, K.*, et al.* (2021). Glioma cells require one-carbon metabolism to survive glutamine starvation. Acta Neuropathol Commun *9*, 16.

Teleman, A.a., Chen, Y.W., and Cohen, S.M. (2005). 4E-BP functions as a metabolic brake used under stress conditions but not during normal growth. Genes and Development *19*, 1844-1848.

Tettweiler, G., Miron, M., Jenkins, M., Sonenberg, N., and Lasko, P.F. (2005). Starvation and oxidative stress resistance in Drosophila are mediated through the eIF4E-binding protein, d4E-BP. Genes and Development *19*, 1840-1843.

Thoreen, C.C., Chantranupong, L., Keys, H.R., Wang, T., Gray, N.S., and Sabatini, D.M. (2012). A unifying model for mTORC1-mediated regulation of mRNA translation. Nature *485*, 109-113.

Trefts, E., and Shaw, R.J. (2021). AMPK: restoring metabolic homeostasis over space and time. Mol Cell *81*, 3677-3690.

Truitt, Morgan L., Conn, Crystal S., Shi, Z., Pang, X., Tokuyasu, T., Coady, Alison M., Seo, Y., Barna, M., and Ruggero, D. (2015). Differential Requirements for eIF4E Dose in Normal Development and Cancer. Cell, 1-13.

Truitt, M.L., and Ruggero, D. (2016). New frontiers in translational control of the cancer genome. Nat Rev Cancer *16*, 288-304.

Tsukiyama-Kohara, K., Poulin, F., Kohara, M., DeMaria, C.T., Cheng, a., Wu, Z., Gingras, a.C., Katsume, a., Elchebly, M., Spiegelman, B.M.*, et al.* (2001). Adipose tissue reduction in mice lacking the translational inhibitor 4E-BP1. Nature medicine *7*, 1128-1132.

Valvezan, A.J., and Manning, B.D. (2019). Molecular logic of mTORC1 signalling as a metabolic rheostat. Nat Metab *1*, 321-333.

Wang, Z., Feng, X., Molinolo, A.A., Martin, D., Vitale-Cross, L., Nohata, N., Ando, M., Wahba, A., Amornphimoltham, P., Wu, X.*, et al.* (2019). 4E-BP1 Is a Tumor Suppressor Protein Reactivated by mTOR Inhibition in Head and Neck Cancer. Cancer Res *79*, 1438-1450.

Warburg, O. (1956). On the origin of cancer cells. Science *123*, 309-314.

Wu, S., and Wagner, G. (2021). Deep computational analysis details dysregulation of eukaryotic translation initiation complex eIF4F in human cancers. Cell Syst *12*, 907-923 e906.

Zid, B.M., Rogers, A.N., Katewa, S.D., Vargas, M.a., Kolipinski, M.C., Lu, T.a., Benzer, S., and Kapahi, P. (2009). 4E-BP Extends Lifespan upon Dietary Restriction by Enhancing Mitochondrial Activity in Drosophila. Cell *139*, 149-160.

Wang, Z., Feng, X., Molinolo, A.A., Martin, D., Vitale-Cross, L., Nohata, N., Ando, M., Wahba, A., Amornphimoltham, P., Wu, X.*, et al.* (2019). 4E-BP1 Is a Tumor Suppressor Protein Reactivated by mTOR Inhibition in Head and Neck Cancer. Cancer Res *79*, 1438-1450.

Warburg, O. (1956). On the origin of cancer cells. Science *123*, 309-314.

Wu, S., and Wagner, G. (2021). Deep computational analysis details dysregulation of eukaryotic translation initiation complex eIF4F in human cancers. Cell Syst *12*, 907-923 e906.

Zid, B.M., Rogers, A.N., Katewa, S.D., Vargas, M.a., Kolipinski, M.C., Lu, T.a., Benzer, S., and Kapahi, P. (2009). 4E-BP Extends Lifespan upon Dietary Restriction by Enhancing Mitochondrial Activity in Drosophila. Cell *139*, 149-160.

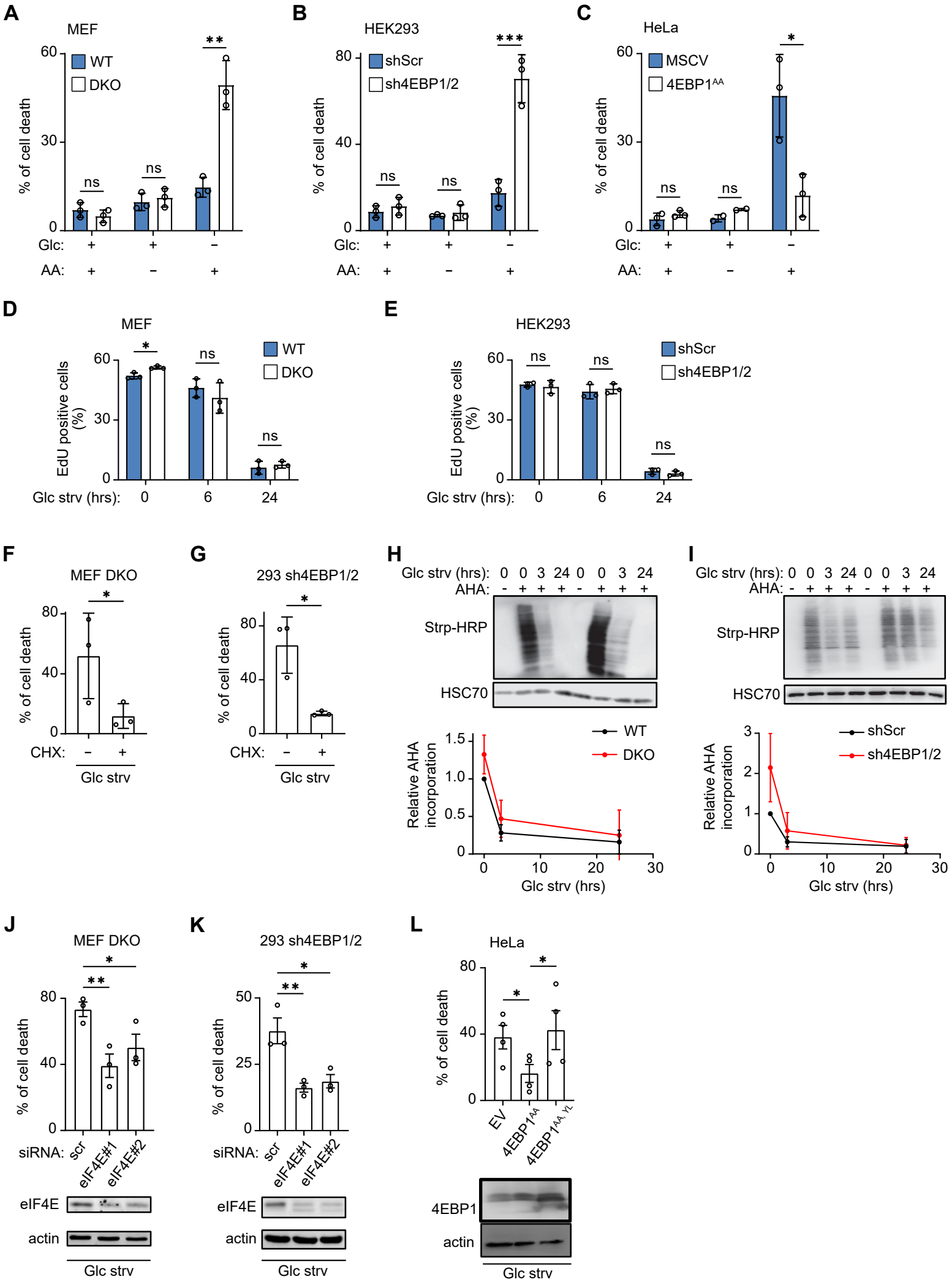
A
MEF
WT
DKO
% of cell death
Glc:
AA:
B
HEK293
shScr
sh4EBP1/2
C
HeLa
MSCV
4EBP1AA
D
MEF
EdU positive cells (%)
Glc strv (hrs):
E
HEK293
F
MEF DKO
CHX:
Glc strv
G
293 sh4EBP1/2
H
Glc strv (hrs): 0 0 3 24 0 0 3 24
AHA: - + + + - + + +
Strp-HRP
HSC70
Relative AHA incorporation
Glc strv (hrs)
I
J
MEF DKO
siRNA: scr eIF4E#1 eIF4E#2
eIF4E
actin
K
293 sh4EBP1/2
L
HeLa
EV
4EBP1AA
4EBP1AA, YL
4EBP1

Figure 1

Figure 2

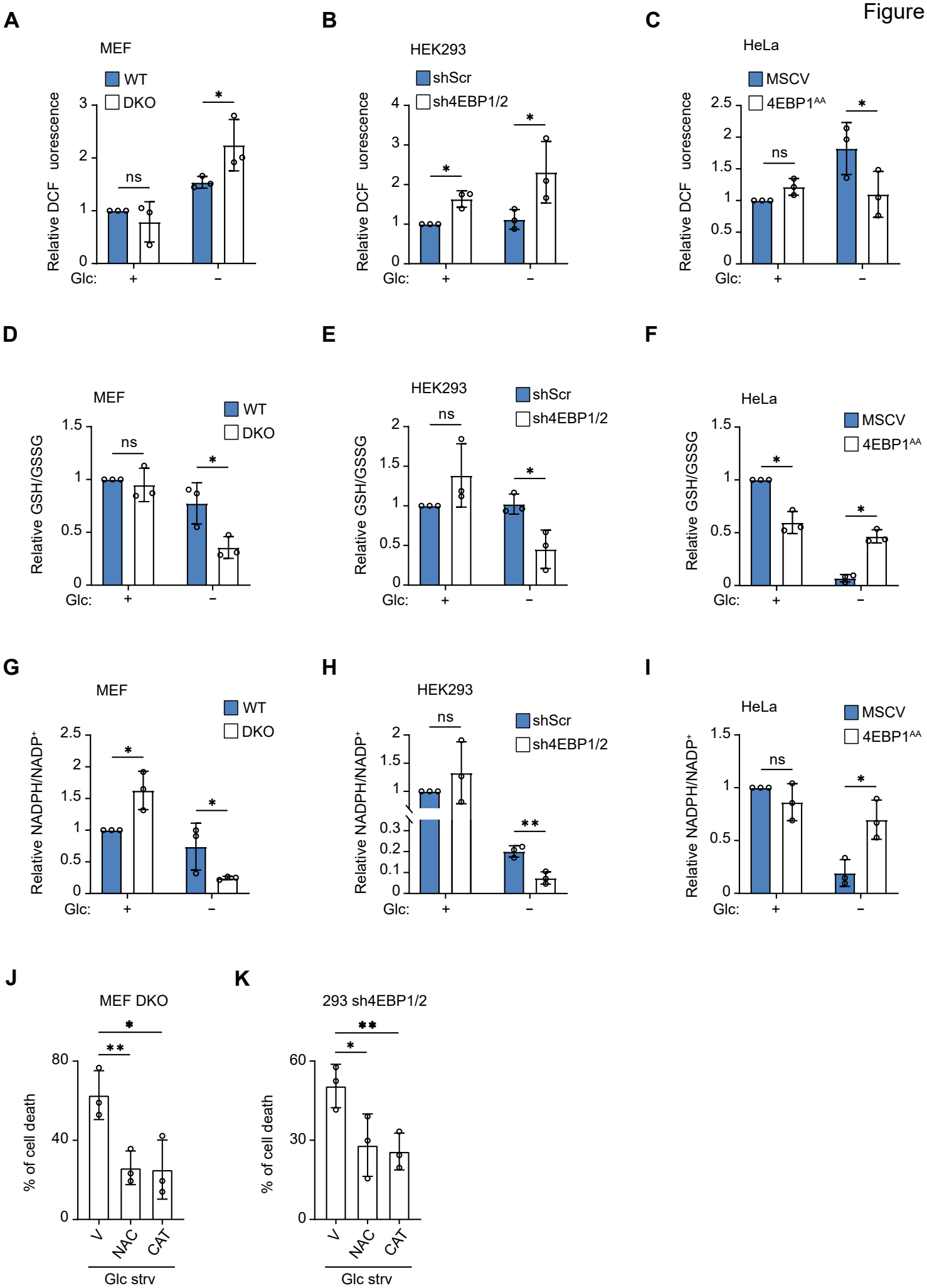
A
MEF
WT
DKO
Relative DCF uorescence
ns
*
Glc: + −
B
HEK293
shScr
sh4EBP1/2
Relative DCF uorescence
*
*
Glc: + −
C
HeLa
MSCV
4EBP1AA
Relative DCF uorescence
ns
*
Glc: + −
D
MEF
WT
DKO
Relative GSH/GSSG
ns
*
Glc: + −
E
HEK293
shScr
sh4EBP1/2
Relative GSH/GSSG
ns
*
Glc: + −
F
HeLa
MSCV
4EBP1AA
Relative GSH/GSSG
*
*
Glc: + −
G
MEF
WT
DKO
Relative NADPH/NADP+
*
*
Glc: + −
H
HEK293
shScr
sh4EBP1/2
Relative NADPH/NADP+
ns
**
Glc: + −
I
HeLa
MSCV
4EBP1AA
Relative NADPH/NADP+
ns
*
Glc: + −
J
MEF DKO
% of cell death
*
**
V
NAC
CAT
Glc strv
K
293 sh4EBP1/2
% of cell death
**
*
V
NAC
CAT
Glc strv

Figure 3

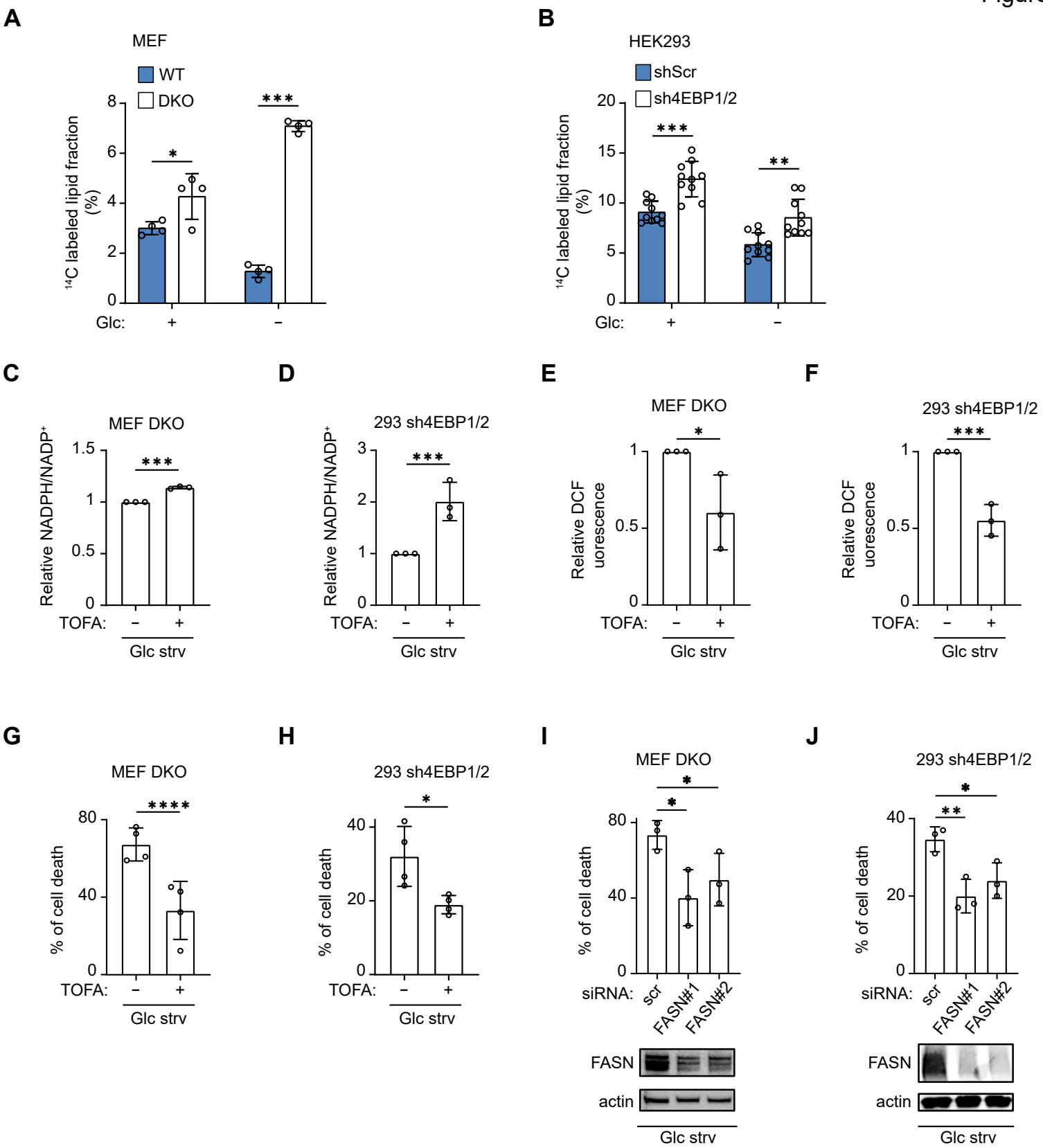
A
MEF
WT
DKO
^{14}C labeled lipid fraction (%)
Glc:
B
HEK293
shScr
sh4EBP1/2
^{14}C labeled lipid fraction (%)
Glc:
C
MEF DKO
Relative NADPH/NADP$^+$
TOFA:
Glc strv
D
293 sh4EBP1/2
Relative NADPH/NADP$^+$
TOFA:
Glc strv
E
MEF DKO
Relative DCF uorescence
TOFA:
Glc strv
F
293 sh4EBP1/2
Relative DCF uorescence
TOFA:
Glc strv
G
MEF DKO
% of cell death
TOFA:
Glc strv
H
293 sh4EBP1/2
% of cell death
TOFA:
Glc strv
I
MEF DKO
% of cell death
siRNA:
scr
FASN#1
FASN#2
FASN
actin
Glc strv
J
293 sh4EBP1/2
% of cell death
siRNA:
scr
FASN#1
FASN#2
FASN
actin
Glc strv

Figure 4

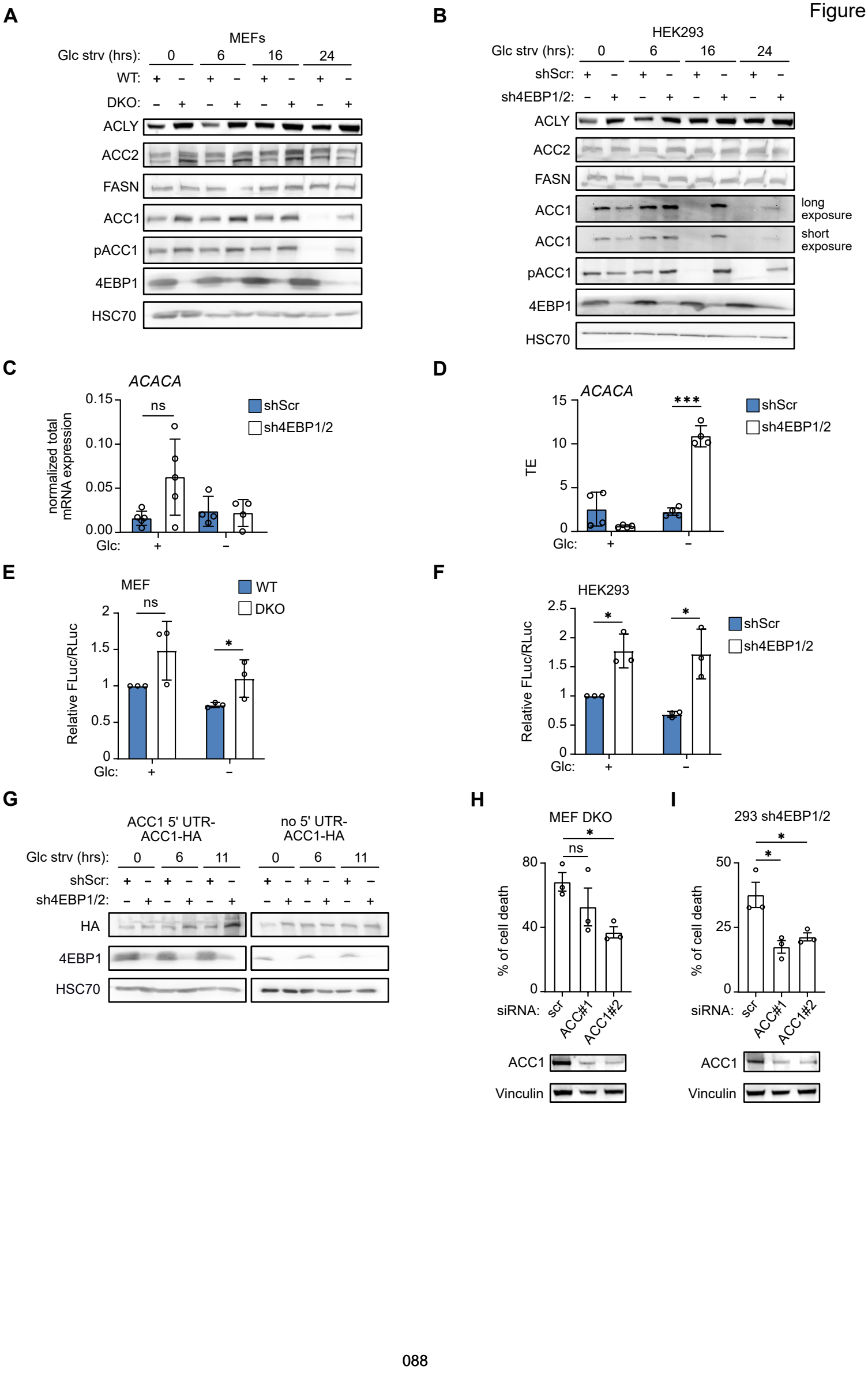
A
MEFs
Glc strv (hrs): 0 6 16 24
WT:
DKO:
ACLY
ACC2
FASN
ACC1
pACC1
4EBP1
HSC70
B
HEK293
Glc strv (hrs): 0 6 16 24
shScr:
sh4EBP1/2:
ACLY
ACC2
FASN
ACC1
long exposure
ACC1
short exposure
pACC1
4EBP1
HSC70
C
ACACA
normalized total mRNA expression
ns
shScr
sh4EBP1/2
Glc:
D
ACACA
TE
***
shScr
sh4EBP1/2
Glc:
E
MEF
Relative FLuc/RLuc
ns
*
WT
DKO
Glc:
F
HEK293
Relative FLuc/RLuc
*
*
shScr
sh4EBP1/2
Glc:
G
ACC1 5' UTR-ACC1-HA
no 5' UTR-ACC1-HA
Glc strv (hrs): 0 6 11 0 6 11
shScr:
sh4EBP1/2:
HA
4EBP1
HSC70
H
MEF DKO
% of cell death
*
ns
siRNA: scr ACC#1 ACC1#2
ACC1
Vinculin
I
293 sh4EBP1/2
% of cell death
*
*
siRNA: scr ACC#1 ACC1#2
ACC1
Vinculin

Figure 5

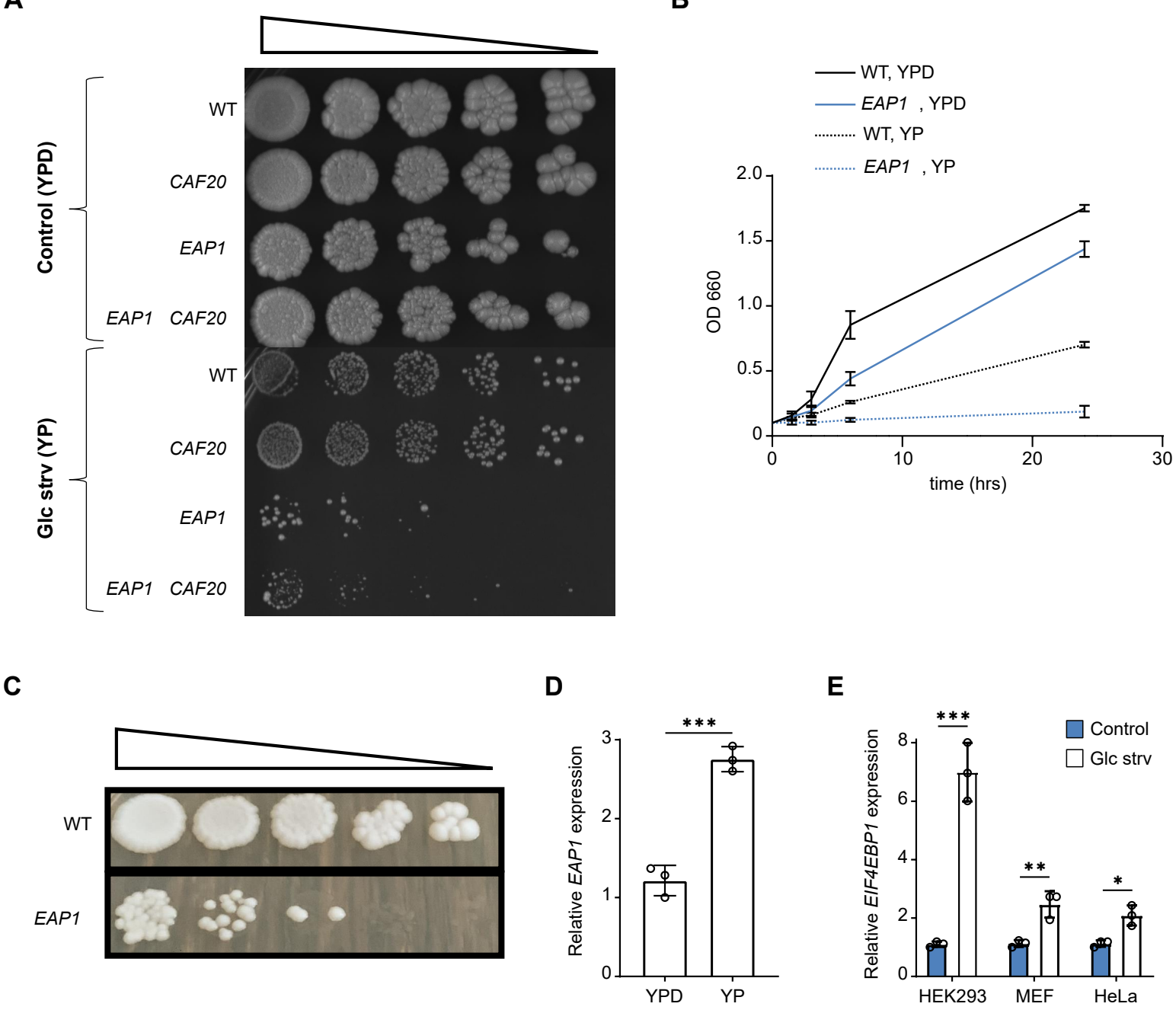
A
Control (YPD)
Glc strv (YP)
WT
CAF20
EAP1
EAP1 CAF20
WT
CAF20
EAP1
EAP1 CAF20
B
WT, YPD
EAP1 , YPD
WT, YP
EAP1 , YP
OD 660
time (hrs)
C
WT
EAP1
D
Relative EAP1 expression
YPD
YP
***
E
Relative EIF4EBP1 expression
Control
Glc strv
HEK293
MEF
HeLa
**
*
***

Figure 6

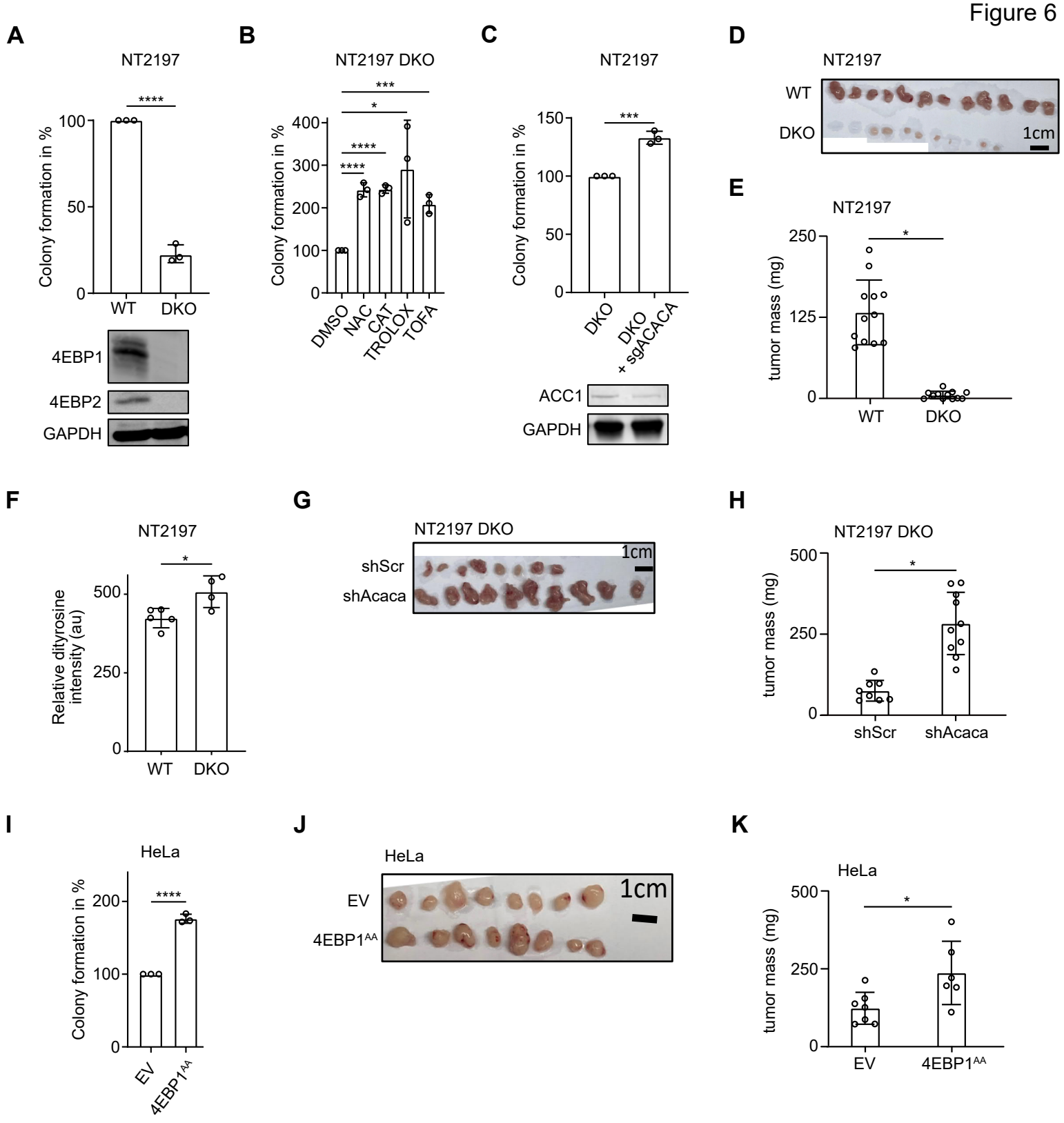
A
NT2197
Colony formation in %
100
50
0
****
WT
DKO
4EBP1
4EBP2
GAPDH
B
NT2197 DKO
Colony formation in %
400
300
200
100
0
***
*
****
****
DMSO
NAC
CAT
TROLOX
TOFA
C
NT2197
Colony formation in %
150
100
50
0
***
DKO
DKO + sgACACA
ACC1
GAPDH
D
NT2197
WT
DKO
1cm
E
NT2197
tumor mass (mg)
250
125
0
*
WT
DKO
F
NT2197
Relative dityrosine intensity (au)
500
250
0
*
WT
DKO
G
NT2197 DKO
shScr
shAcaca
1cm
H
NT2197 DKO
tumor mass (mg)
500
250
0
*
shScr
shAcaca
I
HeLa
Colony formation in %
200
100
0
****
EV
4EBP1AA
J
HeLa
EV
4EBP1AA
1cm
K
HeLa
tumor mass (mg)
500
250
0
*
EV
4EBP1AA

Figure 7

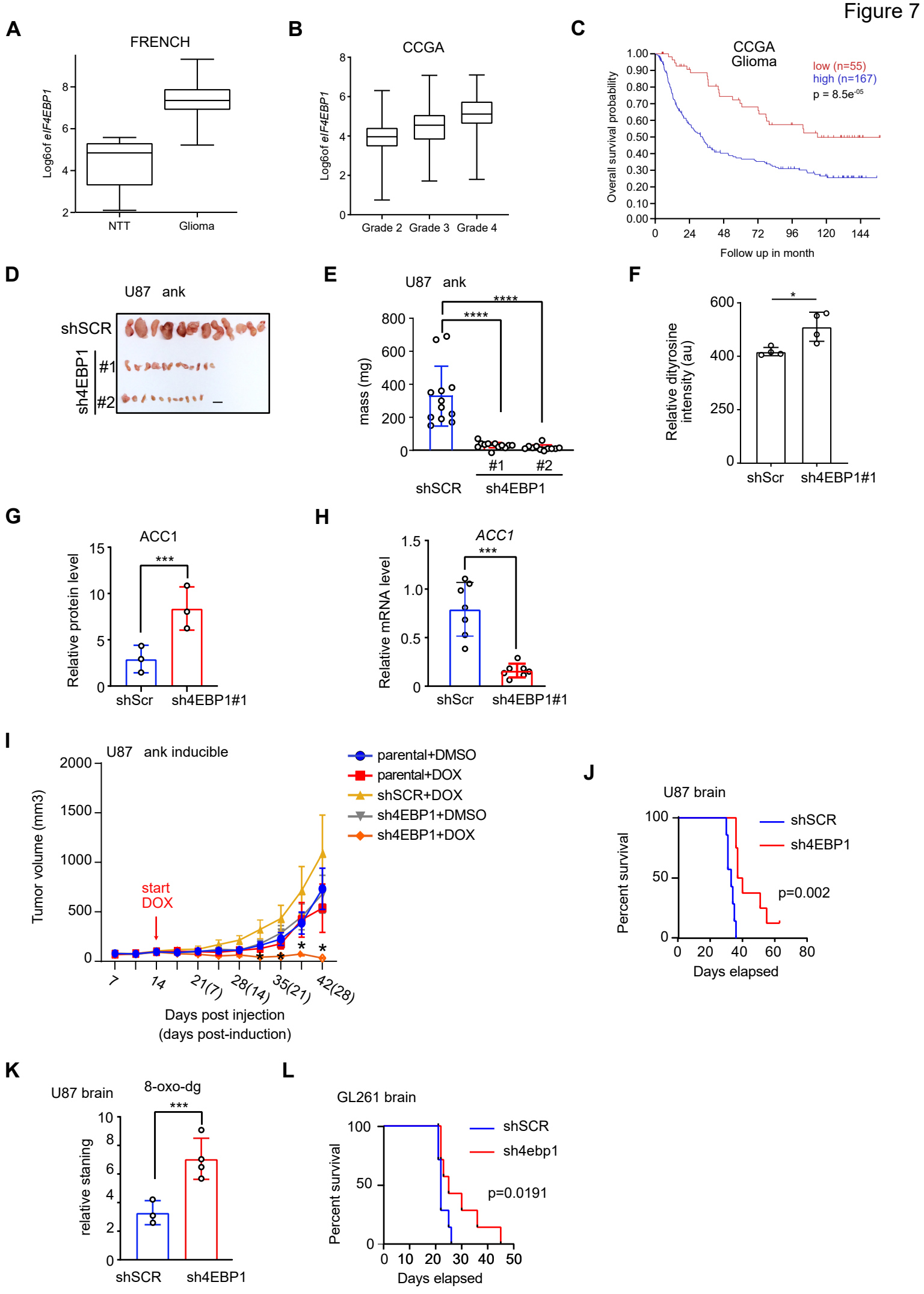
A
FRENCH
Log6of eIF4EBP1
NTT
Glioma
B
CCGA
Log6of eIF4EBP1
Grade 2
Grade 3
Grade 4
C
CCGA
Glioma
low (n=55)
high (n=167)
p = 8.5e-05
Overall survival probability
Follow up in month
D
U87 ank
shSCR
sh4EBP1
#1
#2
E
U87 ank
mass (mg)
****
****
#1
#2
shSCR
sh4EBP1
F
Relative dityrosine intensity (au)
*
shScr
sh4EBP1#1
G
ACC1
Relative protein level
***
shScr
sh4EBP1#1
H
ACC1
Relative mRNA level
***
shScr
sh4EBP1#1
I
U87 ank inducible
Tumor volume (mm3)
parental+DMSO
parental+DOX
shSCR+DOX
sh4EBP1+DMSO
sh4EBP1+DOX
start DOX
Days post injection
(days post-induction)
J
U87 brain
Percent survival
shSCR
sh4EBP1
p=0.002
Days elapsed
K
U87 brain
8-oxo-dg
relative staning
***
shSCR
sh4EBP1
L
GL261 brain
Percent survival
shSCR
sh4ebp1
p=0.0191
Days elapsed

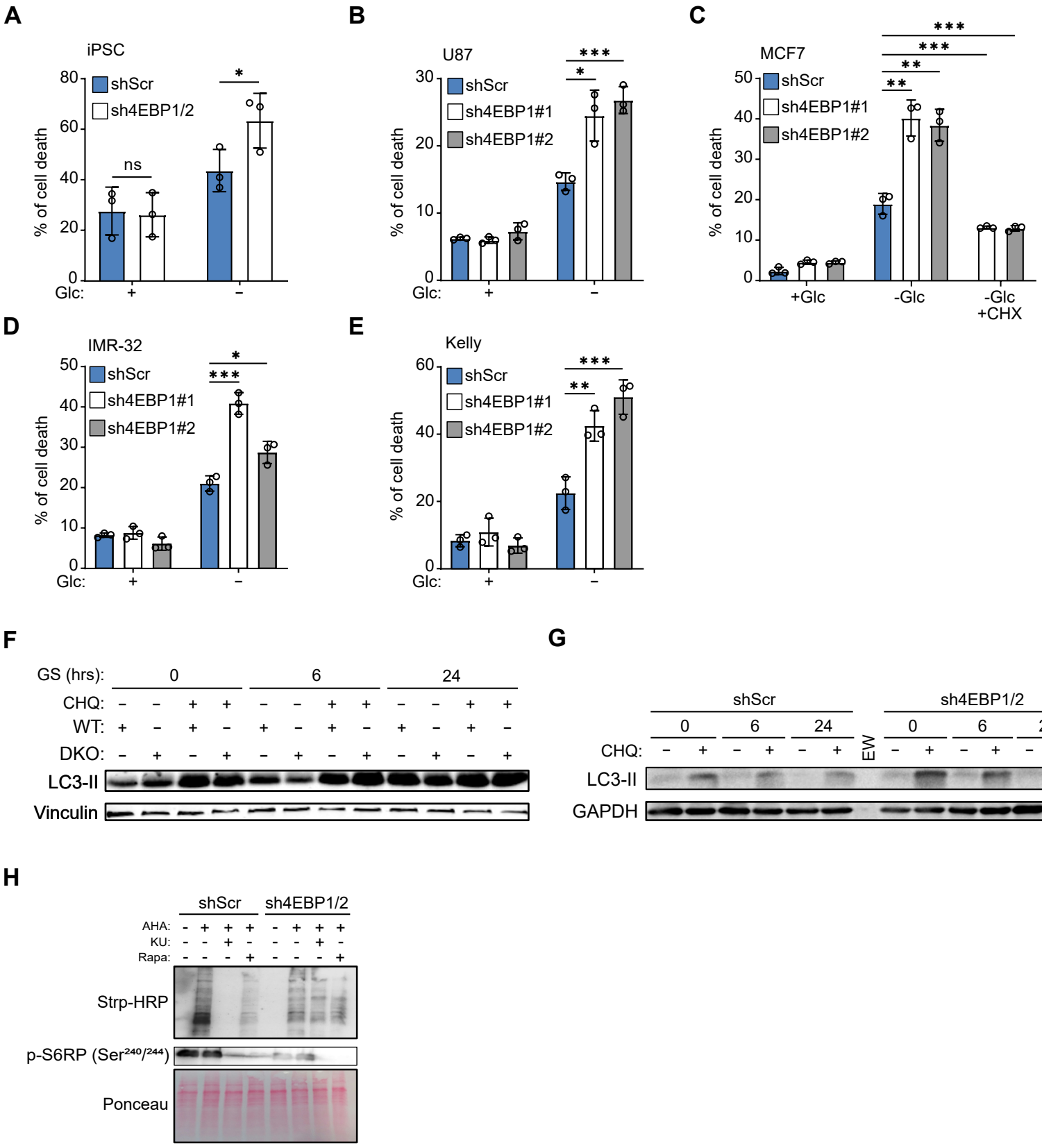

Suppl Figure 1

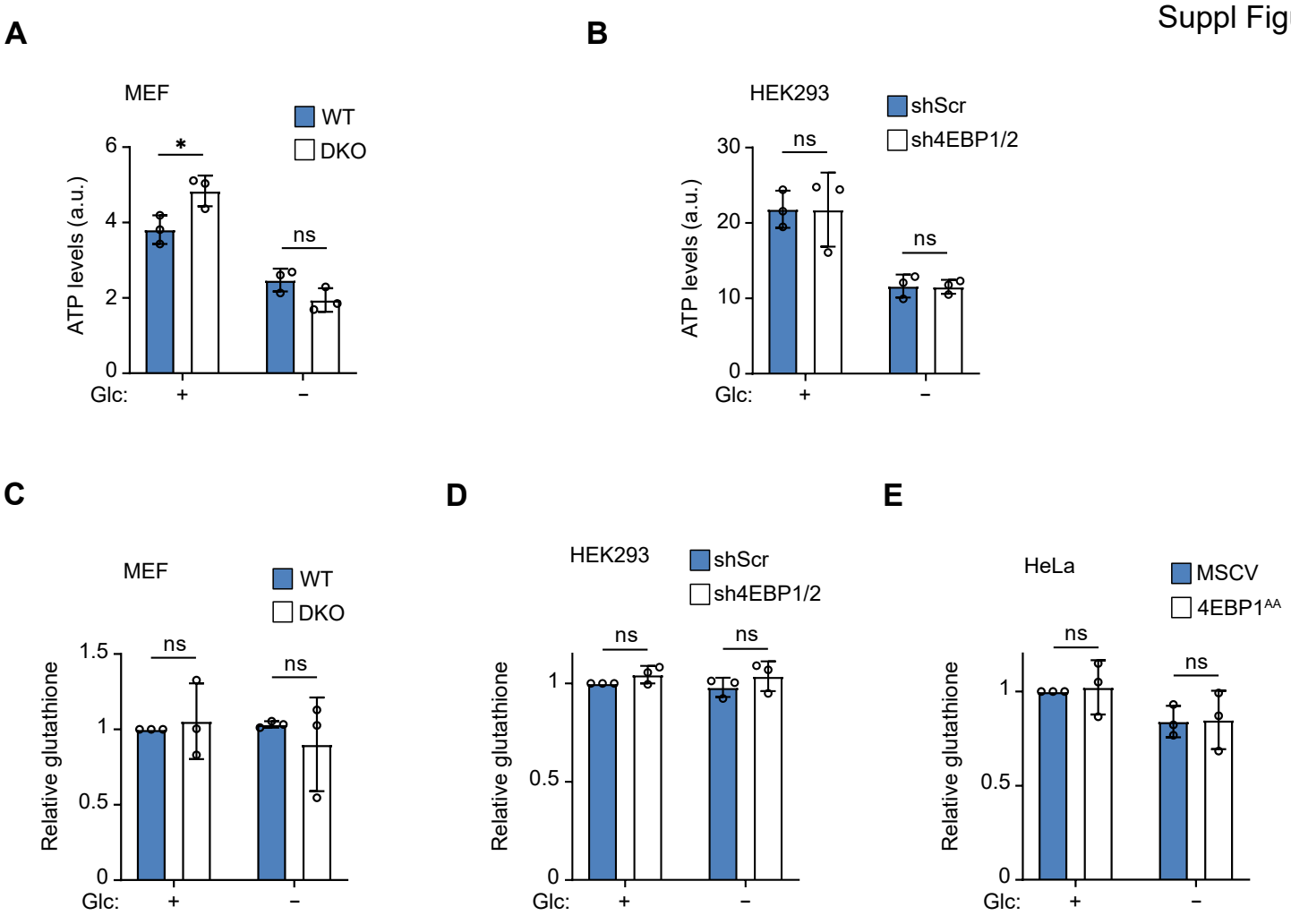
A
MEF
WT
DKO
ATP levels (a.u.)
6
4
2
0
*
ns
Glc:
+
–
B
HEK293
shScr
sh4EBP1/2
ATP levels (a.u.)
30
20
10
0
ns
ns
Glc:
+
–
C
MEF
WT
DKO
Relative glutathione
1.5
1
0.5
0
ns
ns
Glc:
+
–
D
HEK293
shScr
sh4EBP1/2
Relative glutathione
1
0.5
0
ns
ns
Glc:
+
–
E
HeLa
MSCV
4EBP1AA
Relative glutathione
1
0.5
0
ns
ns
Glc:
+
–

A

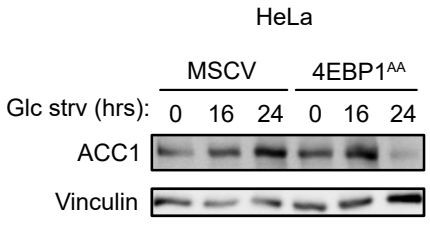

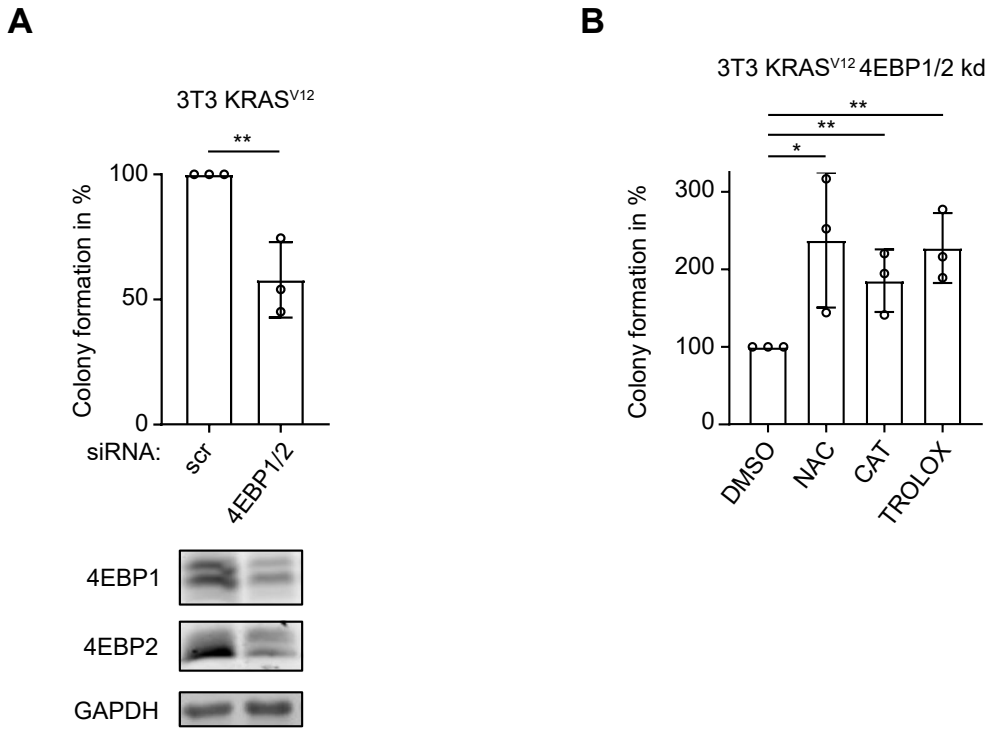
A
3T3 KRAS^{V12}
**
100
50
0
Colony formation in %
siRNA:
scr
4EBP1/2
4EBP1
4EBP2
GAPDH
B
3T3 KRAS^{V12} 4EBP1/2 kd
**
**
*
300
200
100
0
Colony formation in %
DMSO
NAC
CAT
TROLOX

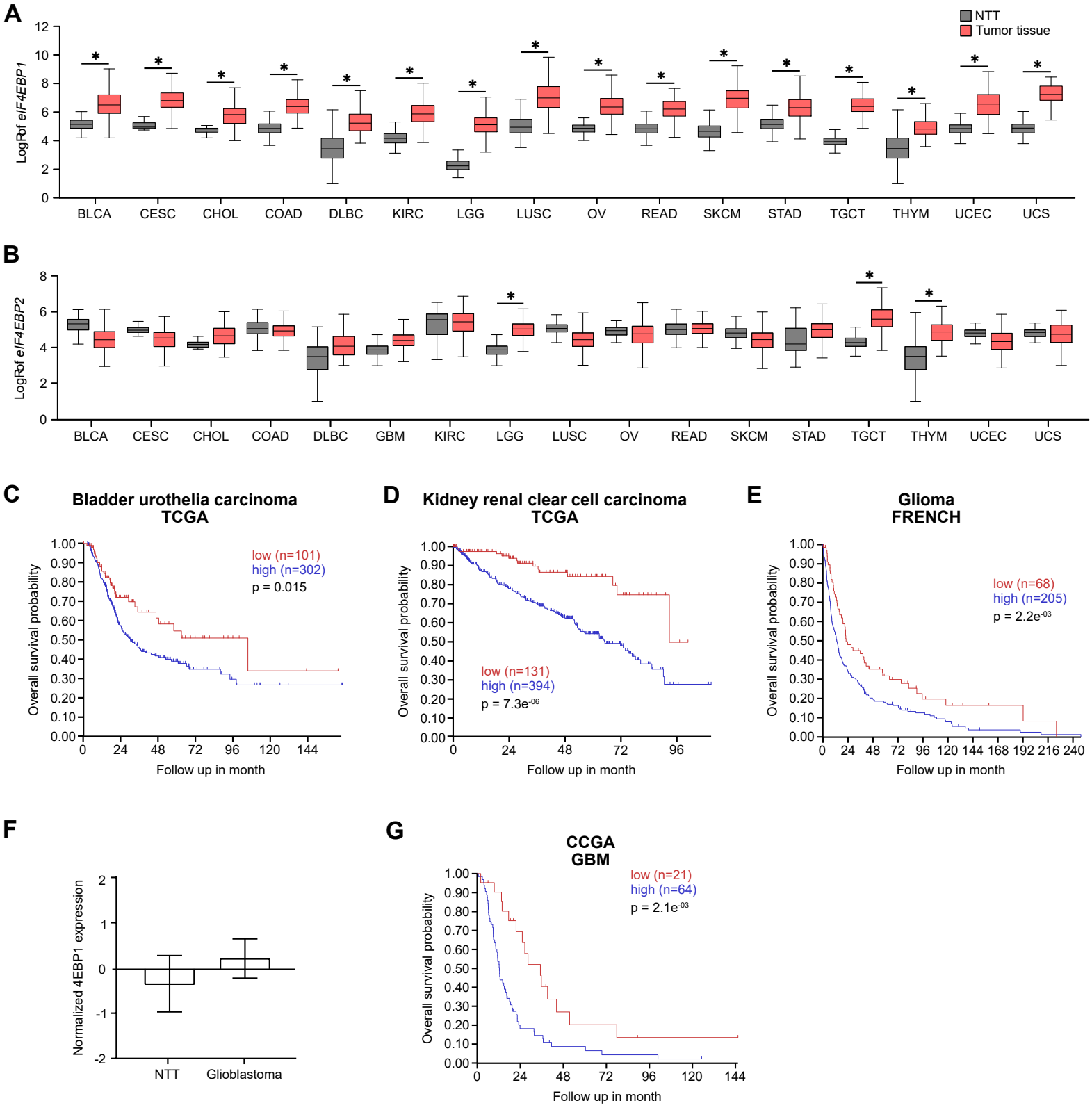

Suppl Figure 5

Suppl Figure 6

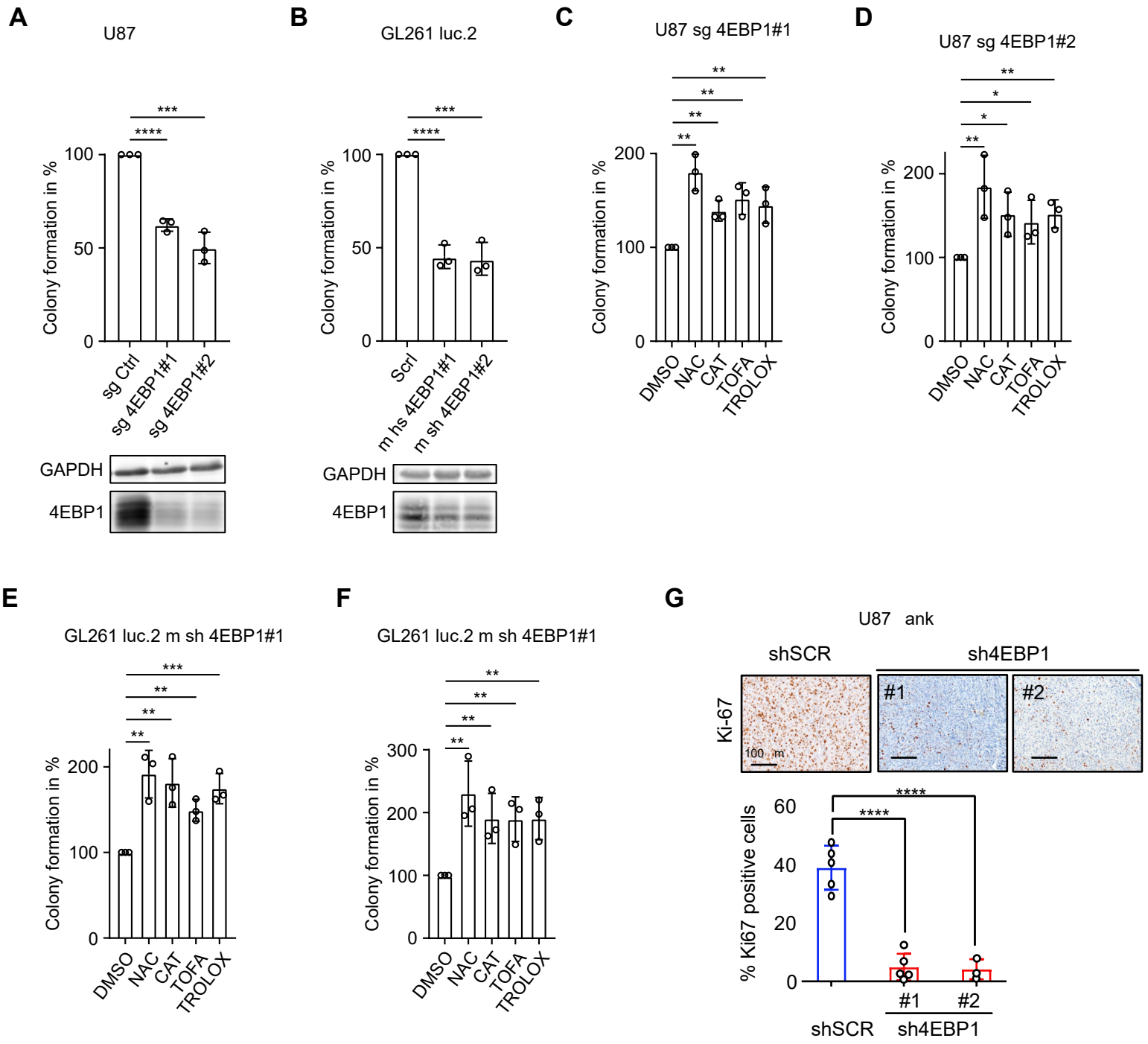

3.2 The type of cell death under glucose starvation

Following the demonstration presented in manuscript 2 that 4EBPs are crucial to support metabolic adaptation and ensure survival under glucose deprivation, the question of how 4EBPs-deficient cells die under glucose starvation remained. Even though it may look trivial, it is not clear which type of cell death is generally induced by prolonged glucose starvation.

Few types of cell death have been proposed to be induced by glucose starvation including apoptosis (Zhao et al. 2008; Caro-Maldonado et al. 2010; Alves et al. 2006), necrosis (Suzuki et al. 2003; Yuneva et al. 2007; León-Annicchiarico et al. 2015), necroptosis (Ding et al. 2016) and entosis (Hamann et al. 2017). Since these types of cell death can be selectively and individually inhibited by specific compounds, the usage of such inhibitors is a common way to delineate the type of cell death (Galluzzi et al. 2018). To characterize the type of cell death occurring in 4EBPs-deficient cells under glucose deprivation the major forms of cell death, namely apoptosis, necroptosis as well as ferroptosis, were blocked by pharmacological inhibition. Ferroptosis, which is strongly connected to GSH depletion and peroxidized lipids, has been shown to be induced by oxygen-glucose deprivation (Li et al. 2018). Since own data showed that glucose deprivation triggers GSH depletion, increased ROS, and accumulation of fatty acids in 4EBPs-deficient cells, there was a presumption that ferroptosis could be involved. Thus, glucose-starved 4EBPs DKO MEFs were incubated with a range of frequently used inhibitors including zVAD, necrostatin 1 stable (NEC1S), and ferrostatin 1 (FER1), which block induction of apoptosis, necroptosis or ferroptosis, respectively. However, none of these compounds significantly reduced cell death in 4EBP-deficient MEFs under glucose depletion (Figure 3.1.1).

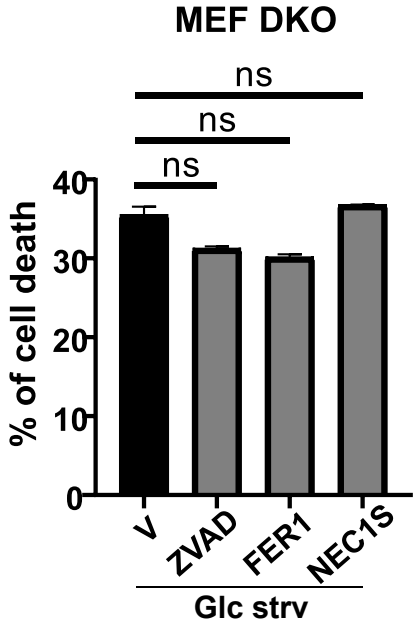

Figure 3.1.1: Treatment of 4EBPs DKO MEFs under glucose starvation. Cells were glucose starved for 48h and treated with vehicle (V) of the indicated cell death inhibitors (10 μM apoptosis inhibitor [ZVAD], 5 μM ferroptosis inhibitor ferrostatin-1 [FER1] or 5 μM necroptosis inhibitor necrostatin-1 stable [NEC1S]). Tested for significance with t-test.

Electron microscopy was then used to further delineate the type of cell death induced in 4EBPs-deficient cells under glucose starvation. This represents another means to identify types of cell death, as it enables to visualize specific subcellular structures including endoplasmic reticulum, mitochondria, nucleus, and cell membrane to search for specific morphological features. For instance, apoptosis is tightly connected to cell condensation, nuclear fragmentation and membrane blebbing (Galluzzi et al. 2018), while necrotic cells show increase in volume until cellular content leaks. Thus, electron microscopy was applied to examine the ultrastructural morphology of both HEK293 sh4EBP1/2 and shScr cells as well as MEF 4EBP1/2 DKO and WT cells under control or glucose-starved conditions (see Figure 3.1.2/3).

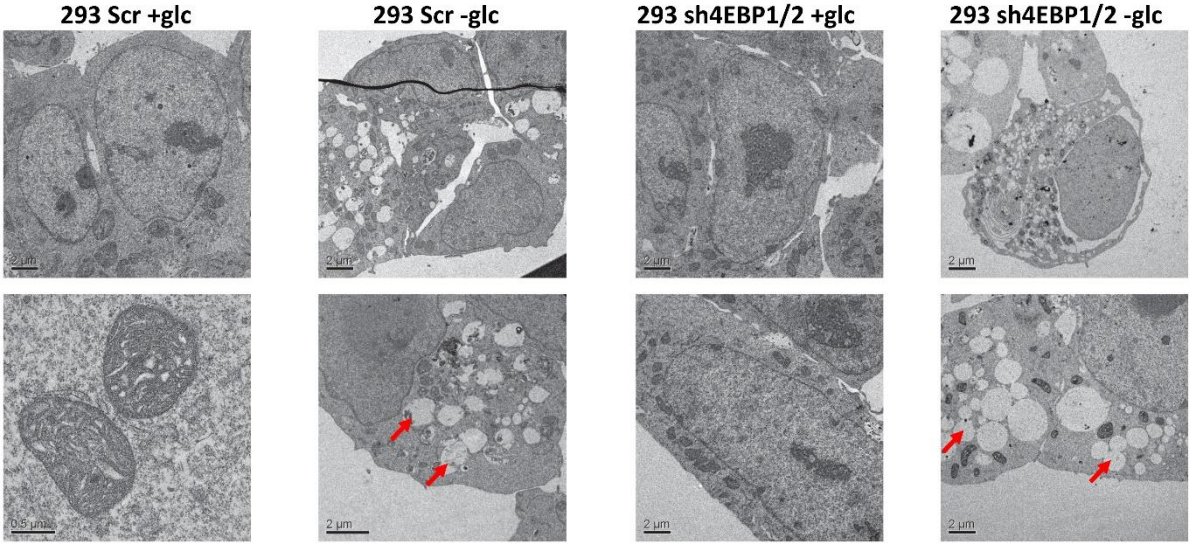

Figure 3.1.2: Representative EM images of control or 4EBPs-deficient HEK293s. Cells were incubated under control conditions or glucose-starved for approximately 30h. Arrows indicate vacuole formation as can be seen in both control and 4EBPs-deficient cells upon glucose starvation. Cell culture, sample preparation and image acquisition were carried out by Tal Levy from the Rotblat's lab.

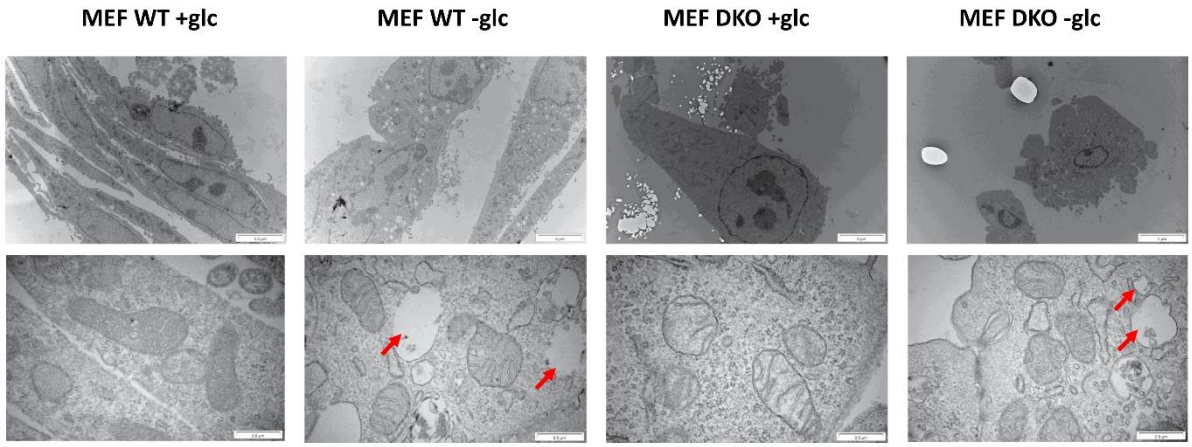

Figure 3.1.3: Representative EM images of WT and 4EBP1/2 DKO MEFs. Cells were incubated under control conditions or glucose-starved for approximately 30h. Arrows indicate vacuole formation as can be seen in both control and 4EBP-deficient cells upon glucose starvation. Cell culture carried out by Kai Völtzke; sample preparation and EM image acquisition performed by Ruchika Anand and Andrea Borchardt as described in (Anand et al. 2016).

Under glucose starvation, morphology of control and 4EBPs-deficient 293 and MEF cells showed no nuclear fragmentation and no membrane blebbing, confirming the absence of apoptosis induction. However, a large number of cytoplasmic vacuoles were seen in glucose-starved conditions when compared to basal conditions. These vacuoles lack any double membrane layers, suggesting that they do not represent autophagosomes. The appearance of such cytoplasmic vacuoles is characteristic of some programmed forms of necrosis, such as paraptosis (Wang et al. 2021). This type of cell death is associated to proteotoxic stress, ER and mitochondria swelling and the formation of cytoplasmic vacuoles (Sperandio et al. 2000). While the mechanisms governing the induction and proceedings of paraptosis are poorly understood, this type of cell death was shown to be suppressed by pharmacological inhibition of protein synthesis (by cycloheximide [CHX]) or of transcription (by actinomycin D [ACD]). This fits well with the own results showing that CHX can rescue the phenotype of 4EBPs-deficient cells under glucose starvation (see Figure 1 of manuscript 2). In addition to CHX, glucose-starved MEF 4EBP1/2 DKO cells could be rescued from cell death by supplementation of ACD (Figure 3.1.4). In conclusion, 4EBP-deficient cells likely undergo paraptosis upon prolonged glucose starvation.

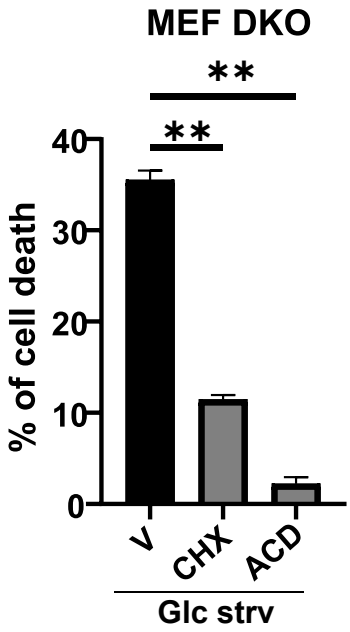

Figure 3.1.4: Treatment of 4EBPs-deficient MEFs under glucose starvation. Cells were glucose starved for 48h and treated with vehicle (V), 1 µg/ml protein synthesis inhibitor cycloheximide (CHX), or 40 nM transcriptional inhibitor actinomycin D (ACD). Tested for significance with t-test.

Paraptosis has not been attributed to any physiological stimuli but rather to treatment with certain compounds that induce ER stress. Mechanistically, however, glucose deprivation was

proposed to cause both reduced protein glycosylation and accumulation of unfolded proteins together leading to proteotoxicity and ER stress (Ding et al. 2016). This could thus possibly lead to paraptosis, especially in conditions where ATP is depleted which preclude induction of apoptosis as previously reported (Leist et al. 1997; Eguchi et al. 1997). Therefore, the type of cell death induced by glucose starvation was studied in a selection of wildtype (and therefore 4EBP-proficient) cells. These experiments showed that glucose starvation-induced cell death was not prevented by zVAD, FER1 or NEC1S but only by treatment with CHX and ACD in a selection of wild type cells including MEF 4EBP1/2 WT cells, NIH3T3 cells, HeLa cells and iPSCs (Figure 3.1.5). It is important to mention that this preliminary screen consists only of technical replicates and thus needs to be reproduced. However, the strong trend detected in these preliminary experiments indicates that glucose starvation does not induce apoptosis, ferroptosis or necroptosis in the examined cell lines but potentially triggers paraptosis.

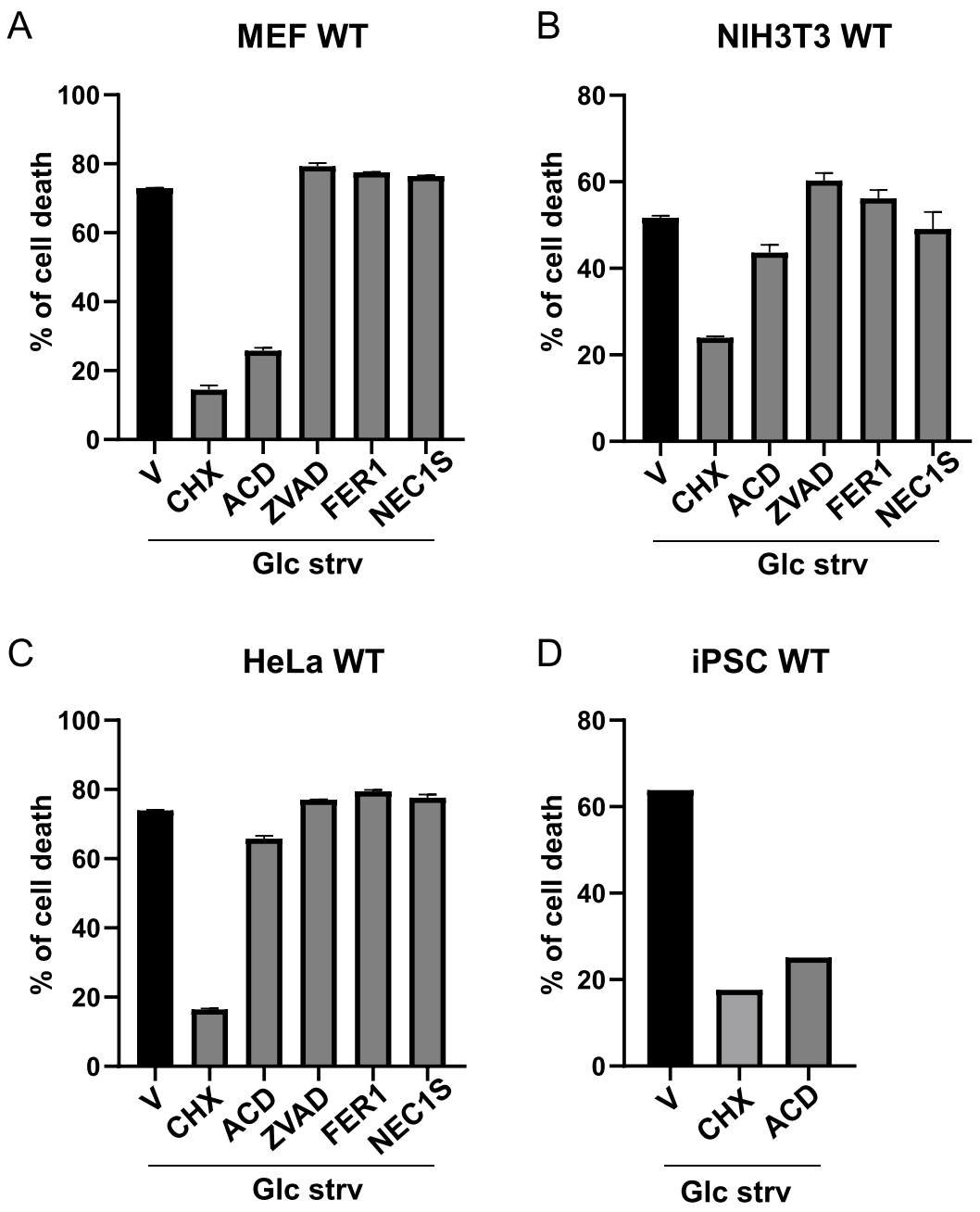

Figure 3.1.5: Treatment of 4EBP-proficient WT cells under glucose starvation. MEF (A), NIH 3T3 (B), HeLa (C) and iPS (D) cells were glucose starved for 72h and treated vehicle (V), apoptosis inhibitor ZVAD, ferroptosis inhibitor ferrostatin-1 (FER1), necroptosis inhibitor necrostatin-1 stable (NEC1S), protein synthesis inhibitor cycloheximide (CHX), or transcriptional inhibitor actinomycin D (ACD). Only technical replicates were measured in this preliminary screen.

Therefore, one might hypothesize that glucose deprivation induces paraptosis or paraptosis-like forms of cell death independently of 4EBPs. The data suggest that 4EBPs may serve to prolong cell survival under glucose-deprived conditions by delaying the induction of paraptosis. Further experiments are needed to fully validate this hypothesis, especially to ensure that the type of cell death is indeed paraptosis. Since glucose starvation reflects a physiological condition that normal cells but also cancer cells frequently encounter, improved understanding of how low levels of glucose mechanistically induce paraptosis or other related forms of cell death would be highly desirable.

4. Manuscript 3 – EIF4EBP1 is transcriptionally upregulated by MYCN and associates with poor prognosis in neuroblastoma

EIF4EBP1 is transcriptionally upregulated by MYCN and associates with poor prognosis in neuroblastoma

Kai Voeltzke[1], Katerina Scharov[1,2], Cornelius Funk[3,4,5], Alisa Kahler[1], Daniel Picard[1,2,6,7], Laura Hauffe[1], Martin F. Orth[3], Marc Remke[1,2,6,7], Irene Esposito[8], Thomas Kirchner[9,10], Alexander Schramm[11], Barak Rotblat[12], Thomas G. P. Grünewald[3,4,5,13], Guido Reifenberger[1,7], Gabriel Leprivier[1*]

[1]Institute of Neuropathology, Heinrich Heine University, Medical Faculty, and University Hospital Düsseldorf, Düsseldorf, Germany.
[2]Department of Pediatric Oncology, Hematology, and Clinical Immunology, Heinrich Heine University, Medical Faculty, and University Hospital Düsseldorf, Düsseldorf, Germany.
[3]Max-Eder Research Group for Pediatric Sarcoma Biology, Institute of Pathology, Faculty of Medicine, LMU Munich, Munich, Germany.
[4]Division of Translational Pediatric Sarcoma Research, German Cancer Research Center (DKFZ), Heidelberg, Germany.
[5]Hopp Children's Cancer Center (KiTZ), Heidelberg, Germany.
[6]Division of Pediatric Neuro-Oncogenomics, DKFZ, Heidelberg, Germany
[7]German cancer consortium (DKTK), partner site Essen/Düsseldorf, Düsseldorf, Germany.
[8]Institute of Pathology, Heinrich Heine University, Medical Faculty, and University Hospital Düsseldorf, Düsseldorf, Germany.
[9]Institute of Pathology, Faculty of Medicine, LMU Munich, Munich, Germany.
[10]German cancer consortium (DKTK) partner site Munich, Munich, Germany.
[11]Department of Medical Oncology, West German Cancer Center, University of Duisburg-Essen, Essen, Germany.
[12]Department of Life Sciences, Ben-Gurion University of the Negev, Beer Sheva, Israel; The National Institute for Biotechnology in the Negev, Beer Sheva, Israel.
[13]Institute of Pathology, Heidelberg University Hospital, Heidelberg, Germany.

Key words: Neuroblastoma, MYCN, mTOR, 4EBP1

***Corresponding author:**
Dr. Gabriel Leprivier, Institute of Neuropathology, Heinrich Heine University Düsseldorf, Moorenstrasse 5, D-40225 Düsseldorf, Germany; E-mail: gabriel.leprivier@med.uni-duesseldorf.de.

ABSTRACT

Background

Neuroblastoma (NB) accounts for 15% of cancer-related deaths in childhood despite considerable therapeutic improvements. While several risk factors, including *MYCN* amplification and alterations in RAS and p53 pathway genes, have been defined in NB, there remains a need for more precise prediction of response to therapy and outcome in the individual patient. Since genes of the mTOR pathway are up-regulated in *MYCN*-amplified NB, we aimed to define the predictive value of the mTOR substrate-encoding gene eukaryotic translation initiation factor 4E-binding protein 1 (*EIF4EBP1*) expression in NB patients.

Methods

Several independent NB patient cohorts with corresponding mRNA expression data were analyzed for *EIF4EBP1* expression. An institutional NB cohort consisting of 69 prospectively collected tumors was employed to immunohistochemically analyze expression of *EIF4EBP1*-encoded protein (4EBP1). In addition, we performed an *in vitro* luciferase reporter gene assay with an episomal *EIF4EBP1* promoter and genetically modulated *MYCN* expression in NB cells.

Findings

EIF4EBP1 mRNA expression was positively correlated with *MYCN* expression and elevated in stage 4 and high-risk NB patients. High *EIF4EBP1* mRNA expression was associated with reduced overall and event-free survival in the entire group of NB patients in three cohorts, as well as in stage 4 and high-risk patients. High levels of 4EBP1 were significantly associated with prognostically unfavorable NB histology. Functional analyses *in vitro* revealed that *EIF4EBP1* expression is transcriptionally controlled by MYCN binding to the *EIF4EBP1* promoter.

Interpretation

High *EIF4EBP1* expression is associated with poor prognosis in NB patients and may serve to stratify patients with high-risk NB.

Funding

G.L. was supported by funding from the Elterninitiative Düsseldorf e.V., the Research Commission of the Medical Faculty of Heinrich Heine University, the Deutsche Forschungsgemeinschaft (Grant LE 3751/2-1), and the German Cancer Aid (Grant 70112624). The laboratory of T.G.P.G. is supported by the Barbara und Wilfried Mohr Foundation. BR is supported by the the Israel Science Foundation (grant No. 1436/19).

Abstract word count (excluding funding section): 249 words.

RESEARCH IN CONTEXT

Evidence before this study

NB represents a particularly heterogeneous cancer entity, with 5-year event-free survival rate ranging from 50% to 98% depending on the patient's risk group. While genes of the nutrient-sensing mTOR pathway were found to be up-regulated in *MYCN*-amplified NB tumors, their clinical relevance and prognostic value in NB patients remain unclear. In particular, the mTOR substrate-encoding gene *EIF4EBP1* was studied in NB by three different groups and high *EIF4EBP1* mRNA expression was observed in *MYCN*-amplified or contradictorily in more favorable stages 1 and 2 patients. Also, *EIF4EBP1* was included in a prognostic gene signature for poor overall survival in NB. However, the prognostic value of *EIF4EBP1* alone was not determined in NB and the expression of *EIF4EBP1* encoded protein, 4EBP1, was not analyzed in NB tumor tissues and not correlated with clinicopathological features such as histological subtypes. Additionally, the transcriptional regulation of the *EIF4EBP1* promoter by MYCN was not characterized.

Added value of this study

This study uncovers the prognostic potential of *EIF4EBP1* at the mRNA and protein levels in NB patients. We report that high *EIF4EBP1* expression is correlated with poor survival in three independent cohorts and that high 4EBP1 levels is associated with a prognostically unfavorable histological subtype. High *EIF4EBP1* expression is also a factor of poor prognosis in stage 4 and high-risk patient groups. Finally, we found that MYCN activates the human *EIF4EBP1* promoter through binding at three binding motifs.

Implications of all the available evidence

EIF4EBP1 mRNA and 4EBP1 protein expression have prognostic value in NB, especially to stratify patients with advanced and more aggressive NB, such as patients with stage 4 disease and high-risk patients including those with unfavorable histological subtype NB. Enhanced *EIF4EBP1* mRNA and 4EBP1 protein expression in NB are driven by direct transcriptional activation of *EIF4EBP1* by MYCN.

INTRODUCTION

Neuroblastoma (NB) is a pediatric malignant tumor that develops from progenitor cells of the sympathetic nervous system and the adrenal glands [1,2]. NB is the most commonly occurring extracranial solid tumor in childhood and the major cause of cancer-related mortality in infants [2]. NB tumors are classified into five stages (1, 2, 3, 4 and 4S) according to tumor size, the presence of metastasis and the outcome of surgical resection [1]. Noteworthy, stage 4S represents a special form of NB in infants that is associated with a high chance of spontaneous regression despite metastatic spread [1]. Apart from surgical resection, treatment options may include response-adjusted chemotherapy for low to intermediate risk groups or a mix of surgery, high-dose chemotherapy, immunotherapy, and radiation for patients belonging to the high-risk group. The risk level is determined based on the tumor stage combined with age at diagnosis, tumor ploidy, genetic alterations and tumor histology [1,3]. However, NB represents a particularly heterogeneous type of cancer, posing challenges to precisely predict therapeutic response and clinical outcome in the individual patient [4,5]. While some NB tumors may spontaneously regress, high-risk patients have an increased likelihood of relapse and available treatment options for relapsed patients are rarely successful. Indeed, the 5-year event-free survival rate for high-risk patients is less than 50%, in contrast to 90-98% for low-risk patients [6]. In addition, success rates of second line treatment in relapsed patients remain poor [5,7]. Therefore, it is critical to define novel stratification factors for NB patients to better predict individual risk and to facilitate administration of the most appropriate therapeutic option.

NB is rarely familial (1-2%) and only few predisposition genes, such as *PHOX2B* and *ALK*, have been reported [4,8–10]. Genetically, several acquired alterations have been detected in NB and linked to patient outcome. These include gain-of-function mutations in *ALK*, gain of chromosome arm 17q, loss of chromosome arm 11q, amplification of *MYCN* [4], and, more recently reported, alterations in genes related to the RAS and p53 pathways [11]. *MYCN* amplification is found in about 20% of NB and is associated with aggressive tumors, therapy resistance and poor survival [6]. *MYCN* is a member of the *MYC* oncogene family and encodes a transcription factor that recognizes a specific DNA element referred to as E-box [12,13]. This

allows MYCN to regulate the transcription of genes involved in cell cycle progression, proliferation, differentiation and survival [6]. MYCN is a strong driver of NB tumorigenesis, as tissue-specific overexpression of MYCN is sufficient to induce NB tumor development in mouse models [14]. Mechanistically, MYCN is proposed to rewire metabolism to enable NB tumor cells to proliferate, in turn preserving the intracellular redox balance while producing enough energy by inducing a glycolytic switch [15–17]. In particular, MYCN actively augments the transcription of multiple genes whose products are involved in the protein synthesis machinery [16]. Even though MYCN represents a highly attractive therapeutic target in NB, as a transcription factor that lacks hydrophobic pockets which can be targeted by drug-like small molecules, it is still considered as being “undruggable” [18,19]. Thus, identification of downstream effectors involved in MYCN-driven NB progression is a promising approach to uncover novel targets for molecularly guided therapeutic approaches.

To better delineate the molecular basis of *MYCN*-amplified NB aggressiveness, several approaches have been undertaken. In particular, RNA-sequencing (RNA-seq) has been used to uncover the set of genes induced in *MYCN*-amplified compared to *MYCN*-non-amplified NB [20]. Strikingly, this analysis identified regulators of protein synthesis which are components of the mechanistic target of rapamycin (mTOR) pathway, including the mTOR target eukaryotic initiation factor 4E binding protein 1 (*EIF4EBP1*). The corresponding protein, 4EBP1, is inhibited through mTOR-mediated phosphorylation when nutrients are available, leading to active mRNA translation initiation [21]. Under nutrient-deprived conditions, when mTOR is inhibited, 4EBP1 gets activated and thus binds to the translation initiation factor eIF4E, in turn blocking cap-dependent mRNA translation initiation [21]. At the cellular level, 4EBP1 is negatively regulating proliferation and mitochondrial activity [22,23]. The exact role of 4EBP1 in cancer is still debated. 4EBP1 was found to exert a tumor suppressive function *in vivo*, as 4EBP1 knock-out leads to enhanced tumor formation in mouse models of head and neck squamous cell carcinoma [24], and prostate cancer [25]. In contrast, 4EBP1 was shown to mediate angiogenesis and facilitate tumor growth in a breast cancer model *in vivo*, highlighting a cancer type-specific function of 4EBP1 [26]. In keeping with that, the clinical relevance of

EIF4EBP1 expression depends on the tumor type. *EIF4EBP1* was reported to be overexpressed in a number of tumor entities in adults [27], including breast cancer [28], in which *EIF4EBP1* is amplified as part of the 8p11-12 amplicon, as well as in ovarian and prostate cancer [29,30]. In breast and liver cancer, high *EIF4EBP1* expression has been associated with poor survival [28,31]. In contrast, *EIF4EBP1* expression was found to be reduced in head and neck cancer, in which low expression is correlated with poor prognosis [24]. In NB, the expression of *EIF4EBP1* is deregulated, even though contradictory findings have been reported. While *EIF4EBP1* was characterized as a gene upregulated in *MYCN*-amplified versus *MYCN*-non-amplified NB tissues and cells [20], another study reported that *EIF4EBP1* levels were higher in favorable stages of NB as compared to advanced stage 4 tumors [32]. In addition, Meng *et al.* showed that *EIF4EBP1* is part of a gene signature that predicts poor overall survival [33]. However, it was not investigated whether *EIF4EBP1* expression alone can predict NB patient prognosis. Thus, the clinical relevance of *EIF4EBP1* expression in NB needs further evaluation. Overexpression of *EIF4EBP1* in cancer is mediated by certain transcription factors, such as MYC [34], androgen receptor [35], and the stress regulators ATF4 [36] and HIF-1α [37], which all bind to and thereby modulate the activity of the *EIF4EBP1* promoter. More specifically, ChIP-sequencing (ChIP-seq) revealed binding of MYCN to the *EIF4EBP1* promoter in NB cells, and MYCN was reported to impact *EIF4EBP1* transcription, pointing to *EIF4EBP1* as a potential MYCN target gene [38,39]. However, how MYCN exactly controls the *EIF4EBP1* promoter is still poorly understood.

In this study, we analyzed publicly available NB patient data sets and revealed that *EIF4EBP1* is overexpressed in NB compared to normal tissues, is significantly co-expressed with *MYCN*, and is elevated in high-risk relatively to low-risk tumor groups. High *EIF4EBP1* levels were found to be significantly linked to poor overall survival in all NB patients, as well as in the more aggressive stage 4 and high-risk groups. In addition, immunohistochemistry staining of NB tissues confirmed the mRNA-based associations and showed that high 4EBP1 protein expression associates with unfavorable histology in NB. Finally, by applying gene reporter

assays and by modulating MYCN expression *in vitro*, we found that MYCN upregulates the *EIF4EBP1* promoter activity by binding to three distinct E-boxes.

MATERIALS AND METHODS

Databases

The RNA-seq, microarray and ChIP-seq data were retrieved from 'R2: Genomics Analysis and Visualization Platform' (http://r2.amc.nl). Data were visualized with IGV or Affinity Designer. For the MYCN occupancy profile in BE(2)-C cells, the ChIP-seq data by Durbin *et al.* (GSE94824) were accessed using the human genome GRCh 38/hg 38. For the initial across dataset analysis, four publicly available and independent cohorts, namely the Versteeg *et al.* (GSE16476), Lastowska *et al.* (GSE13136), Hiyama *et al.* (GSE16237), and Delattre *et al.* (GSE14880) datasets were used. The remaining expression, amplification and survival data consisted of the independent SEQC/ MAQC-III Consortium GSE49710), Kocak *et al.* study (GSE45547) and Neuroblastoma Research Consortium [NRC] (GSE49710), Kocak (GSE45547) and NRC (GSE85047) cohorts. For the expression analysis of TH-MYCN transgenic NB model, the dataset from Balamuth *et al.* (GSE17740) was used.

Immunohistochemistry

For immunohistochemistry, deparaffinated tissue sections were pretreated with citrate buffer at 98°C for 20 min, cooled down to room temperature, and blocked with 2% horse serum, avidin blocking solution and biotin blocking solution (Avidin/Biotin Blocking Kit, SP-2001, Vector Laboratories, Burlingame, CA, USA) for 10 min each. Staining for 4EBP1 was carried out with monoclonal anti-4EBP1 raised in rabbit (1:200; ab32024, Abcam, Cambridge, UK) for 2 h at 37°C. Detection was carried out using the Dako REAL detection system, alkaline phosphatase/RED, rabbit/mouse following manufacturer´s instructions (Detection Kit #K5005, Agilent Technologies, Santa Clara, CA, USA). Immunostained tissue sections were

counterstained with hematoxylin solution according to Mayer (T865.1, Roth, Karlsruhe, Germany).

Evaluation of immunoreactivity of 4EBP1 was carried out in analogy to scoring of hormone receptor Immune Reactive Score (IRS) ranging from 0–12. The percentage of cells with expression of the given antigen was scored and classified in five grades (grade 0 = 0–19%, grade 1 = 20–39%, grade 2 = 40–59%, grade 3 = 60–79% and grade 4 = 80−100%). In addition, the intensity of marker immunoreactivity was determined (grade 0 = none, grade 1 = low, grade 2 = moderate and grade 3 = strong). The product of these two grades defined the final IRS. IRS 0-6 was considered as "low" staining level while IRS 7-12 was categorized as "high" staining level.

Tissue microarrays (TMAs) were constructed by taking three representative cores (each 1 mm in diameter) from respective blocks exhibiting at least 80% viable tumor tissue. Tumor blocks were retrieved from the archives of the Institutes of Pathology of the LMU Munich or the University Hospital Düsseldorf with IRB approval (study numbers 550-16 UE for LMU Munich and 2018-174 for the University Hospital Düsseldorf).

Statistics

All experiments were, if not otherwise stated, independently carried out at least three times. Statistical significance was calculated using Student’s t-test or Mann-Whitney U-test in GraphPad Prism 8. For survival analysis, the cohorts were stratified based on relative expression of *EIF4EBP1*. The median was chosen as expression cutoff to determine high and low *EIF4EBP1* level. Statistical significance was determined by the logrank test. Multivariate analysis was performed using the Cox Regression method in SPSS v21 (IBM). To calculate significance of the scoring of immunohistochemistry staining, the Chi-square test was used. The data are represented as means +/- standard deviation. A p-value of less than 0.05 was considered significant.

Cell culture

Cells were maintained using standard tissue culture procedures in a humidified incubator at 37°C with 5% CO_2 and atmospheric oxygen. NB cell lines IMR-32 and Kelly, and HEK-293-T cells were obtained from American Type Culture Collections (ATCC, Manassas, VA, USA). SHEP-TR-MYCN engineered NB cell lines have been previously described [17]. NB cell lines were cultured in Roswell Park Memorial Institute (RPMI)-1640 medium (Thermo Fisher Scientific, Waltham, MA, USA), while HEK-293-T cells were maintained in Dulbecco's modified Eagle medium (DMEM) (Thermo Fisher Scientific). All cell culture media were supplemented with 10% (volume/volume) fetal bovine serum (FBS) (Sigma-Aldrich, St. Louis, MI, USA) and 1% penicillin/streptomycin (Thermo Fisher Scientific). Cells were treated with 3 µg/ml plasmocin (Invivogen, San Diego, CA, USA) to prevent mycoplasma contamination. To induce MYCN expression, SHEP-TR-MYCN cells were treated with 1 µg/ml doxycycline. All cell lines were routinely confirmed to be mycoplasma-free using Venor®GeM Classic kit (Minerva Biolabs, Berlin, Germany). Cell lines were authenticated by STR-profiling (Genomics and Transcriptomics Laboratory, Heinrich Heine University, Germany).

RNA extraction, cDNA synthesis and quantitative real time PCR

Total RNA was purified from cells using the RNeasy plus mini kit (QIAgen, Hilden, Germany) according to the manufacturer's handbook. RNA concentration and purity were assessed by spectrophotometry using the NanoDrop2000 (Thermo Fisher Scientific). Subsequently, each sample was diluted to a concentration of 100 ng/µl in nuclease-free water. For cDNA synthesis, 1 µg RNA was processed in a total reaction volume of 20 µl using the High-Capacity cDNA Reverse Transcription kit (Applied Biosystems, Waltham, MA, USA), following the manufacturer's protocol. Quantitative real time reverse transcription PCR was performed using SYBR green PCR master mix (Applied Biosystems) and the CFX384 Touch Real-Time PCR Detection System (Bio-Rad Laboratories, Hercules, CA, USA). Relative expression levels of *MYCN* and *EIF4EBP1* were normalized to internal housekeeping genes *GUSB* and *PPIA*. The primer list can be found in supplementary table 1.

Immunoblot analysis of protein expression

Cells were washed with phosphate buffered saline (PBS) and lysed in radioimmunoprecipitation assay (RIPA) buffer (150 mM NaCl, 50 mM Tris-HCl, pH 8, 1% Triton X-100, 0.5% sodium deoxycholate, and 0.1% SDS) supplemented with protease inhibitors (Sigma-Aldrich) and phosphatase inhibitors mix (PhosphoSTOP, Roche, Penzberg, Germany). Cell lysates were centrifuged at 21,000 rpm for 15 min at 4°C to separate cell debris and DNA from protein lysates. Protein concentration was measured with the BCA protein assay kit (Thermo Fisher Scientific), according to manufacturer's protocol. Protein lysates were separated by SDS-PAGE and transferred onto a nylon membrane. The membrane was incubated for 1 h in Tris-buffered saline Tween (TBST) (50 mM Tris-Cl, 150 mM NaCl, pH 7.5, 0.1% Tween-20) containing 5% bovine serum albumin (BSA), to prevent non-specific antibody binding, followed by an overnight incubation at 4°C with the following primary antibodies: 4EBP1 (1:1,000, Cell Signaling Technology, Cambridge, UK #9644), MYCN (1:1,000, Cell Signaling #9405), GAPDH (1:1,000, Cell Signaling #2118), and β-Actin (1:5,000, Sigma-Aldrich #A2228). The secondary antibodies IRDye 800CW Goat anti-Rabbit (1:10,000, LI-COR Biosciences, Bad Homburg, Germany #926-32211) or IRDye 800CW Goat anti-Mouse (1:10,000, LI-COR Biosciences #926-32210) were incubated at room temperature for 1 h, followed by detection of the fluorescent signal with the Odyssey CLx imager (LI-COR Biosciences).

Plasmid construction

The promoter region of the human *EIF4EBP1* gene, spanning from -192 to +1372, was inserted into the SacI and BglII restriction sites of the Firefly Luciferase expressing pGL4.22 plasmid (Promega, Madison, WI, USA). Each of the three identified MYCN binding site was subsequently mutated alone or in a combination of two sites. Each of the E-box sequence has been mutated to CAAGGC. All cloning was performed by GENEWIZ Germany GmbH (Leipzig, Germany).

Luciferase Reporter Assay

For the promoter reporter assay, HEK-293-T cells were seeded into 12-well plates and co-transfected the following day with 500 ng of the *EIF4EBP1* WT or mutant promoter pGL4.22 plasmids, 50 ng of the MYCN overexpressing pcDNA3.1 plasmid or empty pcDNA3.1 plasmid, and 3 ng of the *Renilla* Luciferase expressing pRL-SV40 plasmid (Promega) for normalization. For transfection, plasmids were incubated with 3 µl CalFectin (SignaGen laboratories, Rockville, MD, USA) in Opti-MEM (Thermo Fisher Scientific) for 20 min before adding the mix dropwise onto the cells. 48 h post-transfection, cells were passively lysed and processed according to the protocol of the Dual-Luciferase® Reporter Assay System (Promega), besides using only half the recommended volume of detection buffers. Firefly and *Renilla* luciferase activities were sequentially measured using a Tecan Spark plate reader and the ratio of firefly luciferase to *Renilla* luciferase luminescence was calculated. The experiments were repeated independently for three times.

RESULTS

***EIF4EBP1* expression is increased in NB and correlates with *MYCN* expression**

To assess the clinical significance of *EIF4EBP1* expression, we first examined *EIF4EBP1* mRNA levels in NB tumor tissue samples and normal tissues. We pooled microarray data of four different NB cohorts and retrieved expression data from adrenal tissue used as the corresponding normal tissue (Fig. 1a). This indicated that *EIF4EBP1* expression is significantly elevated in NB compared to adrenal gland ($p<0.0001$, Fig. 1a). We then determined whether *EIF4EBP1* expression is related to the *MYCN* amplification status. By comparing the level of *EIF4EBP1* in *MYCN*-amplified versus *MYCN*-non-amplified NB samples, we found that *EIF4EBP1* is expressed at higher levels in *MYCN*-amplified compared to *MYCN*-non-amplified NB in the SEQC and Kocak cohorts [40,41] ($p<0.0001$, Fig. 1b; $p<0.0001$, Fig. 1c). This further supports and extends previous observations made in a limited number of NB samples (n=20) showing *EIF4EBP1* overexpression in *MYCN*-amplified versus *MYCN*-non-amplified NB

tumors [20]. Since *MYCN* amplification may result in different levels of *MYCN*, we next investigated whether expression levels of *MYCN* and *EIF4EBP1* in NB correlate with each other. Our analyses highlight a significant coexpression between *MYCN* and *EIF4EBP1* in the SEQC (correlation coefficient [r]=0.564, p<0.0001, Fig. 1d) and Kocak ([r]=0.532, p<0.0001, Fig. 1e) cohorts. These findings are in line with the reports that *EIF4EBP1* is a potential MYCN target gene in NB [38,39]. We also assessed whether the expression of *EIF4EBP1* is determined by NB stages or risk groups, and found that *EIF4EBP1* levels are increased according to NB tumor aggressiveness in two cohorts (Fig. 1f&g). In particular, *EIF4EBP1* is expressed at higher levels in stage 4 NB tumors as compared to stage 1 and stage 2 tumors (stage 4 versus stage 1, p<0.0001, Fig. 1f; p<0.0001 Fig. 1g). Interestingly, samples from stage 4S NB showed significantly lower *EIF4EBP1* levels compared to stage 4 tumors (stage 4S versus stage 4, p<0.01, Fig. 1f; p<0.001, Fig. 1g). In support of this finding, we observed that in the SEQC cohort *EIF4EBP1* expression is higher in high-risk compared to low-risk NB, as based on the Children's Oncology Group (COG) classification (p<0.0001, Fig. 1h). Such clinical information was not available in any other publicly available cohorts with mRNA expression data. Taken together, we present evidence that *EIF4EBP1* is commonly overexpressed in NB tumors and that *EIF4EBP1* level is increased in *MYCN*-amplified NB and advanced NB stages.

EIF4EBP1 expression is a factor of poor prognosis in NB

Since we found *EIF4EBP1* mRNA levels to be elevated in aggressive NB subsets, we examined whether *EIF4EBP1* expression is linked to prognosis in NB patients. Kaplan-Meier estimates univocally showed that high *EIF4EBP1* levels (using median expression level as cut off) were significantly associated with reduced overall and event-free survival in three independent cohorts, namely SEQC, Kocak and NRC cohorts [42] (p=3.1e-08, Fig. 2a; p=4.2e-11, Fig. 2b; p=1.7e-06, Fig. 2c, and supplementary Fig. 1a, b&c). To test dependence of *EIF4EBP1* expression as prognostic factor on established factors of poor prognosis, we performed multivariate analysis to determine the statistical interaction between high *EIF4EBP1*

expression and *MYCN* amplification status, tumor stage or age at diagnosis. This indicated that *MYCN* amplification status, tumor stage and age at diagnosis each influenced the prognostic value of high *EIF4EBP1* expression in the SEQC and NRC cohorts (Tables 1&2). Therefore, high *EIF4EBP1* expression is not an independent factor of poor prognosis in NB. However, we uncovered that *EIF4EBP1* expression can predict overall survival in clinically relevant NB subsets, including more advanced and aggressive NB subgroups. Indeed, our analyses highlighted that high *EIF4EBP1* expression significantly predicted reduced overall survival in *MYCN*-non-amplified patients of the SEQC and NRC cohorts (p=3.8e-03, Fig. 2d; p=0.04, Fig. 2e), while it was significant for event-free survival only in the SEQC cohort (supplementary Fig. 1d&e). On the other hand, Kaplan-Meier survival estimates in high-risk NB patients (SEQC cohort) revealed that high *EIF4EBP1* levels were correlated with poor overall survival (p=7.4e-03, Fig. 2f), as well as with reduced event-free survival (supplementary Fig. 1f), suggesting that *EIF4EBP1* expression can stratify patients within the most aggressive NB subset. We additionally analyzed the prognostic value of *EIF4EBP1* expression in stage 4 NB patients. We found high *EIF4EBP1* expression to significantly predict decreased overall and event-free survival of stage 4 patients in two independent cohorts (SEQC and NRC cohorts) (p=3.2e-04 Fig. 2g; p=3.8e-03, Fig. 2h and supplementary Fig. 1g&h). This highlights that *EIF4EBP1* expression robustly stratifies patients within the advanced NB subgroups. Altogether, our analyses support that *EIF4EBP1* expression is a factor of poor prognosis in all NB, as well as in high-risk and stage 4 NB.

High 4EBP1 protein expression is associated with prognostically unfavorable histology of NB

To independently confirm the prognostic value of *EIF4EBP1*/4EBP1 in NB and to determine the biomarker potential of 4EBP1 protein expression in NB, we immunohistochemically analyzed NB TMAs consisting of 69 patient samples. Staining of the TMAs with a 4EBP1-specific antibody revealed a cytoplasmic staining (Fig. 3a), consistent with the expected cellular localization of 4EBP1 [43]. We semi-quantitatively evaluated 4EBP1 staining intensity

and correlated 4EBP1 immunoreactivity with the NB histological subtypes according to the International Neuroblastoma Pathology Classification (INPC), which distinguishes patients with favorable or unfavorable histology based on grade of neuroblastic differentiation and mitosis-karyorrhexis index. We found that tumors with unfavorable histology more frequently exhibited a high 4EBP1 staining score (IRS 7-12) as compared to tumors with favorable histology (Fig. 3b), indicating that high 4EBP1 protein expression is associated with more aggressive NB subsets.

EIF4EBP1 promoter activity and transcription is controlled by MYCN

To delineate how elevated *EIF4EBP1* expression is mechanistically connected to *MYCN* amplification and overexpression in NB, we investigated the transcriptional regulation of *EIF4EBP1* by MYCN. A previous report detected the presence of MYCN on *EIF4EBP1* promoter by ChIP in BE(2)-C, a *MYCN*-amplified NB cell line [38,39]. We validated and further extended this finding by analyzing ChIP-seq data available from an additional *MYCN*-amplified NB cell line, Kelly. This revealed that MYCN binds the endogenous *EIF4EBP1* promoter region (which encompasses exon 1 and a part of intron 1) at three distinct positions, indicating three potential MYCN binding sites (Fig. 4a). *In silico* analysis of the promoter region sequence confirmed the presence of structural E-boxes at the three occupied locations (Fig. 4b). To evaluate the impact of MYCN on the regulation of *EIF4EBP1* promoter activity, we designed a luciferase-based gene reporter assay by cloning the *EIF4EBP1* promoter region (-192 to +1372) in front of a Firefly Luciferase gene (Fig. 4b). The activity of the wildtype *EIF4EBP1* promoter was dose-dependently increased upon forced expression of MYCN in HEK-293-T cells (supplementary Fig. 2a), which was accompanied by an upregulation of endogenous 4EBP1 protein level (supplementary Fig. 2b). To investigate which E-boxes are necessary for the transcriptional activation of the *EIF4EBP1* promoter by MYCN, either a single or a combination of two of the three potential binding sites were mutated. Mutation of either of the three binding sites alone was sufficient to reduce MYCN-induced promoter activity by at least 50% (Fig. 4c). Any combinations of two mutated binding sites virtually abolished promoter

activity driven by MYCN overexpression (Fig. 4c), suggesting that two binding sites, without a specific preference of one over another, are needed for full induction of *EIF4EBP1* promoter activity by MYCN. We next intended to confirm whether MYCN directly regulates *EIF4EBP1* transcription in NB cell lines. To do so, we chose two *MYCN*-amplified NB cell lines, IMR-32 and Kelly, in which we knocked down MYCN expression by siRNA and examined the impact on *EIF4EBP1* mRNA levels by qPCR. The depletion of *MYCN* caused a significant reduction of *EIF4EBP1* transcript levels in both cell lines (Fig. 4d&e). To further support these observations, we assessed the impact of forced MYCN expression on *EIF4EBP1* transcript and protein levels by using SHEP-TR-MYCN cells, which are *MYCN*-non-amplified NB cells engineered to express exogenous MYCN with a tetracycline inducible system [17]. Doxycycline treatment markedly increased *EIF4EBP1* mRNA level over time (Fig. 4f), in parallel with progressive upregulation of MYCN expression (Fig. 4g). This was accompanied by a net increase in the 4EBP1 protein level (Fig. 4g), supporting that MYCN positively controls *EIF4EBP1* mRNA and protein expression in NB cells. In accordance with these findings, analyses of expression data from a transgenic mouse model of MYCN-driven NB (TH-MYCN; [44]) revealed that *EIF4EBP1* expression is upregulated in NB tumors as compared to the corresponding normal tissue, i.e. the ganglia (Fig. 4h). Taken together, our data provide further evidence that *EIF4EBP1* is a transcriptional target of MYCN, potentially providing a mechanistic basis for the observed overexpression of *EIF4EBP1* in *MYCN*-amplified NB patients.

DISCUSSION

MYCN-amplification is accountable for aggressive NB subsets as it has been associated with increased risk of relapse and reduced overall survival of patients [6]. Since MYCN is considered “undruggable”, there is a demand for identifying targetable downstream effectors of MYCN [18,19]. In addition, since NB is a clinically heterogenous disease, ranging from spontaneous regression to progression despite aggressive therapies, novel markers that improve patient risk stratification and hence allow for optimal treatment allocation are

warranted [4]. Here, we report that *EIF4EBP1* expression levels are significantly elevated in NB compared to corresponding non-tumor tissues and positively correlate with both *MYCN* expression and *MYCN* amplification status in at least two independent NB patient cohorts. Furthermore, using three independent NB cohorts, we report that high *EIF4EBP1* expression is a strong predictor of poor overall and event-free survival across all NB patients. This was not independent of *MYCN* amplification status, tumor stage or age at diagnosis, which can be explained in part by the regulation of *EIF4EBP1* promoter by MYCN which we characterized. However, *EIF4EBP1* expression can predict prognosis within distinct patient groups like the *MYCN*-non-amplified patients subset, for which little biomarkers have been identified. Moreover, we observed that high *EIF4EBP1* expression was associated with poor prognosis in the group of patients with aggressive stage 4 NB. Of note, less than a third of stage 4 patients carry a *MYCN* amplification. Thus, it may be worth considering that, in addition to *MYCN* amplification status, levels of *EIF4EBP1* expression could help identifying patients carrying clinically more aggressive tumors within the stage 4 NB patients group. *EIF4EBP1* expression was also linked to worse outcome among high-risk NB patients. Given that *MYCN* amplification is not able of predicting outcome within high-risk NB patients [45], it appears that *EIF4EBP1* expression has a prognostic power beyond *MYCN* amplification in this patient subset. Thus, *EIF4EBP1* expression may represent a promising biomarker for prognostic stratification of high-risk NB patients, in addition to the recently reported genetic alterations in the RAS and p53 pathways [11]. This is further supported by the association we observed between high 4EBP1 protein expression and unfavorable NB histological subtype. Together, our findings highlight a previously underappreciated prognostic factor, i.e., *EIF4EBP1*/4EBP1, which may help refining risk stratification of NB patients, including *MYCN*-non-amplified, stage 4 and high-risk patients, and could potentially assist in tailoring more personalized treatment options. Beyond NB, *EIF4EBP1* expression was reported to be a factor of poor prognosis in breast and liver cancers [28,31], as well as in all TCGA tumor types combined [27]. While our data indicate that *EIF4EBP1* expression has prognostic power in pediatric cancer, together this supports

that *EIF4EBP1* expression represents a factor of poor prognosis in a large number of different tumor types.

Our study also extends previous knowledge by providing further experimental evidence to explain the association between *EIF4EBP1* and *MYCN* expression in NB and the overexpression of *EIF4EBP1* in *MYCN*-amplified NB. Our data revealed that MYCN induces transcription of *EIF4EBP1* by regulating its promoter through multiple binding sites, which was originally suggested by detection of MYCN binding to the *EIF4EBP1* promoter by ChIP analysis [38,39]. However, whether MYCN could transcriptionally regulate the *EIF4EBP1* promoter was still elusive. We demonstrate that MYCN activates the *EIF4EBP1* promoter through binding at three distinct E-boxes, which in turn leads to transcriptional increase of *EIF4EBP1*. Together with the previous ChIP analysis, this supports that *EIF4EBP1* is a direct target gene of MYCN in NB cells. These findings are in line with a previous study reporting that MYC controls *EIF4EBP1* by binding its endogenous promoter in colorectal cancer cells [46], highlighting a general regulation of *EIF4EBP1* by MYC family members in cancer cells.

Expression levels of *EIF4EBP1* appear not only elevated in *MYCN*-amplified versus *MYCN*-non-amplified NB but are also upregulated in *MYCN*-non-amplified tumors relative to control tissue. It might be speculated that in *MYCN*-non-amplified NB, *EIF4EBP1* expression may be regulated by transcription factors other than MYCN. In particular, ATF4, which is critical for the metabolic response of NB cells to glutamine starvation [47,48], has been shown to control *EIF4EBP1* promoter and transcription in pancreatic beta cells [36]. This transcription factor is highly expressed in NB, and in particular in advanced stage 4 [48]. In addition, another transcription factor that is commonly overexpressed in NB is OCT4 [49]. Of note, this transcription factor has been identified by ChIP-seq to bind the promoter region of *EIF4EBP1* in human embryonic stem cells [50,51], thus OCT4 may also activate *EIF4EBP1* transcription in NB cells. Together, these data suggest potential mechanisms underlying the MYCN independent regulation of *EIF4EBP1* expression in *MYCN*-non-amplified NB patients.

Given the prognostic significance of *EIF4EBP1*/4EBP1 in NB, it is possible that 4EBP1 confers advantages to NB tumor growth or tumor cell survival. As evidenced by the presence of

necrotic areas flanked by HIF-1α positive staining [52], NB experience metabolic stress, corresponding to nutrient deprivation and hypoxia, as a consequence of abnormal and immature vascularization [53,54]. One important mechanism for cancer cells to adapt to metabolic stress is through reprogramming of mRNA translation [55]. As a major regulator of mRNA translation, 4EBP1 may aid NB cells to cope with hypoxia and nutrient deprivation. This is supported by the report that 4EBP1 promotes survival of breast tumors under hypoxia by stimulating the synthesis of pro-angiogenic factors, like HIF-1α and VEGF, to facilitate tumor angiogenesis *in vivo* [26]. In addition, the control of mRNA translation was shown to be critical to prevent the deleterious effects of MYCN and MYC overexpression, as we and others previously reported [46, 56]. In fact, 4EBP1, by reducing overall protein synthesis, was reported to prevent cell death induced upon MYC overexpression, likely by blunting accumulation of misfolded proteins and proteotoxic ER stress [46]. It is possible that in a similar manner 4EBP1 contributes to inhibit cell death induced by MYCN overexpression in *MYCN*-amplified NB.

In summary, the findings reported here indicate that *EIF4EBP1* is a direct target gene of MYCN in NB, explaining the observed high expression of *EIF4EBP1* in NB, and that *EIF4EBP1* mRNA and protein expression have prognostic values in NB patients, especially for stratifying high-risk NB patients.

ACKNOWLEDGEMENTS

We would like to thank Dr. Bastian Malzkorn (Institute of Neuropathology, Heinrich Heine University Düsseldorf) for helpful discussions.

DECLARATION OF INTERESTS

The authors declare no conflict of interest.

AUTHORS CONTRIBUTION

Conception and design: Kai Voeltzke and Gabriel Leprivier.

Provision of study material and patients: Irene Esposito and Thomas Kirchner.

Financial and administrative support: Guido Reifenberger.

Data analysis and interpretation: Kai Voeltzke, Thomas G. P. Grünewald, Alexander Schramm, and Gabriel Leprivier.

Critical review and discussion: Barak Rotblat, Marc Remke, Alexander Schramm, Guido Reifenberger, and Gabriel Leprivier.

Experimental support: Kai Voeltzke, Katerina Scharov, Cornelius Funk, Alisa Kahler, Daniel Picard, Laura Hauffe, and Martin F. Orth.

Manuscript writing: Kai Voeltzke, Guido Reifenberger, and Gabriel Leprivier.

Final approval of the manuscript: All authors.

FIGURE LEGENDS

Figure 1: *EIF4EBP1* mRNA expression is associated with *MYCN* mRNA expression and is increased in more advanced and aggressive NB subsets.

(a) Expression levels of *EIF4EBP1* mRNA in a pool of four different NB cohorts (total n=203), compared to healthy control tissues (adrenal gland, n=13). (b, c) Expression levels of *EIF4EBP1* mRNA n *MYCN*-amplified (n=92, SEQC [b] and n=93, Kocak [c]) compared to *MYCN*-non-amplified (n=401, SEQC [b] and n=550 Kocak [c]) NB patients of the SEQC (b) and Kocak (c) cohorts. (d, e) Expression levels of *EIF4EBP1* mRNA plotted against expression levels of *MYCN* mRNA in SEQC (r=0.5637, d) and Kocak (r=0.5321, e) cohorts. (f, g) Expression levels of *EIF4EBP1* mRNA per NB stage in SEQC (f) and Kocak (g) cohorts. (h) Expression levels of *EIF4EBP1* mRNA in high-risk (n=176) compared to non-high-risk (n=322) NB in the SEQC cohort. Data were retrieved from the R2: Genomics Analysis and Visualization Platform. Statistics were determined using Mann-Whitney U-test. Exact p-values are presented. **P*<0.05, ***P*<0.01, ****P*<0.001, *****P*<0.0001.

Figure 2: *EIF4EBP1* mRNA expression correlates with overall survival in NB patients.

(a-c) Kaplan-Meier survival estimates of overall survival of NB patients stratified by their *EIF4EBP1* mRNA expression levels (median cut off) in the SEQC (a), Kocak (b) and NRC (c)

cohorts. (d-h) Kaplan-Meier survival estimates of overall survival of patients with *MYCN*-non-amplified NB (d, e), high-risk NB (f) or stage 4 NB (g, h) stratified by their *EIF4EBP1* mRNA expression levels in the indicated NB cohorts. The number of patients at risk (or censored) are reported under the Kaplan-Meier plot by four-year intervals; such information were not accessible for the Kocak cohort. Significance was determined by log rank test. Data were obtained from the R2: Genomics Analysis and Visualization Platform.

Figure 3: 4EBP1 protein expression is associated with histological subtype of NB.
(a) Representative images of low (left panel) and high (right panel) 4EBP1 immunohistochemical staining levels of selected NB samples represented on the NB TMAs. (b) Distribution of NB cases showing low (IRS 0-6) versus high (IRS 7-12) 4EBP1 protein expression in prognostically favorable versus unfavorable histological subtypes according to International Neuroblastoma Pathology Classification (INPC). Fisher's exact test was used to calculate significance. **P*<0.05.

Figure 4: *EIF4EBP1* promoter activity and expression is regulated by MYCN.
(a) ChIP peaks of MYCN in the *EIF4EBP1* promoter region in Kelly NB cell line. (b) Scheme of the *EIF4EBP1* promoter reporter highlighting the three E-boxes corresponding to MYCN binding sites. (c) HEK-293-T were transfected with wildtype or different E-box mutants *EIF4EBP1* promoter Firefly Luciferase constructs with or without a MYCN expressing plasmid (pMYCN). A *Renilla* Luciferase vector was used as an internal control. (d, e) Relative *MYCN* and *EIF4EBP1* mRNA levels upon siRNA-mediated knockdown of *MYCN* in the *MYCN*-amplified IMR-32 (d) and Kelly (e) cell lines, as measured by qRT-PCR. (f, g) SHEP-TR-MYCN cells were treated with doxycycline (1 µg/ml) for the indicated times; *EIF4EBP1* mRNA levels were determined by qRT-PCR (f) and levels of MYCN and 4EBP1 proteins were monitored by immunoblot using the indicated antibodies (g). (h) Relative *EIF4EBP1* mRNA expression in healthy control tissues (ganglia, n=9) and NB tumors (n=26) of a TH-MYCN transgenic mouse model of NB (Balamuth's dataset; [44]). Data were retrieved from the R2: Genomics Analysis

and Visualization Platform. Statistics were determined using Student's t-test or Mann-Whitney U-test. Exact p-values are presented. *P<0.05, **P<0.01, ***P<0.001, ****P<0.0001.

SUPPLEMENTARY FIGURE LEGENDS

Supplementary Figure 1: *EIF4EBP1* mRNA expression correlates with event-free survival in NB patients.

(a-b) Kaplan-Meier survival estimates of event-free survival of NB patients stratified by their *EIF4EBP1* mRNA expression levels (median cut off) in the SEQC (a), Kocak (b) and NRC (c) cohorts. (d-h) Kaplan-Meier estimates of event-free survival of patients with *MYCN*-non-amplified NB (d, e), high-risk NB (f) or stage 4 NB (g, h) stratified by their *EIF4EBP1* mRNA expression levels in the indicated NB cohorts. The number of patients at risk (or censored) are reported under the Kaplan-Meier plot by four-year intervals; such information were not accessible for the Kocak cohort. Significance was determined by log rank test. Data were obtained from the R2: Genomics Analysis and Visualization Platform.

Supplementary Figure 2: MYCN stimulates *EIF4EBP1* promoter activity and 4EBP1 protein expression in a dose-dependent manner.

(a) HEK-293-T cells were transfected with the wildtype *EIF4EBP1* promoter Firefly Luciferase construct and with the indicated amounts of MYCN expressing plasmid (pMYCN). A *Renilla* Luciferase vector was used as an internal control. (b) MYCN and 4EBP1 protein expression was monitored in cell lysates from (a) by immunoblot analyses using the indicated antibodies.

TABLES

Table 1. Multivariate analysis for overall survival of NB patients in the SEQC cohort.

Table 2. Multivariate analysis for overall survival of NB patients in the NRC cohort.

REFERENCES

[1] Maris JM, Hogarty MD, Bagatell R, Cohn SL. Neuroblastoma. The Lancet 2007;369(9579):2106–20. https://doi.org/10.1016/S0140-6736(07)60983-0.

[2] van Arendonk KJ, Chung DH. Neuroblastoma: Tumor Biology and Its Implications for Staging and Treatment. Children (Basel) 2019;6(1). https://doi.org/10.3390/children6010012.

[3] Tolbert VP, Matthay KK. Neuroblastoma: clinical and biological approach to risk stratification and treatment. Cell Tissue Res 2018;372(2):195–209. https://doi.org/10.1007/s00441-018-2821-2.

[4] Maris JM. The biologic basis for neuroblastoma heterogeneity and risk stratification. Current Opinion in Pediatrics 2005;17(1):7–13. https://doi.org/10.1097/01.mop.0000150631.60571.89.

[5] London WB, Castel V, Monclair T, Ambros PF, Pearson ADJ, Cohn SL et al. Clinical and biologic features predictive of survival after relapse of neuroblastoma: a report from the International Neuroblastoma Risk Group project. J Clin Oncol 2011;29(24):3286–92. https://doi.org/10.1200/JCO.2010.34.3392.

[6] Huang M, Weiss WA. Neuroblastoma and MYCN. Cold Spring Harb Perspect Med 2013;3(10):a014415. https://doi.org/10.1101/cshperspect.a014415.

[7] Simon T, Berthold F, Borkhardt A, Kremens B, Carolis B de, Hero B. Treatment and outcomes of patients with relapsed, high-risk neuroblastoma: results of German trials. Pediatric blood & cancer 2011;56(4):578–83. https://doi.org/10.1002/pbc.22693.

[8] Chen Y, Takita J, Choi YL, Kato M, Ohira M, Sanada M et al. Oncogenic mutations of ALK kinase in neuroblastoma. Nature 2008;455(7215):971–4. https://doi.org/10.1038/nature07399.

[9] Mossé YP, Laudenslager M, Longo L, Cole KA, Wood A, Attiyeh EF et al. Identification of ALK as a major familial neuroblastoma predisposition gene. Nature 2008;455(7215):930–5. https://doi.org/10.1038/nature07261.

[10] Janoueix-Lerosey I, Lequin D, Brugières L, Ribeiro A, Pontual L de, Combaret V et al. Somatic and germline activating mutations of the ALK kinase receptor in neuroblastoma. Nature 2008;455(7215):967–70. https://doi.org/10.1038/nature07398.

[11] Ackermann S, Cartolano M, Hero B, Welte A, Kahlert Y, Roderwieser A et al. A mechanistic classification of clinical phenotypes in neuroblastoma. Science (New York, N.Y.) 2018;362(6419):1165–70. https://doi.org/10.1126/science.aat6768.

[12] Zeid R, Lawlor MA, Poon E, Reyes JM, Fulciniti M, Lopez MA et al. Enhancer invasion shapes MYCN-dependent transcriptional amplification in neuroblastoma. Nat Genet 2018;50(4):515–23. https://doi.org/10.1038/s41588-018-0044-9.

[13] Liu R, Shi P, Wang Z, Yuan C, Cui H. Molecular Mechanisms of MYCN Dysregulation in Cancers. Front. Oncol. 2020;10:625332. https://doi.org/10.3389/fonc.2020.625332.

[14] Weiss WA, Aldape K, Mohapatra G, Feuerstein BG, Bishop JM. Targeted expression of MYCN causes neuroblastoma in transgenic mice. The EMBO journal 1997;16(11):2985–95. https://doi.org/10.1093/emboj/16.11.2985.

[15] Oliynyk G, Ruiz-Pérez MV, Sainero-Alcolado L, Dzieran J, Zirath H, Gallart-Ayala H et al. MYCN-enhanced Oxidative and Glycolytic Metabolism Reveals Vulnerabilities for Targeting Neuroblastoma. iScience 2019;21:188–204. https://doi.org/10.1016/j.isci.2019.10.020.

[16] Boon K, Caron HN, van Asperen R, Valentijn L, Hermus MC, van Sluis P et al. N-myc enhances the expression of a large set of genes functioning in ribosome biogenesis and protein synthesis. The EMBO journal 2001;20(6):1383–93. https://doi.org/10.1093/emboj/20.6.1383.

[17] Tjaden B, Baum K, Marquardt V, Simon M, Trajkovic-Arsic M, Kouril T et al. N-Myc-induced metabolic rewiring creates novel therapeutic vulnerabilities in neuroblastoma. Sci Rep 2020;10(1):7157. https://doi.org/10.1038/s41598-020-64040-1.

[18] Bell E, Chen L, Liu T, Marshall GM, Lunec J, Tweddle DA. MYCN oncoprotein targets and their therapeutic potential. Cancer letters 2010;293(2):144–57. https://doi.org/10.1016/j.canlet.2010.01.015.

[19] Wolpaw AJ, Bayliss R, Büchel G, Dang CV, Eilers M, Gustafson WC et al. Drugging the "Undruggable" MYCN Oncogenic Transcription Factor: Overcoming Previous Obstacles to Impact Childhood Cancers. Cancer Res 2021;81(7):1627–32. https://doi.org/10.1158/0008-5472.CAN-20-3108.

[20] Schramm A, Köster J, Marschall T, Martin M, Schwermer M, Fielitz K et al. Next-generation RNA sequencing reveals differential expression of MYCN target genes and suggests the mTOR pathway as a promising therapy target in MYCN-amplified neuroblastoma. International Journal of Cancer 2013;132(3):E106-15. https://doi.org/10.1002/ijc.27787.

[21] Musa J, Orth MF, Dallmayer M, Baldauf M, Pardo C, Rotblat B et al. Eukaryotic initiation factor 4E-binding protein 1 (4E-BP1): a master regulator of mRNA translation involved in tumorigenesis. Oncogene 2016;35(36):4675–88. https://doi.org/10.1038/onc.2015.515.

[22] Morita M, Gravel S-P, Chénard V, Sikström K, Zheng L, Alain T et al. mTORC1 controls mitochondrial activity and biogenesis through 4E-BP-dependent translational regulation. Cell Metabolism 2013;18(5):698–711. https://doi.org/10.1016/j.cmet.2013.10.001.

[23] Dowling RJO, Topisirovic I, Alain T, Bidinosti M, Fonseca BD, Petroulakis E et al. mTORC1-mediated cell proliferation, but not cell growth, controlled by the 4E-BPs. Science (New York, N.Y.) 2010;328(5982):1172–6. https://doi.org/10.1126/science.1187532.

[24] Wang Z, Feng X, Molinolo AA, Martin D, Vitale-Cross L, Nohata N et al. 4E-BP1 Is a Tumor Suppressor Protein Reactivated by mTOR Inhibition in Head and Neck Cancer. Cancer Res 2019;79(7):1438–50. https://doi.org/10.1158/0008-5472.CAN-18-1220.

[25] Ding M, van der Kwast TH, Vellanki RN, Foltz WD, McKee TD, Sonenberg N et al. The mTOR Targets 4E-BP1/2 Restrain Tumor Growth and Promote Hypoxia Tolerance in PTEN-driven Prostate Cancer. Mol Cancer Res 2018;16(4):682–95. https://doi.org/10.1158/1541-7786.MCR-17-0696.

[26] Braunstein S, Karpisheva K, Pola C, Goldberg J, Hochman T, Yee H et al. A hypoxia-controlled cap-dependent to cap-independent translation switch in breast cancer. Molecular cell 2007;28(3):501–12. https://doi.org/10.1016/j.molcel.2007.10.019.

[27] Wu S, Wagner G. Deep computational analysis of human cancer and non-cancer tissues details dysregulation of eIF4F components and their interactions in human cancers. bioRxiv 2020:2020.10.12.336263. https://doi.org/10.1101/2020.10.12.336263.

[28] Karlsson E, Pérez-Tenorio G, Amin R, Bostner J, Skoog L, Fornander T et al. The mTOR effectors 4EBP1 and S6K2 are frequently coexpressed, and associated with a poor prognosis and endocrine resistance in breast cancer: a retrospective study including patients from the randomised Stockholm tamoxifen trials. Breast cancer research BCR 2013;15(5):R96. https://doi.org/10.1186/bcr3557.

[29] Kremer CL, Klein RR, Mendelson J, Browne W, Samadzedeh LK, Vanpatten K et al. Expression of mTOR signaling pathway markers in prostate cancer progression. The Prostate 2006;66(11):1203–12. https://doi.org/10.1002/pros.20410.

[30] Lee M, Kim EJ, Jeon MJ. MicroRNAs 125a and 125b inhibit ovarian cancer cells through post-transcriptional inactivation of EIF4EBP1. Oncotarget 2016;7(8):8726–42. https://doi.org/10.18632/oncotarget.6474.

[31] Cha Y-L, Li P-D, Yuan L-J, Zhang M-Y, Zhang Y-J, Rao H-L et al. EIF4EBP1 overexpression is associated with poor survival and disease progression in patients with hepatocellular carcinoma. PLOS ONE 2015;10(2):e0117493. https://doi.org/10.1371/journal.pone.0117493.

[32] Fransson S, Abel F, Kogner P, Martinsson T, Ejeskär K. Stage-dependent expression of PI3K/Akt-pathway genes in neuroblastoma. International Journal of Oncology 2013;42(2):609–16. https://doi.org/10.3892/ijo.2012.1732.

[33] Meng X, Li H, Fang E, Feng J, Zhao X. Comparison of Stage 4 and Stage 4s Neuroblastoma Identifies Autophagy-Related Gene and LncRNA Signatures Associated With Prognosis. Front. Oncol. 2020;10:1411. https://doi.org/10.3389/fonc.2020.01411.

[34] Balakumaran BS, Porrello A, Hsu DS, Glover W, Foye A, Leung JY et al. MYC activity mitigates response to rapamycin in prostate cancer through eukaryotic initiation factor 4E-binding protein 1-mediated inhibition of autophagy. Cancer Res 2009;69(19):7803–10. https://doi.org/10.1158/0008-5472.CAN-09-0910.

[35] Liu Y, Horn JL, Banda K, Goodman AZ, Lim Y, Jana S et al. The androgen receptor regulates a druggable translational regulon in advanced prostate cancer. Science Translational Medicine 2019;11(503). https://doi.org/10.1126/scitranslmed.aaw4993.

[36] Yamaguchi S, Ishihara H, Yamada T, Tamura A, Usui M, Tominaga R et al. ATF4-mediated induction of 4E-BP1 contributes to pancreatic beta cell survival under endoplasmic reticulum stress. Cell Metabolism 2008;7(3):269–76. https://doi.org/10.1016/j.cmet.2008.01.008.

[37] Azar R, Lasfargues C, Bousquet C, Pyronnet S. Contribution of HIF-1α in 4E-BP1 gene expression. Mol Cancer Res 2013;11(1):54–61. https://doi.org/10.1158/1541-7786.MCR-12-0095.

[38] Cheung CHY, Hsu C-L, Tsuei C-Y, Kuo T-T, Huang C-T, Hsu W-M et al. Combinatorial targeting of MTHFD2 and PAICS in purine synthesis as a novel therapeutic strategy. Cell death & disease 2019;10(11):786. https://doi.org/10.1038/s41419-019-2033-z.

[39] Hsu C-L, Chang H-Y, Chang J-Y, Hsu W-M, Huang H-C, Juan H-F. Unveiling MYCN regulatory networks in neuroblastoma via integrative analysis of heterogeneous genomics data. Oncotarget 2016;7(24):36293–310. https://doi.org/10.18632/oncotarget.9202.

[40] SEQC/MAQC consortium. SEQC/MAQC consortium: A comprehensive assessment of RNA-seq accuracy, reproducibility and information. Nature biotechnology 2014;32(9):903–14. https://doi.org/10.1038/nbt.2957.

[41] Kocak H, Ackermann S, Hero B, Kahlert Y, Oberthuer A, Juraeva D et al. Hox-C9 activates the intrinsic pathway of apoptosis and is associated with spontaneous regression in neuroblastoma. Cell death & disease 2013;4(4):e586. https://doi.org/10.1038/cddis.2013.84.

[42] Rajbhandari P, Lopez G, Capdevila C, Salvatori B, Yu J, Rodriguez-Barrueco R et al. Cross-Cohort Analysis Identifies a TEAD4-MYCN Positive Feedback Loop as the Core Regulatory Element of High-Risk Neuroblastoma. Cancer discovery 2018;8(5):582–99. https://doi.org/10.1158/2159-8290.CD-16-0861.

[43] Armengol G, Rojo F, Castellví J, Iglesias C, Cuatrecasas M, Pons B et al. 4E-binding protein 1: a key molecular "funnel factor" in human cancer with clinical implications. Cancer Res 2007;67(16):7551–5. https://doi.org/10.1158/0008-5472.CAN-07-0881.

[44] Balamuth NJ, Wood A, Wang Q, Jagannathan J, Mayes P, Zhang Z et al. Serial transcriptome analysis and cross-species integration identifies centromere-associated protein E as a novel neuroblastoma target. Cancer Res 2010;70(7):2749–58. https://doi.org/10.1158/0008-5472.CAN-09-3844.

[45] Lee JW, Son MH, Cho HW, Ma YE, Yoo KH, Sung KW et al. Clinical significance of MYCN amplification in patients with high-risk neuroblastoma. Pediatric blood & cancer 2018;65(10):e27257. https://doi.org/10.1002/pbc.27257.

[46] Tameire F, Verginadis II, Leli NM, Polte C, Conn CS, Ojha R et al. ATF4 couples MYC-dependent translational activity to bioenergetic demands during tumour progression. Nature cell biology 2019;21(7):889–99. https://doi.org/10.1038/s41556-019-0347-9.

[47] Qing G, Li B, Vu A, Skuli N, Walton ZE, Liu X et al. ATF4 regulates MYC-mediated neuroblastoma cell death upon glutamine deprivation. Cancer cell 2012;22(5):631–44. https://doi.org/10.1016/j.ccr.2012.09.021.

[48] Ren P, Yue M, Xiao D, Xiu R, Gan L, Liu H et al. ATF4 and N-Myc coordinate glutamine metabolism in MYCN-amplified neuroblastoma cells through ASCT2 activation. The Journal of pathology 2015;235(1):90–100. https://doi.org/10.1002/path.4429.

[49] Yang S, Zheng J, Ma Y, Zhu H, Xu T, Dong K et al. Oct4 and Sox2 are overexpressed in human neuroblastoma and inhibited by chemotherapy. Oncology reports 2012;28(1):186–92. https://doi.org/10.3892/or.2012.1765.

[50] Gifford CA, Ziller MJ, Gu H, Trapnell C, Donaghey J, Tsankov A et al. Transcriptional and epigenetic dynamics during specification of human embryonic stem cells. Cell 2013;153(5):1149–63. https://doi.org/10.1016/j.cell.2013.04.037.

[51] Čančer M, Hutter S, Holmberg KO, Rosén G, Sundström A, Tailor J et al. Humanized Stem Cell Models of Pediatric Medulloblastoma Reveal an Oct4/mTOR Axis that Promotes Malignancy. Cell Stem Cell 2019;25(6):855-870.e11. https://doi.org/10.1016/j.stem.2019.10.005.

[52] Påhlman S, Mohlin S. Hypoxia and hypoxia-inducible factors in neuroblastoma. Cell Tissue Res 2018;372(2):269–75. https://doi.org/10.1007/s00441-017-2701-1.

[53] Schaaf MB, Garg AD, Agostinis P. Defining the role of the tumor vasculature in antitumor immunity and immunotherapy. Cell death & disease 2018;9(2):115. https://doi.org/10.1038/s41419-017-0061-0.

[54] Lugano R, Ramachandran M, Dimberg A. Tumor angiogenesis: causes, consequences, challenges and opportunities. Cell. Mol. Life Sci. 2020;77(9):1745–70. https://doi.org/10.1007/s00018-019-03351-7.

[55] Leprivier G, Rotblat B, Khan D, Jan E, Sorensen PH. Stress-mediated translational control in cancer cells. Biochimica et biophysica acta 2015;1849(7):845–60. https://doi.org/10.1016/j.bbagrm.2014.11.002.

Figure 1

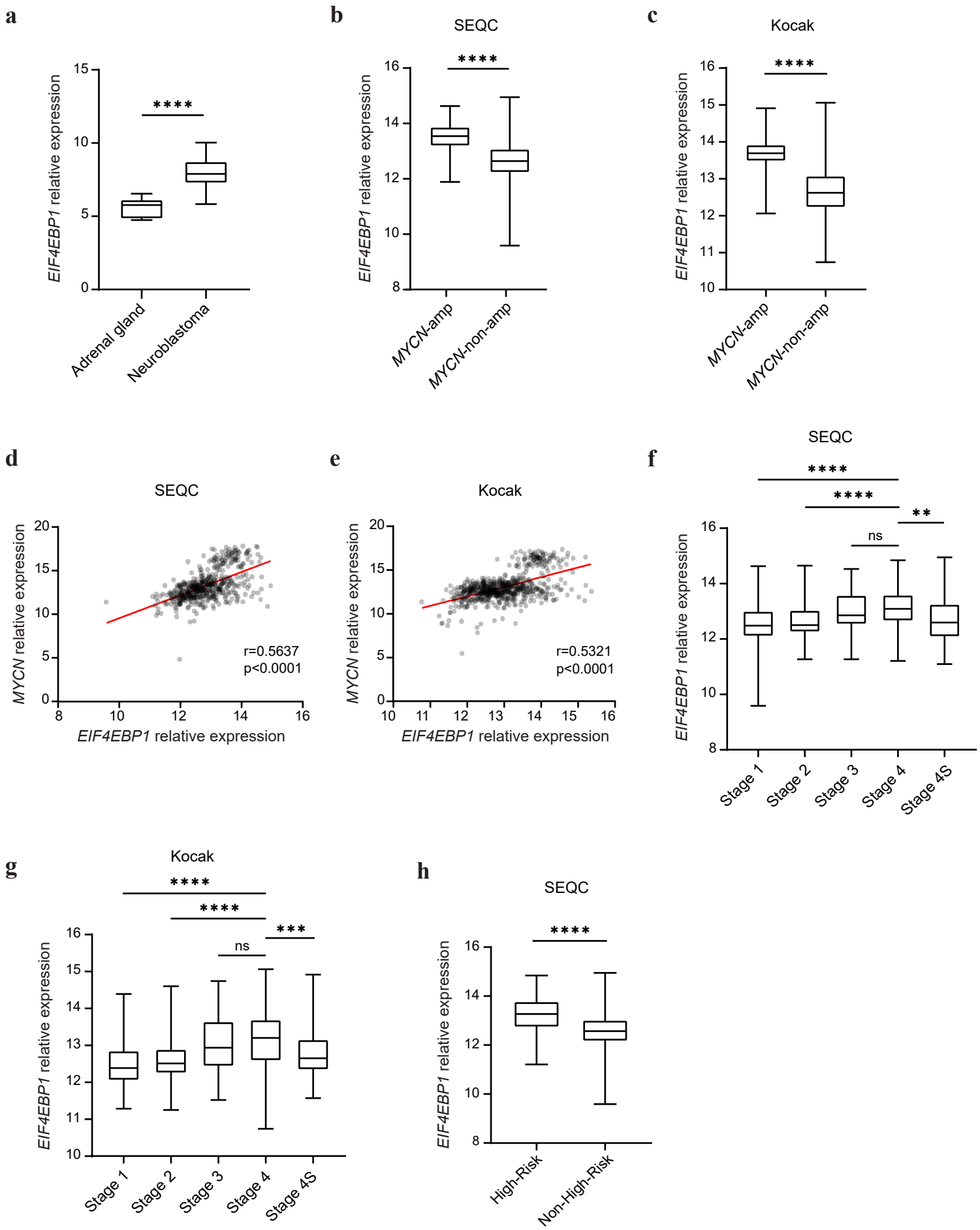
a
EIF4EBP1 relative expression
****
Adrenal gland
Neuroblastoma
b
SEQC
EIF4EBP1 relative expression
****
MYCN-amp
MYCN-non-amp
c
Kocak
EIF4EBP1 relative expression
****
MYCN-amp
MYCN-non-amp
d
SEQC
MYCN relative expression
r=0.5637
p<0.0001
EIF4EBP1 relative expression
e
Kocak
MYCN relative expression
r=0.5321
p<0.0001
EIF4EBP1 relative expression
f
SEQC
****
****
**
ns
EIF4EBP1 relative expression
Stage 1
Stage 2
Stage 3
Stage 4
Stage 4S
g
Kocak
****
****
***
ns
EIF4EBP1 relative expression
Stage 1
Stage 2
Stage 3
Stage 4
Stage 4S
h
SEQC
****
EIF4EBP1 relative expression
High-Risk
Non-High-Risk

Figure 2

a

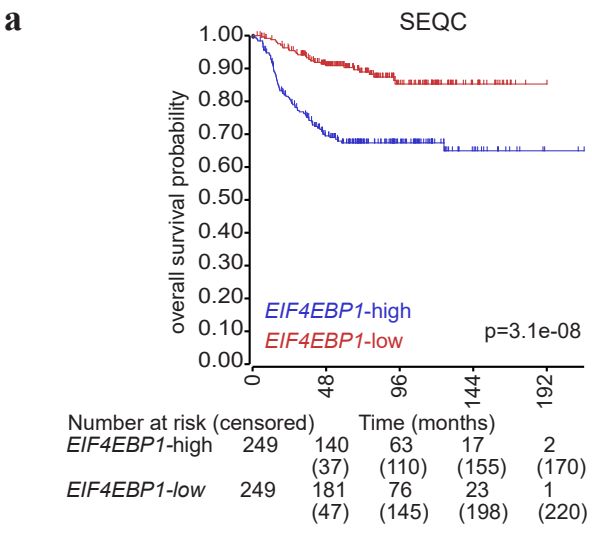

Number at risk (censored) Time (months)

EIF4EBP1-high	249	140 (37)	63 (110)	17 (155)	2 (170)
EIF4EBP1-low	249	181 (47)	76 (145)	23 (198)	1 (220)

b

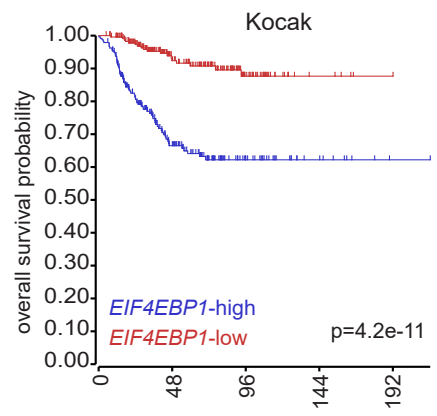

c

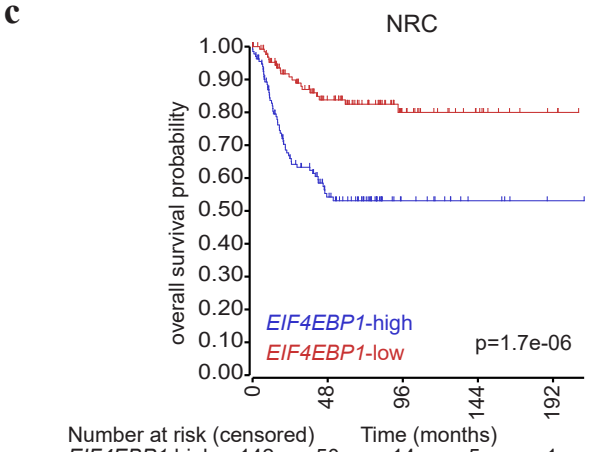

Number at risk (censored) Time (months)

EIF4EBP1-high	142	50 (38)	14 (73)	5 (82)	1 (86)
EIF4EBP1-low	141	72 (51)	26 (95)	11 (110)	3 (118)

d

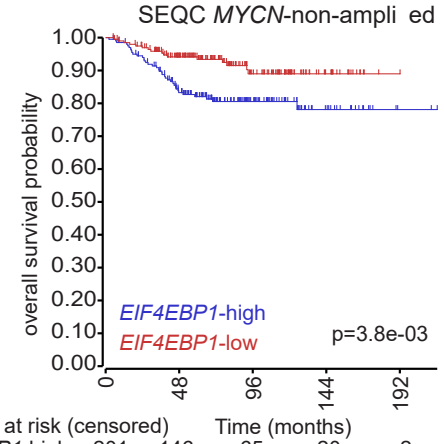

Number at risk (censored) Time (months)

EIF4EBP1-high	201	146 (23)	65 (100)	20 (144)	2 (162)
EIF4EBP1-low	200	148 (52)	68 (116)	20 (164)	1 (183)

e

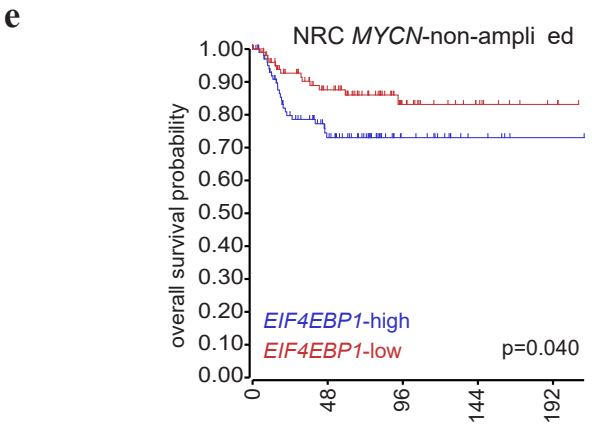

Number at risk (censored) Time (months)

EIF4EBP1-high	111	51 (36)	16 (71)	5 (82)	1 (86)
EIF4EBP1-low	111	62 (38)	23 (75)	10 (88)	3 (95)

f

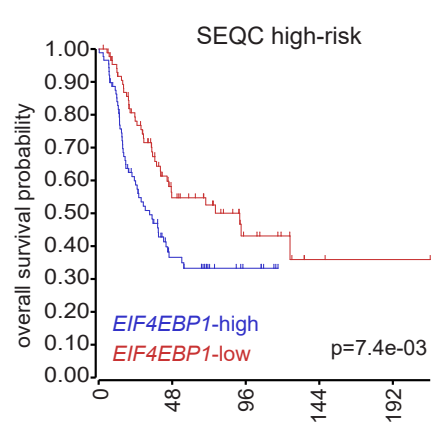

Number at risk (censored) Time (months)

EIF4EBP1-high	88	22 (15)	6 (29)	0 (35)	0 (35)
EIF4EBP1-low	88	32 (22)	11 (39)	2 (47)	1 (48)

g

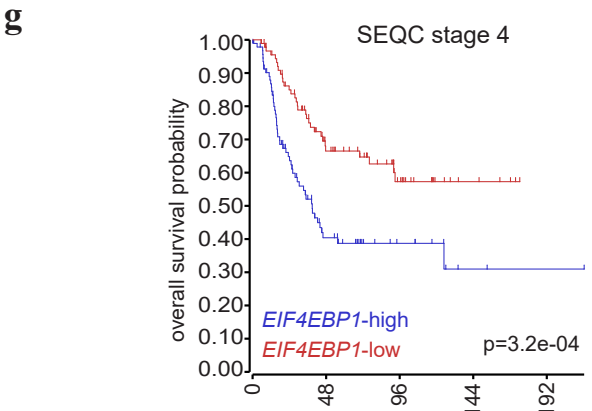

Number at risk (censored) Time (months)

EIF4EBP1-high	92	26 (17)	9 (33)	2 (39)	1 (40)
EIF4EBP1-low	91	44 (20)	20 (40)	5 (55)	0 (60)

h

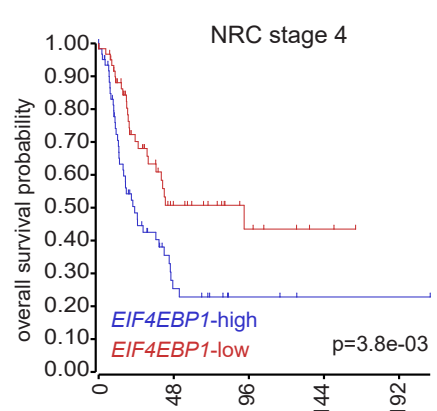

Number at risk (censored) Time (months)

EIF4EBP1-high	62	10 (13)	3 (19)	3 (19)	1 (21)
EIF4EBP1-low	62	17 (21)	6 (31)	2 (35)	0 (37)

Figure 3

a

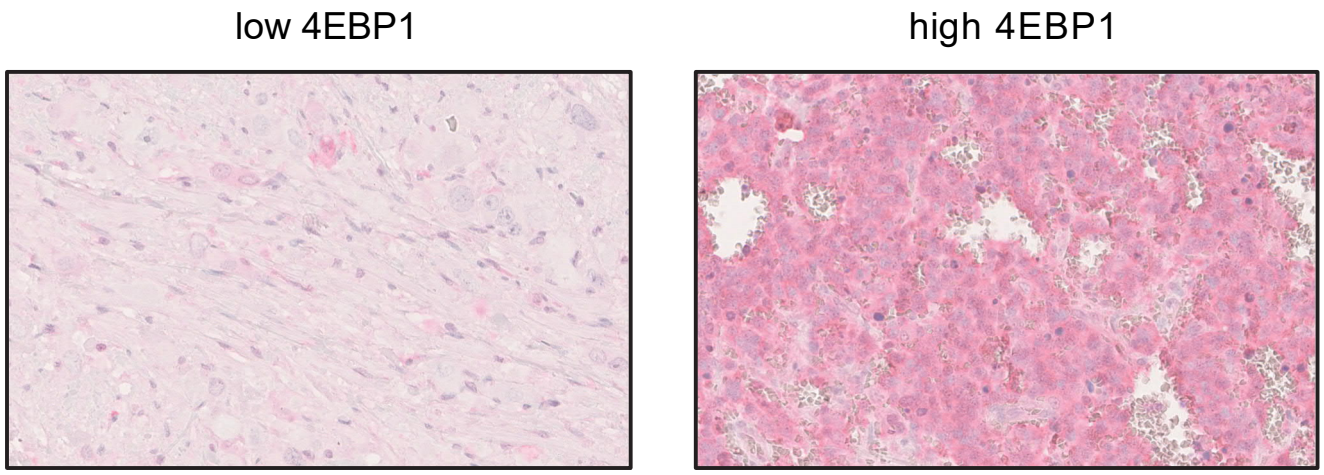
low 4EBP1
high 4EBP1

b

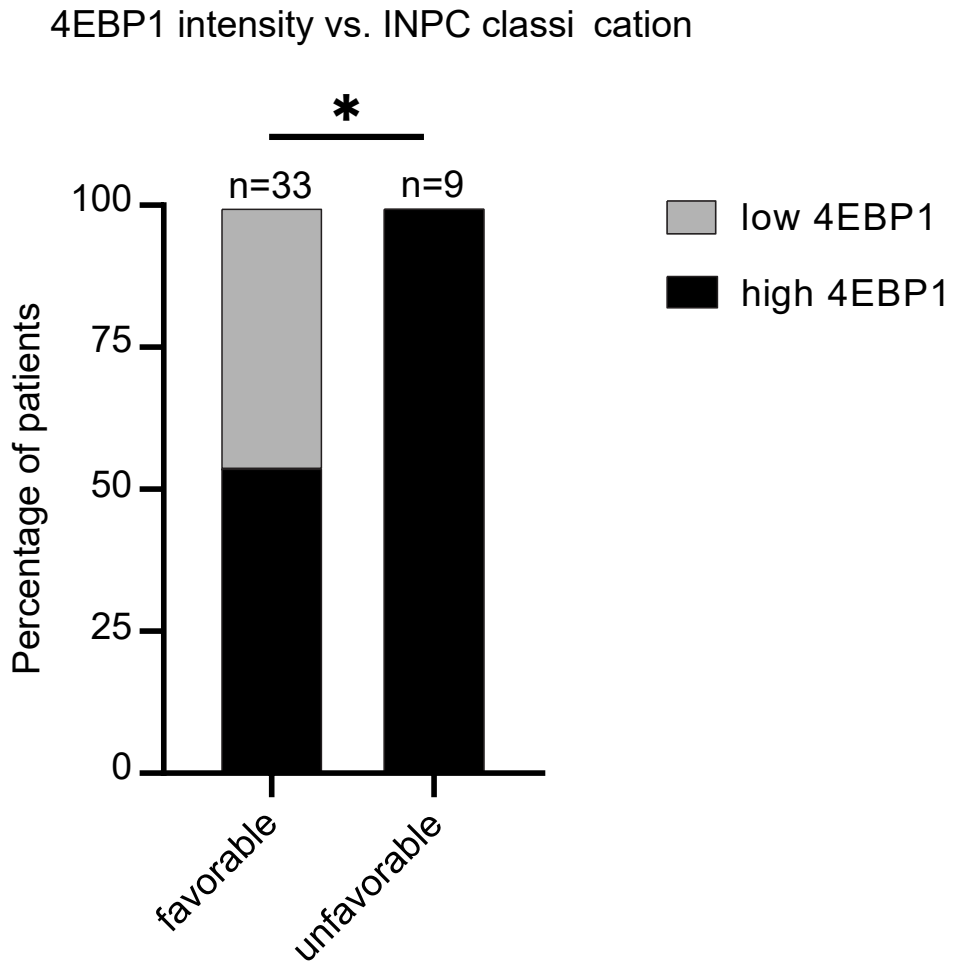
4EBP1 intensity vs. INPC classi cation
*
n=33
n=9
low 4EBP1
high 4EBP1
Percentage of patients
100
75
50
25
0
favorable
unfavorable

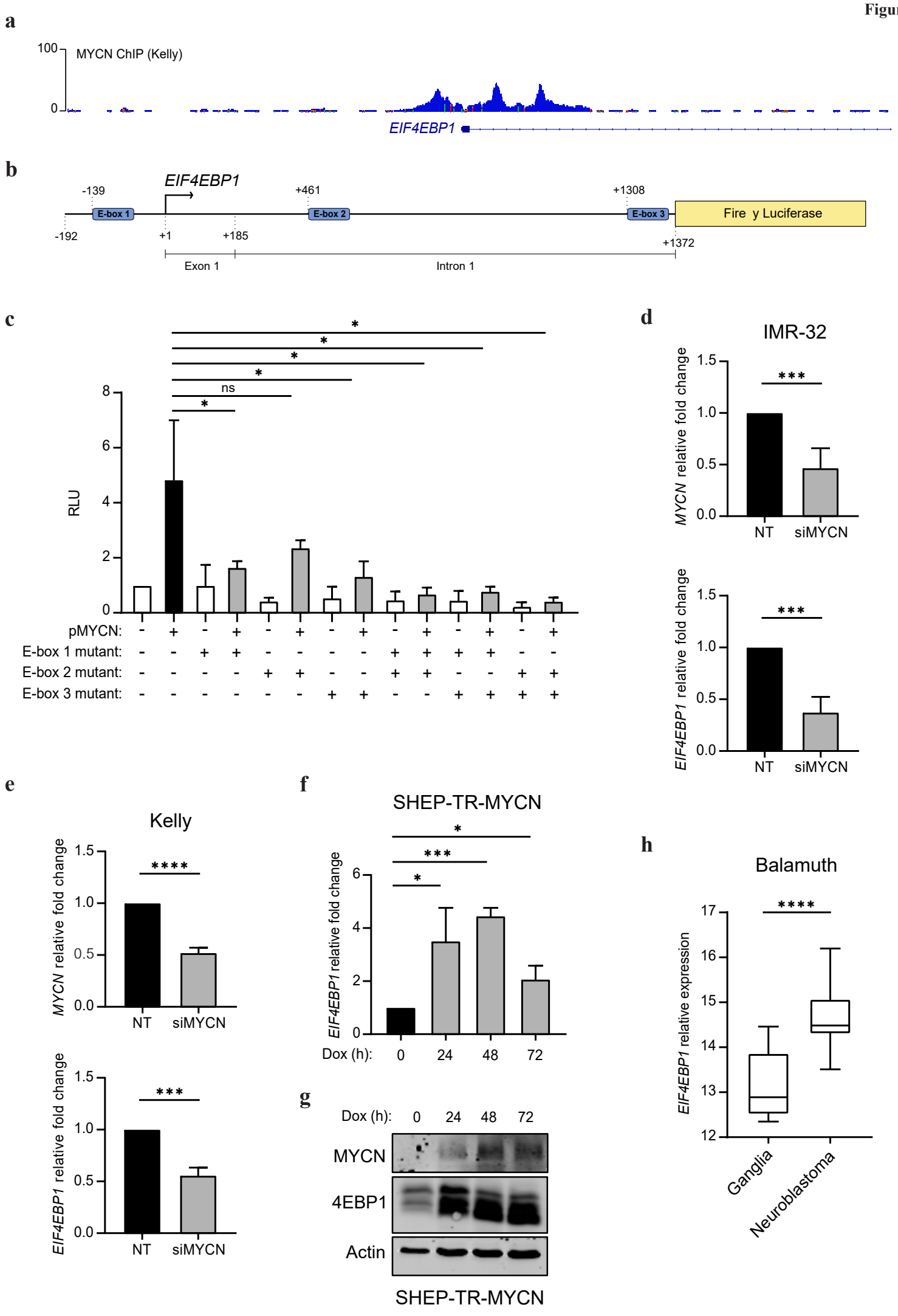
a
100
MYCN ChIP (Kelly)
0
EIF4EBP1
b
EIF4EBP1
-139
+461
+1308
E-box 1
E-box 2
E-box 3
Fire y Luciferase
-192
+1
+185
+1372
Exon 1
Intron 1
c
RLU
ns
pMYCN:
E-box 1 mutant:
E-box 2 mutant:
E-box 3 mutant:
d
IMR-32
MYCN relative fold change
EIF4EBP1 relative fold change
NT
siMYCN
e
Kelly
MYCN relative fold change
EIF4EBP1 relative fold change
f
SHEP-TR-MYCN
EIF4EBP1 relative fold change
Dox (h):
g
MYCN
4EBP1
Actin
SHEP-TR-MYCN
h
Balamuth
EIF4EBP1 relative expression
Ganglia
Neuroblastoma

a

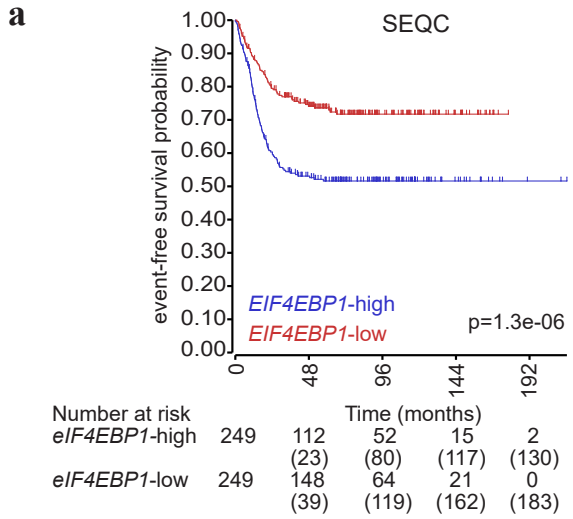

Number at risk					
eIF4EBP1-high	249	112 (23)	52 (80)	15 (117)	2 (130)
eIF4EBP1-low	249	148 (39)	64 (119)	21 (162)	0 (183)

b

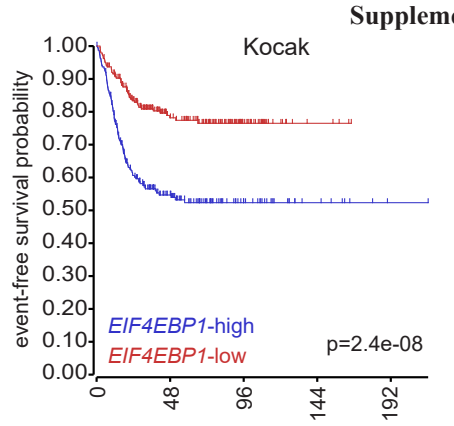

c

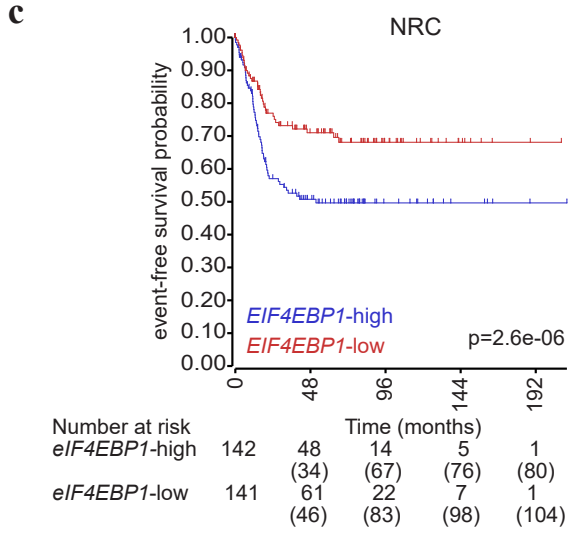

Number at risk					
eIF4EBP1-high	142	48 (34)	14 (67)	5 (76)	1 (80)
eIF4EBP1-low	141	61 (46)	22 (83)	7 (98)	1 (104)

d

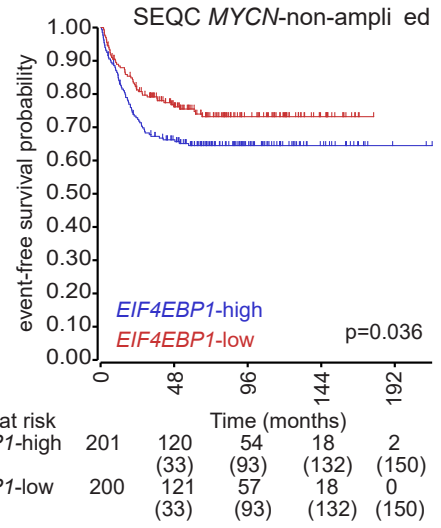

Number at risk					
eIF4EBP1-high	201	120 (33)	54 (93)	18 (132)	2 (150)
eIF4EBP1-low	200	121 (33)	57 (93)	18 (132)	0 (150)

e

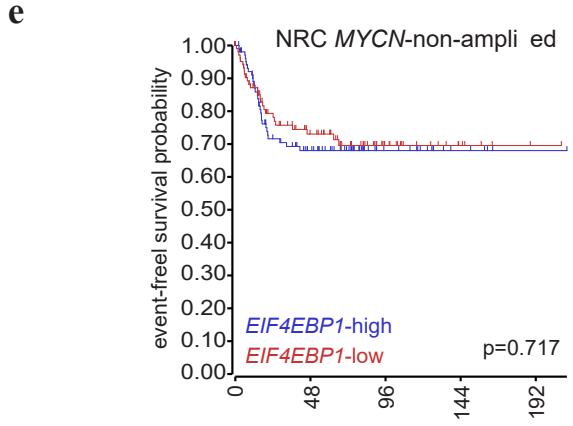

Number at risk					
eIF4EBP1-high	111	50 (31)	16 (65)	5 (76)	1 (80)
eIF4EBP1-low	62	51 (35)	19 (65)	6 (78)	1 (83)

f

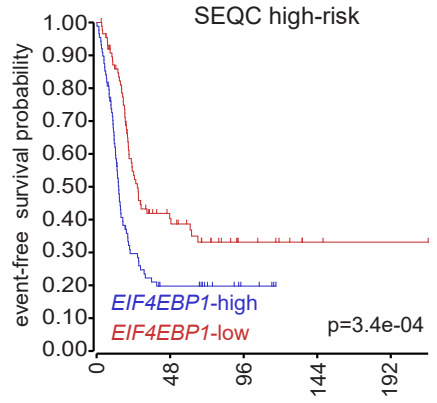

Number at risk					
eIF4EBP1-high	88	14 (6)	4 (16)	0 (20)	0 (20)
eIF4EBP1-low	88	25 (15)	8 (28)	2 (34)	1 (35)

g

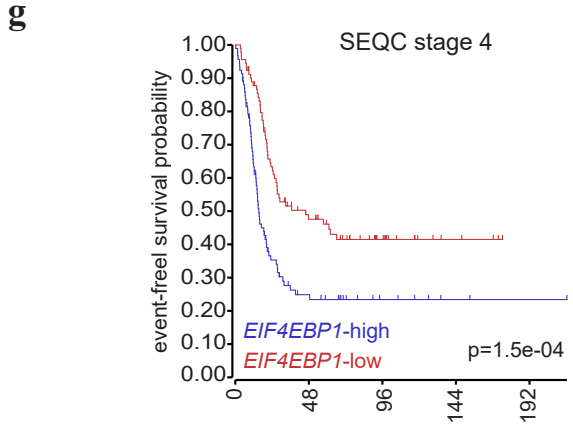

Number at risk					
eIF4EBP1-high	92	17 (10)	6 (20)	2 (24)	1 (25)
eIF4EBP1-low	91	35 (11)	15 (27)	4 (38)	0 (42)

h

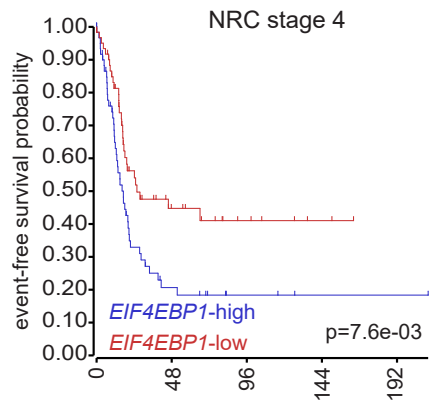

Number at risk					
eIF4EBP1-high	62	9 (10)	3 (15)	1 (17)	1 (17)
eIF4EBP1-low	62	14 (19)	6 (26)	2 (30)	0 (32)

a

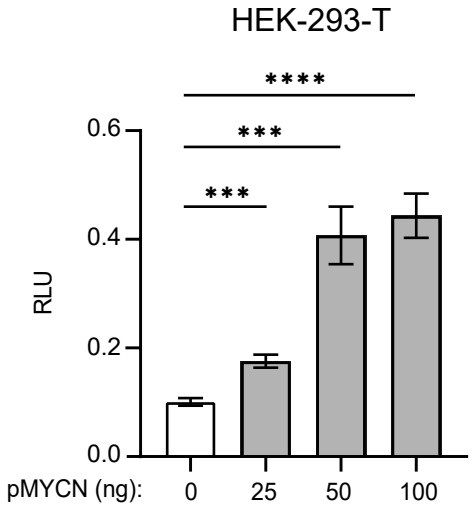
HEK-293-T
****
***
***
0.6
0.4
0.2
0.0
RLU
pMYCN (ng):
0
25
50
100

b

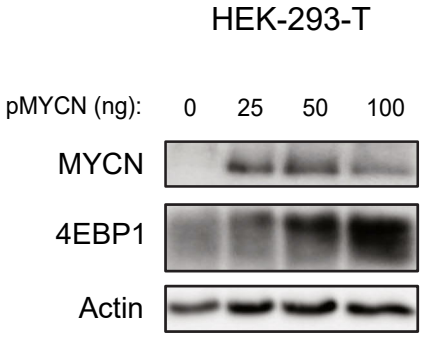
HEK-293-T
pMYCN (ng):
0
25
50
100
MYCN
4EBP1
Actin

Table 1. Multivariate analysis for overall survival of NB patients in the SEQC cohort.

Variables	**HR**	**95.0% CI**	**p value**
MYCN amplification	22.373	8.89-56.306	0
High *EIF4EBP1* mRNA expression	2.16	1.255-3.717	0.005
MYCN amplification*high *EIF4EBP1* mRNA expression	0.222	0.08-0.614	0.004
Variables	**HR**	**95.0% CI**	**p value**
Stage 4	17.618	6.694-46.366	0
High *EIF4EBP1* mRNA expression	5.457	2.026-14.697	0.001
Stage 4*high *EIF4EBP1* mRNA expression	0.292	0.097-0.879	0.029
Variables	**HR**	**95.0% CI**	**p value**
Age at diagnosis	33.018	7.835-139.139	0
High *EIF4EBP1* mRNA expression	12.204	2.832-52.598	0.001
Age at diagnosis*high *EIF4EBP1* mRNA expression	0.16	0.035-0.74	0.019

Table 2. Multivariate analysis for overall survival of NB patients in the NRC cohort.

Variables	**HR**	**95.0% CI**	**p value**
MYCN amplification	4.967	1.118-22.066	0.035
High *EIF4EBP1* mRNA expression	3.031	1.543-5.954	0.001
MYCN amplification*high *EIF4EBP1* mRNA expression	0.656	0.135-3.181	0.601
Variables	**HR**	**95.0% CI**	**p value**
Stage 4	15.050	4.239-53.432	0.018
High *EIF4EBP1* mRNA expression	5.144	1.330-19.895	0
Stage 4*high *EIF4EBP1* mRNA expression	0.36	0.081-1.598	0.179
Variables	**HR**	**95.0% CI**	**p value**
Age at diagnosis	0.27	0.036-2.056	0
High *EIF4EBP1* mRNA expression	0.364	0.048-2.772	0.002
Age at diagnosis*high *EIF4EBP1* mRNA expression	55.427	3.258-942.88	0.005

Supplementary table 1: Primer list

target gene	forward	reverse
eIF4EBP1	AGCCCTTCCAGTGATGAGC	TGTCCATCTCAAACTGTGACTCTT
MYCN	TGAGCGATTCAGATGATGAAGA	GCATCGTTTGAGGATCAGC
GUSB	GTTTTTGATCCAGACCCAGATG	GCCCATTATTCAGAGCGAGTA
PPIA	TTATTTGGGTTGCTCCCTTC	AAGTGTGCCAAATCTGCAAG

5. Discussion

The work summarized in this PhD-thesis aimed at delineating the role of 4EBPs under glucose starvation. Cells frequently encounter periods of low glucose availability, and cancer represents a pathological condition that is characterized by glucose deprivation due to high anabolism and immature vascularization patterns (Schaaf et al. 2018; Lugano et al. 2020). An approach to cope with low levels of glucose is to adjust the cellular metabolism accordingly. This primarily requires a switch from anabolic to catabolic processes, which ensures preservation of energy levels and redox balance, and promotes cell survival. There is some evidence that 4EBPs can act as translational regulators of metabolism to protect cells or organisms under nutrient stress, such as high-fat or calorie-restricted diets (Birse et al. 2010; Teleman et al. 2005; Tsai et al. 2016; Zid et al. 2009). Thus, the hypothesis addressed in this thesis was that 4EBPs would have similar functions upon glucose starvation. Indeed, the findings reported here implicate 4EBPs to be crucial to the metabolic adaptation in response to glucose starvation. In particular, 4EBPs appear to be essential to adapt cellular metabolism to glucose-deprived conditions by blocking fatty acid synthesis (FAS), which in turn allows to conserve the redox balance. The mechanism of selective inhibition of FAS by 4EBPs, through repression of *ACACA* translation, and its impact on redox balance and cell survival under low levels of glucose is illustrated in Figure 5.1.

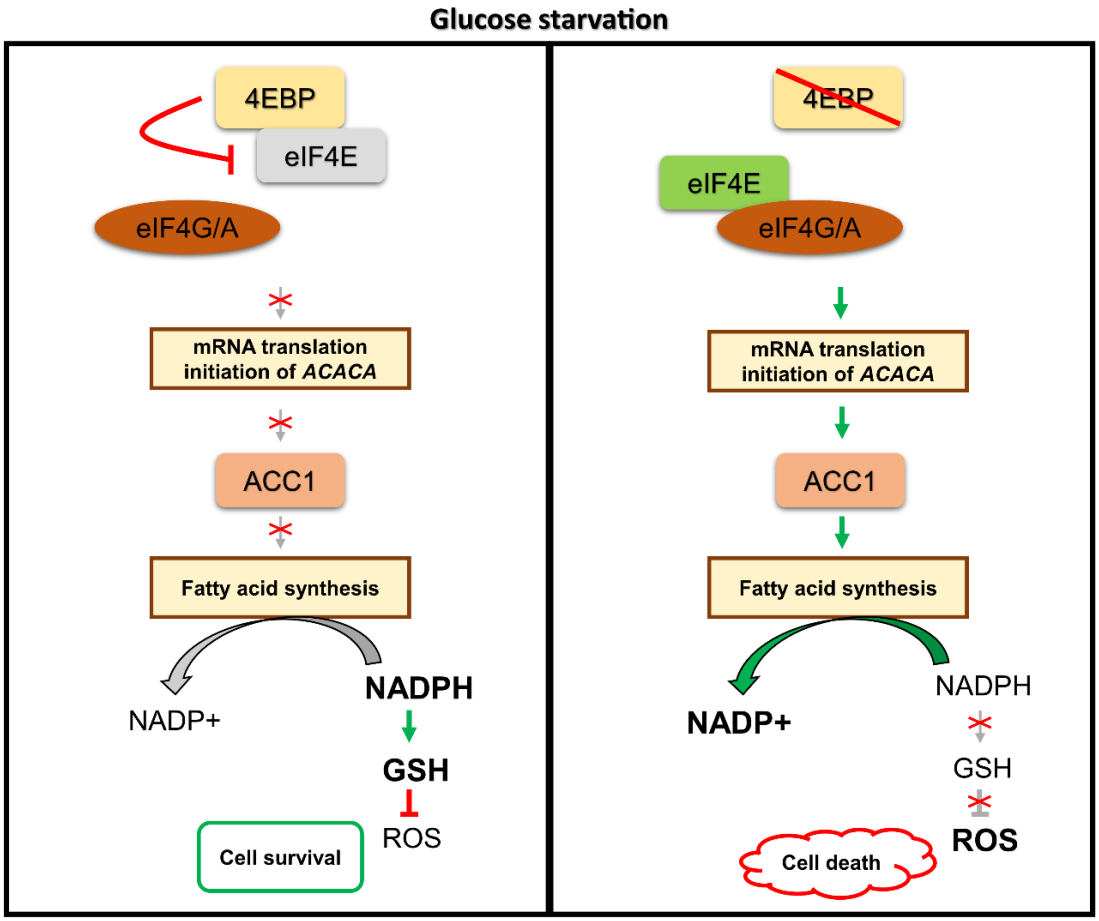

Figure 5.1: Illustration of the mechanisms underlying the protective function of 4EBPs under glucose starvation. In 4EBP-proficient cells (left panel), glucose starvation activates the 4EBPs translational repressors to selectively inhibit the translation of *ACACA*. Decreased levels of ACC1 will limit FAS and thus spare NADPH. The preserved levels of NADPH can be utilized to regenerate GSH, which in turn prevents ROS accumulation thereby promoting cell survival. In 4EBP-deficient cells (right panel), ACC1 synthesis is not blocked under glucose starvation, maintaining fatty acid synthesis activity. In consequence, NADPH is consumed which disrupts the redox balance by raising ROS levels, thus eventually triggering cell death.

The own findings reveal that both under basal conditions (paper 1) or under glucose starvation (manuscript 2) 4EBPs are involved in selectively regulating translation of sets of transcripts rather than restricting global protein synthesis. This raises the question of how 4EBPs can orchestrate such a selectivity since their function to bind and block eIF4E, preventing cap-dependent mRNA translation, seems general as all mRNAs are concerned. Previous reports identified numerous transcripts whose translation is selectively regulated by 4EBP1/2 upon pharmacological suppression of mTORC1 (Thoreen et al. 2012; Hsieh et al. 2012). In these studies, the translation of such transcripts was suppressed by 4EBP1/2, which is expected for negative regulators of mRNA translation. In contrast, the findings in paper 1 reveal that the translation of a comparable number of transcripts is also promoted by the function of 4EBPs. Such a positive regulation of mRNA translation by 4EBPs was previously observed, as 4EBPs were reported to promote selective synthesis of HIF-1α and VEGF in response to hypoxia (Braunstein et al. 2007). The authors concluded that the underlying mechanism of 4EBPs stimulation of mRNA translation occurs through IRES-dependent, therefore cap-independent mRNA translation. In particular, the inhibition of cap-dependent mRNA translation releases ribosomes and the translation initiation factor eIF4G, which becomes available for translation initiation of mRNAs independently of eIF4E. However, the own experiments did not detect an enrichment of IRES-containing transcripts in the gene cluster whose translation is promoted by 4EBP1/2 (see paper 1, Figure 1, cluster #1). Moreover, it was possible to robustly rescue 4EBP-deficient cells from glucose starvation-induced cell death by treatment with the protein synthesis inhibitor cycloheximide, which strongly suggests that 4EBPs are needed to repress rather than promote mRNA translation of certain transcripts under low glucose conditions. In summary, these findings suggest that 4EBPs suppress translation of a selective set of transcripts while, either directly or indirectly, stimulate selective translation of other sets of transcripts, at least under basal and hypoxic conditions, by mechanisms yet to be explored.

Manuscript 2 reports that under glucose-deprived conditions, 4EBPs are selectively repressing the translation of *ACACA* and thus blocking expression of ACC1, the rate-limiting enzyme of the NADPH-consuming FAS pathway. This transcript was not detected to be translationally regulated by 4EBPs under physiological conditions or under pharmaceutical inhibition of mTORC1 (Thoreen et al. 2012), but was identified in quiescent CD4+ T cell (Ricciardi et al. 2018) and in liver tissue of mice fed with a high fat diet (Conn et al. 2021). This strongly

suggests that different stimuli somehow direct 4EBPs to control translation of distinct sets of mRNAs. This assertion raises the question of how 4EBPs mediate selective translational regulation towards certain transcripts. Furthermore, while under amino acid or serum starvation, 4EBPs are involved in selectively inhibiting the translation of pro-proliferative mRNAs (Dowling et al. 2010), to restrain cell proliferation, the own data indicate that 4EBPs are not involved in blocking cell proliferation under glucose starvation. Thus, it is necessary to explain how this can be achieved. One possible explanation could be the presence of specific motifs located in the 5'UTRs of mRNAs, which have been identified by independent studies (Hsieh et al. 2012; Thoreen et al. 2012; Truitt et al. 2015; Jin et al. 2020). These studies revealed that the selectivity for eIF4E/4EBPs translational regulation depends on specific, yet different motifs rather than the length or complexity of the 5'UTR, as previously thought. The authors suggested that the RNA binding protein La-related protein 1 (LARP1) could dictate the selectivity towards specific sets of transcripts (Jin et al. 2020). LARP1 has recently been proposed to repress mRNA translation upon mTORC1 inhibition, similarly to 4EBPs (Lahr et al. 2017). LARP1 and 4EBPs both bind to mRNAs which contain specific motifs in their 5'UTR (namely TOP or PRTE motifs), yet regulate distinct transcripts (Hong et al. 2017). The combined effect of 4EBPs and LARP1 on mRNA translation can putatively explain the selectivity towards specific transcripts (Jin et al. 2020). However, this does not provide a reason for the distinct selectivity triggered by different types of stress. In yeast, two differential sets of RNA-binding proteins, which directly interact with 4EBPs, define the differences of translational targets between the 4EBP orthologues Eap1 and Caf20 (Cridge et al. 2010). This would also explain why Eap1-mutant, but not Caf20-mutant yeast cells exhibited reduced survival compared to control cells under glucose-free conditions. In *Drosophila* and *Xenopus,* certain RNA-binding proteins have been identified to interact with 4EBPs to guide their selectivity towards specific transcripts (Richter und Sonenberg 2005). In mammals, no such RNA-binding proteins affecting 4EBPs functions have yet been discovered (Richter und Sonenberg 2005). Therefore, it is tempting to speculate that in mammals there might be RNA-binding and 4EBPs-interacting proteins that have not been identified to date. Assuming this hypothesis proves correct, it would be conceivable that certain stress stimuli trigger the expression and/or activity of specific RNA interacting proteins to finely control the translational targets of 4EBPs, thereby regulating the response in a stress type-dependent manner.

In the literature the assumption persists that 4EBPs are inactive under optimal conditions as mTORC1 is active and thus maintains them in a phosphorylated state. However, paper 1 shows that a fraction of 4EBPs escapes from mTORC1-mediated inhibition and exerts translational regulatory activity. This raises the question of how 4EBP molecules dodge the inhibition by mTORC1. It is possible that an equilibrium is met between the amount mTORC1 kinase molecules and the number of 4EBP molecules. This could mean that even though

mTORC1 is highly active, it cannot reach a state where the total fraction of its substrates is phosphorylated. Alternatively, 4EBP-specific phosphatases such as protein phosphatase 1G (PPM1G) could be a mechanism for 4EBPs to maintain a dephosphorylated fraction even when mTORC1 is fully active (Liu et al. 2013). In conditions where 4EBPs are overexpressed, as it is the case in NB, the equilibrium could be further shifted towards an increased pool of functional 4EBPs that escape from inhibition by mTORC1. Remarkably, forced overexpression of WT 4EBP1 in HEK-293-T cells caused elevated suppression of cap-dependent mRNA translation under conditions in which mTORC1 is active (Sekiyama et al. 2015). This finding further supports the hypothesis that the ratio between mTORC1 molecules and substrate 4EBP molecules dictate the efficacy of mTORC1-mediated inhibition of 4EBPs.

The biological significance of this active pool of 4EBPs under (patho-)physiological conditions was further addressed. The phenotypic characterization of the impact of *EIF4EBP1* and *EIF4EBP2* targeted deletion in mouse models is particularly informative in this respect. 4EBP1/2 DKO mice developed an obese phenotype compared to WT mice, especially under high fat diet, but also under control diet conditions (Le Bacquer et al. 2007). Under physiological conditions and control diet, 4EBP1/2 DKO mice accumulated more fat, displayed increased cholesterol levels, and showed a reduced metabolic activity as compared to WT mice (Le Bacquer et al. 2007). MTORC1 was detected to be highly active in these mice (Le Bacquer et al. 2007), which strongly suggests that *in vivo* a pool of 4EBPs is active under physiological conditions supporting the *in vitro* findings in paper 1. In addition to these findings, another study found that overexpression of wildtype 4EBP1 protected mice from age-related obesity and reverted low metabolic activity (Tsai et al. 2016). In conclusion, the findings summarized in this thesis and the available literature provide an explanation of the function of 4EBPs *in vivo* under physiological conditions. Deepened understanding of the role of 4EBPs under energy-rich conditions could facilitate clinical interventions in patients with metabolic diseases.

Since 4EBPs were found to be functional even under conditions where mTORC1 is active (paper 1), it is also likely that an upregulation of 4EBPs levels will have a tremendous biological impact. As some cancer types exhibit elevated levels of *EIF4EBP1*/4EBP1, it raises two questions: (1) how is *EIF4EBP1* overexpression mediated? and (2) what is the clinical relevance of *EIF4EBP1* overexpression?

It has been highlighted recently that *EIF4EBP1* expression is frequently increased in cancer (Wu und Wagner 2021). For instance, the 8p11-12 amplification in breast cancer patients is a mechanism that underlies the overexpression of *EIF4EBP1* in these tumors (Karlsson et al. 2011). However, this mechanism does not explain the overexpression observed in other cancer entities, including prostate and liver cancers (Cha et al. 2015; Kremer et al. 2006).

Manuscript 3 presents a mechanism mediating *EIF4EBP1* overexpression in neuroblastoma (NB) cells by the transcriptional action of MYCN. This may explain the increased levels of *EIF4EBP1* in *MYCN*-amplified NB tumors. However, the question of how *EIF4EBP1* levels are increased in *MYCN*-non amplified NB tumors persists. In addition to the three described MYCN binding sites in the promoter region of *EIF4EBP1*, extended analysis of publicly available ChIP-seq data identified binding of other transcription factors to the promoter, including the proto-oncogenes JUND, ETS1 and MYBL2 (Laura Hauffe, personal communication). Since these factors are known to be associated with cancer progression and reported to be frequently overexpressed and aberrantly activated in diverse cancer entities including prostate, breast and liver cancers (Frau et al. 2011; Millena et al. 2016; Fry und Inoue 2018), they could possibly promote *EIF4EBP1* overexpression in these tumor entities. However, this is speculative and needs to be confirmed experimentally. Next to the question of how *EIF4EBP1* levels might be upregulated, it was evaluated whether *EIF4EBP2* and *EIF4EBP3* expression is upregulated in NB. As shown in Figure 6.1 (see appendix), only *EIF4EBP1* is overexpressed in NB, compared to normal tissues, while *EIF4EBP2* expression remained unchanged and *EIF4EBP3* expression is decreased. Comparison of ChIP-seq data of the promoter regions of the three homologs revealed only one binding site for MYCN in the promoter regions of both *EIF4EBP2* and *EIF4EBP3*, in close proximity to the transcription start site. Thus, it might be that one binding site is not sufficient for a robust activation of transcription by MYCN. This speculation is supported by the finding that mutating two of the three MYCN binding sites virtually abolished MYCN-mediated transcriptional activation of *EIF4EBP1*. The relative decrease of *EIF4EBP3* levels in NB as compared to healthy control tissue, however, remains an open question and requires further research. One might speculate that this reduction in mRNA levels is, independently of the function of the encoded protein, repressed by transcription factors involved in NB progression.

The finding of an active fraction of 4EBPs under energy-rich conditions emphasizes the need to investigate the total level of 4EBPs. However, analysis of 4EBPs levels in tumors largely relies on monitoring the amount of phosphorylated 4EBPs only, without assessing the levels of total 4EBPs. This ignores the potential fraction of active 4EBPs and can, specifically in cancer with 4EBP1 overexpression, conceal the full understanding. Numerous studies performed on various tumor samples assumed that detection of high levels of phosphorylated 4EBPs indicate that 4EBPs are inactive, as it would denote active mTORC1 signaling (Musa et al. 2016). However, a fraction of 4EBPs is functional even under optimal growth conditions. The common overexpression in cancer possibly increases the fraction of active 4EBP, which has clinical relevance since high *EIF4EBP1* expression has been associated with poor patient survival in a number of tumor types (Wu und Wagner 2021). Furthermore, the protective role of 4EBPs under glucose starvation, in particular in NB cells, may provide a functional impact

for the observed increased levels of *EIF4EBP1*/4EBP1 in aggressive NB. This cancer is highly glucose-addicted and thus susceptible to glucose scarcity, which it putatively encounters throughout tumor development, growth, and metastasis as pointed out by the presence of necrotic and hypoxic regions (Sepideh Aminzadeh et al. 2015). Similarly, it has been shown that aggressive *MYCN*-amplified NB hijacks another translational repressor, namely eEF2K, to mediate adaptation to nutrient deprivation (Delaidelli et al. 2017). Therefore, the data in this thesis indicate how evolutionarily conserved proteins, and in particular translational repressors such as 4EBPs, are hijacked by cancer cells to adapt their metabolism to stressful conditions and thereby gain a survival advantage.

A possible strategy towards development of therapeutic compounds for treating cancer aims at the inactivation of mTORC1 due to its role in promoting tumor growth/anabolic processes (Zou et al. 2020). The results of this thesis, however, condemns such a simplistic view on the role of mTORC1 and its downstream targets in cancer progression. Depending on the context, mTORC1 inhibition, and thus activation of 4EBPs, could have opposing effects on tumor growth. For instance, a study revolving around treatment of pancreatic tumors in mouse models showed that mTORC1 inhibition reduced cancer cell proliferation only in well-vascularized tumor regions, while it had the opposite effect in poorly vascularized and thus likely glucose-deprived regions (Palm et al. 2015). This supports the findings that activation of 4EBPs (corresponding to mTORC1 inhibition) promotes survival of tumor cells under metabolically challenged conditions, by translationally reprogramming metabolism (see Figure 5.1). In conclusion, future research should focus on developing inhibitors for the downstream targets of mTORC1 and translational regulators 4EBPs.

In summary, the translational regulators 4EBPs are able to selectively control distinct gene sets both under basal and glucose-deprived conditions. While under basal conditions, 4EBPs are non-essential for the survival of cells, under glucose-deprived conditions they adapt the metabolism to maintain the redox balance and to ensure survival. Moreover, *EIF4EBP1*/4EBP1 were found to be overexpressed in NB and overexpression of 4EBPs was associated with high-risk tumors and poor prognosis for patients, and is at least in part controlled by MYCN. Altogether, 4EBPs represent a conserved class of translational regulators involved in adjusting metabolic activities to microenvironmental stimuli in both normal and tumor cells.

6. Appendix

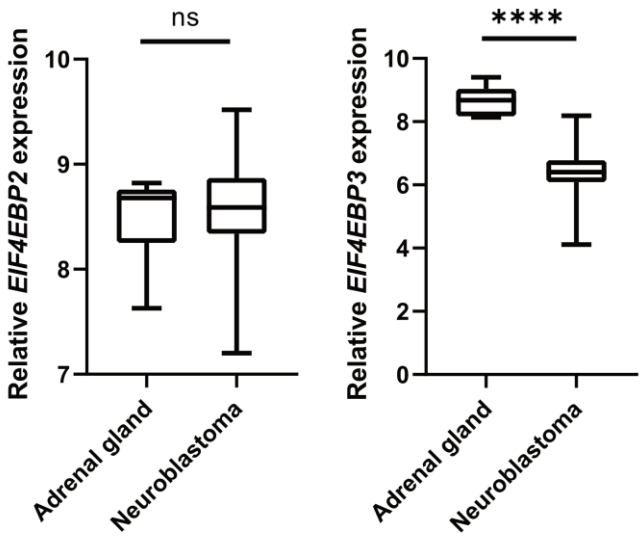

Figure 6.1: The expression levels of EIF4EBP2 and -3 in a pooled cohort of Neuroblastoma (NB) patients compared to healthy control tissue (adrenal gland). *The relative expression of EIF4EBP2 remains unchanged between NB patients and control tissue. The transcript levels of EIF4EBP3 are significantly downregulated in NB patients compared to control tissue. Tested for significance by Mann-Whitney U-test. ns= not significant, *P<0.05, **P<0.01, ***P<0.001, ****P<0.0001*

Table 6.1: List of additional compounds used in this thesis but excluded from the manuscripts.

Name	Company
Actinomycin D	Sigma-Aldrich, St. Louis, MO, USA
zVAD	Invivogen, San-Diego, CA, USA
Ferrostatin-1	Sigma-Aldrich, St. Louis, MO, USA
Nec-1s	Sigma-Aldrich, St. Louis, MO, USA

7. Author contributions to manuscripts

Paper 1

Title: 4EBP1/2 are active under standard cell culture conditions to regulate the translation of specific mRNAs

Published on 11th of November 2020 in Springer Nature – *Cell Death and Disease* (Alasad et al. 2020)

Contribution: Kai Völtzke conceived and designed one experiment of the study. He collected data by culturing and transfecting cells, and performing a luciferase gene reporter assay. He statistically analyzed his data and prepared the according figure panel. Furthermore, he critically revised and commented on the manuscript.

Manuscript 2

Title: 4EBP1/2 support cell survival under metabolic stress by translationally regulating fatty acid synthesis

Manuscript in preparation, to be submitted to CellPress – *Cell* in the first quarter of 2022.

Contribution: Kai Völtzke helped with conception and design of the study. He planned and performed experiments. He further analyzed all data he collected and contributed to create the figures (Figure 1-5). He was substantially involved in the *in vitro* cell culture experiments (Figure 1-4) and the *in vivo* work in budding yeast (Figure 5). He further performed statistical analysis of the data and wrote the parts of the manuscript according to his experiments. Furthermore, he critically evaluated and commented on the whole manuscript.

Manuscript 3

Title: *EIF4EBP1* is transcriptionally upregulated by MYCN and associates with poor prognosis in neuroblastoma

Submitted to Springer Nature – *Cell Death and Disease* on November 9th 2021, and pre-published on bioRxiv (Voeltzke et al. 2021)

Contribution: Kai Völtzke substantially conceived and designed the study. He collected the data from databanks and performed bioinformatics analysis of these data. He contributed to generation of experimental data either by performing experiments or by guiding students to do so. In addition, he created all the figures and performed the statistical analysis. Furthermore, he wrote the manuscript.

---------- ----------

Kai Völtzke Gabriel Leprivier, PhD

Signature and Date Signature and Date

8. References

Abiko, Fumi; Tomoo, Koji; Mizuno, Atsuo; Morino, Shigenobu; Imataka, Hiroaki; Ishida, Toshimasa (2007): Binding preference of eIF4E for 4E-binding protein isoform and function of eIF4E N-terminal flexible region for interaction, studied by SPR analysis. In: *Biochemical and Biophysical Research Communications* 355 (3), S. 667–672. DOI: 10.1016/j.bbrc.2007.01.198.

Alabdullah, M. L.; Ahmad, D. A.; Moseley, P.; Madhusudan, S.; Chan, S.; Rakha, E. (2019): The mTOR downstream regulator (p-4EBP1) is a novel independent prognostic marker in ovarian cancer. In: *Journal of obstetrics and gynaecology : the journal of the Institute of Obstetrics and Gynaecology* 39 (4), S. 522–528. DOI: 10.1080/01443615.2018.1534091.

Alain, Tommy; Morita, Masahiro; Fonseca, Bruno D.; Yanagiya, Akiko; Siddiqui, Nadeem; Bhat, Mamatha et al. (2012): eIF4E/4E-BP ratio predicts the efficacy of mTOR targeted therapies. In: *Cancer research* 72 (24), S. 6468–6476. DOI: 10.1158/0008-5472.CAN-12-2395.

Alasad, Khawla; Voeltzke, Kai; Levin, Liron; Reifenberger, Guido; Leprivier, Gabriel; Rotblat, Barak (2020): 4EBP1/2 are active under standard cell culture conditions to regulate the translation of specific mRNAs. In: *Cell death & disease* 11 (11), S. 968. DOI: 10.1038/s41419-020-03182-6.

Altmann, M.; Schmitz, N.; Berset, C.; Trachsel, H. (1997): A novel inhibitor of cap-dependent translation initiation in yeast: p20 competes with eIF4G for binding to eIF4E. In: *The EMBO journal* 16 (5), S. 1114–1121. DOI: 10.1093/emboj/16.5.1114.

Altschul, S. F. (1993): A protein alignment scoring system sensitive at all evolutionary distances. In: *Journal of molecular evolution* 36 (3), S. 290–300. DOI: 10.1007/BF00160485.

Alves, Nuno L.; Derks, Ingrid A. M.; Berk, Erik; Spijker, René; van Lier, René A. W.; Eldering, Eric (2006): The Noxa/Mcl-1 axis regulates susceptibility to apoptosis under glucose limitation in dividing T cells. In: *Immunity* 24 (6), S. 703–716. DOI: 10.1016/j.immuni.2006.03.018.

Amorim, Inês S.; Kedia, Sonal; Kouloulia, Stella; Simbriger, Konstanze; Gantois, Ilse; Jafarnejad, Seyed Mehdi et al. (2018): Loss of eIF4E Phosphorylation Engenders Depression-like Behaviors via Selective mRNA Translation. In: *J. Neurosci.* 38 (8), S. 2118–2133. DOI: 10.1523/JNEUROSCI.2673-17.2018.

Anand, Ruchika; Strecker, Valentina; Urbach, Jennifer; Wittig, Ilka; Reichert, Andreas S. (2016): Mic13 Is Essential for Formation of Crista Junctions in Mammalian Cells. In: *PLOS ONE* 11 (8), e0160258. DOI: 10.1371/journal.pone.0160258.

Averous, J.; Proud, C. G. (2006): When translation meets transformation: the mTOR story. In: *Oncogene* 25 (48), S. 6423–6435. DOI: 10.1038/sj.onc.1209887.

Aykin-Burns, Nùkhet; Ahmad, Iman M.; Zhu, Yueming; Oberley, Larry W.; Spitz, Douglas R. (2009): Increased levels of superoxide and H2O2 mediate the differential susceptibility of cancer cells versus normal cells to glucose deprivation. In: *The Biochemical journal* 418 (1), S. 29–37. DOI: 10.1042/BJ20081258.

Ayuso, María I.; Hernández-Jiménez, Macarena; Martín, María E.; Salinas, Matilde; Alcázar, Alberto (2010): New hierarchical phosphorylation pathway of the translational repressor eIF4E-binding protein 1 (4E-BP1) in ischemia-reperfusion stress. In: *The Journal of biological chemistry* 285 (45), S. 34355–34363. DOI: 10.1074/jbc.M110.135103.

Azar, Rania; Lasfargues, Charline; Bousquet, Corinne; Pyronnet, Stéphane (2013): Contribution of HIF-1α in 4E-BP1 gene expression. In: *Mol Cancer Res* 11 (1), S. 54–61. DOI: 10.1158/1541-7786.MCR-12-0095.

Balakumaran, Bala S.; Porrello, Alessandro; Hsu, David S.; Glover, Wayne; Foye, Adam; Leung, Janet Y. et al. (2009): MYC activity mitigates response to rapamycin in prostate cancer through eukaryotic

initiation factor 4E-binding protein 1-mediated inhibition of autophagy. In: *Cancer Res* 69 (19), S. 7803–7810. DOI: 10.1158/0008-5472.CAN-09-0910.

Bellance, Nadege; Lestienne, Patrick; Rossignol, Rodrigue (2009): Mitochondria: from bioenergetics to the metabolic regulation of carcinogenesis. In: *Frontiers in bioscience (Landmark edition)* 14, S. 4015–4034. DOI: 10.2741/3509.

Benedetti, Arrigo de; Graff, Jeremy R. (2004): eIF-4E expression and its role in malignancies and metastases. In: *Oncogene* 23 (18), S. 3189–3199. DOI: 10.1038/sj.onc.1207545.

Berg, Jeremy M.; Tymoczko, John L.; Stryer, Lubert (Hg.) (2002): Biochemistry. 5th edition: W H Freeman.

Bhat, Mamatha; Robichaud, Nathaniel; Hulea, Laura; Sonenberg, Nahum; Pelletier, Jerry; Topisirovic, Ivan (2015): Targeting the translation machinery in cancer. In: *Nature reviews. Drug discovery* 14 (4), S. 261–278. DOI: 10.1038/nrd4505.

Birse, Ryan T.; Choi, Joan; Reardon, Kathryn; Rodriguez, Jessica; Graham, Suzanne; Diop, Soda et al. (2010): High-fat-diet-induced obesity and heart dysfunction are regulated by the TOR pathway in Drosophila. In: *Cell Metabolism* 12 (5), S. 533–544. DOI: 10.1016/j.cmet.2010.09.014.

Böhm, Raphael; Imseng, Stefan; Jakob, Roman P.; Hall, Michael N.; Maier, Timm; Hiller, Sebastian (2021): The dynamic mechanism of 4E-BP1 recognition and phosphorylation by mTORC1. In: *Molecular cell* 81 (11), 2403-2416.e5. DOI: 10.1016/j.molcel.2021.03.031.

Braun-Dullaeus, R. C.; Mann, M. J.; Seay, U.; Zhang, L.; Leyen, H. E. von der; Morris, R. E.; Dzau, V. J. (2001): Cell cycle protein expression in vascular smooth muscle cells in vitro and in vivo is regulated through phosphatidylinositol 3-kinase and mammalian target of rapamycin. In: *Arteriosclerosis, thrombosis, and vascular biology* 21 (7), S. 1152–1158. DOI: 10.1161/hq0701.092104.

Braunstein, Steve; Karpisheva, Ksenia; Pola, Carolina; Goldberg, Judith; Hochman, Tsivia; Yee, Herman et al. (2007): A hypoxia-controlled cap-dependent to cap-independent translation switch in breast cancer. In: *Molecular cell* 28 (3), S. 501–512. DOI: 10.1016/j.molcel.2007.10.019.

Brenner, C.; Nakayama, N.; Goebl, M.; Tanaka, K.; Toh-e, A.; Matsumoto, K. (1988): CDC33 encodes mRNA cap-binding protein eIF-4E of Saccharomyces cerevisiae. In: *Molecular and cellular biology* 8 (8), S. 3556–3559. DOI: 10.1128/mcb.8.8.3556-3559.1988.

Buttgereit, F.; Brand, M. D. (1995): A hierarchy of ATP-consuming processes in mammalian cells. In: *Biochemical Journal* 312 (Pt 1) (Pt 1), S. 163–167. DOI: 10.1042/bj3120163.

Buzzai, Monica; Bauer, Daniel E.; Jones, Russell G.; Deberardinis, Ralph J.; Hatzivassiliou, Georgia; Elstrom, Rebecca L.; Thompson, Craig B. (2005): The glucose dependence of Akt-transformed cells can be reversed by pharmacologic activation of fatty acid beta-oxidation. In: *Oncogene* 24 (26), S. 4165–4173. DOI: 10.1038/sj.onc.1208622.

Cai, Weijia; Ye, Qing; She, Qing-Bai (2014): Loss of 4E-BP1 function induces EMT and promotes cancer cell migration and invasion via cap-dependent translational activation of snail. In: *Oncotarget* 5 (15), S. 6015–6027. DOI: 10.18632/oncotarget.2109.

Caro-Maldonado, A.; Tait, S. W. G.; Ramírez-Peinado, S.; Ricci, J-E; Fabregat, I.; Green, D. R.; Muñoz-Pinedo, C. (2010): Glucose deprivation induces an atypical form of apoptosis mediated by caspase-8 in Bax-, Bak-deficient cells. In: *Cell death and differentiation* 17 (8), S. 1335–1344. DOI: 10.1038/cdd.2010.21.

Carracedo, Arkaitz; Cantley, Lewis C.; Pandolfi, Pier Paolo (2013): Cancer metabolism: fatty acid oxidation in the limelight. In: *Nat Rev Cancer* 13 (4), S. 227–232. DOI: 10.1038/nrc3483.

Carroll, Matthew; Dyer, John; Sossin, Wayne S. (2006): Serotonin increases phosphorylation of synaptic 4EBP through TOR, but eukaryotic initiation factor 4E levels do not limit somatic cap-dependent translation in aplysia neurons. In: *Molecular and cellular biology* 26 (22), S. 8586–8598. DOI: 10.1128/MCB.00955-06.

Castelli, Lydia M.; Talavera, David; Kershaw, Christopher J.; Mohammad-Qureshi, Sarah S.; Costello, Joseph L.; Rowe, William et al. (2015): The 4E-BP Caf20p Mediates Both eIF4E-Dependent and Independent Repression of Translation. In: *PLOS Genetics* 11 (5), e1005233. DOI: 10.1371/journal.pgen.1005233.

Cha, Yin-Lian; Li, Pin-Dong; Yuan, Lin-Jing; Zhang, Mei-Yin; Zhang, Yao-Jun; Rao, Hui-Lan et al. (2015): EIF4EBP1 overexpression is associated with poor survival and disease progression in patients with hepatocellular carcinoma. In: *PLOS ONE* 10 (2), e0117493. DOI: 10.1371/journal.pone.0117493.

Chao, Min-Wu; Wang, Li-Ting; Lai, Chin-Yu; Yang, Xiao-Ming; Cheng, Ya-Wen; Lee, Kuo-Hsiung et al. (2015): eIF4E binding protein 1 expression is associated with clinical survival outcomes in colorectal cancer. In: *Oncotarget* 6 (27), S. 24092–24104. DOI: 10.18632/oncotarget.4483.

Cheung, Chantal Hoi Yin; Hsu, Chia-Lang; Tsuei, Chao-Yin; Kuo, Tzu-Ting; Huang, Chen-Tsung; Hsu, Wen-Ming et al. (2019): Combinatorial targeting of MTHFD2 and PAICS in purine synthesis as a novel therapeutic strategy. In: *Cell death & disease* 10 (11), S. 786. DOI: 10.1038/s41419-019-2033-z.

Cho, Sung-Yup; Lee, Seungun; Yeom, Jeonghun; Kim, Hyo-Jun; Lee, Jin-Haeng; Shin, Ji-Woong et al. (2020): Transglutaminase 2 mediates hypoxia-induced selective mRNA translation via polyamination of 4EBPs. In: *Life Science Alliance* 3 (3). DOI: 10.26508/lsa.201900565.

Choo, Andrew Y.; Kim, Sang Gyun; Vander Heiden, Matthew G.; Mahoney, Sarah J.; Vu, Hieu; Yoon, Sang-Oh et al. (2010): Glucose addiction of TSC null cells is caused by failed mTORC1-dependent balancing of metabolic demand with supply. In: *Molecular cell* 38 (4), S. 487–499. DOI: 10.1016/j.molcel.2010.05.007.

Ciccarese, Francesco; Zulato, Elisabetta; Indraccolo, Stefano (2019): LKB1/AMPK Pathway and Drug Response in Cancer: A Therapeutic Perspective. In: *Oxidative Medicine and Cellular Longevity* 2019, S. 8730816. DOI: 10.1155/2019/8730816.

Colon, Nadja C.; Chung, Dai H. (2011): Neuroblastoma. In: *Advances in pediatrics* 58 (1), S. 297–311. DOI: 10.1016/j.yapd.2011.03.011.

Conn, Crystal S.; Yang, Haojun; Tom, Harrison J.; Ikeda, Kenji; Oses-Prieto, Juan A.; Vu, Hieu et al. (2021): The major cap-binding protein eIF4E regulates lipid homeostasis and diet-induced obesity. In: *Nat Metab* 3 (2), S. 244–257. DOI: 10.1038/s42255-021-00349-z.

Cosentino, G. P.; Schmelzle, T.; Haghighat, A.; Helliwell, S. B.; Hall, M. N.; Sonenberg, N. (2000): Eap1p, a novel eukaryotic translation initiation factor 4E-associated protein in Saccharomyces cerevisiae. In: *Molecular and cellular biology* 20 (13), S. 4604–4613. DOI: 10.1128/MCB.20.13.4604-4613.2000.

Cridge, Andrew G.; Castelli, Lydia M.; Smirnova, Julia B.; Selley, Julian N.; Rowe, William; Hubbard, Simon J. et al. (2010): Identifying eIF4E-binding protein translationally-controlled transcripts reveals links to mRNAs bound by specific PUF proteins. In: *Nucleic Acids Research* 38 (22), S. 8039–8050. DOI: 10.1093/nar/gkq686.

Dastidar, Somasish Ghosh; Pham, Michael T.; Mitchell, Matthew B.; Yeom, Steven G.; Jordan, Sarah; Chang, Angela et al. (2020): 4E-BP1 Protects Neurons from Misfolded Protein Stress and Parkinson's Disease Toxicity by Inducing the Mitochondrial Unfolded Protein Response. In: *J. Neurosci.* 40 (45), S. 8734–8745. DOI: 10.1523/JNEUROSCI.0940-20.2020.

Deberardinis, Ralph J.; Lum, Julian J.; Hatzivassiliou, Georgia; Thompson, Craig B. (2008): The biology of cancer: metabolic reprogramming fuels cell growth and proliferation. In: *Cell Metabolism* 7 (1), S. 11–20. DOI: 10.1016/j.cmet.2007.10.002.

Delaidelli, Alberto; Negri, Gian Luca; Jan, Asad; Jansonius, Brandon; El-Naggar, Amal; Lim, Jonathan K. M. et al. (2017): MYCN amplified neuroblastoma requires the mRNA translation regulator eEF2 kinase to adapt to nutrient deprivation. In: *Cell death and differentiation* 24 (9), S. 1564–1576. DOI: 10.1038/cdd.2017.79.

Demontis, Fabio; Perrimon, Norbert (2010): FOXO/4E-BP signaling in Drosophila muscles regulates organism-wide proteostasis during aging. In: *Cell* 143 (5), S. 813–825. DOI: 10.1016/j.cell.2010.10.007.

Dennis, Michael D.; Shenberger, Jeffrey S.; Stanley, Bruce A.; Kimball, Scot R.; Jefferson, Leonard S. (2013): Hyperglycemia mediates a shift from cap-dependent to cap-independent translation via a 4E-BP1-dependent mechanism. In: *Diabetes* 62 (7), S. 2204–2214. DOI: 10.2337/db12-1453.

Dever, Thomas E.; Kinzy, Terri Goss; Pavitt, Graham D. (2016): Mechanism and Regulation of Protein Synthesis in Saccharomyces cerevisiae. In: *Genetics* 203 (1), S. 65–107. DOI: 10.1534/genetics.115.186221.

Ding, Boxiao; Parmigiani, Anita; Divakaruni, Ajit S.; Archer, Kellie; Murphy, Anne N.; Budanov, Andrei V. (2016): Sestrin2 is induced by glucose starvation via the unfolded protein response and protects cells from non-canonical necroptotic cell death. In: *Sci Rep* 6, S. 22538. DOI: 10.1038/srep22538.

Ding, Mei; van der Kwast, Theodorus H.; Vellanki, Ravi N.; Foltz, Warren D.; McKee, Trevor D.; Sonenberg, Nahum et al. (2018): The mTOR Targets 4E-BP1/2 Restrain Tumor Growth and Promote Hypoxia Tolerance in PTEN-driven Prostate Cancer. In: *Mol Cancer Res* 16 (4), S. 682–695. DOI: 10.1158/1541-7786.MCR-17-0696.

Dowling, Ryan J. O.; Topisirovic, Ivan; Alain, Tommy; Bidinosti, Michael; Fonseca, Bruno D.; Petroulakis, Emmanuel et al. (2010): mTORC1-mediated cell proliferation, but not cell growth, controlled by the 4E-BPs. In: *Science (New York, N.Y.)* 328 (5982), S. 1172–1176. DOI: 10.1126/science.1187532.

Dubois, Ludwig; Magagnin, Michaël G.; Cleven, Arjen H. G.; Weppler, Sherry A.; Grenacher, Beat; Landuyt, Willy et al. (2009): Inhibition of 4E-BP1 sensitizes U87 glioblastoma xenograft tumors to irradiation by decreasing hypoxia tolerance. In: *International journal of radiation oncology, biology, physics* 73 (4), S. 1219–1227. DOI: 10.1016/j.ijrobp.2008.12.003.

Eberlé, Delphine; Hegarty, Bronwyn; Bossard, Pascale; Ferré, Pascal; Foufelle, Fabienne (2004): SREBP transcription factors: master regulators of lipid homeostasis. In: *Biochimie* 86 (11), S. 839–848. DOI: 10.1016/j.biochi.2004.09.018.

Eguchi, Y.; Shimizu, S.; Tsujimoto, Y. (1997): Intracellular ATP levels determine cell death fate by apoptosis or necrosis. In: *Cancer Res* 57 (10), S. 1835–1840. Online verfügbar unter https://pubmed.ncbi.nlm.nih.gov/9157970/.

Fernandez, James; Bode, Barry; Koromilas, Antonis; Diehl, J. Alan; Krukovets, Irene; Snider, Martin D.; Hatzoglou, Maria (2002): Translation mediated by the internal ribosome entry site of the cat-1 mRNA is regulated by glucose availability in a PERK kinase-dependent manner. In: *Journal of Biological Chemistry* 277 (14), S. 11780–11787. DOI: 10.1074/jbc.M110778200.

Fingar, Diane C.; Richardson, Celeste J.; Tee, Andrew R.; Cheatham, Lynn; Tsou, Christina; Blenis, John (2004): mTOR controls cell cycle progression through its cell growth effectors S6K1 and 4E-

BP1/eukaryotic translation initiation factor 4E. In: *Molecular and cellular biology* 24 (1), S. 200–216. DOI: 10.1128/MCB.24.1.200-216.2004.

Fingar, Diane C.; Salama, Sofie; Tsou, Christina; Harlow, Ed; Blenis, John (2002): Mammalian cell size is controlled by mTOR and its downstream targets S6K1 and 4EBP1/eIF4E. In: *Genes & Development* 16 (12), S. 1472–1487. DOI: 10.1101/gad.995802.

Flavahan, William A.; Wu, Qiulian; Hitomi, Masahiro; Rahim, Nasiha; Kim, Youngmi; Sloan, Andrew E. et al. (2013): Brain tumor initiating cells adapt to restricted nutrition through preferential glucose uptake. In: *Nat Neurosci* 16 (10), S. 1373–1382. DOI: 10.1038/nn.3510.

Foster, Kathryn G.; Fingar, Diane C. (2010): Mammalian target of rapamycin (mTOR): conducting the cellular signaling symphony. In: *Journal of Biological Chemistry* 285 (19), S. 14071–14077. DOI: 10.1074/jbc.R109.094003.

Frau, Maddalena; Ladu, Sara; Calvisi, Diego F.; Simile, Maria M.; Bonelli, Piero; Daino, Lucia et al. (2011): Mybl2 expression is under genetic control and contributes to determine a hepatocellular carcinoma susceptible phenotype. In: *Journal of hepatology* 55 (1), S. 111–119. DOI: 10.1016/j.jhep.2010.10.031.

Fry, Elizabeth A.; Inoue, Kazushi (2018): Aberrant expression of ETS1 and ETS2 proteins in cancer. In: *Cancer reports and reviews* 2 (3). DOI: 10.15761/CRR.1000151.

Galluzzi, Lorenzo; Vitale, Ilio; Aaronson, Stuart A.; Abrams, John M.; Adam, Dieter; Agostinis, Patrizia et al. (2018): Molecular mechanisms of cell death: recommendations of the Nomenclature Committee on Cell Death 2018. In: *Cell death and differentiation* 25 (3), S. 486–541. DOI: 10.1038/s41418-017-0012-4.

Gebauer, Fátima; Hentze, Matthias W. (2004): Molecular mechanisms of translational control. In: *Nat Rev Mol Cell Biol* 5 (10), S. 827–835. DOI: 10.1038/nrm1488.

Gilbert, Wendy V.; Zhou, Kaihong; Butler, Tamira K.; Doudna, Jennifer A. (2007): Cap-independent translation is required for starvation-induced differentiation in yeast. In: *Science (New York, N.Y.)* 317 (5842), S. 1224–1227. DOI: 10.1126/science.1144467.

Gingras, A. C.; Kennedy, S. G.; O'Leary, M. A.; Sonenberg, N.; Hay, N. (1998): 4E-BP1, a repressor of mRNA translation, is phosphorylated and inactivated by the Akt(PKB) signaling pathway. In: *Genes & Development* 12 (4), S. 502–513. DOI: 10.1101/gad.12.4.502.

Gingras, A. C.; Raught, B.; Gygi, S. P.; Niedzwiecka, A.; Miron, M.; Burley, S. K. et al. (2001): Hierarchical phosphorylation of the translation inhibitor 4E-BP1. In: *Genes & Development* 15 (21), S. 2852–2864. DOI: 10.1101/gad.912401.

Gkogkas, Christos G.; Khoutorsky, Arkady; Ran, Israeli; Rampakakis, Emmanouil; Nevarko, Tatiana; Weatherill, Daniel B. et al. (2013): Autism-related deficits via dysregulated eIF4E-dependent translational control. In: *Nature* 493 (7432), S. 371–377. DOI: 10.1038/nature11628.

Graber, Tyson E.; Holcik, Martin (2007): Cap-independent regulation of gene expression in apoptosis. In: *Mol. BioSyst.* 3 (12), S. 825–834. DOI: 10.1039/B708867A.

Graff, Jeremy R.; Konicek, Bruce W.; Carter, Julia H.; Marcusson, Eric G. (2008): Targeting the eukaryotic translation initiation factor 4E for cancer therapy. In: *Cancer Res* 68 (3), S. 631–634. DOI: 10.1158/0008-5472.CAN-07-5635.

Gwinn, Dana M.; Shackelford, David B.; Egan, Daniel F.; Mihaylova, Maria M.; Mery, Annabelle; Vasquez, Debbie S. et al. (2008): AMPK phosphorylation of raptor mediates a metabolic checkpoint. In: *Molecular cell* 30 (2), S. 214–226. DOI: 10.1016/j.molcel.2008.03.003.

Haghighat, A.; Mader, S.; Pause, A.; Sonenberg, N. (1995): Repression of cap-dependent translation by 4E-binding protein 1: competition with p220 for binding to eukaryotic initiation factor-4E. In: *The EMBO journal* 14 (22), S. 5701–5709. Online verfügbar unter https://pubmed.ncbi.nlm.nih.gov/8521827/.

Hamann, Jens C.; Surcel, Alexandra; Chen, Ruoyao; Teragawa, Carolyn; Albeck, John G.; Robinson, Douglas N.; Overholtzer, Michael (2017): Entosis Is Induced by Glucose Starvation. In: *Cell reports* 20 (1), S. 201–210. DOI: 10.1016/j.celrep.2017.06.037.

Hardie, D. Grahame; Ross, Fiona A.; Hawley, Simon A. (2012): AMPK: a nutrient and energy sensor that maintains energy homeostasis. In: *Nat Rev Mol Cell Biol* 13 (4), S. 251–262. DOI: 10.1038/nrm3311.

Hartman, Nathaniel W.; Lin, Tiffany V.; Zhang, Longbo; Paquelet, Grace E.; Feliciano, David M.; Bordey, Angélique (2013): mTORC1 targets the translational repressor 4E-BP2, but not S6 kinase 1/2, to regulate neural stem cell self-renewal in vivo. In: *Cell reports* 5 (2), S. 433–444. DOI: 10.1016/j.celrep.2013.09.017.

Hay, Nissim; Sonenberg, Nahum (2004): Upstream and downstream of mTOR. In: *Genes & Development* 18 (16), S. 1926–1945. DOI: 10.1101/gad.1212704.

Herzig, Sébastien; Shaw, Reuben J. (2018): AMPK: guardian of metabolism and mitochondrial homeostasis. In: *Nat Rev Mol Cell Biol* 19 (2), S. 121–135. DOI: 10.1038/nrm.2017.95.

Hinnebusch, Alan G.; Ivanov, Ivaylo P.; Sonenberg, Nahum (2016): Translational control by 5'-untranslated regions of eukaryotic mRNAs. In: *Science (New York, N.Y.)* 352 (6292), S. 1413–1416. DOI: 10.1126/science.aad9868.

Holcik, Martin; Sonenberg, Nahum (2005): Translational control in stress and apoptosis. In: *Nat Rev Mol Cell Biol* 6 (4), S. 318–327. DOI: 10.1038/nrm1618.

Holditch, Sara J.; Brown, Carolyn N.; Atwood, Daniel J.; Pokhrel, Deepak; Brown, Sara E.; Lombardi, Andrew M. et al. (2019): The consequences of increased 4E-BP1 in polycystic kidney disease. In: *Hum Mol Genet* 28 (24), S. 4132–4147. DOI: 10.1093/hmg/ddz244.

Hong, Sungki; Freeberg, Mallory A.; Han, Ting; Kamath, Avani; Yao, Yao; Fukuda, Tomoko et al. (2017): LARP1 functions as a molecular switch for mTORC1-mediated translation of an essential class of mRNAs. In: *eLife Sciences Publications, Ltd*, 26.06.2017. Online verfügbar unter https://elifesciences.org/articles/25237, zuletzt geprüft am 21.10.2021.

Hsieh, Andrew C.; Costa, Maria; Zollo, Ornella; Davis, Cole; Feldman, Morris E.; Testa, Joseph R. et al. (2010): Genetic dissection of the oncogenic mTOR pathway reveals druggable addiction to translational control via 4EBP-eIF4E. In: *Cancer cell* 17 (3), S. 249–261. DOI: 10.1016/j.ccr.2010.01.021.

Hsieh, Andrew C.; Liu, Yi; Edlind, Merritt P.; Ingolia, Nicholas T.; Janes, Matthew R.; Sher, Annie et al. (2012): The translational landscape of mTOR signalling steers cancer initiation and metastasis. In: *Nature* 485 (7396), S. 55–61. DOI: 10.1038/nature10912.

Hsieh, Andrew C.; Nguyen, Hao G.; Wen, Lexiaochuan; Edlind, Merritt P.; Carroll, Peter R.; Kim, Won; Ruggero, Davide (2015): Cell type-specific abundance of 4EBP1 primes prostate cancer sensitivity or resistance to PI3K pathway inhibitors. In: *Sci. Signal.* 8 (403), ra116. DOI: 10.1126/scisignal.aad5111.

Hsu, Chia-Lang; Chang, Hsin-Yi; Chang, Jen-Yun; Hsu, Wen-Ming; Huang, Hsuan-Cheng; Juan, Hsueh-Fen (2016): Unveiling MYCN regulatory networks in neuroblastoma via integrative analysis of heterogeneous genomics data. In: *Oncotarget* 7 (24), S. 36293–36310. DOI: 10.18632/oncotarget.9202.

Hsu, Peggy P.; Sabatini, David M. (2008): Cancer cell metabolism: Warburg and beyond. In: *Cell* 134 (5), S. 703–707. DOI: 10.1016/j.cell.2008.08.021.

Huang, Chung-I; Wang, Chih-Chun; Tai, Tzong-Shyuan; Hwang, Tzer-Zen; Yang, Chuan-Chien; Hsu, Chin-Mu; Su, Yu-Chieh (2019): eIF4E and 4EBP1 are prognostic markers of head and neck squamous cell carcinoma recurrence after definitive surgery and adjuvant radiotherapy. In: *PloS one* 14 (11), e0225537. DOI: 10.1371/journal.pone.0225537.

Ibrahimo, Salma; Holmes, Leah E. A.; Ashe, Mark P. (2006): Regulation of translation initiation by the yeast eIF4E binding proteins is required for the pseudohyphal response. In: *Yeast (Chichester, England)* 23 (14-15), S. 1075–1088. DOI: 10.1002/yea.1415.

Igreja, Cátia; Peter, Daniel; Weiler, Catrin; Izaurralde, Elisa (2014): 4E-BPs require non-canonical 4E-binding motifs and a lateral surface of eIF4E to repress translation. In: *Nat Commun* 5, S. 4790. DOI: 10.1038/ncomms5790.

Jagoe, R. Thomas; Lecker, Stewart H.; Gomes, Marcelo; Goldberg, Alfred L. (2002): Patterns of gene expression in atrophying skeletal muscles: response to food deprivation. In: *FASEB journal : official publication of the Federation of American Societies for Experimental Biology* 16 (13), S. 1697–1712. DOI: 10.1096/fj.02-0312com.

Jeon, Sang-Min; Chandel, Navdeep S.; Hay, Nissim (2012): AMPK regulates NADPH homeostasis to promote tumour cell survival during energy stress. In: *Nature* 485 (7400), S. 661–665. DOI: 10.1038/nature11066.

Jin, Hua; Xu, Weijin; Rahman, Reazur; Na, Daxiang; Fieldsend, Allegra; Song, Wei et al. (2020): TRIBE editing reveals specific mRNA targets of eIF4E-BP in Drosophila and in mammals. In: *Science Advances* 6 (33), eabb8771. DOI: 10.1126/sciadv.abb8771.

Joyner, Ryan P.; Tang, Jeffrey H.; Helenius, Jonne; Dultz, Elisa; Brune, Christiane; Holt, Liam J. et al. (2016): A glucose-starvation response regulates the diffusion of macromolecules. In: *eLife* 5. DOI: 10.7554/eLife.09376.

Kang, Min-Ji; Vasudevan, Deepika; Kang, Kwonyoon; Kim, Kyunggon; Park, Jung-Eun; Zhang, Nan et al. (2017): 4E-BP is a target of the GCN2-ATF4 pathway during Drosophila development and aging. In: *The Journal of cell biology* 216 (1), S. 115–129. DOI: 10.1083/jcb.201511073.

Karlsson, Elin; Pérez-Tenorio, Gizeh; Amin, Risul; Bostner, Josefine; Skoog, Lambert; Fornander, Tommy et al. (2013): The mTOR effectors 4EBP1 and S6K2 are frequently coexpressed, and associated with a poor prognosis and endocrine resistance in breast cancer: a retrospective study including patients from the randomised Stockholm tamoxifen trials. In: *Breast cancer research : BCR* 15 (5), R96. DOI: 10.1186/bcr3557.

Karlsson, Elin; Waltersson, Marie Ahnström; Bostner, Josefine; Pérez-Tenorio, Gizeh; Olsson, Birgit; Hallbeck, Anna-Lotta; Stål, Olle (2011): High-resolution genomic analysis of the 11q13 amplicon in breast cancers identifies synergy with 8p12 amplification, involving the mTOR targets S6K2 and 4EBP1. In: *Genes, chromosomes & cancer* 50 (10), S. 775–787. DOI: 10.1002/gcc.20900.

Khan, D.; Katoch, A.; Das, A.; Sharathchandra, A.; Lal, R.; Roy, P. et al. (2015): Reversible induction of translational isoforms of p53 in glucose deprivation. In: *Cell death and differentiation* 22 (7), S. 1203–1218. DOI: 10.1038/cdd.2014.220.

Kim, Joungmok; Guan, Kun-Liang (2019): mTOR as a central hub of nutrient signalling and cell growth. In: *Nat Cell Biol* 21 (1), S. 63–71. DOI: 10.1038/s41556-018-0205-1.

Kim, Joungmok; Kundu, Mondira; Viollet, Benoit; Guan, Kun-Liang (2011): AMPK and mTOR regulate autophagy through direct phosphorylation of Ulk1. In: *Nat Cell Biol* 13 (2), S. 132–141. DOI: 10.1038/ncb2152.

Komar, Anton A.; Hatzoglou, Maria (2011): Cellular IRES-mediated translation: the war of ITAFs in pathophysiological states. In: *Cell Cycle* 10 (2), S. 229–240. DOI: 10.4161/cc.10.2.14472.

Kremer, Celeste L.; Klein, Rob R.; Mendelson, Jenny; Browne, Walden; Samadzedeh, Linda K.; Vanpatten, Kristie et al. (2006): Expression of mTOR signaling pathway markers in prostate cancer progression. In: *The Prostate* 66 (11), S. 1203–1212. DOI: 10.1002/pros.20410.

Lachance, Pascal E. D.; Miron, Mathieu; Raught, Brian; Sonenberg, Nahum; Lasko, Paul (2002): Phosphorylation of eukaryotic translation initiation factor 4E is critical for growth. In: *Molecular and cellular biology* 22 (6), S. 1656–1663. DOI: 10.1128/MCB.22.6.1656-1663.2002.

Lahr, Roni M.; Fonseca, Bruno D.; Ciotti, Gabrielle E.; Al-Ashtal, Hiba A.; Jia, Jian-Jun; Niklaus, Marius R. et al. (2017): La-related protein 1 (LARP1) binds the mRNA cap, blocking eIF4F assembly on TOP mRNAs. In: *eLife* 6. DOI: 10.7554/eLife.24146.

Lang, Michael J.; Martinez-Marquez, Jorge Y.; Prosser, Derek C.; Ganser, Laura R.; Buelto, Destiney; Wendland, Beverly; Duncan, Mara C. (2014): Glucose starvation inhibits autophagy via vacuolar hydrolysis and induces plasma membrane internalization by down-regulating recycling. In: *Journal of Biological Chemistry* 289 (24), S. 16736–16747. DOI: 10.1074/jbc.M113.525782.

Laplante, Mathieu; Sabatini, David M. (2009): An emerging role of mTOR in lipid biosynthesis. In: *Current biology : CB* 19 (22), R1046-52. DOI: 10.1016/j.cub.2009.09.058.

Laplante, Mathieu; Sabatini, David M. (2012): mTOR signaling in growth control and disease. In: *Cell* 149 (2), S. 274–293. DOI: 10.1016/j.cell.2012.03.017.

Lawrence, J. (1997): PHAS/4E-BPs as regulators of mRNA translation and cell proliferation. In: *Trends in biochemical sciences* 22 (9), S. 345–349. DOI: 10.1016/s0968-0004(97)01101-8.

Lazaris-Karatzas, A.; Montine, K. S.; Sonenberg, N. (1990): Malignant transformation by a eukaryotic initiation factor subunit that binds to mRNA 5' cap. In: *Nature* 345 (6275), S. 544–547. DOI: 10.1038/345544a0.

Le Bacquer, Olivier; Combe, Kristell; Patrac, Véronique; Ingram, Brian; Combaret, Lydie; Dardevet, Dominique et al. (2019): 4E-BP1 and 4E-BP2 double knockout mice are protected from aging-associated sarcopenia. In: *Journal of cachexia, sarcopenia and muscle* 10 (3), S. 696–709. DOI: 10.1002/jcsm.12412.

Le Bacquer, Olivier; Petroulakis, Emmanuel; Paglialunga, Sabina; Poulin, Francis; Richard, Denis; Cianflone, Katherine; Sonenberg, Nahum (2007): Elevated sensitivity to diet-induced obesity and insulin resistance in mice lacking 4E-BP1 and 4E-BP2. In: *J Clin Invest* 117 (2), S. 387–396. DOI: 10.1172/JCI29528.

Lee, Bianca J.; Boyer, Jacob A.; Burnett, G. Leslie; Thottumkara, Arun P.; Tibrewal, Nidhi; Wilson, Stacy L. et al. (2021): Selective inhibitors of mTORC1 activate 4EBP1 and suppress tumor growth. In: *Nature chemical biology*. DOI: 10.1038/s41589-021-00813-7.

Lee, Ho Jeong; Venkatarame Gowda Saralamma, Venu; Kim, Seong Min; Ha, Sang Eun; Raha, Suchismita; Lee, Won Sup et al. (2018): Pectolinarigenin Induced Cell Cycle Arrest, Autophagy, and Apoptosis in Gastric Cancer Cell via PI3K/AKT/mTOR Signaling Pathway. In: *Nutrients* 10 (8). DOI: 10.3390/nu10081043.

Leist, M.; Single, B.; Castoldi, A. F.; Kühnle, S.; Nicotera, P. (1997): Intracellular adenosine triphosphate (ATP) concentration: a switch in the decision between apoptosis and necrosis. In: *The Journal of experimental medicine* 185 (8), S. 1481–1486. DOI: 10.1084/jem.185.8.1481.

León-Annicchiarico, Clara Lucía; Ramírez-Peinado, Silvia; Domínguez-Villanueva, Dídac; Gonsberg, Anika; Lampidis, Theodore J.; Muñoz-Pinedo, Cristina (2015): ATF4 mediates necrosis induced by glucose deprivation and apoptosis induced by 2-deoxyglucose in the same cells. In: *The FEBS Journal* 282 (18), S. 3647–3658. DOI: 10.1111/febs.13369.

Leprivier, Gabriel; Remke, Marc; Rotblat, Barak; Dubuc, Adrian; Mateo, Abigail-Rachele F.; Kool, Marcel et al. (2013): The eEF2 kinase confers resistance to nutrient deprivation by blocking translation elongation. In: *Cell* 153 (5), S. 1064–1079. DOI: 10.1016/j.cell.2013.04.055.

Leprivier, Gabriel; Rotblat, Barak (2020): How does mTOR sense glucose starvation? AMPK is the usual suspect. In: *Cell Death Discov.* 6 (1), S. 27. DOI: 10.1038/s41420-020-0260-9.

Leprivier, Gabriel; Rotblat, Barak; Khan, Debjit; Jan, Eric; Sorensen, Poul H. (2015): Stress-mediated translational control in cancer cells. In: *Biochimica et biophysica acta* 1849 (7), S. 845–860. DOI: 10.1016/j.bbagrm.2014.11.002.

Li, Li; Hao, Yu; Zhao, Yu; Wang, Huijuan; Zhao, Xiujun; Jiang, Yan; Gao, Fulu (2018): Ferroptosis is associated with oxygen-glucose deprivation/reoxygenation-induced Sertoli cell death. In: *International journal of molecular medicine* 41 (5), S. 3051–3062. DOI: 10.3892/ijmm.2018.3469.

Liang, Jiyong; Mills, Gordon B. (2013): AMPK: a contextual oncogene or tumor suppressor? In: *Cancer Res* 73 (10), S. 2929–2935. DOI: 10.1158/0008-5472.CAN-12-3876.

Lin, Sheng-Cai; Hardie, D. Grahame (2018): AMPK: Sensing Glucose as well as Cellular Energy Status. In: *Cell Metabolism* 27 (2), S. 299–313. DOI: 10.1016/j.cmet.2017.10.009.

Lin, T. A.; Kong, X.; Haystead, T. A.; Pause, A.; Belsham, G.; Sonenberg, N.; Lawrence, J. C. (1994): PHAS-I as a link between mitogen-activated protein kinase and translation initiation. In: *Science (New York, N.Y.)* 266 (5185), S. 653–656. DOI: 10.1126/science.7939721.

Lindqvist, Lisa M.; Tandoc, Kristofferson; Topisirovic, Ivan; Furic, Luc (2018): Cross-talk between protein synthesis, energy metabolism and autophagy in cancer. In: *Current Opinion in Genetics & Development* 48, S. 104–111. DOI: 10.1016/j.gde.2017.11.003.

Liu, Grace Y.; Sabatini, David M. (2020): mTOR at the nexus of nutrition, growth, ageing and disease. In: *Nature reviews. Molecular cell biology* 21 (4), S. 183–203. DOI: 10.1038/s41580-019-0199-y.

Liu, Jianyu; Stevens, Payton D.; Eshleman, Nichole E.; Gao, Tianyan (2013): Protein phosphatase PPM1G regulates protein translation and cell growth by dephosphorylating 4E binding protein 1 (4E-BP1). In: *Journal of Biological Chemistry* 288 (32), S. 23225–23233. DOI: 10.1074/jbc.M113.492371.

Lugano, Roberta; Ramachandran, Mohanraj; Dimberg, Anna (2020): Tumor angiogenesis: causes, consequences, challenges and opportunities. In: *Cell. Mol. Life Sci.* 77 (9), S. 1745–1770. DOI: 10.1007/s00018-019-03351-7.

Lynch, Mary; Fitzgerald, Chris; Johnston, Kelly A.; Wang, Shanping; Schmidt, Emmett V. (2004): Activated eIF4E-binding protein slows G1 progression and blocks transformation by c-myc without inhibiting cell growth. In: *The Journal of biological chemistry* 279 (5), S. 3327–3339. DOI: 10.1074/jbc.M310872200.

Ma, Xiaoju Max; Blenis, John (2009): Molecular mechanisms of mTOR-mediated translational control. In: *Nat Rev Mol Cell Biol* 10 (5), S. 307–318. DOI: 10.1038/nrm2672.

Mader, S.; Lee, H.; Pause, A.; Sonenberg, N. (1995): The translation initiation factor eIF-4E binds to a common motif shared by the translation factor eIF-4 gamma and the translational repressors 4E-binding proteins. In: *Molecular and cellular biology* 15 (9), S. 4990–4997. DOI: 10.1128/MCB.15.9.4990.

Marambio, Paola; Toro, Barbra; Sanhueza, Carlos; Troncoso, Rodrigo; Parra, Valentina; Verdejo, Hugo et al. (2010): Glucose deprivation causes oxidative stress and stimulates aggresome formation and autophagy in cultured cardiac myocytes. In: *Biochimica et biophysica acta* 1802 (6), S. 509–518. DOI: 10.1016/j.bbadis.2010.02.002.

Martínez-Reyes, Inmaculada; Chandel, Navdeep S. (2020): Mitochondrial TCA cycle metabolites control physiology and disease. In: *Nat Commun* 11 (1), S. 102. DOI: 10.1038/s41467-019-13668-3.

Mascarenhas, Claire; Edwards-Ingram, Laura C.; Zeef, Leo; Shenton, Daniel; Ashe, Mark P.; Grant, Chris M. (2008): Gcn4 is required for the response to peroxide stress in the yeast Saccharomyces cerevisiae. In: *Molecular biology of the cell* 19 (7), S. 2995–3007. DOI: 10.1091/mbc.e07-11-1173.

Masoro, Edward J. (2000): Caloric restriction and aging: an update. In: *Experimental Gerontology* 35 (3), S. 299–305. DOI: 10.1016/S0531-5565(00)00084-X.

Mehrpour, Maryam; Esclatine, Audrey; Beau, Isabelle; Codogno, Patrice (2010): Overview of macroautophagy regulation in mammalian cells. In: *Cell Res* 20 (7), S. 748–762. DOI: 10.1038/cr.2010.82.

Millena, Ana Cecilia; Vo, BaoHan T.; Khan, Shafiq A. (2016): JunD Is Required for Proliferation of Prostate Cancer Cells and Plays a Role in Transforming Growth Factor-β (TGF-β)-induced Inhibition of Cell Proliferation. In: *Journal of Biological Chemistry* 291 (34), S. 17964–17976. DOI: 10.1074/jbc.M116.714899.

Miron, M.; Verdú, J.; Lachance, P. E.; Birnbaum, M. J.; Lasko, P. F.; Sonenberg, N. (2001): The translational inhibitor 4E-BP is an effector of PI(3)K/Akt signalling and cell growth in Drosophila. In: *Nat Cell Biol* 3 (6), S. 596–601. DOI: 10.1038/35078571.

Morita, Masahiro; Gravel, Simon-Pierre; Chénard, Valérie; Sikström, Kristina; Zheng, Liang; Alain, Tommy et al. (2013): mTORC1 controls mitochondrial activity and biogenesis through 4E-BP-dependent translational regulation. In: *Cell Metabolism* 18 (5), S. 698–711. DOI: 10.1016/j.cmet.2013.10.001.

Moruno, Félix; Pérez-Jiménez, Eva; Knecht, Erwin (2012): Regulation of autophagy by glucose in Mammalian cells. In: *Cells* 1 (3), S. 372–395. DOI: 10.3390/cells1030372.

Mossmann, Dirk; Park, Sujin; Hall, Michael N. (2018): mTOR signalling and cellular metabolism are mutual determinants in cancer. In: *Nat Rev Cancer* 18 (12), S. 744–757. DOI: 10.1038/s41568-018-0074-8.

Musa, J.; Orth, M. F.; Dallmayer, M.; Baldauf, M.; Pardo, C.; Rotblat, B. et al. (2016): Eukaryotic initiation factor 4E-binding protein 1 (4E-BP1): a master regulator of mRNA translation involved in tumorigenesis. In: *Oncogene* 35 (36), S. 4675–4688. DOI: 10.1038/onc.2015.515.

National Center for Biotechnology Information (NCBI)[Internet]. Online verfügbar unter https://www.ncbi.nlm.nih.gov/, zuletzt geprüft am September 2021.

Nehdi, Atef; Sean, Polen; Linares, Izzar; Colina, Rodney; Jaramillo, Maritza; Alain, Tommy (2014): Deficiency in either 4E-BP1 or 4E-BP2 augments innate antiviral immune responses. In: *PLOS ONE* 9 (12), e114854. DOI: 10.1371/journal.pone.0114854.

Orozco, Jose M.; Krawczyk, Patrycja A.; Scaria, Sonia M.; Cangelosi, Andrew L.; Chan, Sze Ham; Kunchok, Tenzin et al. (2020): Dihydroxyacetone phosphate signals glucose availability to mTORC1. In: *Nat Metab* 2 (9), S. 893–901. DOI: 10.1038/s42255-020-0250-5.

Oulhen, Nathalie; Boulben, Sandrine; Bidinosti, Michael; Morales, Julia; Cormier, Patrick; Cosson, Bertrand (2009): A variant mimicking hyperphosphorylated 4E-BP inhibits protein synthesis in a sea urchin cell-free, cap-dependent translation system. In: *PLOS ONE* 4 (3), e5070. DOI: 10.1371/journal.pone.0005070.

Palm, Wilhelm; Park, Youngkyu; Wright, Kevin; Pavlova, Natalya N.; Tuveson, David A.; Thompson, Craig B. (2015): The Utilization of Extracellular Proteins as Nutrients Is Suppressed by mTORC1. In: *Cell* 162 (2), S. 259–270. DOI: 10.1016/j.cell.2015.06.017.

Palorini, Roberta; Votta, Giuseppina; Pirola, Yuri; Vitto, Humberto de; Palma, Sara de; Airoldi, Cristina et al. (2016): Protein Kinase A Activation Promotes Cancer Cell Resistance to Glucose Starvation and Anoikis. In: *PLOS Genetics* 12 (3), e1005931. DOI: 10.1371/journal.pgen.1005931.

Pende, Mario; Um, Sung Hee; Mieulet, Virginie; Sticker, Melanie; Goss, Valerie L.; Mestan, Jurgen et al. (2004): S6K1(-/-)/S6K2(-/-) mice exhibit perinatal lethality and rapamycin-sensitive 5'-terminal oligopyrimidine mRNA translation and reveal a mitogen-activated protein kinase-dependent S6 kinase pathway. In: *Molecular and cellular biology* 24 (8), S. 3112–3124. DOI: 10.1128/MCB.24.8.3112-3124.2004.

Petroulakis, Emmanuel; Parsyan, Armen; Dowling, Ryan J. O.; LeBacquer, Olivier; Martineau, Yvan; Bidinosti, Michael et al. (2009): p53-dependent translational control of senescence and transformation via 4E-BPs. In: *Cancer cell* 16 (5), S. 439–446. DOI: 10.1016/j.ccr.2009.09.025.

Pettersson, Filippa; Del Rincon, Sonia V.; Emond, Audrey; Huor, Bonnie; Ngan, Elaine; Ng, Jonathan et al. (2015): Genetic and pharmacologic inhibition of eIF4E reduces breast cancer cell migration, invasion, and metastasis. In: *Cancer research* 75 (6), S. 1102–1112. DOI: 10.1158/0008-5472.CAN-14-1996.

Pickering, Becky M.; Willis, Anne E. (2005): The implications of structured 5' untranslated regions on translation and disease. In: *Seminars in cell & developmental biology* 16 (1), S. 39–47. DOI: 10.1016/j.semcdb.2004.11.006.

Pifferi, Fabien; Terrien, Jérémy; Marchal, Julia; Dal-Pan, Alexandre; Djelti, Fathia; Hardy, Isabelle et al. (2018): Caloric restriction increases lifespan but affects brain integrity in grey mouse lemur primates. In: *Commun Biol* 1 (1), S. 30. DOI: 10.1038/s42003-018-0024-8.

Pike, Lisa S.; Smift, Amy L.; Croteau, Nicole J.; Ferrick, David A.; Wu, Min (2011): Inhibition of fatty acid oxidation by etomoxir impairs NADPH production and increases reactive oxygen species resulting in ATP depletion and cell death in human glioblastoma cells. In: *Biochimica et biophysica acta* 1807 (6), S. 726–734. DOI: 10.1016/j.bbabio.2010.10.022.

Poulin, F.; Gingras, A. C.; Olsen, H.; Chevalier, S.; Sonenberg, N. (1998): 4E-BP3, a new member of the eukaryotic initiation factor 4E-binding protein family. In: *The Journal of biological chemistry* 273 (22), S. 14002–14007. DOI: 10.1074/jbc.273.22.14002.

Qin, Xiaoyu; Jiang, Bin; Zhang, Yanjie (2016): 4E-BP1, a multifactor regulated multifunctional protein. In: *Cell Cycle* 15 (6), S. 781–786. DOI: 10.1080/15384101.2016.1151581.

Qu, Yuanyuan; Zhao, Rui; Wang, Hongkai; Chang, Kun; Yang, Xiaoqun; Zhou, Xiaoyan et al. (2016): Phosphorylated 4EBP1 is associated with tumor progression and poor prognosis in Xp11.2 translocation renal cell carcinoma. In: *Sci Rep* 6, S. 23594. DOI: 10.1038/srep23594.

Ren, Yi; Shen, Han-Ming (2019): Critical role of AMPK in redox regulation under glucose starvation. In: *Redox Biology* 25, S. 101154. DOI: 10.1016/j.redox.2019.101154.

Ricciardi, Sara; Manfrini, Nicola; Alfieri, Roberta; Calamita, Piera; Crosti, Maria Cristina; Gallo, Simone et al. (2018): The Translational Machinery of Human CD4+ T Cells Is Poised for Activation and Controls the Switch from Quiescence to Metabolic Remodeling. In: *Cell Metabolism* 28 (6), 895-906.e5. DOI: 10.1016/j.cmet.2018.08.009.

Richter, Joel D.; Sonenberg, Nahum (2005): Regulation of cap-dependent translation by eIF4E inhibitory proteins. In: *Nature* 433 (7025), S. 477–480. DOI: 10.1038/nature03205.

Robichaud, N.; Del Rincon, S. V.; Huor, B.; Alain, T.; Petruccelli, L. A.; Hearnden, J. et al. (2015): Phosphorylation of eIF4E promotes EMT and metastasis via translational control of SNAIL and MMP-3. In: *Oncogene* 34 (16), S. 2032–2042. DOI: 10.1038/onc.2014.146.

Rousseau, D.; Gingras, A. C.; Pause, A.; Sonenberg, N. (1996a): The eIF4E-binding proteins 1 and 2 are negative regulators of cell growth. In: *Oncogene* 13 (11), S. 2415–2420. Online verfügbar unter https://pubmed.ncbi.nlm.nih.gov/8957083/.

Rousseau, D.; Kaspar, R.; Rosenwald, I.; Gehrke, L.; Sonenberg, N. (1996b): Translation initiation of ornithine decarboxylase and nucleocytoplasmic transport of cyclin D1 mRNA are increased in cells overexpressing eukaryotic initiation factor 4E. In: *Proceedings of the National Academy of Sciences of the United States of America* 93 (3), S. 1065–1070. DOI: 10.1073/pnas.93.3.1065.

Russell, Ryan C.; Yuan, Hai-Xin; Guan, Kun-Liang (2014): Autophagy regulation by nutrient signaling. In: *Cell Res* 24 (1), S. 42–57. DOI: 10.1038/cr.2013.166.

Rutkovsky, Alexandria C.; Yeh, Elizabeth S.; Guest, Stephen T.; Findlay, Victoria J.; Muise-Helmericks, Robin C.; Armeson, Kent; Ethier, Stephen P. (2019): Eukaryotic initiation factor 4E-binding protein as an oncogene in breast cancer. In: *BMC Cancer* 19 (1), S. 491. DOI: 10.1186/s12885-019-5667-4.

Sabatini, David M. (2017): Twenty-five years of mTOR: Uncovering the link from nutrients to growth. In: *PNAS* 114 (45), S. 11818–11825. DOI: 10.1073/pnas.1716173114.

Salt, I. P.; Johnson, G.; Ashcroft, S. J.; Hardie, D. G. (1998): AMP-activated protein kinase is activated by low glucose in cell lines derived from pancreatic beta cells, and may regulate insulin release. In: *Biochemical Journal* 335 (Pt 3) (Pt 3), S. 533–539. DOI: 10.1042/bj3350533.

Sarbassov, D. D.; Ali, Siraj M.; Kim, Do-Hyung; Guertin, David A.; Latek, Robert R.; Erdjument-Bromage, Hediye et al. (2004): Rictor, a novel binding partner of mTOR, defines a rapamycin-insensitive and raptor-independent pathway that regulates the cytoskeleton. In: *Current biology : CB* 14 (14), S. 1296–1302. DOI: 10.1016/j.cub.2004.06.054.

Saxton, Robert A.; Sabatini, David M. (2017): mTOR Signaling in Growth, Metabolism, and Disease. In: *Cell* 168 (6), S. 960–976. DOI: 10.1016/j.cell.2017.02.004.

Schaaf, Marco B.; Garg, Abhishek D.; Agostinis, Patrizia (2018): Defining the role of the tumor vasculature in antitumor immunity and immunotherapy. In: *Cell death & disease* 9 (2), S. 115. DOI: 10.1038/s41419-017-0061-0.

Schultz, Luciana; Chaux, Alcides; Albadine, Roula; Hicks, Jessica; Kim, Jenny J.; Marzo, Angelo M. de et al. (2011): Immunoexpression status and prognostic value of mTOR and hypoxia-induced pathway members in primary and metastatic clear cell renal cell carcinomas. In: *The American journal of surgical pathology* 35 (10), S. 1549–1556. DOI: 10.1097/PAS.0b013e31822895e5.

Seki, Nobuhiko; Takasu, Tasaburo; Sawada, Shigeki; Nakata, Masao; Nishimura, Rieko; Segawa, Yoshihiko et al. (2010): Prognostic significance of expression of eukaryotic initiation factor 4E and 4E

binding protein 1 in patients with pathological stage I invasive lung adenocarcinoma. In: *Lung Cancer* 70 (3), S. 329–334. DOI: 10.1016/j.lungcan.2010.03.006.

Sekiyama, Naotaka; Arthanari, Haribabu; Papadopoulos, Evangelos; Rodriguez-Mias, Ricard A.; Wagner, Gerhard; Léger-Abraham, Mélissa (2015): Molecular mechanism of the dual activity of 4EGI-1: Dissociating eIF4G from eIF4E but stabilizing the binding of unphosphorylated 4E-BP1. In: *PNAS* 112 (30), E4036-45. DOI: 10.1073/pnas.1512118112.

Sepideh Aminzadeh; Silvia Vidali; Wolfgang Sperl; Barbara Kofler; René G. Feichtinger (2015): Energy metabolism in neuroblastoma and Wilms tumor. In: *Translational Pediatrics* 4 (1), S. 202–232. Online verfügbar unter https://tp.amegroups.com/article/view/5636/6417.

Shackelford, David B.; Shaw, Reuben J. (2009): The LKB1-AMPK pathway: metabolism and growth control in tumour suppression. In: *Nat Rev Cancer* 9 (8), S. 563–575. DOI: 10.1038/nrc2676.

Shaw, Reuben J.; Kosmatka, Monica; Bardeesy, Nabeel; Hurley, Rebecca L.; Witters, Lee A.; DePinho, Ronald A.; Cantley, Lewis C. (2004): The tumor suppressor LKB1 kinase directly activates AMP-activated kinase and regulates apoptosis in response to energy stress. In: *Proceedings of the National Academy of Sciences of the United States of America* 101 (10), S. 3329–3335. DOI: 10.1073/pnas.0308061100.

Shim, H.; Chun, Y. S.; Lewis, B. C.; Dang, C. V. (1998): A unique glucose-dependent apoptotic pathway induced by c-Myc. In: *Proceedings of the National Academy of Sciences of the United States of America* 95 (4), S. 1511–1516. DOI: 10.1073/pnas.95.4.1511.

Signer, Robert A. J.; Le Qi; Zhao, Zhiyu; Thompson, David; Sigova, Alla A.; Fan, Zi Peng et al. (2016): The rate of protein synthesis in hematopoietic stem cells is limited partly by 4E-BPs. In: *Genes & Development* 30 (15), S. 1698–1703. DOI: 10.1101/gad.282756.116.

Sikalidis, Angelos K.; Mazor, Kevin M.; Kang, Minji; Liu, Hongyun; Stipanuk, Martha H. (2013): Total 4EBP1 Is Elevated in Liver of Rats in Response to Low Sulfur Amino Acid Intake. In: *Journal of Amino Acids* 2013, S. 864757. DOI: 10.1155/2013/864757.

Simons, Andrean L.; Mattson, David M.; Dornfeld, Ken; Spitz, Douglas R. (2009): Glucose deprivation-induced metabolic oxidative stress and cancer therapy. In: *Journal of cancer research and therapeutics* 5 Suppl 1 (Suppl 1), S2-6. DOI: 10.4103/0973-1482.55133.

Singh, Rajat; Cuervo, Ana Maria (2011): Autophagy in the cellular energetic balance. In: *Cell Metabolism* 13 (5), S. 495–504. DOI: 10.1016/j.cmet.2011.04.004.

Smith, M. R.; Jaramillo, M.; Liu, Y. L.; Dever, T. E.; Merrick, W. C.; Kung, H. F.; Sonenberg, N. (1990): Translation initiation factors induce DNA synthesis and transform NIH 3T3 cells. In: *The New biologist* 2 (7), S. 648–654. Online verfügbar unter https://pubmed.ncbi.nlm.nih.gov/2083255/.

Sonenberg, Nahum; Hinnebusch, Alan G. (2009): Regulation of translation initiation in eukaryotes: mechanisms and biological targets. In: *Cell* 136 (4), S. 731–745. DOI: 10.1016/j.cell.2009.01.042.

Soufi, Abdenour; Dalton, Stephen (2016): Cycling through developmental decisions: how cell cycle dynamics control pluripotency, differentiation and reprogramming. In: *Development (Cambridge, England)* 143 (23), S. 4301–4311. DOI: 10.1242/dev.142075.

Sperandio, S.; Belle, I. de; Bredesen, D. E. (2000): An alternative, nonapoptotic form of programmed cell death. In: *Proceedings of the National Academy of Sciences of the United States of America* 97 (26), S. 14376–14381. DOI: 10.1073/pnas.97.26.14376.

Suzuki, Atsushi; Kusakai, Gen-ichi; Kishimoto, Atsuhiro; Lu, Jie; Ogura, Tsutomu; Esumi, Hiroyasu (2003): ARK5 suppresses the cell death induced by nutrient starvation and death receptors via

inhibition of caspase 8 activation, but not by chemotherapeutic agents or UV irradiation. In: *Oncogene* 22 (40), S. 6177–6182. DOI: 10.1038/sj.onc.1206899.

Svitkin, Y. V.; Pause, A.; Haghighat, A.; Pyronnet, S.; Witherell, G.; Belsham, G. J.; Sonenberg, N. (2001): The requirement for eukaryotic initiation factor 4A (eIF4A) in translation is in direct proportion to the degree of mRNA 5' secondary structure. In: *RNA (New York, N.Y.)* 7 (3), S. 382–394. DOI: 10.1017/s135583820100108x.

Svitkin, Yuri V.; Herdy, Barbara; Costa-Mattioli, Mauro; Gingras, Anne-Claude; Raught, Brian; Sonenberg, Nahum (2005): Eukaryotic translation initiation factor 4E availability controls the switch between cap-dependent and internal ribosomal entry site-mediated translation. In: *Molecular and cellular biology* 25 (23), S. 10556–10565. DOI: 10.1128/MCB.25.23.10556-10565.2005.

Tahmasebi, Soroush; Alain, Tommy; Rajasekhar, Vinagolu K.; Zhang, Jiang-Ping; Prager-Khoutorsky, Masha; Khoutorsky, Arkady et al. (2014): Multifaceted regulation of somatic cell reprogramming by mRNA translational control. In: *Cell stem cell* 14 (5), S. 606–616. DOI: 10.1016/j.stem.2014.02.005.

Teleman, Aurelio A.; Chen, Ya-Wen; Cohen, Stephen M. (2005): 4E-BP functions as a metabolic brake used under stress conditions but not during normal growth. In: *Genes & Development* 19 (16), S. 1844–1848. DOI: 10.1101/gad.341505.

Thoreen, Carson C.; Chantranupong, Lynne; Keys, Heather R.; Wang, Tim; Gray, Nathanael S.; Sabatini, David M. (2012): A unifying model for mTORC1-mediated regulation of mRNA translation. In: *Nature* 485 (7396), S. 109–113. DOI: 10.1038/nature11083.

Truitt, Morgan L.; Conn, Crystal S.; Shi, Zhen; Pang, Xiaming; Tokuyasu, Taku; Coady, Alison M. et al. (2015): Differential Requirements for eIF4E Dose in Normal Development and Cancer. In: *Cell* 162 (1), S. 59–71. DOI: 10.1016/j.cell.2015.05.049.

Tsai, Shihyin; Sitzmann, Joanna M.; Dastidar, Somasish G.; Rodriguez, Ariana A.; Vu, Stephanie L.; McDonald, Circe E. et al. (2015): Muscle-specific 4E-BP1 signaling activation improves metabolic parameters during aging and obesity. In: *J Clin Invest* 125 (8), S. 2952–2964. DOI: 10.1172/JCI77361.

Tsai, Shih-Yin; Rodriguez, Ariana A.; Dastidar, Somasish G.; Del Greco, Elizabeth; Carr, Kaili Lia; Sitzmann, Joanna M. et al. (2016): Increased 4E-BP1 Expression Protects against Diet-Induced Obesity and Insulin Resistance in Male Mice. In: *Cell reports* 16 (7), S. 1903–1914. DOI: 10.1016/j.celrep.2016.07.029.

Tsukiyama-Kohara, K.; Poulin, F.; Kohara, M.; DeMaria, C. T.; Cheng, A.; Wu, Z. et al. (2001): Adipose tissue reduction in mice lacking the translational inhibitor 4E-BP1. In: *Nat Med* 7 (10), S. 1128–1132. DOI: 10.1038/nm1001-1128.

Tsukumo, Yoshinori; Alain, Tommy; Fonseca, Bruno D.; Nadon, Robert; Sonenberg, Nahum (2016): Translation control during prolonged mTORC1 inhibition mediated by 4E-BP3. In: *Nature Communications* 7, S. 11776. DOI: 10.1038/ncomms11776.

Umenaga, Yu; Paku, Keum Soon; In, Yasuko; Ishida, Toshimasa; Tomoo, Koji (2011): Identification and function of the second eIF4E-binding region in N-terminal domain of eIF4G: comparison with eIF4E-binding protein. In: *Biochemical and Biophysical Research Communications* 414 (3), S. 462–467. DOI: 10.1016/j.bbrc.2011.09.084.

Vacanti, Nathaniel M.; Divakaruni, Ajit S.; Green, Courtney R.; Parker, Seth J.; Henry, Robert R.; Ciaraldi, Theodore P. et al. (2014): Regulation of substrate utilization by the mitochondrial pyruvate carrier. In: *Molecular cell* 56 (3), S. 425–435. DOI: 10.1016/j.molcel.2014.09.024.

Voeltzke, Kai; Scharov, Katerina; Funk, Cornelius; Kahler, Alisa; Picard, Daniel; Hauffe, Laura et al. (2021): EIF4EBP1 is transcriptionally upregulated by MYCN and associates with poor prognosis in neuroblastoma. In: *bioRxiv*, 2021.12.08.471784. DOI: 10.1101/2021.12.08.471784.

Wan, Jing; Shi, Fang; Xu, Zhanzhan; Zhao, Min (2015): Knockdown of eIF4E suppresses cell proliferation, invasion and enhances cisplatin cytotoxicity in human ovarian cancer cells. In: *International Journal of Oncology* 47 (6), S. 2217–2225. DOI: 10.3892/ijo.2015.3201.

Wang, Chunmei; Cigliano, Antonio; Jiang, Lijie; Li, Xiaolei; Fan, Biao; Pilo, Maria G. et al. (2015): 4EBP1/eIF4E and p70S6K/RPS6 axes play critical and distinct roles in hepatocarcinogenesis driven by AKT and N-Ras proto-oncogenes in mice. In: *Hepatology (Baltimore, Md.)* 61 (1), S. 200–213. DOI: 10.1002/hep.27396.

Wang, Shuai; Guo, Yazhou; Yang, Chen; Huang, Ruijie; Wen, Yuting; Zhang, Chunyan et al. (2021): Swainsonine Triggers Paraptosis via ER Stress and MAPK Signaling Pathway in Rat Primary Renal Tubular Epithelial Cells. In: *Frontiers in pharmacology* 12, S. 715285. DOI: 10.3389/fphar.2021.715285.

Wang, Xuemin; Beugnet, Anne; Murakami, Mirei; Yamanaka, Shinya; Proud, Christopher G. (2005): Distinct signaling events downstream of mTOR cooperate to mediate the effects of amino acids and insulin on initiation factor 4E-binding proteins. In: *Molecular and cellular biology* 25 (7), S. 2558–2572. DOI: 10.1128/MCB.25.7.2558-2572.2005.

Wang, Zhiyong; Feng, Xiaodong; Molinolo, Alfredo A.; Martin, Daniel; Vitale-Cross, Lynn; Nohata, Nijiro et al. (2019): 4E-BP1 Is a Tumor Suppressor Protein Reactivated by mTOR Inhibition in Head and Neck Cancer. In: *Cancer Res* 79 (7), S. 1438–1450. DOI: 10.1158/0008-5472.CAN-18-1220.

Ward, Patrick S.; Thompson, Craig B. (2012): Metabolic reprogramming: a cancer hallmark even warburg did not anticipate. In: *Cancer cell* 21 (3), S. 297–308. DOI: 10.1016/j.ccr.2012.02.014.

Weber, Carmen A.; Sekar, Karthik; Tang, Jeffrey H.; Warmer, Philipp; Sauer, Uwe; Weis, Karsten (2020): β-Oxidation and autophagy are critical energy providers during acute glucose depletion in Saccharomyces cerevisiae. In: *PNAS* 117 (22), S. 12239–12248. DOI: 10.1073/pnas.1913370117.

Wiebe, Shane; Nagpal, Anmol; Truong, Vinh T.; Park, Jeehyun; Skalecka, Agnieszka; He, Alexander J. et al. (2019): Inhibitory interneurons mediate autism-associated behaviors via 4E-BP2. In: *Proceedings of the National Academy of Sciences of the United States of America* 116 (36), S. 18060–18067. DOI: 10.1073/pnas.1908126116.

Wilson, Wayne A.; Hawley, Simon A.; Hardie, D.Grahame (1996): Glucose repression/derepression in budding yeast: SNF1 protein kinase is activated by phosphorylation under derepressing conditions, and this correlates with a high AMP:ATP ratio. In: *Current biology : CB* 6 (11), S. 1426–1434. DOI: 10.1016/s0960-9822(96)00747-6.

Winder, W. W.; Hardie, D. G. (1996): Inactivation of acetyl-CoA carboxylase and activation of AMP-activated protein kinase in muscle during exercise. In: *The American journal of physiology* 270 (2 Pt 1), E299-304. DOI: 10.1152/ajpendo.1996.270.2.E299.

Wolpert, Lewis (2011): Principles of development. 4. ed. Oxford: Oxford University Press.

Woods, A.; Munday, M. R.; Scott, J.; Yang, X.; Carlson, M.; Carling, D. (1994): Yeast SNF1 is functionally related to mammalian AMP-activated protein kinase and regulates acetyl-CoA carboxylase in vivo. In: *Journal of Biological Chemistry* 269 (30), S. 19509–19515. Online verfügbar unter https://pubmed.ncbi.nlm.nih.gov/7913470/.

Wu, Su; Wagner, Gerhard (2021): Deep computational analysis details dysregulation of eukaryotic translation initiation complex eIF4F in human cancers. In: *Cell systems*. DOI: 10.1016/j.cels.2021.07.002.

Yamaguchi, Suguru; Ishihara, Hisamitsu; Yamada, Takahiro; Tamura, Akira; Usui, Masahiro; Tominaga, Ryu et al. (2008): ATF4-mediated induction of 4E-BP1 contributes to pancreatic beta cell survival under endoplasmic reticulum stress. In: *Cell Metabolism* 7 (3), S. 269–276. DOI: 10.1016/j.cmet.2008.01.008.

Yuneva, Mariia; Zamboni, Nicola; Oefner, Peter; Sachidanandam, Ravi; Lazebnik, Yuri (2007): Deficiency in glutamine but not glucose induces MYC-dependent apoptosis in human cells. In: *J Cell Biol* 178 (1), S. 93–105. DOI: 10.1083/jcb.200703099.

Zhang, Chen-Song; Hardie, D. Grahame; Lin, Sheng-Cai (2020): Glucose Starvation Blocks Translation at Multiple Levels. In: *Cell Metabolism* 31 (2), S. 217–218. DOI: 10.1016/j.cmet.2020.01.005.

Zhang, Chen-Song; Jiang, Bin; Li, Mengqi; Zhu, Mingjiang; Peng, Yongying; Zhang, Ya-Lin et al. (2014): The lysosomal v-ATPase-Ragulator complex is a common activator for AMPK and mTORC1, acting as a switch between catabolism and anabolism. In: *Cell Metabolism* 20 (3), S. 526–540. DOI: 10.1016/j.cmet.2014.06.014.

Zhang, Tao; Guo, Jianrong; Li, Huili; Wang, Jiliang (2018): Meta-analysis of the prognostic value of p-4EBP1 in human malignancies. In: *Oncotarget* 9 (2), S. 2761–2769. DOI: 10.18632/oncotarget.23031.

Zhao, Yuxing; Coloff, Jonathan L.; Ferguson, Emily C.; Jacobs, Sarah R.; Cui, Kai; Rathmell, Jeffrey C. (2008): Glucose metabolism attenuates p53 and Puma-dependent cell death upon growth factor deprivation. In: *Journal of Biological Chemistry* 283 (52), S. 36344–36353. DOI: 10.1074/jbc.M803580200.

Zid, Brian M.; Rogers, Aric N.; Katewa, Subhash D.; Vargas, Misha A.; Kolipinski, Marysia C.; Lu, Tony Au et al. (2009): 4E-BP extends lifespan upon dietary restriction by enhancing mitochondrial activity in Drosophila. In: *Cell* 139 (1), S. 149–160. DOI: 10.1016/j.cell.2009.07.034.

Zou, Zhilin; Tao, Tao; Li, Hongmei; Zhu, Xiao (2020): mTOR signaling pathway and mTOR inhibitors in cancer: progress and challenges. In: *Cell Biosci* 10 (1), S. 31. DOI: 10.1186/s13578-020-00396-1.